An analysis of the impact of trash screen design on debris related blockage at culvert inlets

Janice Blanc

Submitted for the degree of Doctor of Philosophy

Heriot-Watt University
School of the Built Environment

March 2013

Abstract

The construction of a culvert within a river channel alters the local hydraulic characteristics which often increases upstream water elevation as a result of the volume of water being constricted as it enters the culvert. This effect can be exacerbated if there is a build up of debris either at the inlet or trapped within the culvert. As a consequence culverts, especially those which are prone to becoming blocked, may considerably increase the potential for out of channel flows and therefore the risk of serious flooding. While trash screens may be fitted at a culvert inlet to prevent debris from entering, unless they are well designed and maintained they may increase the potential for flooding if they become blocked by trapping debris that would have passed unrestricted through the culvert. Guidelines for screen design focus mainly on ensuring sufficient screen area is provided to handle the expected debris load, while recommendations for individual screen elements, such as bar spacing, are generally based on anecdotal evidence and site specific environmental or safety concerns. However, many different trash screen configurations can influence blockage potential. To gain a better understanding of how blockage, and therefore any potential associated flood risk, of culvert trash screens is influenced by screen geometry and position, a Froude-scaled physical model was developed to facilitate assessment of the efficiency of different trash screen configurations. To minimize scaling issues related to complex geometry, and to ensure the focus of the research remained on the influence of screen design rather than on factors specific to the debris, wooden dowel was used to represent different debris lengths. Detailed analysis based on 147,000 debris passes is used to show that, as would be expected, potential for screen blockage by debris increases as the ratio of debris length to bar spacing increases. However, in addition, a key finding has been that the screen position relative to the zone of flow acceleration created as the flow is constricted on approach to the culvert inlet is a significant driving factor in the blocking potential of the screen. Detailed statistical analysis was used to define blockage potential in terms of all contributing factors. The derived model was used to develop end user focussed tools, a nomograph and an interactive spreadsheet, to aid estimation of blockage at a screen for a given geometry and position.

Acknowledgements

I would like to express my gratitude to Dr. Scott Arthur and Dr. Grant Wright for their continuous guidance, encouragement and support throughout this research. Grateful thanks are also due to Dr. Nicholas Wallerstein for his interest and assistance.

Acknowledgements are also due to the technical staff of the School of the Built Environment at Heriot-Watt University for their expert assistance. Many thanks go to Mr David Murray for his resourcefulness and thoroughness during the construction and revision of the experimental test rig, to Mr James Maguire for helping put it back together again whenever required, and to Mr Tom Stenhouse for his interest, assistance and quick response to overcoming operational problems with the flume.

I would also like to extend my thanks to Duncan Sharp and Wajid A Khan for their assistance during the data gathering process and to the City of Edinburgh Council for allowing access to their telemetry system.

This research project was financially supported by the SAWA Interreg IVB project and the Engineering and Physical Sciences Research Council (EPSRC), whose funding is gratefully acknowledged.

ACADEMIC REGISTRY

Research Thesis Submission

Name*:*	Janice Blanc		
School/PGI:	School of the Built Environment, IIE		
Version: *(i.e. First, Resubmission, Final)*	Final	Degree Sought (Award **and** Subject area)	Doctor of Philosophy (Civil Engineering)

Declaration

In accordance with the appropriate regulations I hereby submit my thesis and I declare that:

1) the thesis embodies the results of my own work and has been composed by myself
2) where appropriate, I have made acknowledgement of the work of others and have made reference to work carried out in collaboration with other persons
3) the thesis is the correct version of the thesis for submission and is the same version as any electronic versions submitted*.
4) my thesis for the award referred to, deposited in the Heriot-Watt University Library, should be made available for loan or photocopying and be available via the Institutional Repository, subject to such conditions as the Librarian may require
5) I understand that as a student of the University I am required to abide by the Regulations of the University and to conform to its discipline.

* *Please note that it is the responsibility of the candidate to ensure that the correct version of the thesis is submitted.*

Signature of Candidate*:*		Date:	

Submission

Submitted By *(name in capitals):*	
Signature of Individual Submitting:	
Date Submitted:	

For Completion in the Student Service Centre (SSC)

Received in the SSC by *(name in capitals):*			
Method of Submission **(***Handed in to SSC; posted through internal/external mail***):**			
E-thesis Submitted (*mandatory for final theses***)**			
Signature:		Date:	

Table of Contents

List of Tables

List of Figures

List of Abbreviations

ADV	Acoustic Doppler Velocimeter
AES	Afflux Estimation System
AR&R	Australian Rainfall and Runoff
CAR	Water Environment (Controlled Activities) (Scotland) Regulations 2005
CES	Conveyance Estimation System
CIRIA	Construction Industry Research and Information Association
CSO	Combined sewage overflow
DEFRA	Department of Environment, Food and Rural Affairs
EA	Environment Agency
EHMWPE	Extra high molecular weight polyethylene
EU	European Union
FHWA	Federal Highway Administration
Fr	Froude Number
FSM	Froude scale modelling
HDPE	High-density polyethylene
HMWB	Heavily modified water body
HW	Headwater
LWD	Large woody debris
NFM	Natural flood management
POST	Parliamentary Office of Science & Technology
Re	Reynolds number
RoSPA	Royal Society for the Prevention of Accidents
SEPA	Scottish Environment Protection Agency
TW	Tailwater
UK	United Kingdom
UKBAP	UK Biodiversity Action Plan
USA	United States of America
WFD	Water Framework Directive

List of Associated Publications

Blanc, J., Wallerstein, N.P., Arthur, S., Wright, G.B., 2011. Modelling the Impact of Trash Screen Design on Debris Related Blockage at Culvert Inlets. *Rivers 2011, Proceedings of the 3rd International Conference on Managing Rivers in the 21st Century:* Sustainable Solutions for Global Crisis of Flooding, Pollution and Water Scarcity, 6th-9th December 2011, Penang, Malaysia.

Blanc, J., Wallerstein, N.P., Arthur, S. & Wright, G.B., in press. An analysis of the performance of debris screens at culverts. Proceedings of the ICE – Water Management, Accepted for publication December 2012.

Chapter 1
Introduction

1.1. Overview

Floods are a natural occurrence and the risks they pose are wide ranging. However, in societal terms, the main concern is the risk to people and property. Globally, the number of recorded flood events is increasing. Flooding currently accounts for a large proportion of the average annual damage and loss of life caused by natural events with around 9000 deaths annually and flood related costs of over £10bn a year (Golding, 2009). For example, in 2007 over 200 major floods worldwide affected 180 million people and resulted in around 8000 deaths. In financial terms the 2007 floods caused an estimated £40 billion worth of damage (Pitt, 2008). In 2008 the expected annual damages from urban flooding in the United Kingdom (UK) were estimated at £0.27 billion (Dawson *et al*., 2008) but it has been suggested that as a result of urban growth, land use changes and climate changes this could rise to between £2 billion and £15 billion by 2080 (Evans *et al*., 2004b; Hall *et al*., 2005). The first Scottish National Flood Risk Assessment, produced by the Scottish Environment Protection Agency (SEPA), reports that approximately one in 22 of all residential properties and one in 13 of all non-residential properties in Scotland are at risk from flooding and notes that the average annual damage to homes, businesses and agriculture from all sources of flooding is estimated to be between £720 million and £850 million (SEPA, 2011). In addition, climate change trends suggest that Scotland will experience more frequent extreme weather events, including intense summer rainfall (SEPA, 2012a). Along with potential climate changes, changes in land use can fundamentally influence the water balance of a catchment through, for example, abstraction from rivers or ground water sources for irrigation, the different evaporative demands of different crop types or a switch from agricultural to urban use.

Assessing the risk of flooding to human life and property and working towards minimising flood risk has become a major concern. This is in part due to increased public awareness of these issues and the drive resulting from reports such as the Pitt review, produced as a response to the UK floods of 2007 (Pitt, 2008). This focus on risk assessment rather than relying on post flood action is supported by the Department of Environment, Food and Rural Affairs (DEFRA) strategy ,'Making Space for Water', (DEFRA, 2004) and the implementation of the Water Framework Directive (WFD) (EU, 2000).

Flooding has an impact on many aspects of life including the natural environment and ecosystems, social systems, infrastructure and the built environment, and economic activity (Hall *et al*., 2003). Flooding can result in damage due to direct contact with floodwaters but indirect damage may also occur as a further consequence of the flood and the disruption of economic and social activities. The assessment of damage can be broken down into tangible and intangible damages. Tangible damages include: physical damage to buildings and their contents, damage to infrastructure, loss of industrial production, traffic disruption and costs directly relating to emergency response. Intangible damages are harder to quantify but as significant and include: loss of life, short and long term health effects, ecological impacts, impact of post-flood recovery, and the increased vulnerability of survivors (Floodsite, 2009).

The economic cost of flooding can be substantial. There may be a significant loss of economic production due to damaged facilities, energy and telecommunication failures, and the interruption of supply of intermediary goods such as prefabricated product components and processed materials (Messner & Meyer, 2005). Other examples include loss of time and profits due to traffic disruption, disturbance of markets after floods, and the disadvantages connected with reduced market and public services. Direct damage is only a small part of the effect of flooding upon humans; there are also huge social and environmental impacts including loss of homes, goods and working environments and increased health risks (ICE, 2001; OFWAT, 2002). Flooding can also result in serious injury and fatalities. It is acknowledged that indirect, environmental and socio-economic damage need to be a major consideration when fully analysing flood impacts (FEMA, 1998; Penning-Rowsell & Green, 2000) and in the UK there has been a noticeable shift away from the dependence on purely economic analysis towards a more holistic approach that takes into account the distress and social impacts of flooding (ICE, 2001; Hall *et al*., 2003; Werritty *et al.*, 2007). This is in line with Article 6 of the European Union (EU) Directive on the assessment and management of flood risks (Floods Directive), which requires the assessment and mapping of social, economic and environmental flood risk (EU, 2007).

Many factors and situations may contribute to flood risk. The work detailed here is concerned with one potential flood risk; that associated with flooding at culvert inlet screens when they become blocked by a build up of debris.

1.2. Flood Risks Associated with Culverts

Flood risk in urban areas has often been managed through the construction of culverts. This has resulted in river maintenance difficulties and reduced the ability of channels to cope with increasingly intense summer storms. Many of these installations were designed to accommodate major flooding using guidelines and predictions available at the time of installation. However, the recommended volumes may no longer be adequate due to recent and predicted future climate change impacts and land use changes.

Since the mid-1990s the potential for increased flood risk associated with culverts has been recognised and both the Environment Agency (EA) (CIWEM, 2010) and SEPA now discourage culverting. The Scottish Executive (2004), in advice to local authorities on planning and flooding, notes that culverts are a frequent cause of local flooding, particularly if the design or maintenance is inadequate. In their Position Statement to support the implementation of the Water Environment (Controlled Activities: Scotland) Regulations 2005 (CAR) (TSO, 2005), SEPA notes that culverts have a range of harmful local and system-wide impacts on the environment and indicate their aim is to "Protect the physical character, habitat, transport of sediment, free passage of fauna, establishment of other ecology, access to light, and chemical quality in small and urban watercourses from the harmful effects of culverting" (SEPA, 2005, Section 1.2). SEPA states that it:

- "Is opposed to the enclosed culverting of watercourses for land gain and will actively seek to discourage such proposals"
- "Will presume against unjustified enclosed culverting (box or cylinder) of watercourses as bridging structures for transport routes"
- "Will presume against other forms of unjustified open culverting of watercourses (e.g. brick, stone or concrete open channels)"
- "Will seek improvements to existing culverts in line with this position statement when replacement or significant maintenance works are proposed"

Furthermore, where it has been demonstrated that culverting is the only viable option, SEPA "will seek adoption of mitigation measures to protect habitats, passage of fauna, and river form and flow".

In addition to minimizing the negative environmental aspects, the aim of SEPA's position statement is to mitigate the problems of increased flood risk associated with poorly designed culverts. For example Figure 1.1a shows a well designed culvert with appropriate capacity and consideration of environmental issues while Figure 1.1b shows a poor culvert design where the risk of blockage may be increased through the use of multiple small barrels which are individually more prone to blockage. A summary of risk factors for culvert blockage is shown in Table 1.1.

(a)  (b) 

Figure 1.1 (a) Good culvert design (b) Poor culvert design (Image b from Benn *et al*., 2004)

Table 1.1 Risk Factors for Culvert Blockage (EA, 2009. Table 4.2 page 18)

Factor	Issues
Size	The smaller the culvert, the more likely it is to become blocked. The preferred option is to avoid multiple barrel culverts and adopt the largest size practicable.
Bends, steps and changes of cross-section	These should be avoided as they can trap larger items of debris which start to cause a blockage.
Length	The longer the culvert, the greater the probability that debris will be trapped somewhere, and the more difficult it is to remove a blockage.
Hydraulic design	A culvert that flows with a free water surface, even in large floods, is less likely to trap large debris than one which flows full.
Inverted siphon culverts (those where the barrel dips down to pass under an obstruction	These are more likely to block due to the accumulation of debris during periods of low flow. Such culverts should be avoided except in circumstances where there is no other practicable option.

Alteration to a river channel by the construction of a culvert may change the characteristics of the flow upstream, often increasing the backwater elevation if the culvert inlet acts as the point of control and this effect can be exacerbated by the presence of debris if it becomes trapped within the culvert or at its inlet. As a consequence culverts, especially those which are prone to becoming blocked, may considerably increase the potential for out of channel flows and therefore the risk of serious flooding. Often the problem is minor, for example a blocked culvert may result in a road flooding, which causes disruption but has no lasting damage. In other cases the problems can be more substantial. For example in August 2004, 57 people had to be airlifted to safety after the vehicles they were travelling in became trapped between two debris flows in Glen Ogle. The debris flows were the result of culverts carrying streams under the road becoming blocked due to exceptionally high rainfall and high soil saturation which had triggered debris slides into the headwaters of the streams (Winter *et al.*, 2008).

Blocked culverts may also put lives at risk either directly through the flood waters or as a result of structural damage to buildings and infrastructure. The following examples illustrate the potential serious risk caused by flooding at culverts. In Merthyr Tydfil in December 1979 two residents were drowned when water trapped behind a culvert was released when the blockage cleared (RSSB, 2004). Three deaths occurred in Carlisle during 2005 during the worst flooding in that city for over 100 years (Pitt, 2008). In 2007, five members of a family were killed in Gosford, New South Wales when a road collapsed because of a failure to adequately maintain the underlying culvert (McCarthy, 2008) and during the flooding that year in the UK one case of accidental drowning was recorded as being the direct result of an individual becoming trapped by a temporary grille covering a concrete culvert (Pitt, 2008). More recently, in 2011, a member of the public died while trying to unblock a culvert during a storm to try and ease flooding in the village of Smithton near Inverness (Freuchie Flood Action Group, 2011).

Within the UK, most urban streams and brooks no longer act as the main disposal mechanism for foul sewage as a result of the 1936 Public Health Act which required local authorities to provide public sewers (HMSO, 1936). However, many are treated as a convenient disposal system by local residents and/or still receive combined sewage overflow (CSO) discharges. In addition, industrial and commercial waste may enter the watercourse either through deliberate disposal or accidental spillage. A wide range of discarded items including toys, plastic bags, garden waste, traffic cones and shopping trolleys find their way into urban watercourses, which consequently increase the risk of blockage and associated flooding (ICE, 2001). In addition to debris resulting from deliberate tipping, a considerable amount of debris finds its way naturally to the watercourse. The volumes of debris are dependent on the extended riparian environment as debris may have originated from within the watercourse or its immediate surroundings, or may have been transported there from a more distant location through natural or anthropogenic processes.

Blockage by debris is one of the main factors contributing to flood risk associated with culverts but other forms of culvert failure are also a hazard. Flooding may occur due to collapse of the culvert, an example of which took place on the I-70, East of Vail, Colorado, USA in 2003 when four lanes of the highway were damaged. City streets and 28 homes also suffered damage. The culvert failed due to rusting of a corrugated metal pipe (Perrin & Jhaveri, 2004). Culvert collapse can also occur where culvert construction, installation or maintenance has been poor, or where the load on the culvert from overhead traffic exceeds the design load.

Culvert failure may also be the result of insufficient capacity. This may be due to poor design, unexpected extreme conditions or changes to the catchment such as land use changes since installation.

It is recognised that full hydraulic assessment of a potential culvert, its catchment and hydrology including potential future challenges and changes (particularly climate change derived) will help to determine the appropriate capacity for the culvert and contribute towards minimising any flood risk.

1.3. The Use of Trash Screens

Trash screens (sometimes referred to as debris screens or grilles) are often installed at the upstream end of culverts to prevent the entry of debris. Some example screens are shown in Figures 1.2 to 1.5. Unless the screens are well designed and maintained they may be a hazard in themselves and actually increase the potential for flooding if they trap debris that would have passed through the culvert without causing any problems. Table 1.2 summarises the hazards associated with trash screens.

Figure 1.2 Debris screen at culvert on the Stenhouse burn at Ellen's Glen Loan in Edinburgh

Figure 1.3 Debris screen in Inch Park Edinburgh

Figure 1.4 Debris blocking screen at culvert on the Stenhouse burn at Lasswade Road Edinburgh

Figure 1.5 Debris screen at culvert on the Braidburn at Redford Road in Edinburgh

Table 1.2 Hazards associated with trash screens (EA, 2009. Table 4.1 page 14)

Hazards associated with not providing a screen	Hazards that may arise as a consequence of installing a screen in a watercourse
Death or injury as a result of someone entering a culvert or being swept in during a flood Flooding resulting from blockage of the culvert by debris Damage to the interior of a culvert or the services it contains (uncommon)	Flooding caused by debris accumulating on a screen and blocking it Injury to those responsible for maintaining and cleaning the screen Environmental degradation – visual impact, restrictions to wildlife movement, lighting nuisance, health impacts of accumulating trash at the site, vandalism Structural failure Restriction on access in an emergency

Trash screens differ from security screens in that their main purpose is to prevent the passage of debris into the culvert rather than restrict access or minimize health and safety concerns. Trash screens are also generally only installed at the upstream end of a culvert. According to the EA (2009, p5), “The screen should trap as little debris as possible commensurate with the aim of preventing material that could cause a blockage from progressing downstream”. Current guidelines and standards for the use of trash screens are discussed in detail in Chapter 2.

Once site requirements have been taken into consideration, currently the main focus of screen design is on ensuring sufficient screen area is provided to handle the expected debris load. However a number of other trash screen configuration elements may also have an influence on the potential for blocking debris passage and a better understanding of the influence of these elements is required to ensure screen designs can be optimised in order to minimise any flood risk associated with blockage at culvert trash screens. This is important as culverts will continue to play an integral role in urban watercourses for the foreseeable future.

1.4. Future Challenges

1.4.1. Increased urbanisation

In 2007 half of the world's population lived in cities. The total global urban population is expected to almost double over the next 20 years, resulting in over five billion city dwellers, over 60% of the predicted global population (Hall, 2007; Zevenbergen *et al*., 2008). Within England, it was predicted that land in urban/industrial use will increase by 20% between 2000 and 2016 with a need for up to five million new homes (Robinson *et al*., 2000). Urbanisation has a significant effect on the hydrological cycle, and in particular, on the physical structure of streams and rivers and rainfall-runoff processes. Increases in impervious surfaces can result in magnification of runoff during storm events, bank erosion and the alteration of stream channels (e.g. Walsh *et al*., 2005a, 2005b; Pizzuto *et al*., 2008). These changes are summarised in Figure 1.6.

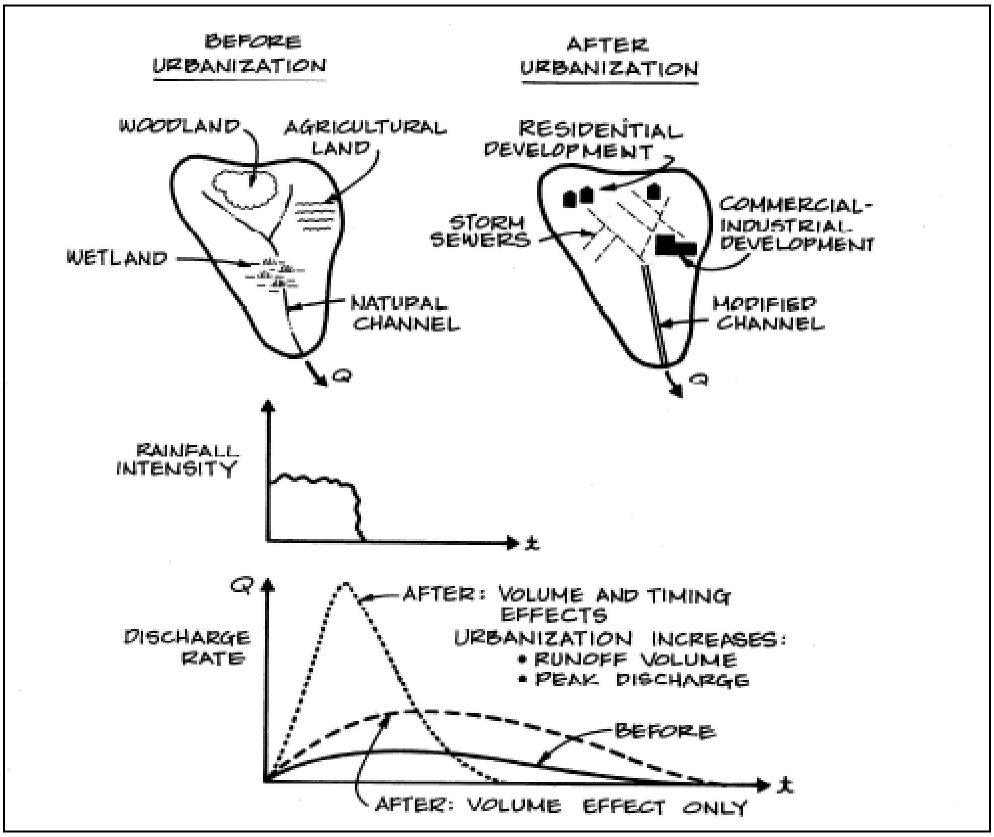

Figure 1.6 Typical hydrologic-hydraulic impact of urbanisation (Walesh, 1989)

This urban development has resulted in a process of 'urbanisation' of natural drains and streams around the growing urban areas. Two of the most significant forms of this are concrete lining and culverting (ICE, 2001) both of which lead to environmental degradation of streams. Pickett *et al*. (2011), in a review of progress made in managing urban ecological systems, discuss the problems resulting from "Urban Stream Syndrome", a term used by Walsh (2005b) to describe the degradation of streams in urban areas. Rivers and streams have an important role in a number of processes including transporting surface runoff, providing habitat and migration pathways for aquatic species, and attenuating pollution. Changes to rivers and streams resulting from urbanisation may therefore alter the transport of energy, materials, and certain ecosystem functions (e.g. Groffman *et al*., 2002; Elmore & Kaushal, 2008; Kaushal *et al.*, 2008; Roach *et al*., 2008).

Increased urbanisation can further increase rainfall over and above any climate change related increase due to higher temperatures leading to increased convection and the supply of sources of water vapour along with particles to seed raindrop formation from combustion and industrial processes. Mansell (2003) suggests that an increase in precipitation of up to 15% can occur in and downwind of large urban areas.

In addition to the increasing flood risk due to changes in runoff patterns there is also an increase in susceptibility to flooding as pressures grow to build in unsuitable areas such as flood plains.

1.4.2. Climate change

Flood risk issues associated with culverts may become more pronounced if climate change leads to more extreme rainfall events. Current climate change predictions indicate that severe weather events will become more frequent. Rainfall could increase by up to 40% leading to an increase in surface runoff and corresponding flood volumes (UKWIR, 2004). Evans *et al*. (2004b) suggest both socio-economic and climate changes may lead to an increase in flood damages of 200%. In order to understand the implications of the potential increase in flood risk a major report was commissioned by the Parliamentary Office of Science and Technology (POST). The Foresight Flood and Coastal Defence project studied the impact of four different future scenarios on flood risk (Foresight, 2006). The scenarios represented a range of environmental and economic conditions. The report indicated that with existing policies and measures flood risk would increase under all scenarios. However, the level of damage was scenario dependant. For example, under the 'world markets' scenario the increase in economic value of property would result in higher levels of financial damage.

1.4.3. Legislation

The key legislative performance requirements of a culvert as defined by Balkham *et al.* (2010) are:

- Environmental legislation
- Health and safety legislation
- Duties as the riparian owner
- Legislation relating to the infrastructure associated with the culvert

The existing legal framework relating to culverts varies from country to country within the UK. Each system confers rights, powers and duties on the owners of culverts and the relevant statutory bodies. In Scotland, the recent Flood Risk Management (Scotland) Act 2009 (Scottish Government, 2009) transposes the 'Floods Directive' (EU, 2007) into Scottish Law. This will increase the role of SEPA within flood risk management and place new requirements on the Scottish Government, SEPA and responsible authorities. There will be a requirement to map and assess structures that may cause or reduce flood risk which will include culverts and culvert trash and safety screens. The new legislation should provide a simplified route to promoting flood management schemes and culvert works as local authorities can confirm the requirements for work within a flood management plan without the need for Scottish Government approval. Under the CAR, culverting of a watercourse is considered a controlled activity and authorisation must be obtained from SEPA for all such works.

In England and Wales, the Flood and Water Management Act (TSO, 2010), which was passed in 2010, should result in a more integrated approach to flood management between Local Authorities, water boards and drainage companies. It strengthens the consent requirements for culverts by allowing existing culverts to be designated as flood management assets which require consent before they can be modified or removed. In addition consent is now required for all new culverts.

The continued implementation of aspects of the WFD will have an impact on culverting through the requirement to maintain or improve the ecological status of watercourses. Under the WFD Annex II (Article 4(3)), culverted watercourses are designated 'Heavily Modified Water Bodies (HMWB)' because they have been substantially changed in character as a result of human activity. The Directive requires that culverted watercourses, along with other HMWBs, meet the lower standard of 'Good Ecological

Potential' rather than the higher standard, for other water bodies, of 'Good Ecological Status'. Annex V of the WFD details the requirements for each status.

The legal requirements regarding the disposal of debris removed from culverts or trash screens varies across countries within the UK but generally a license is required in order to remove or transport the debris. Within Scotland the routine disposal of debris from culverts and any associated screens is covered by the rules of the CAR. In addition all maintenance operations within the UK may have obligations under the appropriate Construction (Design and Management) Regulations and Confined Spaces Regulations.

1.4.4. *Changes in flood management practice*

Over time the approach to flood management has changed. An initial focus on land drainage and flood defence throughout the 1950s, 60s and 70s moved towards a flood control approach and then to flood management in the 1980s and 90s (Floodsite, 2009). All these approaches had a strong focus on engineering measures. Now a more integrated flood risk management approach is being taken with the aim of balancing the reduction of the consequences of floods against other considerations. For example, natural flood management (NFM), defined by POST (2011) as "the alteration, restoration or use of landscape features to reduce flood risk" is now being promoted as a cost-effective catchment scale approach to managing flood risk. One NFM strategy is to slow the passage of water through planting riverbank or floodplain woodland. In addition, overland flow paths may be reduced through the use of grass or tree buffer strips. Although both these strategies may have a positive effect on peak flood rates they may also contribute to heavy debris load in the watercourse, particularly during storm events, which could result in increasing blockage risk at downstream culverts.

1.5. International Approaches to Flood Risk at Culverts

Flood risk associated with culverts is not just a problem within the UK and a number of other countries are adopting strategies to control culvert installation and reduce any associated risks relating to changed hydraulic conditions or potential blockage.

For example, within the United States of America (USA), the Federal Highways Administration (FHWA) has recently produced an updated version of their culvert design guide (Schall *et al*., 2012). This third edition brings together all information relating to culvert design into a single publication including consideration of animal and fish passage; details of culvert assessment, repair and rehabilitation, and information about available software packages. This national guideline is supported by a document detailing approaches to debris control at culverts and bridges (Bradley *et al*., 2005) and a number of state and region specific guides (e.g. AMEC, 2008; TxDOT, 2012).

A national guideline document, Australian Rainfall and Runoff (AR&R), is published by Engineers Australia (Pilgrim, 1987). As part of the Council of Australian Governments National Climate Change Adaptation Framework a number of projects have recently been undertaken to provide information to allow updating of AR&R, one of which, Project 11, considered blockage at hydraulic structures (Weeks *et al*., 2012).

Within New Zealand, requirements for culvert installation vary across the country and a number of regions have produced standards and guidelines relating to the installation of culverts and any associated debris control (e.g. Stevenson *et al*., 2008). In addition the Ministry for the Environment has developed some general guidelines (e.g. Ministry for the Environment, 2004).

1.6. Aims and Objectives of this Research

The work presented in this thesis focuses on one potential flood risk; that associated with flooding at culvert inlet screens when they become blocked by a build up of debris.

The research outlined in the following chapters set out to determine, using an experimental approach, if aspects of trash screen geometry and location had an influence on potential blockage by debris. The research aims to define blockage potential at a culvert inlet trash screen in relation to a number of screen configuration elements.

This aim was supported by four main objectives.

1. To develop a robust physical model that would allow investigation of individual trash screen configuration elements
2. To use the constructed model to undertake comprehensive testing to identify which structural elements had an influence on blockage potential
3. To use the gathered data to develop an empirical relationship that defines blockage potential in terms of the influencing components
4. To assess the impact of the findings on current screen design guidelines

1.7. Thesis Layout

This thesis documents the experimental analysis of the influence of trash screen configuration on blockage and details the development of an empirical relationship that defines blockage potential in relation to a range of screen configuration elements.

Chapter 1 has introduced the scope and background of the research area and summarised the main aims and objectives of this project.

Chapter 2 gives details of culvert and trash screen design options and provides an overview of the hydraulic conditions that need to be considered where culverts and trash screens are installed. It reviews existing design and implementation guidelines and standards for culverts and trash screens and considers what may be required to enhance these recommendations.

Chapter 3 covers sources of debris, methods of debris transport and accumulation and the impacts of debris blockage. It also considers existing methods of debris control at structures within watercourses. Finally, it reviews available research relating to the debris control performance of trash screens and identifies the need for further studies.

Chapter 4 briefly looks at the use of modelling in hydraulic research and details the approach selected. A description of the experimental set up is provided along with details of the testing methodology and a discussion of the limitations and potential errors.

Chapter 5 describes the extensive experimental programme undertaken to assess the influence of a number of aspects of screen geometry and position on debris blockage potential. The results obtained during testing are detailed, analysed and discussed.

Chapter 6 describes the development of a best fit empirical model defining blockage potential in relation to individual influencing elements. It then discusses the development of a simplified linear model that can be used to predict potential blockage for input parameters out-with the tested range. The use of the simplified model in two end user focused tools, a nomograph and an interactive spreadsheet, is then outlined.

Chapter 7 summarises the analysis undertaken during this research and highlights the main conclusions drawn from this project and their implications for future trash screen designs. Finally, recommendations for further work are proposed.

Chapter 2

Culvert and Trash Screen Design and Hydraulics

2.1. Introduction

This chapter introduces the use and structure of culverts and trash screens and provides the theoretical background and equations that define the hydraulic conditions relevant to culvert installations. A number of possible design options are reviewed. Key issues that must be taken into consideration when designing culvert and trash screen installations including current policies, guidelines and recommendations are discussed.

2.2. Culverted Waterways

Culverts are covered artificial channels or pipelines that carry a watercourse under an obstruction such as a road, railway or an area of developed land. They may also be used to manage flood flows adjacent to developments where the natural channel is considered inadequate. They are one of the most common forms of drainage structure and are widely used throughout the world. They vary considerably in size and design, from narrow pipes through to large square sided channels. There is no clear definition of what constitutes a culvert but the following characteristics are common to most (Balkham *et al*., 2010):

- The length in the direction of flow is significantly greater than the width of the culvert
- The base of the watercourse through the culvert is part of the structure of the culvert
- A culvert will generally be capable of flowing full under flood conditions
- A culvert is generally more prone to obstruction by debris than a bridge

Once a culvert is installed, if flood flows increase due to climate change or upstream land-use development, it is very difficult to change the capacity without significant re-engineering. The latest UK culvert design and operation guide published by the Construction Industry Research and Information Association (CIRIA) encourages designers to consider options other than culverts where a practical alternative exists (Balkham *et al*., 2010).

The installation of new culverts is discouraged for a number of reasons which include:

- Potential raised water levels upstream and a higher flood risk
- Potential negative impact on the river environment
- A greater risk of blockage than with an open channel which increases the flood risk
- Increased health and safety risks when compared with an open channel
- Increased complexity and costs for maintenance and repair

Alternatives to a installing a new culvert may include:

- Redesigning to avoid the need to cross a watercourse
- Using a different crossing approach such as a bridge or ford
- Diverting the watercourse

Where culverts are already in place, removal and channel restoration, often referred to as 'Daylighting', is an option. Daylighting offers an alternative to replacing existing culverts with larger capacity ones as well as potentially providing multiple benefits to society (e.g. provision of recreational areas and opportunity for community involvement), the economy (e.g. revenue generated from recreation, reduced maintenance requirements) and the environment (e.g. improved ecological habitat and improved air and water quality). Consideration of potential benefits of daylighted culverts for society is in keeping with the Ecosystems Services approach currently becoming established within the UK (Haines-Young & Potschin, 2008). This approach was defined by Smith and Maltby (2003) as "... a strategy for the integrated management of land, water and living resources that promotes conservation and sustainable use in an equitable way". Ecosystem services were defined by the Millennium Ecosystem Assessment (2005) as the benefits people gain from ecosystems.

Daylighting projects can vary from the simple task of removing the culvert roof and retaining the rest of the structure and the natural bed material, to major reconstruction work including soft-bioengineering measures and river restoration techniques (Wild *et al*., 2011). An example of a simple approach to daylighting is shown in Figure 2.1 where a daylighted street stream along a downtown residential street in Nebelbach, Zurich was completed in 1991. An example of daylighting undertaken as part of a more extensive flood alleviation project was undertaken in Lewisham, London in 2003/4 and combined flood risk management with a strategy for river restoration. In this project a new 'low-flow' meandering channel was cut through Sutcliffe Park in Lewisham, London, following the original alignment of the River Quaggy (Figure 2.2). The existing culvert was not removed and flow is now regulated between the open and culverted watercourses by a sluice allowing the culvert to operate as a flood control measure (River Restoration Centre, 2012).

Figure 2.1 A daylighted street stream along a downtown residential street in Nebelbach, Zurich

Figure 2.2 Sutcliffe Park after River Quarry restoration. A network of boardwalks, pathways and viewing points were designed to encourage access to the river and ponds (River Restoration Centre, 2012)

However, despite these recommendations, at times culverts provide the only practical solution. As a result there is a need to ensure their design, installation and maintenance has limited impact on the environment, optimises their operation, readily facilitates maintenance, and minimises any potential increase in flood risk. To achieve this there is a need to understand the impact of design and installation of both the culvert and any associated screens on local hydraulics including the potential causes and effects of blockage.

2.3. General Culvert Design

2.3.1. Overview

A considerable amount of information is available regarding the design of culvert structures (e.g. Dasika, 1995; Montes, 1997; Hager & Del Giudice, 1998; Johnson & Brown, 2000; Balkam *et al*., 2010). While these tend to focus on ensuring adequate capacity, appropriate flow control, and sufficient load bearing, a number of them also offer guidelines for other factors that may need to be reviewed before installing a culvert.

A number of different areas need to be considered when designing culverts:

- Engineering aspects including flood capacity; headwater (HW), tailwater (TW) and velocity limitations; storage requirements; buoyancy protection; structural load requirements
- Site criteria including location; upstream and downstream reach length and slope; requirements for debris and siltation control; culvert alignment
- Inlet structure
- Outlet structure
- Erosion and sedimentation control
- Safety requirements
- Environmental implications
- Operation and maintenance requirements

2.3.2. Engineering aspects

Design flow

Generally in urban areas, the recommended design flow for culvert installations is for flow with an estimated one percent chance of being exceeded in any one year (i.e. the 100-year flow). In Scotland the 0.5 per cent (i.e. 200-year flow) is recommended. In other areas such as agricultural areas a lower design standard such as a 10 percent (10-year flood may be acceptable (Balkham *et al*., 2010). An additional allowance is recommended to take account of the possible impacts of climate change which will vary depending on the individual structure, but a design flow that is 20 per cent higher than the basic calculated design flow is normally recommended (DEFRA, 2006).

As well as considering potential flow volumes, both minimum and maximum velocities should be considered when designing a culvert. There needs to be a balance between maintaining flow rates low enough to minimise scour and ensuring rates are high enough to prevent siltation. The maximum velocity should also be consistent with channel stability requirements at the culvert outlet. Working within these limits the resulting velocities must fall within ranges compatible with any requirements for fish passage at the site.

Water Levels

Culvert performance is likely to be affected by the downstream water surface elevation. Therefore, conditions which might promote high TW elevations during flood events need to be assessed during the design stage. Downstream obstructions, channel constrictions, tidal effects, junctions with other watercourses and the impacts of any natural flood management techniques applied in the catchment should be investigated to assess their potential impact.

Buoyancy

The buoyancy of the culvert barrel may be an issue particularly for flexible culverts. Uplift caused by water in or around a culvert may cause the outlet or inlet ends of the barrel to rise and bend. Under some circumstances, the uplift force may be great enough to dislodge the embankment. As a consequence, the use of headwalls, end walls, sloped paving, or other means of anchoring may need to be considered. Buoyancy is more likely to be a significant problem where the culvert slope is steep, the potential HW is deep (debris blockage may increase headwater), the upstream fill slope is flat, or where there are large culvert skews or the inlet has mitred ends.

Load

As well as potential buoyancy issues due to the water, water contributes to the overall load on the culvert. Loads affecting culvert design include the culvert weight, fluid loads, earth and pavement loads, and the weight and impact of surface vehicles or structures. A failure to assess potential loads during the design phase and design the culvert appropriately may result in the culvert structure collapsing under the load resulting in damage to the culvert itself and potentially also the surrounding area.

2.3.3. Site criteria

Location in channel

Not all locations along a watercourse are suitable for culvert placement. Selection of an appropriate location can reduce the impact of the river crossing on the environment, minimise the risk of damage to the crossing structure itself, and limit future maintenance costs (SEPA, 2008). It is recommended that culvert construction in locations where channel lateral migration likely to be rapid, such as at the apex of active meanders (Figure 2.3) should be avoided. In addition, areas of known sediment deposition (Figure 2.4) should be avoided as accumulation at the structure will reduce flow capacity (SEPA, 2010)

If the culvert becomes blocked the watercourse will find an alternative route so some consideration of the potential for flow along the surrounding area needs to be considered. Any alternative paths may be limited by factors including the height of upstream or downstream banks, access requirements and safety risks.

Figure 2.3 Areas of active lateral migration are not suitable areas for crossings (SEPA, 2010)

Figure 2.4 Actively eroding areas are not suitable areas for crossings (SEPA, 2010)

Local topography

Where possible the culvert length and slope should follow the contours of the existing topography, with the culvert invert aligned with the channel bottom and the skew angle of the stream and the culvert entrance matching the geometry of the embankment.

To minimise head losses and erosion the culvert barrel should follow the natural alignment and gradient of the watercourse. A straight culvert alignment is desirable to avoid blockage, and may also reduce construction costs, and maximise hydraulic efficiency. An example of the benefits of considering appropriate culvert alignment can be found in the successful installation of recent culverts by the Maryland State Highway Administration (Kosicki & Davis, 2001) who recently initiated new design procedures to limit the impact of constructing culverts in streams. Their new procedures included training of engineers in basic and advanced courses in stream morphology. However, straight culverts are not always an economical or practical option. Culverts may be required that bend either vertically or horizontally. Culverts that have one or more changes in slope within the barrel are commonly referred to as broken-back culverts (Figure 2.5).

(a) (b)

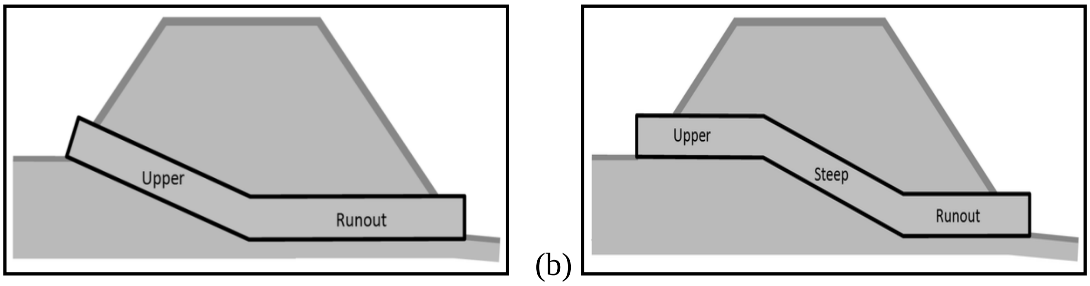

Figure 2.5 Broken back culverts (a) single break (b) double break (Aquaveo, 2012)

One section of a broken-back culvert is usually steep which can result in damaging high outlet velocities and the water velocity in the flatter run out section is usually supercritical. The velocity can be reduced by energy dissipation devices or ensuring a hydraulic jump forms within the barrel upstream from the culvert outlet although the precise locating of a hydraulic jump can be difficult to ensure (Hotchkiss *et al.*, 2003).

Horizontal bends may be used to avoid obstacles or realign the flow but, if a non-linear arrangement is required, particular attention should be given to maintenance access and erosion, sedimentation, and debris control. Examples of different alignment options for culverts are shown in Figures 2.6 and 2.7.

Figure 2.6 Changing the watercourse slope can increase the chance of blockage (adapted from FCSCP, 2002 p243)

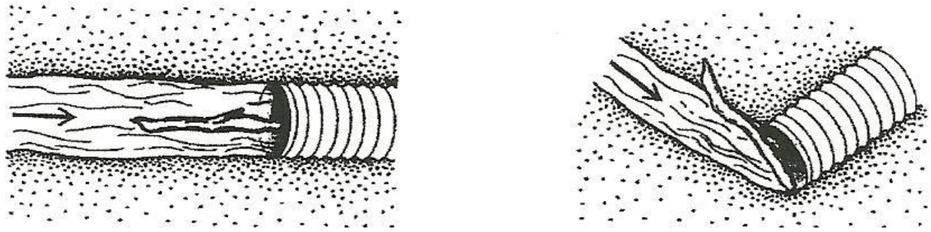

Figure 2.7 Aligning the culvert at an angle to the watercourse can increase the chance of blockage (adapted from FCSCP, 2002 p243)

Site development

When considering future needs any infrastructure developments must be considered especially in growing urban areas as developments such as road widening will have an impact. As well as restricting the length of new culverts, existing culverts should not be extended without a hydraulic assessment to investigate any potential change in capacity that may occur.

2.3.4. Inlet structure

Overview

The design of the inlet structure is a fundamental part of the culvert design as both hydraulic efficiency and cost can be significantly affected by inlet conditions. In addition, minor changes to the geometry of the inlet can have significant impacts upon the hydraulic efficiency of the culvert (Sterling Jones *et al*., 2006; Kells, 2008).

The culvert inlet forms the transition from the channel into the culvert barrel. Since the natural channel is usually wider than the culvert barrel, a flow contraction occurs at the inlet edge and this may be the primary flow control. The provision of a more gradual flow transition will lessen the energy loss and create a more hydraulically efficient inlet condition.

Many different inlet configurations can be used. These include both prefabricated and constructed-in-place installations. Commonly used inlet configurations include projecting culvert barrels (Figure 2.8), cast-in-place concrete headwalls, gabion or brick headwalls (Figure 2.9), pre-cast or prefabricated end sections (Figure 2.10), and culvert ends mitred to conform to the fill slope (Figure 2.10b).

Figure 2.8 Culvert inlet with projecting barrel

(a)  (b) 

Figure 2.9 Culvert inlet with (a) brick and (b) Gabion head walls

(a)  (b) 

Figure 2.10 Prefabricated culvert inlets (a) vertical head wall (b) mitred to match fill slope

Headwalls and wingwalls

Constriction of the natural channel at a culvert inlet forces the flow through a reduced opening. As a result of this contraction, vortices and areas of high velocity flow may scour away the embankment adjacent to the culvert. In some cases, a scour hole may also form upstream of the culvert floor due to acceleration of flow as it enters the culvert. The use of headwalls, wingwalls, and aprons will help to protect the slopes and channel bed at the culvert inlet.

Headwalls may be used for a variety of reasons:

- To increase the efficiency of the inlet
- To provide embankment stability
- To provide embankment protection against erosion
- To provide protection from buoyancy
- To shorten the length of the required structure

Wingwalls are generally used where the side slopes of the channel adjacent to the entrance are unstable, or where the culvert is skewed to the normal channel flow. Wingwalls can also be used to gain a hydraulic advantage for box culverts by maintaining the approach velocity and alignment, and improving the inlet edge configuration (e.g. Normann *et al*., 2001). However, their major advantage is in eliminating erosion around a headwall.

If high HW depths are likely, or the approach velocity in the channel is high enough to cause substantial scour, a short channel apron should be provided at the toe of the headwall.

Inlet performance

Side-tapered and slope-tapered inlets may reduce the flow contraction. In addition, depressed inlets, such as slope-tapered inlets, increase the effective head on the flow control section, thereby potentially further increasing culvert efficiency.

Inlet performance can also be improved through the use of bevelled edges at the entrance of the culvert (Figure 2.11). Bevelled edges reduce the contraction of the flow by effectively enlarging the face of the culvert.

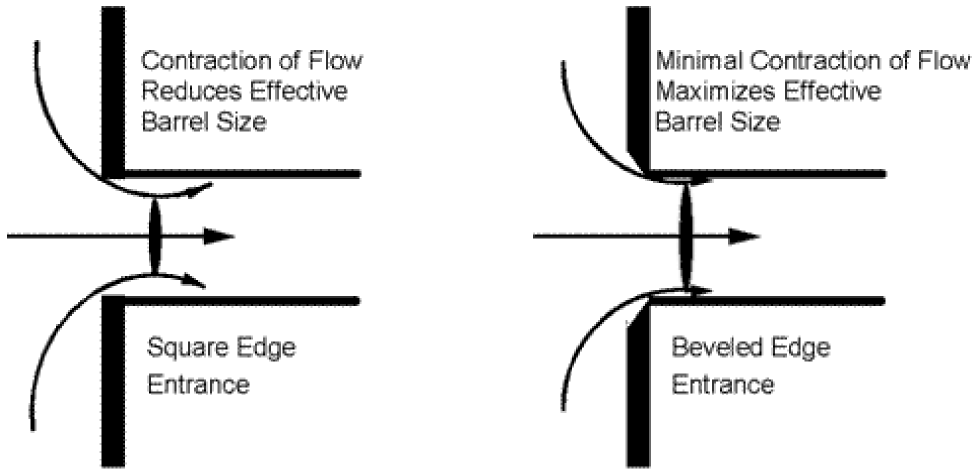

Figure 2.11 Entrance contraction (schematic) (Schall *et al*., 2008).

Debris control devices

Many culverts function adequately without the need for debris control. However debris control at the inlet should be considered for the following conditions:

- The watercourse is expected to transport a heavy volume of debris
- The culvert is located in a steep region
- The culverts is located under a high fill
- Access for clearance is limited

The EA (2009) discourage the use of screens for debris control unless the benefits are significant. They recommend that other options should always be considered and, under the Water Resources Act 1991 and the Land Drainage Act 1991, require that approval is sought and where necessary a formal consent given before a screen is installed in a watercourse. SEPA require that where "...screens are fitted on the inlet or outlet of the culvert, these must be designed so that there is at least 230mm of space between the bars of the screen or fence, up to the high water level" (SEPA, 2005).

Alternatives to the installation of a trash screen include looking at ways of reducing the debris load in the watercourse, for example by changes to land management practices and discouraging illegal dumping. Methods of debris control are discussed further in Chapter 3.

2.3.5. Culvert body

Barrel shape and size

The most commonly used culvert shapes include circular, box (rectangular), elliptical, pipe-arch, and arch (Table 2.1).

Table 2.1 Culvert barrel shapes (adapted from TSO, 2004)

Type	**Shape**	**Common Materials**
Pipe		Concrete Plastic Corrugated Steel
Box	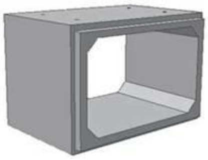	Pre-cast concrete In situ concrete
Pipe Arch		Corrugated steel
Multiple cell		Corrugated steel Pre-cast concrete
Complex, non standard		In situ concrete Pre-cast concrete with additions

The shape selection is normally based on the cost of construction, design limitations such as upstream water surface elevation or embankment height, cover above and below the barrel and the required hydraulic and structural performance. For example, multiple barrel constructions may be used where embankment or roadway levels are too low to allow a single barrel large enough to handle the expected flow. Multiple barrels may also be used to offer secondary flow paths under high flow conditions (Figure 2.12).

Figure 2.12 Double barrel culvert at Cameron Toll shopping centre in Edinburgh

The length of a culvert influences its capacity when operating under outlet control and it is therefore recommended that the length should be kept to the minimum required to meet current and expected future needs. In addition, safety and maintenance requirements may influence the selection. For example, within the UK current guidelines for the design of highway culverts (TSO, 2004) recommend that where a culvert is longer than 12m it should be a minimum of 1.2m in diameter to facilitate access for maintenance.

The culvert body can influence the potential for blockage by debris. The dominant factor in determining the degree of blockage is the size of the structure's clear opening. Rigby *et al*. (2002), after investigations of culvert blockage during large storms, concluded that culvert or bridge openings greater than about 6 m are likely to only partially block if they block at all; while culverts with openings of less than about 6m exhibit a full range of blockage from partial to complete.

Barrel material

The longevity of the culvert barrel is an important design consideration. At most locations, commonly used culvert materials are very durable. However, there are environmental conditions which will deteriorate all culvert materials. The two major problems affecting the longevity of culvert barrels are abrasion and corrosion (Figure 2.13).

(a)  (b) 

Figure 2.13 (a) Corroded metal culvert in Eastern Ontario (Moore, 2008) (b) Corroded culvert along I-70, Colorado (Molinas & Mommandi, 2009)

Abrasion is the result of erosion of culvert material due to the natural movement of sediment bedload in the watercourse. Both metal and concrete culverts may also be subject to corrosion. Metal culverts are affected by acidic and alkaline conditions that may occur in both the soil and water, and also by the soils electrical conductivity. Concrete culverts are sensitive to saltwater environments and may react to sulphates and carbonates within the soil. They may also be affected by sulphuric acid resulting from the combining of water and sulphur dioxide produced by anaerobic bacteria, particularly where the culvert soffit is buried beneath the stream bed. Selection of the most appropriate material for the surrounding environment can prolong the culverts functional life.

In addition to the requirement for corrosion and abrasion resistance, the selection of a culvert material may depend upon structural strength, hydraulic roughness and durability. The three most common culvert materials are concrete, non-reinforced corrugated aluminium, and corrugated steel. Culverts may also be lined with other materials to inhibit corrosion and abrasion, or to reduce hydraulic resistance. For example, corrugated metal culverts may be lined with asphaltic concrete.

2.3.6. Outlet structure

The culvert outlet forms the transition between the culvert barrel and the downstream channel. Culvert outlets are commonly subject to scour. Scour at a culvert outlet can be classified into two separate types: local scour and general stream degradation (Normann *et al*., 2001). Both types of scour can occur simultaneously at a culvert outlet. Local scour is typified by a scour hole produced at the culvert outlet (e.g. Figure 2.14). This is the result of high exit velocities, and the effects generally extend only a limited distance downstream. Material scoured from the hole is deposited immediately downstream, and may result in the formation of a low bar. The scour hole is generally deepest during periods of high flow.

(a)  (b) 

Figure 2.14 High-velocity discharge from undersized culverts causes downstream scour. (a) Culvert was placed at grade in 1979. (b) By 1998, undersized culvert had caused over 1 foot of downstream scour (FSSSWG, 2008).

General stream degradation is the result of natural causes producing a lowering of the stream bed over time and is independent of culvert efficiency. Protection against scour at culvert outlets varies from limited riprap placement to complex and expensive energy dissipation devices such as hydraulic jump basins, impact basins, drop structures, and stilling wells.

2.3.7. Erosion and sedimentation control

Culverts may create or exacerbate bank and bed erosion and/or promote sediment deposition. This is due to an alteration of the normal watercourse water velocities and disruption to the natural transport of sediment. If the armour layer on the river bed is damaged by bed scour at the culvert inlet or outlet, softer underlying sediment may erode, leading to major damage. This destroys the immediate habitat and also increases the amount of fine sediment transported downstream. This sediment can smother habitats important for fish spawning, aquatic invertebrates and aquatic plants. Sediment may also be deposited at bridges and culverts causing damage to the structure and increasing local flood risk. This leads to the need for regular dredging at the structure, which can have impacts on the ecology and water quality of the river.

The most common culverts to experience sedimentation problems within the culvert barrel are multi-barrel installations. In multi-barrel constructions commonly one or more of the barrels will have a tendency to accumulate sediment, especially during periods of low flow. However, self-cleaning can occur during periods of high discharge. To help prevent blockage from siltation, all but one of the multiple pipes may be placed higher than the others. This allows the lower pipe to maintain cleaning velocities, and the higher pipes help provide flow capacity for major storms.

Erosion provides an input of coarse sediment from the bed and banks. This may have an impact downstream raising the level of the bed therefore reducing the capacity of the channel. Localised erosion around the culvert itself can lead to the structure being damaged and its hydraulic capacity reduced.

2.3.8. Safety requirements

The primary safety considerations in the design and construction of a culvert are its structural and hydraulic adequacy. A well designed and maintained culvert should not present a significantly greater risk to health and safety than the open watercourse it replaces. Additional safety considerations include traffic safety and public safety.

The entrance to a culvert is generally thought to be a significant hazard. Most often the risk is thought to be to children who choose to enter the culvert (Figure 2.15) and risk injury or death by drowning.

Figure 2.15 Potential safety issues with children gaining access to culverts

There is also the risk that someone may fall into the watercourse in a flood, be swept into the culvert, and be drowned. However, within the UK the probability of death by drowning is small: based on drowning figures up to 2002 the Royal Society for the Prevention of Accidents (RoSPA) estimates the risk to be 0.76 per 100,000 of the population (RoSPA, 2002). As an example, 427 cases of accidental drowning were recorded within in the UK in 2002, 167 of these occurred in rivers or streams (RoSPA, 2002) and in 2003, 144 of the 381 reported deaths caused by drowning occurred in rivers and streams (EA, 2009). While there is no record of whether any of these cases involved drainage structures, as noted in Section 1.2, the Pitt review (Pitt, 2008) reports one death directly resulting from entrapment in a flooded drain and a death was recorded in 2011 as being the direct result of a member of the public attempting to clear a blocked culvert during a flood (Freuchie Flood Action Group, 2011).

As well as the risk of death or injury as a result of a person entering a culvert, either voluntarily or as a result of being swept in during a flood, other hazards are associated with culverts including flooding resulting from blockage of the culvert by debris and damage to the interior of a culvert or the services it contains. Additional hazards may be present where debris screens have been installed. These include flooding resulting from debris accumulation on the screen, injury to persons maintaining and cleaning the screens, environmental degradation, structural failure, and restricted emergency access.

A number of mitigation measures may be considered to reduce these hazards. Where entry into the culvert is considered unsafe then the use of signs, fencing, shrub planting and/or screens at the inlet and/or outlet need to be considered. Although they may be required for safety, screens promote debris build-up and the subsequent reduction of hydraulic performance and so should only be used where fencing or alternative methods of preventing access are not appropriate. While the design of security screens are similar to the debris screens discussed in Section 2.4, the main design focus is on screen bar spacing to ensure access is restricted. Maintenance of safety screens once they are installed is essential if they are to continue to prevent access as damaged or badly fitting screens may not prevent access (Figure 2.16).

Figure 2.16 Poorly maintained security screens do not always prevent access to culverts (Martinson, 2010)

Safety screens can also be a danger under flood conditions if there is a risk of someone falling into a watercourse and being swept into the structure and pinned against it by rising flood waters. Only limited literature is available detailing the most appropriate design for safety screens. Engel and Lau (1981), cited in Weisman (1989), state the requirement to ensure that while the screen must fully meet its purpose of preventing access, it also needs to be oriented and positioned to allow someone to climb out of the water if they get swept onto it. They suggest that to accomplish this, the grating must begin upstream of the region of rapid acceleration of flow into the culvert and recommend a parabolic curved screen. While these recommendations were based on research looking at only a limited number of specific sites, a further study looking at the use of a parabolic safety screen in Albuquerque, New Mexico (Allred-Coonrod, 1994) also found that a parabolic screen was an appropriate shape and in addition suggested the screen should be designed to ensure a hydraulic jump occurred at the screen to aid in sliding a body upwards to safety.

The fundamental key to safety is the correct design and installation of the culvert and a number of different factors should be considered at the design stage including culvert length and orientation, location and accessibility, slope, flow conditions and any flash flood risks, barrel size, invert materials and the potential for noxious gases in confined spaces.

2.3.9. Environmental implications

Overview

Culverting may result in significant effects on environmental features and wildlife habitats. The linear nature of a watercourse may be altered stopping species from spreading naturally (CIWEM, 2010). In addition the presence of a culvert may result in a modified substrate, altered flow, and reduced algal and plant growth as well as isolating the culverted portion of the stream from the surrounding environment (Macdonald & Davies, 2007).

Pollution

SEPA (2005) notes that culverted urban watercourses are often highly polluted due to problems with incorrectly connected foul sewers, overflow from blocked sewers, or runoff from contaminated surfaces or areas of contaminated surface water. In addition, culverted sections can create serious access difficulties which limit effective pollution control.

Impact on fish migration

At some culvert locations, the need to accommodate migrating fish is a fundamental design consideration. The installation may affect fish passage due to a number of reasons including:

- Reduced light in long culverts
- Increased flow velocity through a culvert
- Vertical jumps and drops
- Too shallow flows
- Absence of resting places

A complete barrier can lead to loss of migratory fish upstream which may ultimately lead to a decline in populations throughout the river system. In a recent study, Nislow *et al.* (2011) note that that "Stream sections located above predicated impassable culverts had fewer than half the number of species and less than half the total fish abundance, while stream sections above and below passable culverts had essentially equivalent richness and abundance". For example, in 1996 the River Tweed Foundation identified 1000 culverts in the River Tweed catchment which were impassable to fish on watercourses otherwise capable of supporting salmonid species (SEPA, 2005). Another example is the vertical discontinuity caused by the installation of a culvert in the Boise National Forest which prevents migration of Kokanee salmon (FSSSWG, 2008) (Figure 2.17).

Figure 2.17 Culvert in the Boise National Forest prevents migration of Kokanee Salmon (FSSSWG, 2008)

A number of measures can be taken to minimize the impact on fish passage. Ensuring the culvert base is below the natural bed level will allow a natural bed to be maintained during low flows. Maintaining the natural bed level will also help retain the natural slope. Where possible the culvert should also maintain the natural channel width, to minimise the risk of erosion. The culvert installation should ensure natural low flow depths are preserved and the water velocities and depths in the culvert under different flow conditions need to be adequate for fish passage. The use of multiple small barrel culverts should be restricted as fish can be discouraged from entering small size diameter openings. For longer culverts or culverts where depth/velocity is an issue baffles can provide the necessary resting places required for fish passage (Figure 2.18).

Figure 2.18 Culvert next to Redford Road, Edinburgh showing environmental features

Specific requirements will vary depending on the species of fish. The Scottish Executive (2000), in a consultation paper, provides design guidelines for facilitating fish passage in river crossings but a major problem is the limited knowledge of the capabilities of many species of fish and other organisms that migrate through the river network. Species, and different life stages within species, can move at different times of the year and during different flow conditions. The variability means that designing culverts to meet specific depth, velocity, and turbulence requirements for multiple species during all flow conditions is not a practical option.

The additional impact caused by adding a debris screen at the inlet is uncertain. According to the EA (2009) the installation of a trash screen is only likely to impact on the migration of mature salmon species, other fish species are unlikely to be affected by bars with a minimum clear spacing of 140mm. However SEPA (2008) recommend a minimum spacing of 230mm between bars where fish passage is an issue.

Impact on mammal habitats

A number of priority species identified by the UK Biodiversity Action Plan (UKBAP), such as otters and voles, depend on good quality river corridor habitats (HMSO, 1994). As well as impacting on fish lifecycles, culverts that do not maintain the riparian corridor can create barriers for mammals, restricting access to feeding grounds and limiting the opportunity to establish new populations. For example according to SEPA (2008) road accidents are one of the major causes of otter death in Scotland. A significant contributing factor is thought to be that where no facilities for mammal passage have been provided the high water velocities in culverts during spate conditions mean they cannot swim through road crossing structures and so they use the road – greatly increasing their chance of being killed. Current UK guidelines require mammal runs to be incorporated into culverts where the watercourse forms the natural passage across a road (TSO, 2004). Figure 2.18 shows an example of a recent culvert installation that includes a mammal run. Where mammal passage is facilitated, drainage culverts can be beneficial by mitigating any potentially harmful effects of busy transport corridors by providing a vital habitat linkage (Yanes *et al*., 1995; Clevenger *et al*., 2001; Dodd Jr. *et al*., 2004; Rees *et al*., 2009). In a study of the use of culverted road crossings in Maryland, USA, 57 different species of animal were found to make use of the culvert as a crossing in 265 culverts studied (Pelsinsky, 2012) (Figure 2.19).

Figure 2.19 Mammals using culverts in Maryland, USA (Pelsinsky, 2012)

Impact on access, recreation, amenity provision and environmental aesthetics

Culverting generally leads to the loss of green amenity space along river banks and can reduce access for recreational opportunities such as fishing, walking or water sports.

If there is no alternative to a culvert, the design of the structure should include consideration of aesthetic values and fit as naturally as possible into the existing environment. Debris screens when installed often have a stark visual appearance and may be considered out of place with the character of the local environment in certain settings. However, this does not always need to the case as designs can be made to either blend with the environment or to become a feature of it. For example, course debris catchers and a trash screen for smaller debris were installed as part of a £12 million Cockshaw Burn Flood Relief scheme (Homes and Communities Agency, 2012). Rather than install standard control devices the EA worked alongside a local community partnership in Hexham to establish a public environmental artworks programme alongside the working flood defences. The project resulted in a well used walk, the 'Hexham Flood Trail', that is a significant community resource. A course debris trap has been created using stout oak pillars (Figure 2.20); while immediately downstream a trash screen is intended to catch smaller size debris (Figure 2.21).

The accumulation of trash on screens tends to make it even less attractive, but this can be reduced by regular cleaning. The waste collected from the screens can present a further problem as it may need to be stored temporarily on site before being removed for disposal. If temporary storage is required consideration should be given to the visual and environmental impact of the storage area and any potential safety issues associated with storing the debris at the culvert site and its periodic collection and transportation.

Figure 2.20 A course debris trap has been created as part of the Hexham flood defences using stout oak pillars carved by artist Steve Hyslop (Image Copyright Oliver Dixon)

Figure 2.21 A trash screen created as part of the Hexham flood defences by artist-blacksmith Matthew Fedden (Image Copyright Oliver Dixon)

2.4. Water Flow in a Culverted Channel

2.4.1. Overview of channel flow

Flow along a watercourse may be described as open channel or pipe flow. Open channel flow occurs where there is a free surface at atmospheric pressure; pipe flow is the result of flow under pressure through a closed conduit. A number of different classifications have been made to distinguish flow types (e.g. Novak *et al*., 2001; Chadwick *et al*., 2004; Mott, 2006). All these characterizations of flow depend on two main parameters: time and distance. Flows are either steady (parameters not varying with time) or unsteady, and uniform (parameters not varying with distance) or non-uniform.

The most commonly adopted classification follows that detailed by Chadwick *et al*. (2004) who suggest four flow types:

- Steady uniform flow where discharge and depth are constant
- Steady non-uniform flow where discharge is constant but the depth varies
- Unsteady uniform flow where the discharge varies but the depth is constant
- Unsteady non-uniform flow where both discharge and depth vary

Open channel flow may be laminar or turbulent depending on the value of the Reynolds number (Re) which is defined in Equation 1 where V is the mean flow velocity (m/s), R is the hydraulic radius (m) and υ is the coefficient of kinematic viscosity(m^2/s).

$$Re = \frac{VR}{\upsilon} \tag{1}$$

Flow in an open channel is generally classed as laminar where Re is less than 500 and fully turbulent where Re is greater than 2000 although the limits are not as clear as those observed in pipe flow and values of greater than 1000 are often also considered to indicate turbulent flow. Flow in rivers and canals will be turbulent with unsteady flow in rivers and predominantly steady in canals (Novak *et al*., 2001).

Three phases of flow can be identified: subcritical, critical and supercritical. Subcritical flow occurs when the flow velocity is less than ‘critical’ and depth is deeper than critical depth. It generally occurs where the channel is shallow. Supercritical flow is characterised by high flow velocity and depths less than the critical depth. It occurs where the bed slope is steep or where there is a rapid change from potential energy to kinetic energy. Subcritical flow can only move to supercritical flow through a smooth transition passing through the critical depth while supercritical flow can only return to subcritical flow through a hydraulic jump. The phases of flow can be identified using the associated Froude number (Fr) which can be defined for rectangular channels by the average flow velocity (V, m/s), and average cross sectional depth (d, m)(Equation 2). Flow is supercritical where Fr > 1, critical where Fr = 1 and subcritical where Fr < 1.

$$\mathrm{Fr} = \frac{\mathrm{V}}{\sqrt{\mathrm{gd}}} \tag{2}$$

For a rectangular channel the critical depth (d_c, m) can be defined in terms of discharge (Q, m^3/s) and free surface width (B, m) (Equation 3).

$$\mathrm{d_c} = \sqrt[3]{\frac{\mathrm{Q}^2}{\mathrm{gB}^2}} \tag{3}$$

The specific energy of the flow (E) can be expressed in terms of the depth (d, m) and velocity (V, m/s) (Equation 4). In rivers and canals the flow is generally subcritical.

$$\mathrm{E} = \mathrm{d} + \frac{V^2}{2\mathrm{g}} \tag{4}$$

2.4.2. Flow within a culvert

A number of different factors may affect the flow of water through a culvert:

- The size of the culvert
- Entrance geometry
- Length
- Roughness
- Slope
- TW. The TW depth usually depends on the size, shape, slope and resistance to flow or roughness of the stream

Novak *et al*. (2001) suggest two main groups to describe the flow (Table 2.2): entrance submerged and free flow at entrance. Each of these groups is then split further depending on a number of factors including exit condition, culvert length, flow within culvert barrel, and slope. Balkham *et al.* (2010) split the flow initially into two groups: inlet control and outlet control. They then further divide the flow into free flow, full flow and overtopping flow.

Table 2.2 Types of flow in culvert barrel (adapted from Novak *et al*., 2001 p401)

H/D	**Entrance Conditions**	**Exit Conditions**	**Flow**	**Length**	**Slope**	**Control**	**Remarks**
> 1	Submerged	Submerged	Full	Any	Any	Outlet	Pipe Flow
> 1.2	Submerged	Free	Full	Long	Any	Outlet	Pipe Flow
> 1.2	Submerged	Free	Part Full	Short	Any	Outlet	Orifice
> 1.2	Free	Free and > Critical	Part Full	Any	Mild	Outlet	Subcritical
> 1.2	Free	Free and < Critical	Part Full	Any	Mild	Outlet	Subcritical
> 1.2	Free	Free and < Critical	Part Full	Any	Steep	Inlet	Supercritical
> 1.2	Free	Free and > Critical	Part Full	Any	Steep	Inlet	Hydraulic Jump in barrel

2.5. Culvert Flow Control

2.5.1. Overview

A control point occurs where there is a defined relationship between the flow rate at any point and the upstream water surface elevation. At any given time the flow within the culvert will be determined by the inlet geometry (inlet control) or by a combination of the inlet and barrel geometry and the TW depth (outlet control). Any one culvert may switch between inlet and outlet control as a result of changes to discharge, capacity and downstream conditions. This may cause relatively sudden rises in HW.

2.5.2. Inlet control

For inlet control, the control point is at the entrance to the culvert (Figure 2.22). The entrance characteristics of the culvert are such that entrance headlosses are predominant in determining the HW of the culvert. Water is carried through the culvert barrel more efficiently than the water enters the culvert. The culvert performance is influenced by both the headwater and the inlet configuration. The flow passes through critical depth near the inlet and becomes supercritical in the culvert barrel. Depending on the TW, a hydraulic jump may occur downstream of the inlet. The type of flow under inlet control depends on the degree of submergence of the inlet and outlet ends of the culvert. Figure 2.23 shows examples of flow under inlet control. Inlet control is a feature of steep culverts.

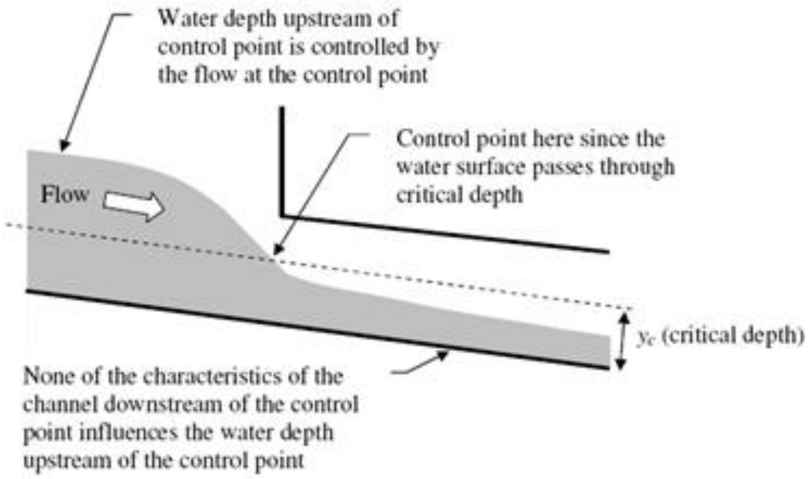

Figure 2.22 Inlet control (EA, 2010, Chapter 7)

2.5.3. Outlet control

Factors influencing the performance of a culvert under inlet control also influence culverts in outlet control. In addition, barrel characteristics (roughness, area, shape, length, and slope) and TW elevation affect culvert performance in outlet control. The headlosses due to TW and barrel friction are predominant in controlling the HW of the culvert. The entrance allows water to enter the culvert faster than the backwater effects of the TW and barrel friction will allow it to flow through the culvert. Figure 2.24 shows examples of flow under outlet control.

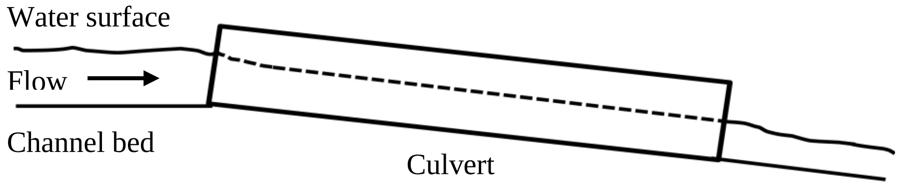

a) Neither end of the culvert is submerged. The flow passes through critical depth just downstream of the culvert entrance and the flow in the barrel is supercritical. The barrel flows partly full over its length, and the flow approaches normal depth at the outlet end.

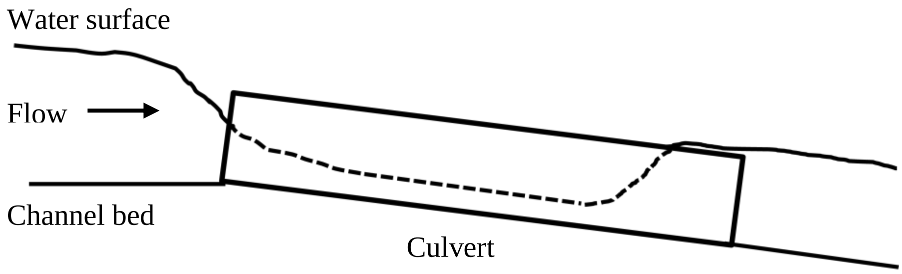

b) Flow just downstream of the inlet is supercritical and a hydraulic jump forms in the culvert barrel.

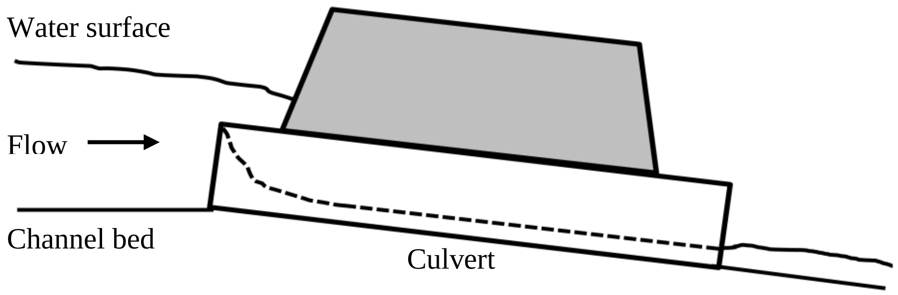

c) The inlet is submerged with free flow at the outlet. Flow is supercritical and the barrel flows partly full over its length. Critical depth is located just downstream of the culvert entrance and the flow is approaching normal depth at the downstream end of the culvert.

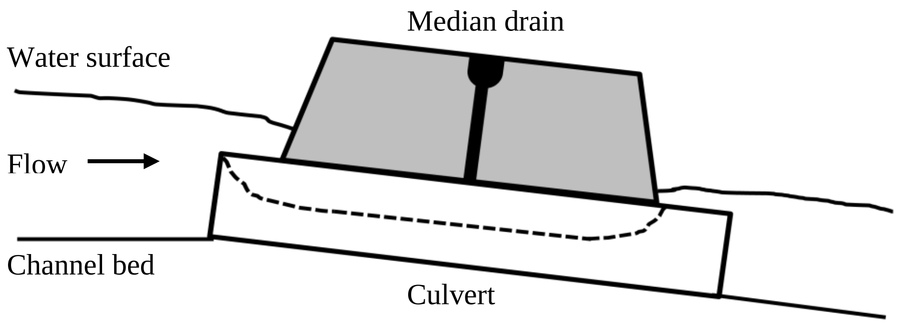

d) Submergence of both inlet and outlet with the formation of a hydraulic jump in the barrel. The drain ventilates the barrel preventing development of sub-atmospheric pressures which might create unstable conditions resulting in alternation between full and partly full flow.

Figure 2.23 Examples of inlet control (based on ISU, 2009)

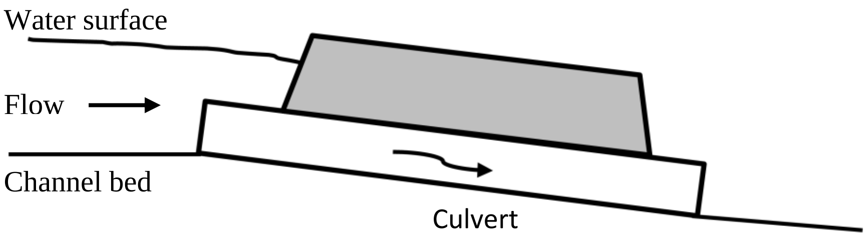

a) Full flow in the culvert barrel.

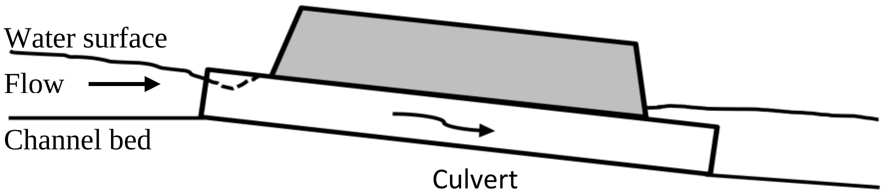

b) Outlet submerged with the inlet unsubmerged. For this case, the headwater is shallow enough to expose the inlet crown as the flow contracts to the culvert.

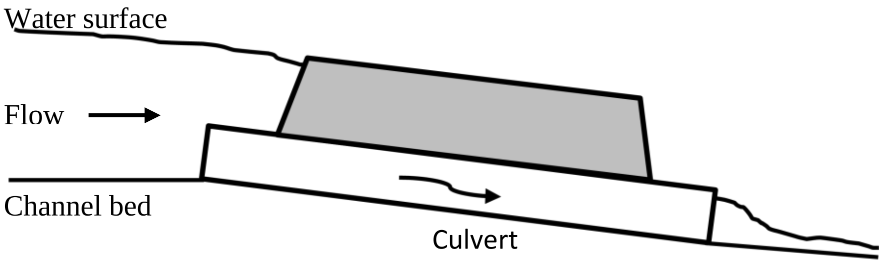

c) The entrance is submerged such that the culvert flows full for its entire length while the outlet is unsumberged. This is rare requiring an extremely high headwater to maintain full barrel flow with no tailwater. The outlet velocities are usually high under this condition.

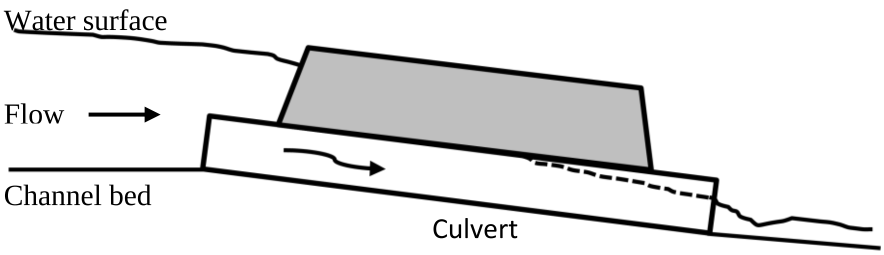

d) The culvert entrance is submerged and the outlet end flows freely with low tailwater. Under these conditions, the barrel flows partly full over at least part of its length (subcritical flow) and the flow passes through critical depth just upstream from the outlet.

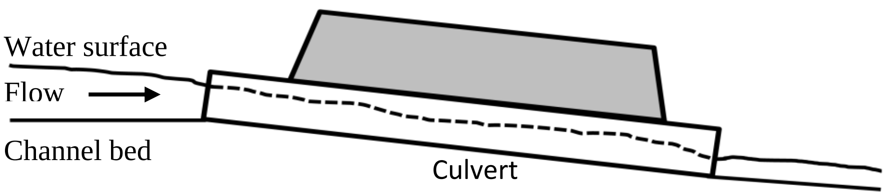

e) Neither the inlet nor the outlet end of the culvert is submerged. The barrel flows partly full over its entire length, and the flow profile is subcritical.

Figure 2.24 Examples of outlet control (based on ISU, 2009)

2.6. Hydraulic Performance of a Culvert

Although the physical structure of a culvert is generally simple, they are hydraulically complex. The behaviour of flow in the section of the channel upstream of the culvert can significantly affect the performance of the culvert as well as have an impact on levels of erosion and sediment transportation (Day, 1997). The hydraulic performance of a culvert depends upon a combination of entrance, exit and friction losses, length of barrel, and the downstream backwater effect. If the culvert contains bends and joins then additional losses will occur at these points. Some additional losses will also be a factor where debris or security screens are fitted. The proportion of the total head loss through the culvert caused by the screen is small for a clean screen. Normann *et al.* (2001) state that the head losses due to a bar grate can be estimated using Equation 5 where H_g (m) is the head losses due to the bar grate, V_g (m/s) is the velocity between the bars, V_u(m/s) is the approach velocity and g is acceleration due to gravity.

$$H_g = 1.5\left(\frac{V_g^2 - V_u^2}{2g}\right) \tag{5}$$

They also note that an alternative estimation method for vertical screen bars as shown in Equation 6 is noted by Metcalf & Eddy (1972) and Mays *et al.* (1983).

$$H_g = K_g \left(\frac{W}{X}\right)\left(\frac{v_g^2}{2g}\right)\sin\theta_g \tag{6}$$

For Equation 6, K_g is a dimensionless bar shape factor, W is the maximum cross-sectional width of the bars facing the flow (m), X is the minimum clear spacing between bars(m) and θ_g (degrees) is the angle of the screen with respect to the horizontal. Equations 5 and 6 were derived empirically and only considered clean screens. Additional losses will occur if the screens are blocked with debris.

Hydraulic performance is also influenced by whether the inlet and/or outlet are submerged. If the inlet is not fully submerged then the controlling relationship is the energy balance between the upstream (1) and critical (2) sections which are almost adjacent to one another, as is shown in Figure 2.25 and described in Equation 7 where HW_i (m) is headwater depth above the inlet control section invert, D (m) is the interior height of culvert barrel, H_c (m) is specific head at critical depth, Q is discharge (m^3/s), A

(m^2) is full cross-sectional area of the culvert barrel, S is the culvert barrel slope and K and M are regression constants. K_u is a conversion factor for units (1.811 for SI) (Sterling Jones *et al*., 2006).

$$\frac{HW_i}{D} = \frac{H_c}{D} + K\left[\frac{K_u Q}{AD^{0.5}}\right]^M + 0.7S \tag{7}$$

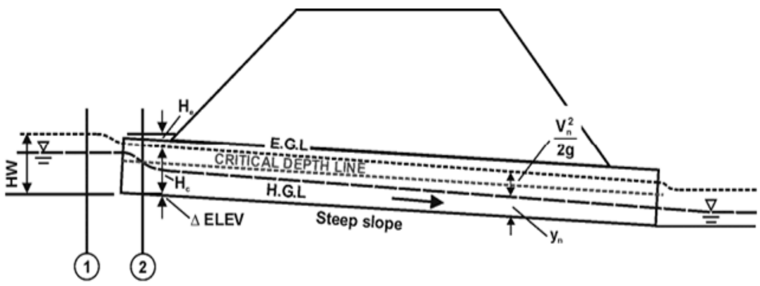

Figure 2.25 Typical inlet flow control conditions (Sterling Jones *et al*., 2006)

Where the outlet is submerged the controlling relationship is between the upstream section and downstream section (Figure 2.26) and the energy balance contains all the frictional losses and elevation changes between the upstream and TW channels. Under these conditions the head relates to the total energy as shown in Equation 8, where HW_o is headwater depth above the outlet invert, TW is tailwater depth above the outlet invert, V_u is approach velocity, V_d is downstream velocity and HL is total energy loss. The total energy losses include the entrance, friction, and exit losses.

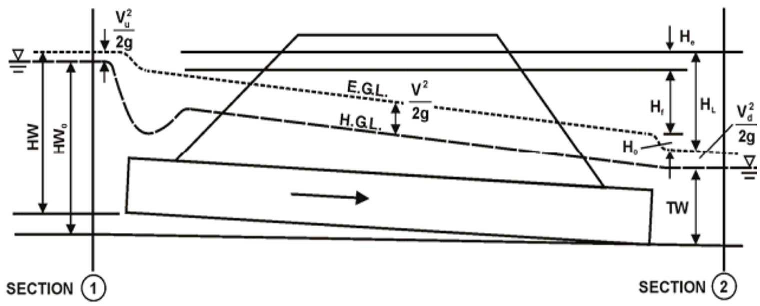

Figure 2.26 Outlet control under full flow (Sterling Jones *et al*., 2006)

$$HW_0 + \frac{V_u^2}{2g} = TW + \frac{V_d^2}{2g} + H_L \tag{8}$$

2.7. General Trash Screen Design

2.7.1. Screen layout

The layout of a trash (or debris) screen will depend on the required screen area and local site conditions but it also needs to have minimum impact on the culvert's hydraulic operation.

The main components of a trash screen are shown in Figure 2.27. Not all components are required for every trash screen. The functions of each component are described in Table 2.3. The type of screen required will depend on the nature of the debris, the required function and the site location and conditions.

Table 2.3 Main components of a screen (EA 2009, p39)

Component	**Description**
Sloping screen	This provides the main screen area.
Horizontal screen	This provides the main screen area.
Coarse screen	This can collect initial larger debris to reduce both the impact on and potential damage to the main trash screen. Where present, the coarse screen is often located some distance upstream of the main screen, and there may be two or more coarse screens at intervals.
Working platform	This provides access to the screen for clearance of the trash. Even where is constructed from open tread panels, the area of the working platform should not be included as part of the effective screen area.
Access gates and removable panels	These provide access to the required sections of the screen to aid trash removal.
Access hatch	This is provided in the working platform to enable access to the culvert for periodic inspection.
Fencing/handrailing	This increases security and reduces the hazard associated with a potential fall into the channel.
Access ladder	This is provided to enable access to the main trash screen and the culvert in order to: • clear trash from the screen in routine/non-routine events • inspect the culvert • respond to emergency or safety-related issues.

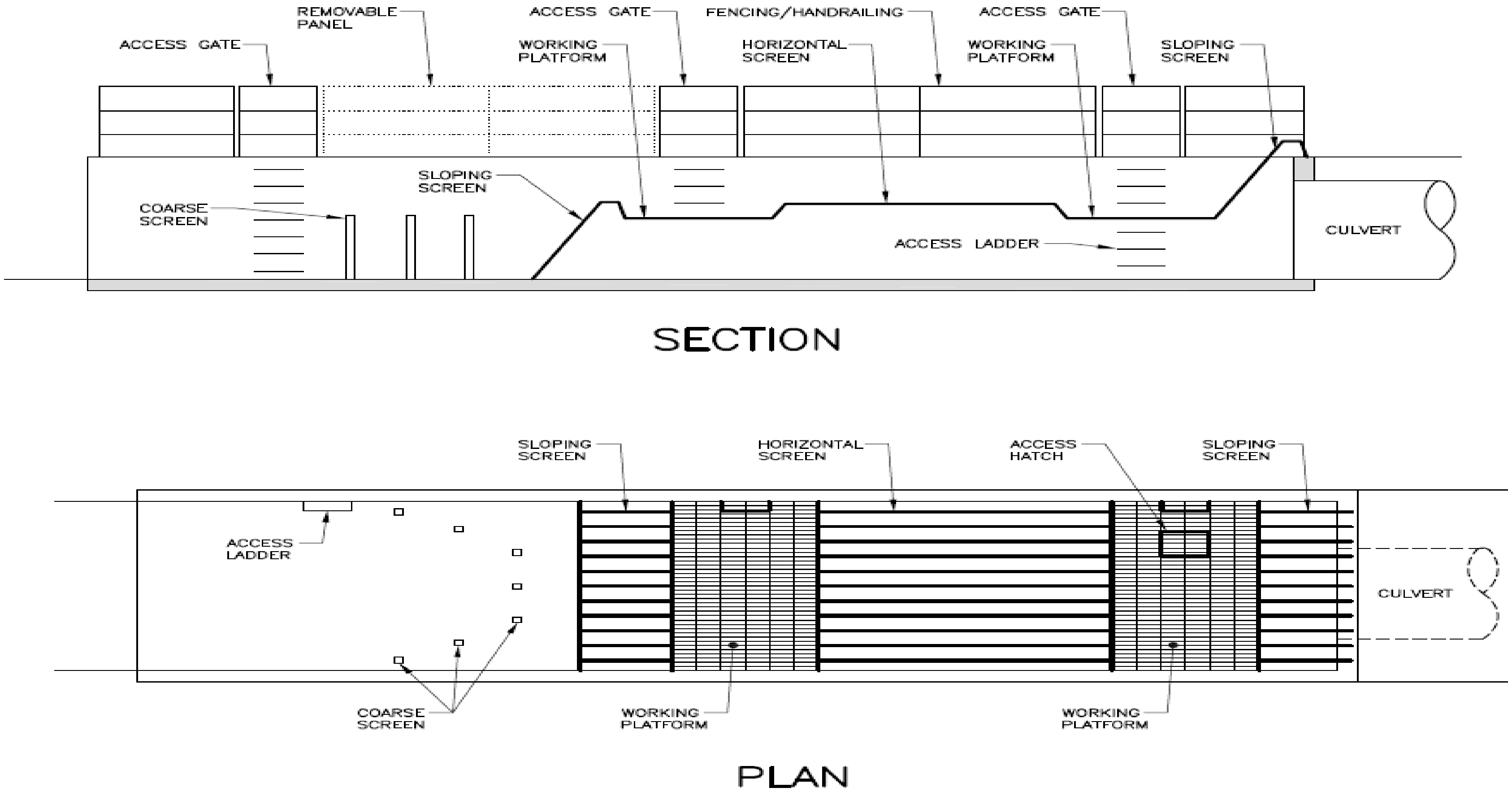

Figure 2.27 Cross section and Plan drawings of the components of a trash screen (EA, 2009 p38)

2.7.2. Screen area

Once site requirements have been taken into consideration the main current focus of screen design is on ensuring sufficient screen area is provided to handle the expected debris load. According to the EA, the majority of failures of new screens have been due to underestimating the size of screen required. The recommended method for calculating the required screen area is outlined in the current Trash and Security Screen Guide produced by the EA (2009). It suggests that screen area should be between three and 30 times the minimum culvert area and should be calculated based on estimated maximum debris amount (Da). This is the anticipated maximum amount of annual debris (m^3) arriving at the screen in non-routine events. For sites where no actual data is available or the available data covers less than two years, standard estimates can be used based on the catchment type (Figure 2.28).

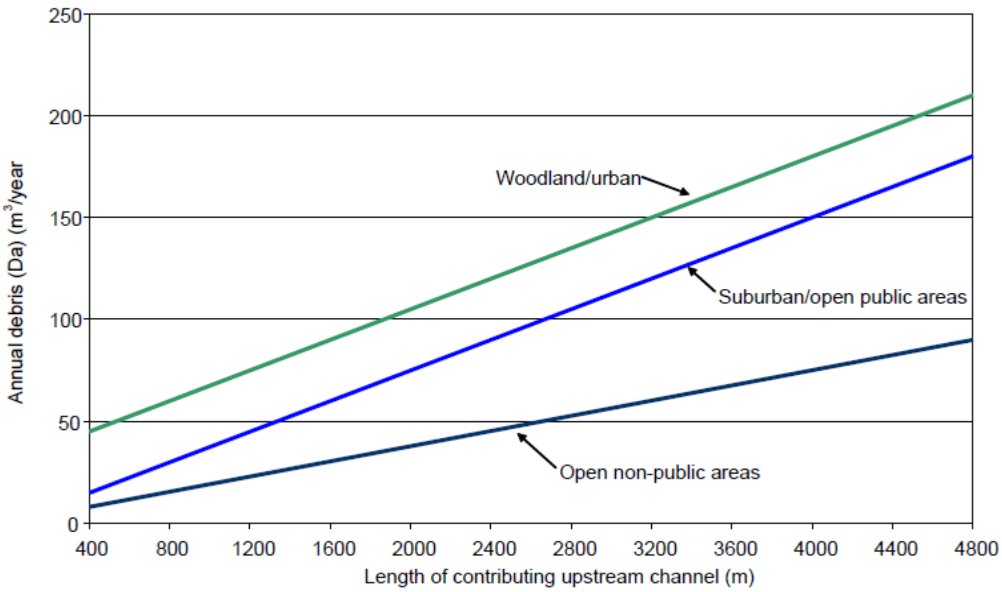

Figure 2.28 Amount of debris expected from different catchment types (EA, 2009)

The design debris amount (dDa) can be calculated from these standard estimates by measuring the contributing length of the watercourse that falls into each of the catchment types and summing the individual values to give an overall Da. This value then needs to be adjusted based on the average gradient of the main contributing upstream length according to the rules described in Table 2.4. This gradient is known as the S1085 slope.

Table 2.4 Gradient adjustments for dDa calculations (EA 2009, p43)

Average Gradient	**Design Debris Amount (dDa)**
Greater than 1 in 250	1.00 Da
1 in 250 to 1 in 500	0.75 Da
1 in 500 to 1 in 1000	0.50 Da
Less than 1 in 1000	0.25 Da

Along with the dDa, a blinded depth factor (Bdf) needs to be determined (Table 2.5). This is based on the predominant catchment type and reflects the degree of screen blockage by the potential debris type. Where there is a mix of catchment types, then Bdf is calculated as an average value taking into consideration the contributing length of each type.

Table 2.5 Blinded Depth Factor (EA 2009, p43)

Predominant Catchment Type	**Blinded Depth Factor (Bdf)**
Woodland	0.63
Urban	0.23
Suburban	0.20
Open public areas	0.37
Open non-public areas (including farmland)	0.32

The required screen size is then calculated using the determined dDa and Bdf values and the likely number of significant events during a year (Equation 9). A significant event is classed as an event that has sufficient force to lift debris off the bed and banks. The method states that unless strong site evidence indicates otherwise the number of events should be taken as three (EA 2009), however, no specific justification is given within the guidelines for this recommendation.

$$\text{Screen Area (m}^2) = \frac{\text{dDa}}{\text{No.of signifcant events} \times \text{Bdf}} \tag{9}$$

The recommended minimum and maximum areas relative to the culvert opening are based on analysis of the performance of trash screens over 15 years and therefore are likely to be a reasonable representation of required values. However, the evidence based method used to determine required screen area in the current guidelines is based on a maximum annual debris load from non-routine events while routine operation, cleaning and maintenance of screens focuses on normal daily/weekly debris loads. Therefore the designed area may not be appropriate for the purpose. In addition, the standard values for dDa (Figure 2.28) were determined using only a limited number of culverts from a single catchment: 17 sites from the Ravensbourne catchment, London (Magenis, 1988) and therefore may not be representative of debris loads from catchments with different contributing areas, rainfall/runoff patterns and demographics.

Once the required area has been determined, achieving that area can be difficult especially in urban areas where space may be limited. In the latest trash screen design guidelines (EA, 2009) two approaches are suggested:

- A long screen located diagonally across the watercourse
- A long screen running parallel to the watercourse where the flow is transferred sideways into a parallel channel

There are a number of problems with these approaches as diagonal screens will reduce the cross-section of the channel and any required change in flow direction will result in additional head losses and increase the potential that debris will get trapped. An alternative approach is to have a series of screens with courser screens upstream.

2.7.3. Screen angle

Current guidelines recommend that screens should be placed at a preferred angle of 45 degrees and a maximum of 60 degrees to the horizontal. 45 degrees potentially offers a higher screen area than a screen at 60 degrees in the same location. The use of a screen with an angle of less than 45 degrees would offer a means to further increase the area of the screen while keeping the top of the screen in the same position. However the current guidelines suggest that these lower angles do not keep the working platform high enough above high flows to ensure safety. Angles steeper than 60 degrees have a high manual handling risk (EA, 2009).

2.7.4. Bars and bar spacing

According to the EA (2009, p14) "The screen should trap as little debris as possible commensurate with the aim of preventing material that could cause a blockage from progressing downstream". To achieve this, the spacing between the bars of a screen should allow as much debris to pass cleanly through the culvert as possible while still achieving the objective of either preventing culvert blockage or unauthorised access. In addition the spacing must not conflict with any requirements for the passage of fish or wildlife. The recommendations for bar spacing for trash screens vary depending on the function of the structure the screen is associated with and the expected debris. For example, an intake at a power station requires a much finer screen (often referred to as a weed screen) to prevent material being drawn into the pumps than would be required at a large culvert which may be designed to allow passage of small debris. Bar spacings of 150mm up to 300mm are suggested but the final design needs to be site specific. Where a screen is required for security purposes it is recommended that the space between the bars should not exceed 140mm. This maximum spacing should include any gaps between the screen and the inlet structure and the bed of the watercourse.

Bar design is a compromise between strength and hydraulic impact. Narrow bars have less of an impact on stream hydraulic performance but must still be robust enough to cope with debris impact and any potential vandalism. In addition the bars must allow for safe and effective raking therefore if cross bars are required to add strength they must be recessed far enough to avoid the rake. Often bars are hooked at the top to allow easier collection of debris on the working platform when raking. Current UK recommended bar dimensions are not less than 8 × 75 mm for flat bars. Thicker (10 or 12 mm) bars may be advisable where extra strength is required. While Clark *et al*. (2010) suggest that rounding the upstream edges of the bars will slightly improve the hydraulic performance and may reduce the propensity for the screen to trap small debris the limited benefit is unlikely to be a justifiable additional cost. The use of circular bars will improve hydraulic performance but there may be a corresponding reduction in rigidity when compared to rectangular cross section bars of the same diameter. The maximum unsupported length of a bar should not exceed 1.5 m. Where any bar lengths exceed 1.5m, bracing should be used. Current guidelines suggest that galvanized mild steel is generally considered to be the best material for bar construction (EA, 2009), however a number of installation companies are now recommending using high-density polyethylene (HDPE) or extra high molecular weight polyethylene (EHMWPE) as an alternative to steel (e.g. Hydrothane Systems, 2011; Structure Guard, 2011). The use of HDPE or EHMWPE reduces the screens' weight and may reduce maintenance requirements by offering greater abrasion resistance and reducing the potential for corrosion. The use of HDPE screens also limits bio-fouling and frazil ice build up which can result in blockage. As screens using these materials are relatively new their durability and resistance to vandalism is as yet unclear. In addition no available research was found documenting comparative performance of screens constructed from different materials under particular environmental conditions such as extreme high or low temperatures, wild fires, high debris loads or flood flows.

2.8. Trash Screen Hydraulics

Laws & Livesey (1978) suggest that there are three main factors that should be considered when assessing the hydraulic impact of a screen:

- The properties of the flow through a screen
- The effect of a screen on time-averaged velocity distributions
- The effect of a screen on turbulence distributions

Meusburger *et al*. (2001) note that data from many field measurements show that flow conditions near trash screens are fully three-dimensional, turbulent and locally transient. A number of experimental studies have been undertaken looking at the hydraulic impact of trash screens; the main focus of which has been to establish head loss across the screens for performance efficiency improvements at power station inlets. The results of the studies have been used to develop correlations for calculating head loss. While the Kirschmer equation (Equation 10) is one of the most widely used (e.g. Osborn, 1968), Tsikata *et al*. (2009) note that other equations are also in use including: the energy equation (Equation 11), an equation generated by Davis (1952) (Equation 12) and an equation used by the U.S. Bureau of Reclamation to determine head loss regardless of bar shape or screen angle (Wahl, 1992) (Equation13). For Equations 10 to 13, Δh = head loss (m), h_1 = upstream flow depth (m), h_2= downstream flow depth (m), h_v =

velocity head of flow approaching rack (m), U_1= average upstream velocity (m/s), U_2 = average downstream velocity (m/s), U = average velocity through net flow area (m/s), V_g is the velocity between the bars (m/s), V_u is the approach velocity (m/s) R = net flow area/gross area (m^2), β = bar shape factor, W = maximum width of bar upstream of flow (m), b = minimum clear spacing between bars (m), θ = angle of inclination of rack with horizontal, g = gravitational acceleration (m/s^2), α = kinetic energy coefficient.

$$\Delta h = \beta \left(\frac{W}{b}\right)^{\frac{4}{3}} h_v \sin\theta \tag{10}$$

$$\Delta h = 1.5\left(\frac{V_g{}^2 - V_u{}^2}{2g}\right) \tag{11}$$

$$\Delta h = h_1 - h_2 + \frac{\left(\alpha_1 U_1{}^2 - \alpha_2 U_2{}^2\right)}{2g} \tag{12}$$

$$\Delta h = \left(1.45 - 0.45R - R^2\right)\left(\frac{U^2}{2g}\right) \tag{13}$$

These relationships were all based on average flow velocities and flow depths in open channels, very few studies have undertaken a detailed analysis of flow through trash screens.

Yeh (1989) notes a number of early investigations of flow through screens (Taylor, 1944; Taylor & Davies, 1944; Taylor & Batchelor, 1949; Andrew, 1951; Baines & Peterson, 1951; Elder, 1959). For example, Yeh reports that in a study looking at screens perpendicular to the direction of stream flow, the most common orientation for trash screens, Baines & Peterson (1951) investigated pressure differences across the screen, velocity distributions, and turbulence. In addition to the study by Yeh investigating free-surface flow through a screen, a number of other studies have also been undertaken some examples of which include: an experimental investigation of various types and angles of screens by Stefan & Fu (1978), an assessment of the performance of screens in terms of debris capture and fish passage (Padilla & Clark, 2008) and an experimental study of turbulent flow near trash racks (Tsikata *et al.*, 2009).

Stefan & Fu (1978) found that the value of the head loss coefficient increases slightly as the Reynolds number increases. Yeh (1989) reports that transverse support bars of the screens appear to significantly disturb the flow and notes that as the screen slope relative to the bed is decreased, more transverse support bars are submerged, causing additional head loss. The study by Padilla & Clark (2008) shows that screens at all angles had little effect on velocities in front of and in back of the screen although under higher velocity scenarios changes in the average velocity profile across the screen were discernable. At debris rack installation angles of 30, 45, and 60 degrees, the flow velocity was found to decrease at the top and increase at the bottom of the flume as the flow travelled from upstream of the screen to downstream of the screen. Tsikata *et al*. (2009) used a physical model to investigate turbulent flow. They found that the head loss coefficient increased as the area of bars relative to the open area increased but decreased as the cross sectional depth of the bar was reduced. While these studies all considered free surface flow, a study by Clark *et al*. (2010) looked at head loss across a submerged trash rack. They found that head loss across a trash rack increased with increasing approach velocity, approach flow angle and bar area relative to clear area. In addition they reported that head loss was reduced where bars did not have a rectangular cross section. Streamlining both upstream and downstream edges of the bars was found to reduce energy loss more than streamlining just one edge. However, they concluded that any head loss associated with water surface disturbances near a trash rack were negligible in open channel flow.

These investigations considered trash screens constructed from straight bars, placed either vertically or inclined. While this configuration is used for almost all trash screens, some safety screens have adopted a parabolic shape as this is considered to increase the likelihood that a person will be swept up the screen to safety if swept into the watercourse. Allred-Coonrod (1994) used a physical model to assess the performance of a parabolic screen under supercritical conditions and concluded that pining forces against the screen would be negligible and by designing to ensure a hydraulic jump was induced on the screen a body would be pushed up to safety. This study also looked at the effects of the screen becoming blocked by using plastic sheet to block off 50% to 70% of the screen. Blocking the screen did not prevent model bodies from swept up the screen. One other study of the impact of blockage of the screen was reported by Xiang *et al*. (2009). In the presence of debris they found that while velocity profiles upstream from the screen were not significantly affected, downstream profiles showed higher velocities at the bottom of the flume than at the top. This was due to floating debris blocking the screen at the top of the flume.

While all these studies report useful findings in terms of trash screen hydraulics the investigations were based on screens in an open channel and therefore do not include any assessment of environments where there is a change in hydraulic conditions created by flow constriction at a culvert.

2.9. Screen Cleaning and Debris Removal

Debris accumulating at screens will need to be removed. The design of the screen must allow safe raking for debris removal under routine and non-routine conditions. Where there is a possibility of damage to surrounding areas from flooding resulting from blockage of the screen, access must be available for alternative clearing methods such as vehicle-mounted grabs if manual clearing when submerged is not possible. Three methods of screen cleaning are commonly used:

- Manually using suitably hooked rakes (Figure 2.29)
- Mechanically by specific grab systems or mobile plant (Figure 2.30)
- Mechanically by automated screen-clearing mechanisms. If an automated method is used its performance should be remotely monitored

Figure 2.29 Timber and debris being manually cleared from screen on River Gaunless (Photographs from Environment Agency, Yorkshire & North East)

Figure 2.30 Examples of mechanical screen cleaners (Photographs from C W Engineering, http://www.cw-engineering.co.uk/screen_cleaners.html)

To ensure raking can be undertaken safely the recommended maximum length for any single section of screen is 2m. If more area is required than can be provided by this length of screen, multiple stages should be used with working platforms between each stage. The design of the screen is required to enable manual handling of debris between each working platform. To do this a maximum vertical distance of 1.2m between each platform is recommended (EA, 2009).

2.10. Culvert and Trash Screen Operation and Maintenance.

There are over 300,000 culverts in the UK that require maintenance to minimise any associated flood risk (Wallerstein, 2010). Maintenance will be required under both routine and non-routine operating conditions and therefore safe access must be available at all times. In addition to regular routine visits as part of standard maintenance programs, culverts and trash screens may need to be cleared at other times due to unexpected blockages caused by dumping or high debris loads in the watercourse. To identify these situations remote water-level monitoring can be used, linked by telemetry to an operational centre. Installation of CCTV at the site may also be beneficial although will increase the operational costs. For example, the Scottish Borders Council installed four trash screen monitors at key sites to monitor the upstream water levels and to provide alarms when the level reached a set threshold that would have created a flood risk potential. The alarms are transmitted along with collected data back to the Councils Border Care Office where appropriate directed action can be taken (Hydro-logic, 2007). Edinburgh City Council also uses this approach to monitor water levels at culverts across the city. Water levels are monitored and once a predefined level is reached maintenance staff are automatically notified of the problem which may allow a rapid response to clear blockages thereby reducing the risk of flooding. For example, a camera and water level monitor are located on a culvert with a trash screen located near Ellen’s Glen Loan in Edinburgh (Figure 2.31).

The water level is recorded every three hours when operating normally. If the water level reaches the preset alarm level a message is automatically sent to the council and levels are monitored every 15 minutes until the level returns to below the alarm level. An example output from the water level monitor with levels triggering alarms is shown in Figure 2.32. In addition photographs taken of the culvert inlet (Figure 2.33) can be used to support maintenance decisions.

Figure 2.31 Culvert at Ellen's Glen Loan, Edinburgh

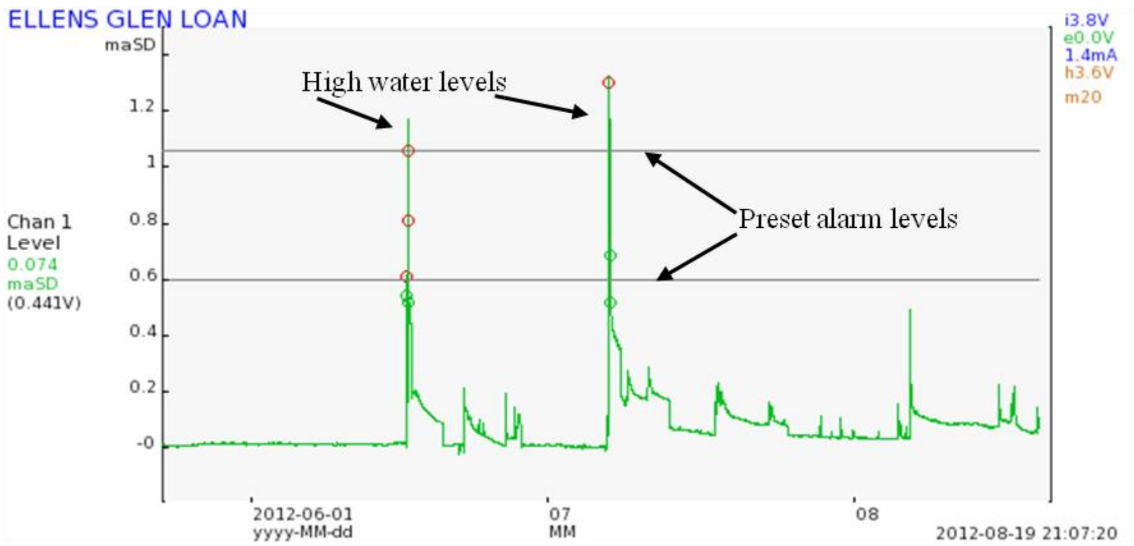

Figure 2.32 Sample output from Edinburgh City Councils Isodaq Timeview Telemetry system – monitoring Ellens Glen Loan

(a) (b) (c) (d)
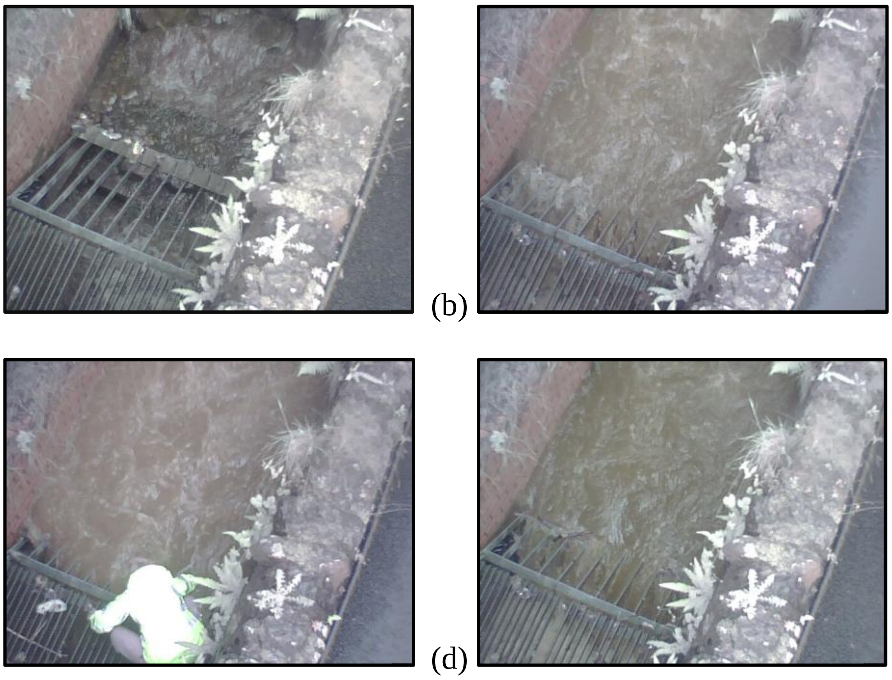

Figure 2.33 Sample photographs from Edinburgh City Councils Isodaq Timeview Telemetry system: (a) Base water flow (b) High water levels trigger an alarm (c) Maintenance crew response to alarm ensures any trapped debris is cleared. (d) Monitoring can continue until water levels return to normal.

While the majority of debris screens are secured in a fixed position, an option may be to secure the screen in such a way that it can be raised or lowered as the needs demands. This allows the trash screen to be temporarily removed from the watercourse to prevent blockage when required. This can be done by using a lifting mechanism which may be triggered automatically when the water levels reach a preset height or remotely by an operative after an alarm or weather warning. Alternatively the screens may be raised manually on site (Figure 2.34).

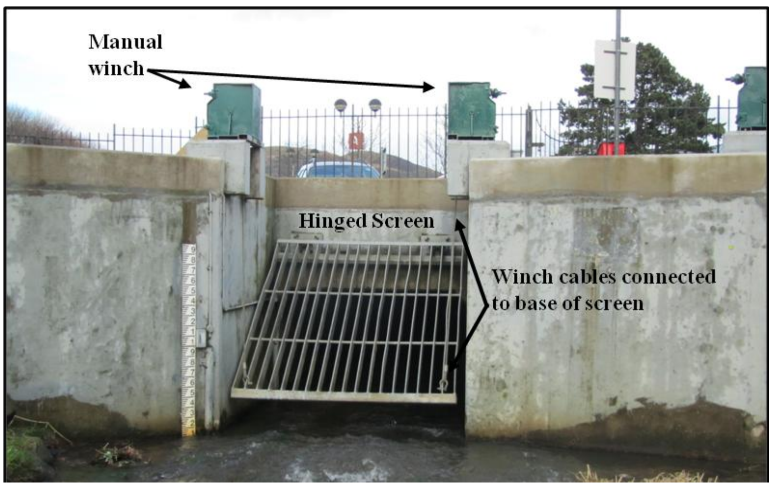

Figure 2.34 Manually raised trash screen

2.11. Chapter Summary

This chapter has introduced the use and structure of culverts and trash screens and provided the theoretical background and equations that define the hydraulic conditions relevant to culvert installations.

Culverts carry watercourses under an obstruction and may also be used to manage flood flows. While the installation of new culverts is now discouraged and controlled, a considerable number of existing culverts are still in use. Projects designed to reduce the impact of culverts through methods such as 'daylighting' are becoming increasingly common.

Despite a number of concerns regarding the impact of culverts, under some circumstances they offer the only practical solution to watercourse routing therefore there is a need to ensure their design, installation and maintenance have minimal impact on the environment and flood risk.

A number of factors must be considered when designing culverts including a number of engineering aspects; site considerations; inlet and outlet structure; erosion, sedimentation and debris control; safety requirements and potential environmental impacts.

The hydraulic performance of a culvert depends on a combination of entrance, exit and friction losses; length of barrel; downstream backwater effects and the presence or absence of a debris screen. It is also influenced by whether the inlet or outlet is submerged and the type of flow occurring in the culvert barrel.

Culverts can operate under either inlet or outlet control. Under inlet control the capacity of the entrance is the limiting factor while for outlet control water can enter the culvert faster than it can flow through the barrel.

Where trash screens are installed, their layout will depend on the required area and local site conditions. Current guidelines, produced by the EA, provide a method for determining the required screen area and suggest screens of between three and 30 times the culvert entrance area. The area calculation is based on an estimation of the maximum amount of debris predicted to arrive at the screen in a non routine event. The guidelines also recommend a screen angle of between 45 and 60 degrees. No specific recommendations are given for bar spacing unless there are particular safety concerns regarding unauthorised access in which case a bar spacing of no greater than 140mm is recommended.

Maintenance is required to ensure safe and secure operation of the culvert and screen and to clear any debris trapped by the screens. Debris can be cleared by both manual and mechanical raking. There are over 300 000 culverts within the UK that require maintenance which must be possible under both routine and non routine operating conditions. In addition to regular maintenance visits, the risk of potential flooding due to raised water levels can be monitored through the use of automated water level monitors, telemetry and CCTV.

Chapter 3
Debris and Debris Control

3.1. Introduction

Chapter 2 provided an overview of how blockages of watercourses, bridges and culverts by debris have had a significant impact on recent flooding events and are commonly recognised as a major contributing factor to flooding. Notably, analysis of a consultation regarding the 2007 floods in the UK, the Pitt Review (Pitt, 2008), reports that many of the responses to the consultation blame the extent of the flooding on the build up of debris. Blockage of a culvert inlet by debris may have an impact on hydraulic conditions, the culvert structure, the local geomorphology, and the surrounding environment as well as potentially having social and economic impacts.

This chapter describes the sources of debris commonly found in watercourses and outlines the processes involved in debris transport within a watercourse and the mechanisms involved in debris deposition and accumulation at river structures. It then summarises current approaches to debris control within a watercourse, reviews the available research relating to the debris control performance of trash screens and discuses the need for further research in this area.

3.1.1. Hydraulic impact

When a culvert becomes blocked the main impact is an increased water level upstream due to the culverts reduced capacity. This is illustrated in Figure 3.1 which shows the channel approach to a small culvert located in a residential area of Edinburgh. Figure 3.1a shows the screen free of debris while Figure 3.1b shows the screen after it has become blocked by a significant quantity of debris which has impeded flow through the screen and caused an increase in upstream flow depth.

The reduced capacity and increased upstream water level will also result in a higher discharge velocity at the outlet.

The limited research currently available regarding the effects of debris on the hydraulic performance of culvert trash screens is discussed in Section 3.7.

(a)

(b)

Figure 3.1 (a) Approach flow to a screen clear of debris, (b) increase in flow depth upstream of the same screen caused by significant blockage

The increase in water depth is highlighted by the depth of water above the ledge that is exposed when the screen is clear.

3.1.2. Structural impact

The culvert inlet structure may be damaged by initial debris impacts, by debris drag forces or by increased loads as a result of debris jams. The debris may also result in scour (e.g. Melville & Dongol, 1992; Pagliara & Carnacina, 2010), and abrasion of the structure which could lead to corrosion damage. Damaged inlets have reduced hydraulic capacities which may lead to greater risk of flooding.

3.1.3. Geomorphology

As well as temporary flow changes due to flooding, a prolonged build up of debris that is not cleared may result in a permanent change to the flow path of the watercourse as it cuts a new channel in an attempt to overcome the blockage.

3.1.4. Socio-economic impact

As discussed in Section 1.2, flooding related to blockage at culverts can have significant social and economic consequences. Flooding resulting from blockage at culverts, particularly culverts associated with a road, can have significant impact on the transportation of goods and services. This can be a major problem if it restricts the movement of emergency services. For example, the draft Environmental Assessment for the City of Peabody, Massachusetts, Goldthwaite Brook Flood Mitigation Project (FEMA, 2009) notes that floods in the main city square, resulting from overflowing culverts, isolated the main fire and police station, resulting in delayed response.

As well as social effects, flooding has a significant economic impact. A flood study undertaken by Forbes Rigby Pty Ltd for the Wollongong City Council notes that in Thirroul, a storm in August 1998 caused $75 million of property damage of which a significant proportion could be attributed to culvert blockage (Weeks *et al*., 2009). In addition increased routine and emergency maintenance requirements from high debris loads may have an economic impact.

3.1.5. Environmental impact

The accumulation of debris can have an adverse impact on the aesthetics of an area and increase public concern about flood risk. The build up of debris can also affect fish and mammal migration paths (see Section 2.3.9). In addition a persistent blockage can result in the formation of a stagnant water pool which may have potential health risks.

3.2. Sources of Debris

3.2.1. Overview

A watercourse normally carries floating as well as submerged debris. The volumes of debris can increase substantially during flood flow conditions and can cause blockage problems at hydraulic structures such as culverts. An accumulation of debris at a culvert changes the flow patterns and may create adverse flow conditions including substantially raised water levels resulting in flooding. The selection of an appropriate control measure will depend on the type and volume of debris arriving at the structure. To help in establishing appropriate controls it is useful to classify the different types of debris. Within the UK the EA has split debris into five main types as outlined in Table 3.1.

Table 3.1 Debris Classification used by the EA. (EA, 2009)

Debris Type	**Examples of debris**
Small vegetation	Leaves, twigs, garden waste, small branches and plants
Large vegetation	Trees, large branches, shrubs, mats of weeds
Domestic refuse	Packaging, small containers (cans, bottles, cartons), plastic bags
Large household refuse	Furniture, mattresses, carpets
Large non-domestic refuse	Cars, shopping trolleys, ladders, pallets, straw bales

The FHWA in the USA, who have responsibility for the maintenance of many hydraulic structures, has a slightly different classification system splitting debris into eight main groupings (Table 3.2). A classification system similar to the FHWA system, but with different grouping names, is currently used within Australia; in addition it also includes a distinct grouping for urban debris (Weeks *et al*., 2012). Although these three classification systems differ they all have a common purpose which is to aid the better management and control of debris within a watercourse.

Table 3.2 Debris Classification used by the FHWA. (Bradley *et al*., 2005)

Debris Type	**Examples of debris**
Small floating debris	Small limbs or sticks, orchard prunings, leaves, and refuse
Medium floating debris	Tree limbs or large sticks
Large floating debris	Logs or trees
Fine detritus	Silt, sand, and fine gravel more or less devoid of floating debris
Coarse detritus	Coarse gravel or rock ranging in size from 16 to 256 mm
Boulders	Material comprised of large rock ranging in size from 256 to 2048 mm
Flowing debris	A heterogeneous fluid mass of clay, silt, sand, gravel, rock, refuse, trees, and/or branches. - a combination of the different types of debris mentioned above
Ice debris	An accumulation or transport of ice floes in the waterway

3.2.2. Natural debris

Natural debris includes all types of organic material found in a water course. While organic debris in the watercourse is generally the result of natural processes, the growth in interest in both ecological sustainability and natural flood management processes over the past few years has resulted in the deliberate introduction of woody debris to streams and rivers to improve habitat provision or reduce river flow rates (see for example Antón *et al*., 2007; Mott, 2010; Thomas & Nisbett, 2012; Manning *et al*., 2013). In addition organic material may be deliberately introduced to the river banks and immediate area around the watercourse to help create and manage deadwood habitats which are considered as key to improving the condition of native woodland as part of the UKBAP (e.g. Humphrey & Bailey, 2012).

Inputs of wood into rivers varies widely depending on factors such as location in the watershed (e.g. Bilby & Ward, 1989), land use and disturbance history (e.g. Gregory &

Davis, 1992). Debris may enter the watercourse in small regular quantities and also on occasions in large volumes. Fetherston *et al*. (1995) refer to this as chronic or episodic: chronic inputs are frequent but small in volume and are the result of tree mortality and incremental bank erosion; episodic inputs result in large volumes of debris and are the result of irregular events such as storms, fires and landslides.

The volume of woody debris is dependent on the full riparian zone environment as it may have originated from within the watercourse or its immediate surroundings, or may have been transported there from a more distant location. Swanson *et al*. (1975) state that the main sources of woody debris entering a watercourse from the surroundings are blown down trees, tree tops and branches resulting from storm damage, and debris slides from steep banks. These processes are likely to be particularly effective on trees or branches already dead or weakened by fire or disease. Both healthy and weakened trees may also enter the watercourse indirectly through bank erosion, debris slides and mudflows. This view is supported by Hogan (1987) who suggests that large pieces of woody debris that originate from within the riparian zone may be the result of trees being uprooted either directly by drag forces or indirectly through erosion. Diehl and Bryan (1993) also suggest that bank instability is a major contributing factor to the potential volume of debris that can enter a watercourse.

A study by Magenis (1988) reported that the volume of debris arriving at a culvert could be estimated based on the length of open channel upstream of the screen and the landuse of the contributing reach. This research also included an assessment of the volume of debris from anthropogenic sources and forms the basis of the estimation of anticipated maximum amount of annual debris used in the recommended calculation for screen area in the current design guidelines (see Section 2.5.2). A number of more recent studies have also assessed potential natural debris loads in watercourses. For example, in a review of watersheds in Japan, Seo and Nakamura (2009) reported that the volume of large woody debris (LWD) entering the watercourse depended on the scale of the contributing watershed. Export per unit area was relatively high in small watersheds, peaked in intermediate watersheds, and decreased in large watersheds. However this study was restricted to a limited range of environments so may not be indicative of volumes under other conditions.

Average debris length, diameter and volume per piece of debris is generally dependant on stream width and increases with stream size with most mobile pieces shorter than watercourse width (e.g. Beschta & Robison, 1990; Nakamura & Swanson, 1994).

3.2.3. Anthropogenic debris

As well as natural debris, items from a variety of other sources can find their way into the watercourse. The main sources of anthropogenic debris are:

- fly-tipping sites
- industrial and/or commercial areas
- farms
- residential properties

The volume and makeup of the anthropogenically sourced debris will depend on the size and type of the catchment area feeding into the watercourse. Increasing catchment area increases both the quantity of available material and runoff. The type of contributing catchment is also significant as, within the UK, the degree of fly-tipping directly into or near streams is strongly correlated with the level of urban and suburban poverty (Webb *et al*., 2006; EA, 2009; Wallerstein & Arthur, 2012). Within more deprived areas householders are less likely to have access to transport to dispose of rubbish at civic amenity sites and also often have less storage available for their waste due to the higher density of the population so they have a greater need to dispose of it more regularly (Webb *et al*., 2006). Fly tipping can be a significant problem; in both environmental and economic terms. The annual cost to Scottish local authorities for clearing up instances of illegally dumped waste exceeds £2.5 million each year (SEPA, 2012b).

Small items of debris that routinely find their way into the watercourse such as packaging materials, plastic bags and toys can contribute to blockage if they result in an accumulation of debris in a culvert or at a screen. Larger items, for example shopping trolleys, packing crates or items of furniture such as a mattress (see Figure 1.7) may be enough to cause a blockage on their own. In addition, extreme flood events may result in very large items being swept into a watercourse and blocking a structure. For example, Figure 3.2a shows cars that have become trapped at a culvert inlet after a major storm event. Cars were also a problem during the major floods in Boscastle in 2004. A number of cars were swept into the river along with other debris and caused significant blockages (Figure 3.2b). A recent study has been undertaken to assess the impact of vehicles blocking bridges after being swept into a river (Teo *et al*., 2011). Obstructions caused by vehicle blockages at bridges were found to increase water surface elevations for a considerable distance upstream of the blockage, and there was a significant impact on flow propagation and hydrodynamic processes along adjacent floodplains.

(a)

(b)

Figure 3.2 (a) Cars blocking a culvert after a storm on 8th June 2008, Newcastle, New South Wales, Australia (Weeks *et al*., 2012) (b) Cars and woody debris at site of the old bridge, Boscastle during 2004 flood. (Photograph © David Flower)

3.3. Factors Influencing Debris Transport

Debris availability is influenced both by the degree of flood inundation of urban areas and the frequency of flooding. Where there are long gaps between flood events more debris will have accumulated in the surrounding area therefore there is the potential for higher debris loads being swept into the river during a single event than may occur if flooding is more frequent.

During a flood, debris is swept into the watercourse from the surrounding banks and redistributed throughout the river network. This process depends on the flood volume, discharge, channel characteristics, the size and geometry of the pieces of debris relative to the channel width, orientation of the debris relative to the channel alignment, weight and buoyancy of the debris, and the hydraulic characteristics and geometry of the banks and channels (Braudrick *et al*., 1997; Braudrick & Grant, 2001; Haga *et al*., 2002; Bradley *et al*., 2005; Bocchiola *et al*., 2006a, 2006b). Once in the watercourse debris may move by rolling, sliding or floating.

While it is recognised that both organic and non-organic debris contribute to blockages within rivers, the main research focus has been on woody debris. Braudrick *et al.*, (1997) in a study of woody debris transport, identified three general modes of transport which depend on the input rate of logs:

- Uncongested: debris moving without piece-to-piece interaction. Movement tends to be linear with respect to time
- Congested: logs move together as a single mass. Movement of congested LWD transport tends to be in pulses with respect to time
- Semi-congested: intermediate between the two regimes

A considerable number of studies have been undertaken looking at the transportation patterns of woody debris once in a watercourse. Many of these focused on assessing the forces necessary to initiate movement and factors influencing debris transport such as drag, torque and buoyancy while also considering the impact of woody debris on channel hydraulics and morphology (e.g. Braudrick *et al*., 1997; Diehl, 1997; Braudrick & Grant, 2000; Manga & Kirchner, 2000; Wallerstein *et al*., 2001; Bocchiola *et al*., 2002; Hygelund & Manga, 2003; Bradley *et al*., 2005; Mazzorana *et al*., 2011; Shields & Alonso, 2012). In a recent study, Shields and Alonso (2012) used an outdoor grassed channel to assess flow forces on large pieces of wood. The combined effect of buoyancy, drag, and lift forces acting on a cylindrical log were found to be at maximum when the log was either resting on the bed or just submerged and oriented perpendicular to the flow.

Deihl (1997) notes that observations of debris transport suggest predominantly uncongested transport with only short-term contact between logs, a finding also noted during a field study by Lyn *et al*. (2003). This later study also reports that the orientation of the debris in the stream may be a function of size, with longer logs having a tendency to orientate parallel to the flow direction and shorter debris exhibiting a wider range of orientations. Diehl also notes that LWD is not consistently aligned with the flow, but suggests that rotation is due to the influence of eddies and vortices. This tendency to re-orientate due to flow patterns may be significant in determining how debris is transported close to structures within a watercourse as the presence of an obstacle will alter flow paths upstream and immediately around the obstacle.

Other studies report on changes in hydraulic properties resulting from local disturbance of flow patterns due to obstacles such as tree trunks, logs jams or artificial structures (e.g. Young, 1991; Gippel, 1995; Shields & Gippel, 1995; Abbe & Montgomery, 1996; Lyn *et al*., 2003; Bocchiola *et al*., 2006a, 2006b; Manners *et al*., 2007). For example, in a flume based experimental investigation of how the motion of LWD in rivers is influenced by the presence of obstacles, Bocchiola *et al*. (2006b) found that the probability that a piece of LWD is stopped by an obstacle and whether it stops by leaning against one obstacle or by bridging two obstacles depends both on the length of the LWD and on the flow conditions.

The distance travelled by debris once mobilised has also been considered by a number of studies and was found to depend on a number of factors; one of the most significant being water depth. In a field experiment looking at transport of small woody debris in a mountain stream in Japan, Haga *et al*. (2002) showed that the distance travelled by the logs is strictly related to the water depth at the peak flow. Similar findings showing the influence of flood water depth on debris transport were reported by Braudrick & Grant (2001).

Both the distance transported and the initiation of transport will also be influenced by the size and geometry of the debris. Coniferous wood debris tends to be cylindrical and therefore is more readily transported and routed through a river system. In contrast, widely spreading or multiple stemmed hardwoods are more likely forms snags and only travel short distances. Where the wood is without a rootwad or leaf canopy, its motion is the result of a balance between the downstream driving forces of fluid drag and buoyancy (Hygelund & Manga, 2003) and the resisting forces of log weight and friction between the log and the channel bed (Braudrick & Grant, 2000). Light, buoyant logs tend to flow with the main current while much larger logs or trees with large roots can 'dredge' the bottom and therefore tend to move very slowly (Abbe & Montgomery, 1996).

Studies looking at the transport of debris from its source to the watercourse are extremely limited. Johnson *et al*. (2000) used a combination of field study and analysis of aerial photographs to investigate the influence of flood induced wood flotation and transport within a riparian forest. They found high spatial variability of riparian responses to large floods and suggest that while flood waters had an impact on riparian forests the effect was much greater where wood was transported within the water. In addition they report that the dynamics of the flood and forest interactions were strongly influenced by the state of the forest prior to the flood, which was a result of previous floods and land-use practices.

While a number of different authors have reported on studies of debris in the riparian environment, in a review of studies looking at large in-stream wood, Wohl *et al*., (2010) note that historically, most of the field studies looking at large wood transport have focused on the Pacific North West area of the USA. However, as the review notes, in the last decade or so research has been undertaken in many different geographical areas and environments including Europe (e.g. Comiti *et al*., 2006), Asia (e.g. Seo *et al*., 2008), South Africa (e.g. Gomi *et al*., 2006), Australia (e.g. Webb & Erskine, 2003), New Zealand (e.g. Baillie & Davis, 2002), South America (e.g. Andreoli *et al*., 2007) and other regions of North America (e.g. Marcus *et al*., 2002). This increasing diversity in environments being studied highlights the growing need for understanding the interaction between debris load and transport in river systems in terms of ecological, geological and hydrological impacts.

3.4. Factors Influencing Debris Deposition and Accumulation at a Culvert

Within the UK currently four mechanisms for debris accumulation and blockage at a culvert have been identified (EA, 2009):

- Sedimentation: progressive build up of sediment within the culvert barrel
- Gradual blockage: blockage from the surface downwards by floating debris
- Abrupt blockage: blockage by urban materials such as sheet metal, fences and sheds
- Sudden blockage – total instantaneous blockage by a large item or items of debris

Accumulation of debris at a culvert or trash screen is very site specific and as a result little data is available to help determine the probability of accumulations resulting in blockage. Blockage probability is a function of three main factors: debris availability, probability of transport, and the probability of deposition and accumulation. Table 3.3 details risk factors influencing debris accumulation within a culvert.

Table 3.3 Risk factors influencing debris accumulation at culverts. (Adapted from EA, 2009)

Culvert feature	Risk
Size of culvert barrel	Generally the smaller the culvert the greater the risk of blockage
Number of barrels	Risk of blockage is higher for multiple barrels, but blockage of one barrel only causes partial loss of capacity
Bends, Steps and changes in cross section	Can trap larger pieces of debris
Services	Services that pass through a culvert can trap debris
Length	The longer the culvert the greater the risk
Hydraulic design	Free surface flow within a culvert is less like to result in trapped debris than full flow
Inlet and approach conditions	Sharps bends at the entrance may induce deposition and debris build up
Inverted syphons	High propensity to block

Both experimental and field studies have been used to assess the potential for debris deposition and accumulation within a river. For example, an experimental study by Braudrick & Grant (2001), which investigated the motion and the deposition patterns of wood dowels, suggests that the probability of LWD to be deposited depends on particular flow variables and on the size of the debris. While many of the studies have focussed on the formation of woody debris jams within the watercourse (e.g. Abe & Montgomery, 1996; Manners *et al*., 2007; Bochiola *et al*., 2008; Manners & Doyle, 2008), a limited number have specifically investigated debris accumulation at artificial structures (e.g. Melville & Dongol, 1992; Lyn *et al*., 2003; Pagliara & Carnacina, 2010; Mazzorana *et al*., 2011; Wallerstein & Arthur, 2012).

The study by Lyn *et al*. (2003) examined factors contributing to the initiation and development of debris piles at bridge piers and involved both laboratory and field analysis. The laboratory study suggested a greater potential for debris accumulation at lower water depths while the field observations show that delivery of debris to the structure was episodic rather than continuous and that the debris pile could be initiated and grow to a considerable size before the peak of an event. In addition it was noted that similar hydrological events can produced significantly different patterns of accumulation.

Melville & Dongol (1992) and Pagliara & Carnacina (2010) studied the role of debris accumulations in the development of scour at bridge piers but limited consideration was given to the potential volume of debris that may accumulate. However, a recent study undertaken by Mazzorana *et al*. (2011) considered identifying potential volumes of debris at structures such as bridges, key to refining hazard mapping. They used a modelling approach to both estimate the potential volume of woody material entering a watercourse during a flood event from banks and floodplains and evaluate woody material transport to key critical configurations such as bridges.

While the majority of studies considering structures in watercourses have focused on debris accumulations at bridges, a recent study by Wallerstein & Arthur (2012) used trash screen monitoring records and GIS data sets relating to 140 sites in Belfast to develop simple empirical models that enable estimation of the probability of delivery of significant debris loads to screens. The study found that the potential for debris arrival at a screen was related to key channel, flow, land use and social deprivation variables. In addition it was found that the significance of the driving variables and the extent of their influence varied depending on the time of year. Their models do not currently factor in culvert or trash screen design.

3.5. The Need for Debris Control

Perham (1987), cited in Abt *et al*. (1992), noted the requirement for floating-debris control to protect hydraulic structures. He indicated that floating debris can have an extremely harmful effect on flood control works, power-generation intakes, and navigation facilities. While a variety of structural and non-structural approaches have been taken to help minimise the problems caused by debris blockage at culverts, little research is available on the efficiency of different control measures. Wallerstein *et al*.

(1997) offer a review of a number of debris control approaches in different areas of the USA and Europe and note that “debris control and exclusion systems involve considerable capital cost, and difficult and expensive maintenance procedures and they may themselves impair the efficient operation of the structure they were intended to protect”. For example, as screens designed to exclude debris from hydro-electric power plant intakes result in head loss, the need to minimize bar spacing to prevent debris entry into the turbines must be balanced against the loss of potential energy for power generation. Therefore careful consideration of the whole system is required before deciding on the most appropriate approach to debris control.

3.6. Structural Approaches to Debris Control

A number of different structural measures can be taken at culvert inlets to try and reduce the impact of debris. These include mechanisms designed to trap and store the debris such as racks and sediment traps and devices designed to orientate the debris to facilitate its passage through the culvert such as fins and deflector poles. The choice of structure will depend on site conditions and more than one device can be employed at a single culvert.

3.6.1. Deflectors

Structures can be placed at the culvert inlet to deflect the major portion of debris away from the culvert entrance. They are normally "V" shaped in plane with the apex upstream (Figure 3.3).

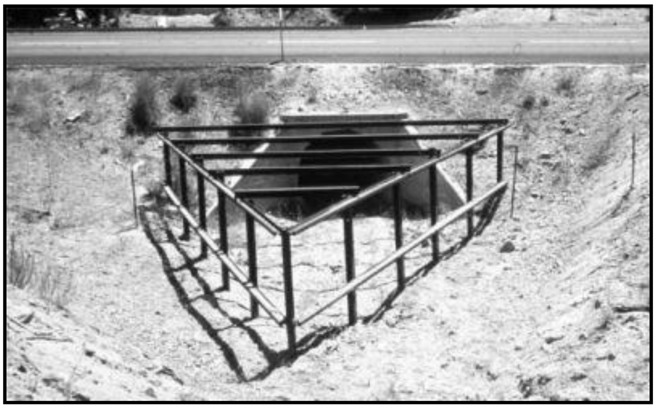

Figure 3.3 Steel debris deflectors, looking downstream

The structural stability and orientation of these deflectors make them particularly suitable for large culverts, high velocity flow, and large woody debris or large boulders. The debris is deflected to the sides or top of the structure where it can be temporarily stored in areas set aside or designed for this purpose. An alternative use of deflectors is to use poles to attempt to orientate the debris within the flow (Figure 3.4a). Under extreme conditions, rather than facilitate the transport of debris, the deflectors can act as a collection point. This may result in a blockage as happened at the site of the Eel River (Figure 3.4b).

(a)  (b) 

Figure 3.4 Debris deflectors installed at State Route 59 south crossing of the Eel River in central Indiana, before (a) and after (b) after a major flow event (Bradley *et al*., 2005 and Lyn *et al*., 2003)

3.6.2. Racks, screens and grilles

As discussed in Section 1.3, racks or screens are commonly fitted at culvert openings to reduce the risks of flooding resulting from culvert blockage (e.g. Figure 3.5). An overview of trash screen design is given in Section 2.7. General design guidance for trash racks including bar spacing, head loss, rack location, vibration response, and angle of inclination have been offered in a number of countries for many years. In the USA, Hydraulic Engineering Circular No. 9, produced by the FHWA offers general guidance which may be supplemented by specific guidelines produced by individual states. The latest edition (Bradley *et al*., 2005) replaces earlier editions published in 1964 and 1971 (Reihsen, 1964; Reihsen & Harrison, 1971). Within the UK, current guidance is offered by the EA (Balkam *et al*. 2010; EA, 2009). Studies undertaken to investigate the efficiency of trash racks are reviewed in Section 3.9.

Figure 3.5 Debris Racks (Bradley *et al*., 2005; TSO, 2004)

3.6.3. Risers

Risers are structures placed directly over the culvert inlet in order to prevent flowing debris and fine detritus reaching the culvert inlet (Figure 3.6). They can also be used as relief inlets if the main culvert entrance becomes blocked. Risers require a relatively high embankment and are most commonly used where debris consists of flowing masses of clay, silt, sand, sticks, or medium floating debris without boulders. They are vulnerable to impact damage and may be structurally unstable under high-velocity flow conditions. As with deflectors, an adequate area for storing the retained debris must be provided.

(a)  (b) 

Figure 3.6 (a) Riser in basin with anti-vortex device on top (b) Riser placed during initial construction of culvert provides relief in case the culvert entrance becomes plugged (Bradley et al., 2005)

3.6.4. Cribs

Debris cribs are open structures placed vertically over the culvert inlet to prevent inflow of coarse bedload and light floating debris (Figure 3.7). They are particularly useful for small-size culverts where course detritus is likely to be an issue. Cribs are similar to risers but can be almost enveloped without blocking the culvert. Due to the debris type and site conditions associated with cribs and risers, they appear to be the most consistently successful in producing efficient, maintenance-free installations.

(a)  (b) 

Figure 3.7 (a) Debris crib of pre-cast concrete sections (b) Redwood debris crib with spacing to prevent passage of fine material (Bradley *et al*., 2005)

3.6.5. Fins

The orientation of debris relative to the direction of stream flow has a major impact on the potential for blocking the culvert entrance. Walls built into the stream channel upstream of the culvert can align debris, such as logs, with the axis of the culvert so that the debris will pass through the culvert barrel without clogging the inlet (Figure 3.8).

Debris fins have been used most successfully with large culverts. If the fin is sloped upward toward the culvert, the debris that does not pass through the culvert can float upward and prevent debris from blocking the culvert inlet. As the height of fins generally does not exceed the height of the culvert they are ineffective once the culvert had become submerged.

(a)  (b) 

Figure 3.8 (a) Concrete debris fins with sloping leading edge as extension of culvert walls (b) Combined installation of concrete debris fin and metal pipe debris riser (Bradley *et al*., 2005)

3.6.6. Dam, basins and silt traps

In addition to the problems caused by floating debris, sediment and dense debris carried in the bedload can cause significant blockage problems within a culvert. The amount entering the culvert can be reduced by construction of sediment dams or basins to trap the debris upstream of the culvert inlet (Figure 3.9). The basin or dam should be located far enough upstream and the openings should be sized to allow the suspended sediment sufficient time to settle out prior to entering the culvert. These constructions are particularly effective in areas where heavy silt and/or sand loading occurs during flood events and velocity levels are not high enough to allow scouring of the streambed and culvert. However there must be adequate storage in the basin and the site must be easily accessible for to allow the sediment to be cleared.

(a) 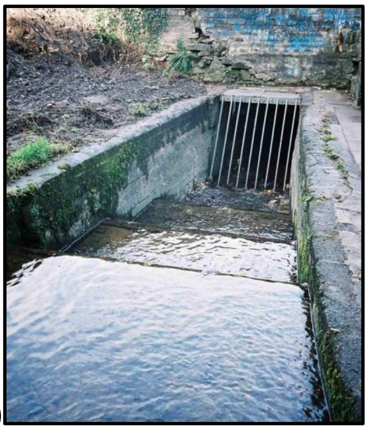 (b) 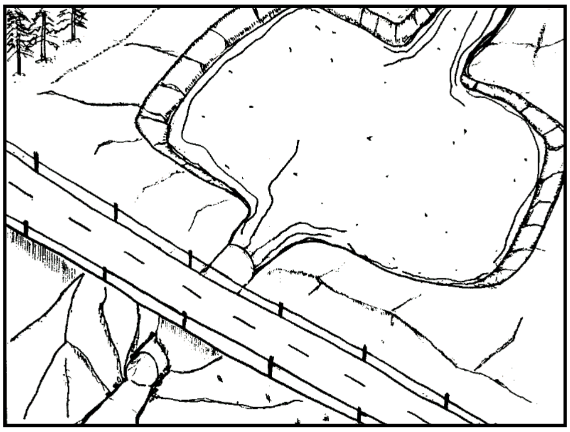

Figure 3.9 (a) Screen protecting culvert with sediment trap upstream (b) Diagram of sediment catch basin upstream of a culvert (FEMA, 2001).

3.6.7. Relief culverts

Relief culverts located at the same site but above the flow line of the primary culvert offer an alternate route for the flow if the main culvert gets plugged. These culverts are also less likely to block due to deposition as they will only come into operation during high flows. This is not always a practical or economical option.

3.7. Non-Structural Approaches to Debris Control

3.7.1. Operation and Maintenance Routines

The establishment of a maintenance regime is a fundamental part of the planning and design requirements for culvert screen installations. This needs to include plans for regular cleaning and disposal of the cleared debris and strategies for emergency response if the screen becomes blocked during a flood event. The owner needs to be aware of their responsibilities as failure to address maintenance issues has previously led to legal action (EA, 2009).

A key consideration in any targeted programme of maintenance is whether the blockage is contributing to a real flood risk. In some situations the negative visual/public impression given by debris blockages can be greater than any potential impact on flood risk. A consistent assessment procedure is required to ensure the maintenance regime adopted is justified. Another important consideration is that many temporary blockages occur during flooding where the feasibility of removal is more limited. While operation and maintenance focuses on small, routine debris loads many racks are designed to handle periodic large volumes of debris and not all screens will be at equal risk from blockage. This difference can cause problems in ensuring the rack is cleared appropriately. Some form of prioritisation of the most ‘at risk’ screens will increase the efficiency of the maintenance programme and help reduce potential flood risk. Work towards developing a predictive tool that will provide a means of ranking culverts in terms of blockage potential is currently ongoing (e.g. Wallerstein & Arthur, 2012).

As noted in Section 2.10, the use of technology such as telemetry to routinely monitor at-risk screens or to automatically alert maintenance crews to potential problems can greatly enhance the efficiency of operation and maintenance programs.

3.7.2. Debris management plans

Removal of debris from banks and the watercourse

Focused maintenance on areas known to be a high risk for dumping can remove debris before it gets a chance to enter the watercourse. In addition, rapid clear up of natural debris from heavily wooded or parkland areas both after high winds and seasonally after leaf fall can significantly reduce the available material that could potentially block culvert trash screens.

Once debris has entered the watercourse, trash collecting boats can be used to remove debris from larger rivers before it becomes a problem at downstream structures. For example, a boat with the capability of holding up to 3 tonnes of debris clears floating debris from the river Thames. The volume of debris routinely cleared requires the holding baskets to be emptied three to four times a day.

Reducing anthropogenic generated debris

Reducing domestic and large household refuse will have a significant impact in urban areas. This type of debris can reach the watercourse directly from residential areas or from known fly-tipping hotspots. Often this type of debris is only mobile under high flow conditions. This can result in a large volume of debris accumulating at a screen following heavy rainfall in the catchment. The public are often unaware of the risks from this type of debris and engaging with the local community to ensure they are aware of the potential consequences of dumping near the culvert or in the upstream area would be a useful step to potentially reducing the problem. The EA (2009) suggest a public awareness campaign targeted specifically at riparian owners may also reduce the debris load from domestic refuse.

Regular maintenance of the riparian environment to remove debris before it is transported downstream and increased monitoring of known fly-tipping sites will also reduce the problem.

Large non-domestic refuse is often associated with industrial land. Working with the site owner to ensure debris is secured to prevent it entering the watercourse or if necessary taking enforcing acting against the site owner may be an option (EA 2009). Alternatively a physical barrier can be put in place between the site and the watercourse.

However, it must be constructed in such a way as to ensure it does not compromise the flood flow capacity of the watercourse or prevent access for maintenance.

Reducing natural debris

LWD is important for river ecosystems as it provides food for organisms and its presence increases the physical diversity of the channel. Its removal can have serious environmental consequences. However, a heavy LWD load can increase the risk of flooding by causing wood jams (Young, 1991). Land management techniques now seek to achieve a debris load that is sufficient to sustain the ecosystem while minimising any risk resulting from debris transport and blockage of structures (e.g. Gippel, 1995; HEC, 2006).

While a reduction in small vegetation along the watercourse is unlikely to have a significant impact on the volume of debris arriving at a culvert screen, a reduction in large vegetation may have a significant impact. Small vegetation is most likely to be a hazard where there is a substantial contributing upstream length of the watercourse. The large vegetation load may be reduced by routine removal of debris from the watercourse and/or the management of upstream vegetation to reduce the volume of debris entering the watercourse. This will require cooperation between the culvert owners and riparian owners. Environmental aspects must be considered if large vegetation or woody debris is to be routinely removed from the river banks or watercourse as this may have a detrimental impact on the waters ecosystem (e.g. Gurnell *et al*., 2002; Wallerstein & Thorne, 2004).

3.8. Research relating to debris control performance of trash screens

3.8.1. Overview of research to date

A number of studies have been undertaken looking at the use of trash screens for debris control (e.g. Ott *et al*., 1987; Strong & Ott, 1988; Abt *et al*., 1992; Lemon *et al*., 1999; Wahl & Einhellig, 2000; Katopodis *et al*., 2005; Ho *et al*., 2006; Padilla & Clark, 2008; Xiang *et al*., 2009, Clark *et al*., 2010). The majority of these investigations have focused on variations in screen discharge capacity, head loss across the screens, and the effect of the screen on turbine efficiency. Very few studies have been undertaken looking at screen performance in terms of debris blockage efficiency. An investigation by Abt *et* *al*. (1992) assessed the performance of a trash screen upstream of an inlet drop structure under supercritical flow conditions. They found that localised flooding occurred once approximately 41% of the screen had become blocked. In addition it was noted that the location of the blockage was important as blockages at the top of the screen due to floating debris had less impact than blockages at the base of the screen due to non-floating debris. Experimental studies undertaken by Padilla & Clark (2008) and Xiang *et al*. (2009) were aimed at increasing the understanding of screen design for both debris removal and fish passage and assessed the efficiency of racks at trapping debris consisting mostly of Egeria, an aquatic plant. Although assessing different rack configurations and environments the general findings in both studies were that racks at lower angles are more efficient at trapping debris and racks with narrow bar spacings are more efficient at trapping debris than racks with wide bar spacings regardless of the angle of the rack.

3.8.2. Need for further research

Although considerable research has been undertaken looking at aspects of trash screen hydraulics (see Section 2.8) and debris deposition and accumulation (see Section 3.4) very few studies have considered the impact of debris blockage on trash screens. In addition, while the studies noted in the previous section assessed blockage at trash screens in open channels, currently no reported experimental assessment of trash screens at culvert inlets is available. Therefore in order to understand the performance of trash screens at culverts, there is a need to assess screen performance under the specific hydraulic conditions created by the restriction of flow through a culvert. The research reported in the following chapters aims to provide an assessment of screen performance under these conditions through the objectives listed in Section 1.6: the development of a physical model to represent a culverted watercourse, the use of the model to investigate the performance of various trash screen configurations, the development of an empirical relationship that defines blockage potential in terms of the influencing components, and assessing the impact of the findings on current screen design guidelines.

3.9. Chapter Summary

Worldwide, a number of different classification systems for debris found in rivers have been defined. While there are minor differences between the systems they are all aimed at aiding better assessment of debris loads with a view to increasing the efficiency of debris management and control.

Two main categories are defined: debris from natural sources and debris from anthropogenic sources. The volume of natural debris found in a watercourse depends on a number of factors such as location within the watercourse, land use, previous disturbance and prevailing weather conditions. Debris may have originated from overhanging or adjacent vegetation or may have blown in or been transported by overland flow. Anthropogenic debris may be the result of deliberate fly-tipping at known hot spots or through items from domestic, industrial, commercial or agricultural sources either intentionally or unintentionally arriving at a watercourse.

During a flood, debris is swept into the watercourse from the surrounding area. The method of debris transport depends on various factors including the flood volume, discharge, channel characteristics, the size and geometry of the pieces relative to the channel width, orientation of the debris relative to the channel alignment, and the hydraulic characteristics and geometry of the banks and channels.

Debris generally travels as individual pieces within a watercourse and while the general tendency is for debris to orientate itself parallel to the flow direction, it will rotate and realign as a result of eddies and vortices. This may influence the transport patterns of debris at and approaching both natural and artificial obstacles.

Blockage probability is a function of three main factors: availability, probability of transport, and the probability of deposition and accumulation. Four mechanisms for debris accumulation and blockage at a culvert have been identified: sedimentation, blockage by floating debris, blockage by urban materials such as sheet metal or fences and total instantaneous blockage by large items. Both experimental and field studies have been used to assess the potential for debris deposition and accumulation at structures within a river most of which have focused on debris accumulation at bridges.

Blockage of a culvert affects local hydraulic conditions, potentially most significantly raising upstream water levels and increasing flood risk. In addition there may be geomorphological, structural, social, economic and environmental implications.

There is a recognised need for debris control to prevent potential blockage and while a number of different structural and non structural approaches have been used there is little research available outlining the efficiency of different methods.

Structural methods include the use of deflectors; racks, screens or grilles; risers; cribs; fins; dams, basins and silt traps; and relief culverts. Non-structural methods include efficient operation and maintenance routines and debris management plans.

A limited number of studies have been undertaken to assess the use of trash screens for debris control; these have generally focused on variations in screen discharge capacity, head loss, and the effect of the screen on turbine efficiency. Very few studies have considered screen performance in terms of debris blockage efficiency. In addition most of the research has considered screens in open channels. In order to understand the performance of trash screens at culverts, there is a need to assess screen performance under the specific hydraulic conditions created by the restriction of flow through a culvert. The research reported in the following chapters aims to provide an assessment of screen performance under these conditions through the objectives listed in Section 1.6.

Chapter 4
Experimental Set up and Approach

4.1. Introduction

This chapter briefly reviews the historical use of models in hydraulic research before assessing modelling options currently available. It then justifies the selection of the approach adopted during this project before describing the set up of the physical model developed and used to carry out an extensive series of laboratory tests in order to meet the objectives outlined in Section 1.6. Finally, accuracy of the equipment used and an assessment of potential errors and limitations in the approach are discussed and, where possible, quantified.

4.2. The Historical Use of Models in Hydraulic Research

Early scale-model experiments, assessing the efficiency of waterwheels, were conducted by John Smeaton in the 1750's (Hughes, 1993) but the work of Froude in the late 1800's helped establish the role of model test predictions as valuable engineering tools (Vassalos, 1999). Although Peakall *et al*. (1996) note a number of early attempts to model fluvial and coastal processes (e.g. Thomson, 1879; Reynolds, 1887; Gilbert, 1914), it was only after the development of dimensional analysis by Buckingham (1915) that scale modelling techniques in engineering were widely adopted (e.g. ASCE 1942; Murphy 1950). From the mid 1940's hydraulic scale models have played a key role in the design of hydraulic structures. Since then numerous modelling texts have been published and are widely available (e.g. Etema *et al*., 2000; Novak *et al*., 2010).

4.3. Modelling Options

In order to investigate site conditions or design structures or machines, the engineering hydraulics can be determined either through the application of pure theory or via empirical and modelling methods. Within hydraulic research the adoption of a purely theoretical approach is rare and tends to be restricted to limited cases where laminar flow dominates. All other methods are based to some degree on modelling. In the simplest terms, modelling can be described as the use of any method to represent a process. Ideally, this representation would accurately simulate all aspects of the process.

However, this is rarely achievable due to either insufficient understanding of all aspects of the process or because of the inherent complexity. As a result, a model is almost always a simplified representation of a process. Although these simplified models cannot provide absolute answers, they can offer a means to improve understanding of a process.

Models can be split into two categories: Mathematical and Physical. The Mathematical grouping includes mathematical, numerical and computational models. Physical models include hydraulic and analogue models, both of which can be considered as scale models.

4.3.1. Mathematical, numerical and computational modelling

Mathematical models use algebraic and differential equations to represent processes and interactions. They are based on assumptions about the physics of the processes and the environment that sets limits to the application of the model. Numerical models are approximations of mathematical models. Both these model types offer solutions to general situations.

Computational models are implementations of numerical models using a computer system and specific data. Hotchkiss *et al*. (2008) compare a number of packages that are available for a variety of hydraulic engineering problems. Some example packages that can be used to model culvert and debris screen hydraulics include ISIS, HEC-RAS, MIKE11, Hydro, Hydrocalc Hydraulics, XPSWMM, and Culvert Master. Methods and software to estimate water levels in channels and at bridges and culverts have also been developed by UK operating authorities involved in flood risk management. These are the Conveyance Estimation System (CES) and Afflux Estimation System (AES) (EA, 2009). The CES is a comprehensive software package that allows the user to estimate the flow capacity of any channel reach using details of dimensions, form and vegetation. AES is a package designed to allow estimation of the hydraulic impact of a bridge or a culvert on a watercourse including any increases in water level upstream due to constriction. An integrated software package incorporating both the CES and AES systems, The Conveyance and Afflux Estimation System (CES/AES**)**, differs from other tools in that it is based on a combination of appropriate modelling methods and also on new analysis using contemporary laboratory data and field measurements and allows estimation of water levels in rivers, watercourses and drainage channels that contain bridges or culvert crossings. The CES/AES software has also been integrated into the 1D river-modelling packages, ISIS Flow and InfoWorks RS (HR Wallingford, 2009). However there are still limitations to the CES/AES systems as they do not effectively handle unsteady flows, looped river systems or currently all allow modelling of trash screens, complex culvert layouts or blocked culverts or screens. In a review of roles of computational models in the Environment Agency's flood defence activities, Samuels (2004) reports that there is "...a need to automate the representation of blockage of structures by debris, preferably transient rather than permanent to facilitate probabilistic risk analysis of the effects of blockage". While the review notes that commonly used commercial 1D modelling tools such as HEC-RAS, HYDRO-1D, ISIS and MIKE11 have the capability of modelling trash screens through manual blockage estimation, the impact of blockage is generally assessed by reducing the cross sectional area of the culvert inlet through the modelling of a sluice gate at the culvert entrance. This has the advantage of allowing the impact of varying degrees of blockage to be modelled. HYDRO-1D and ISIS do have the capability of modelling trash screens over the faces of a culvert and allow the user to specify both the geometry and proportion of the screen blocked by debris (Samuels, 2004). A review of the existing CES/AES packages indicates that there are plans to include handling of trash screens in later versions (HR Wallingford, 2009).

4.3.2. Physical models

Hughes (1993 pp 9-10) defines a physical model as, "... a physical system reproduced (usually at a reduced size) so that the major dominant forces acting on the system are represented in the model in correct proportion to the actual physical system."

Physical models allow a problem to be observed under more controlled conditions than field tests would allow and therefore can provide valuable information to help build, calibrate and validate theoretical or empirical models. Processes can be observed, usually in a reduced time-frame, within a controlled and manageable environment. While simplified, the results produced are generally considered more reliable and credible than those resulting from field tests. They also allow for a wider range of data to be gathered than is usually possible from field tests and the data collection is generally easier and cheaper. Physical models may also allow incorporation of variables which are not known in advance and which may have markedly non-linear effects on flow dynamics or morphology. They can also be used to assess unique conditions caused by complex boundary conditions and site specific geometries. Design problems for these conditions may not be practically solvable by theory or standard reference data so often physical modelling, either alone or combined with numerical modelling, can offer a solution.

However, in comparison to computer based modelling, there are a number of possible disadvantages with physical modelling. Physical models are often more expensive both in time and cost than computer models, other limitations include: scale effects; over simplification and abstraction from reality; and cost issues involving space, time, personnel resourcing and equipment. Simplification of some model components can aid the scaling process.

An ideal model achieves similitude with the prototype. Model similitude can be established using a number of different methods (Hughes, 1993):

- By differential equations
- By dimensional analysis
- By scale series

The requirements for similitude will vary depending on the problem under investigation and the required results. Complete similitude requires the model to be geometrically, kinematically and dynamically similar to the prototype. A model and prototype are geometrically similar when all dimensions in all 3 coordinates have the same linear scale ratio (Figure 4.1)

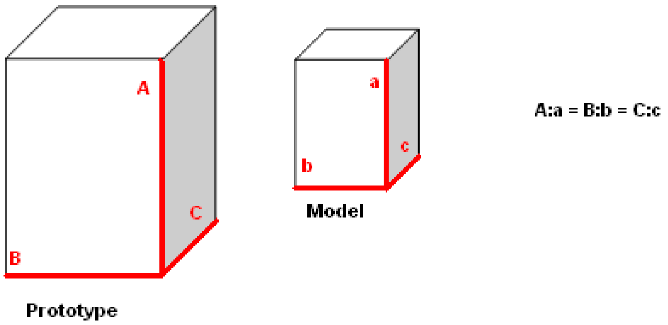

Figure 4.1 Illustration of geometric similarity between model and prototype

Kinematic similarity is the similarity of time as well as geometry. It exists between model and prototype if the paths of moving particles are geometrically similar and if the ratios of the velocities of particles are similar. Dynamic similarity exists when the model and the prototype have the same length scale ratio, time scale ratio, and force scale ratio. In an ideal model every variable would be perfectly scaled; however, it is rarely possible to fulfil this requirement. In physical models involving fluid flow it is not usually possible to have simultaneous equality of all the force ratios required for true dynamic similarity: Reynolds number (Re), a dimensionless number that gives a measure of the ratio of inertial forces to viscous forces; Froude number (Fr), the ratio between the flow velocity and the speed of a wave in shallow water; Mach number, an expression of the ratio of the speed of an object moving through a fluid and the local speed of sound; and Weber number, a dimensionless number that represents the relative importance of a fluid's inertia compared to its surface tension. For example, complete similarity cannot be achieved in a scaled model in which both Fr and Re are relevant if water is the liquid in both the prototype and model, a full scale model would have to be used to achieve the required similarity. As a compromise, the scaling is generally based on the dominant force.

4.4. Selected Approach

In free surface flows, such as those encountered in culverted waterways, gravitational forces dominate and so the most important of the force ratios is Fr. In physical models representing this type of environment, matching the model and protoype flow Re number is therefore generally less critical as long as a fully turbulent flow regime (Re > 2000) is achieved and Fr approaches equality between model and prototype. Allowing some variation of Re from prototypical values allows more flexibility in the model scaling than variation in Fr. This technique is known as Froude scale modelling (FSM) and has been used successfully in movable-bed modelling and also in fixed-bed modelling of flow interaction with artificial structures such as spillways, conduits and breakwaters (e.g. French 1985; Wallerstein *et al.*, 2001; Novak *et al*., 2010) and so was considered an appropriate approach for the purposes of the experimental analysis undertaken during this project. Table 4.1 shows the relationship between prototype and model based on Froude scaling.

Table 4.1 Froude scaling ratios (r) between prototype (p) and model (m)

Factor	Ratio
Froude Number (Fr)	$Fr_p = Fr_m$
Length (L)	$L_r = \frac{L_p}{L_m}$
Velocity (V)	$V_r = \sqrt{L_r}$
Time (t)	$t_r = \sqrt{L_r}$
Discharge (Q)	$Q_r = L_r^{\frac{5}{2}}$
Force (F)	$F_r = L_r^{3}$

4.5. Development of the Physical Test Rig

A flume facility located within the School of the Built Environment at Heriot-Watt University was used to build a Froude scaled physical model to perform the experimental tests. The flume was 22m long, 0.75m wide and 0.5m deep with a variable bed-slope (Figure 4.2a). The initial flume slope was set at 0.006 which is representative of many river regimes within the UK and is comparable with slopes used in other flume experiments that examined debris transport (for example Bocchiola *et al.* 2006a, 2006b).

The flume walls were constructed from glass and the raised floor of the flume from marine plywood. The floor of the flume was raised to allow the culvert invert to be set flush with the channel bed which is typical of the majority of culvert installations. A circular culvert was built within this structure 8.25m downstream of the water inlet to allow flow conditions to stabilize before reaching the culvert. The culvert was made from a section of uPVC pipe 0.3m in diameter and 2m long. The culvert inlet had a headwall made from a sheet of 1cm thick smooth plastic which was vertical and set flush with the inlet orifice (Figure 4.2b). This structure was scaled to represent a prototype circular culvert situated in a straight watercourse with consistent roughness and a flow approach in line with the inlet. A trash screen was constructed that could be placed at various angles (20 to 80 degrees) over the culvert inlet. The screen was constructed from rectangular cross section (0.003m × 0.012m) steel bars. Each individual bar was moveable so that a variety of bar spacings could be achieved at each screen angle (Figure 4.2c). The original test rig construction required the screen to be attached to the culvert head wall. While this position met all the requirements of the initial testing, for later phases of testing an enhancement was made to the set up which allowed the screen to be placed at various positions upstream of the culvert inlet. Schematic diagrams indicating the position of the culvert within the flume, the locations velocity and depth were recorded and positions of the trash screens are shown in Figure 4.3. Table 4.2 details the geometric dimensions of the model and prototype.

The water supply to the flume was provided via a gravity fed pipe from a constant head tank and passed into the flume through a stilling tank. The flow rate of water entering the flume was controlled via a discharge valve. On exiting the flume the water passed into a holding tank sufficiently far downstream to ensure there was no relevant back water effect and was then pumped back up to the constant head tank and re-circulated.

(a)


(b)


(c)
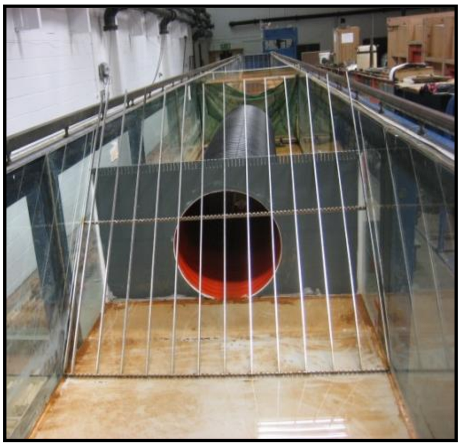

Figure 4.2 (a) Flume (b) Model Culvert and headwall (c) Model Trash screen

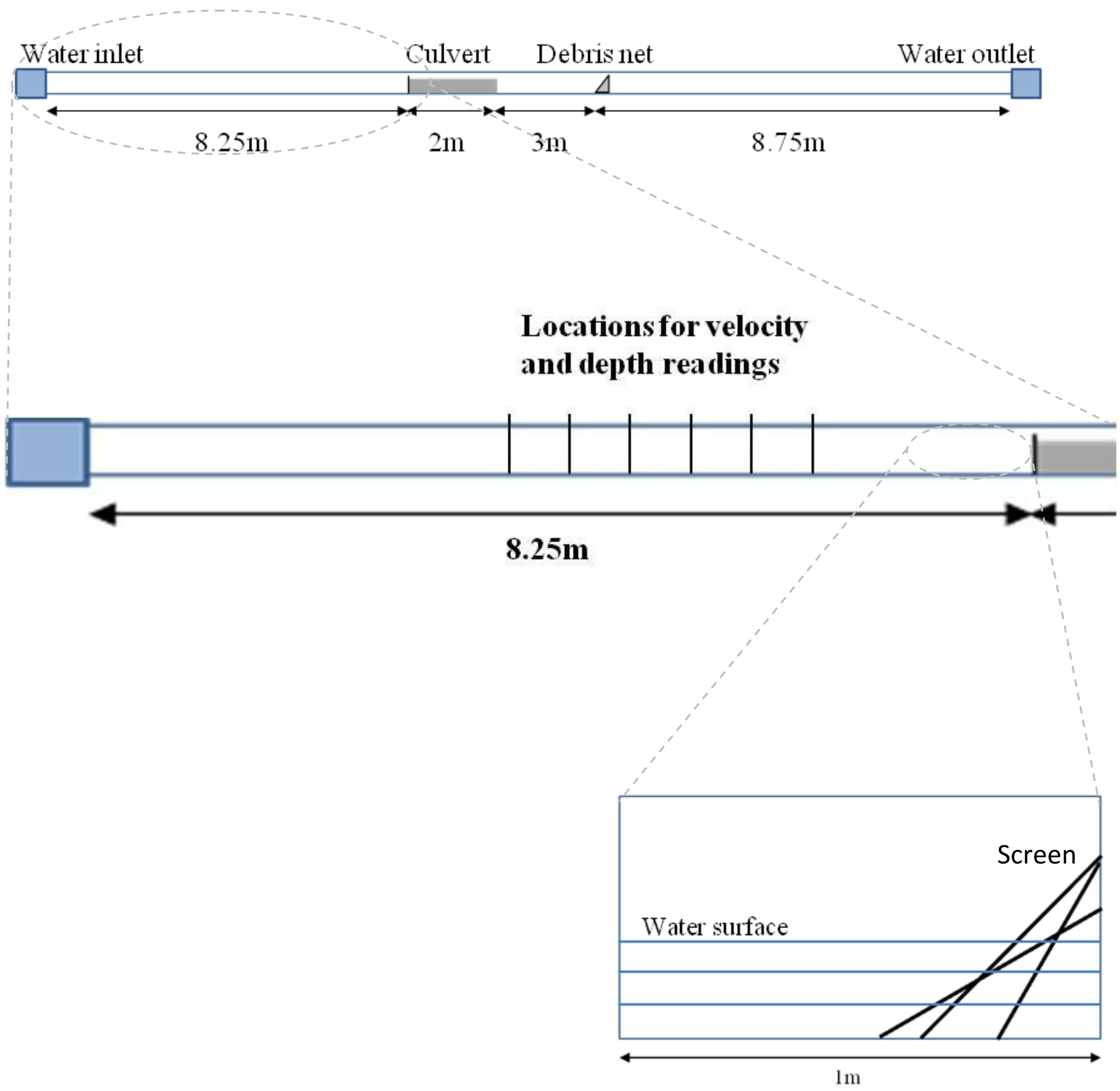

Figure 4.3 Physical Model Schematic showing positin of culvert within the flume, locations of upstream depth and velocity measurements and phase one testing screen locations.

Table 4.2 Froude scaled dimensions for model and prototype

	Model	Prototype
Channel width (m)	0.750	2.500
Upstream reach (m)	8.250	27.500
Downstream reach (m)	15.500	51.670
Initial channel slope (m/m)	0.006	0.006
Culvert length (m)	2.000	6.667
Culvert diameter (m)	0.300	1.000
Bar cross section (m)	0.003 × 0.012	0.010 × 0.040
Bar spacing (1) (m)	0.030	0.100
Bar spacing (2) (m)	0.040	0.133
Bar spacing (3) (m)	0.050	0.167
Bar spacing (4) (m)	0.060	0.200
Bar spacing (5) (m)	0.080	0.267
Bar spacing (6) (m)	0.100	0.333
Bar Spacing (7) (m)	0.150	0.500

The aim of the experimental assessment was to determine the influence of aspects of a trash screen positioned at the culvert inlet. To retain the focus on flow conditions at the inlet, the culvert was allowed to operate under inlet control conditions for the entire range of experiments. A Froude similarity approach was taken which allowed a relaxation in Reynolds number. However, viscous forces can be influential in scale models so to minimise potential errors resulting from viscous effects, the flume slope and discharges were selected such that turbulent sub-critical flow was maintained upstream of the culvert inlet. Elastic effects are very small in water and so no detailed consideration was given to scaling Mach number. Steady flow conditions were adopted, a compromise to most prototypical conditions but this approach was utilized in order to constrain the potential complexity of the model so that the impact of the controlling parameters under investigation could be isolated. Three discharges were used during the testing ($0.005m^3/s$, $0.021m^3/s$, $0.035m^3/s$). The two lower discharges were selected to represent a low flow where water depth at the culvert inlet was 25 percent of the culvert diameter and a moderate flow with a water depth at the inlet of 50 percent of the culvert diameter. The third discharge represented a relatively high flow with water depth at the inlet of 63 percent of the culvert diameter. Ideally a higher discharge would have been used but a discharge of 0.035m^3/s was the highest, repeatable, steady flow that could be achieved with the experimental test rig. Table 4.3 summarises the hydraulic conditions used during the testing with the prototype equivalents, calculated using the ratios defined in Table 4.1, shown in brackets.

Table 4.3 Hydraulic conditions for model (and prototype)

Screen Angle (degrees)	Discharge (m^3/s)	Average upstream depth (m^3/s)	Upstream depth averaged velocity (m/s)	Fr	Re	Depth averaged velocity at the screen (m/s)
30 (30)	0.005 (0.103)	0.07 (0.23)	0.097 (0.18)	0.12 (0.12)	1923 (34821)	0.093 (0.17)
30 (30)	0.021 (0.442)	0.14 (0.47)	0.196 (0.36)	0.17 (0.17)	7300 (12241)	0.198 (0.36)
30 (30)	0.035 (0.703)	0.20 (0.67)	0.232 (0.42)	0.17 (0.17)	11963 (182409)	0.240 (0.44)
45 (45)	0.005 (0.103)	0.07 (0.23)	0.097 (0.18)	0.12 (0.12)	1923 (34821)	0.107 (0.20)
45 (45)	0.021 (0.442)	0.14 (0.47)	0.196 (0.36)	0.17 (0.17)	7300 (12241)	0.232 (0.42)
45 (45)	0.035 (0.703)	0.20 (0.67)	0.232 (0.42)	0.17 (0.17)	11963 (182409)	0.295 (0.54)
60 (60)	0.005 (0.103)	0.07 (0.23)	0.097 (0.18)	0.12 (0.12)	1923 (34821)	0.164 (0.30)
60 (60)	0.021 (0.442)	0.14 (0.47)	0.196 (0.36)	0.17 (0.17)	7300 (12241)	0.249 (0.45)
60 (60)	0.035 (0.703)	0.20 (0.67)	0.232 (0.42)	0.17 (0.17)	11963 (182409)	0.349 (0.64)

While the range of prototype conditions represented by the experimental discharges is relatively small, they allow simulation of flow environments in a small channel representative of baseflows, small storm events and also flows resulting from early runoff from medium and large storm events. The data gathered using this range of conditions will not necessarily reflect how screens operate under more extreme flood conditions. However, in order to understand the full extent of screen performance it was considered important to first establish how screens perform under normal operating conditions. The findings of the research detailed in this and the following chapters can then be used to help refine future programmes of research aimed at assessing screen performance under flood conditions.

The discharge was varied by adjusting the control valve at the inlet. Discharges were estimated using Equation 14 where Q is discharge (m^3/s), V is flow velocity (m/s) and A is cross sectional area of the channel (m^2).

$$Q = VA \tag{14}$$

Flow velocities were measured midstream using a high-resolution acoustic doppler velocimeter (ADV): a side-looking, fixed-stem Nortek Vectrino. To determine average upstream flow velocities, velocity readings were taken at six locations positioned at 5m intervals between points 1.75m and 4.25m upstream of the culvert inlet (see Figure 4.3). This stretch of channel was used to reduce any impacts resulting from turbulence as water entered the flume or from flow restrictions at the culvert inlet. Depth (d) was measured at the same six locations using a point gauge. To account for turbulent flow, 10 depth readings were taken over a five minute period and an average value was used. Velocities were measured at a water depth 0.6d from the surface. This one point method for estimating depth averaged velocity is commonly used where water depth is less than one metre **(**Hershey, 2009). At each of the six locations (Figure 4.3) the velocity was recorded at a frequency of 25Hz over five minutes and an average value was calculated to estimate the velocity for that location. A depth averaged velocity was then calculated for the upstream reach by averaging the values for the six individual locations. The velocities and depths were measured twice daily for the first two weeks of testing. This showed that comparable values for velocity and depth were recorded on each occasion a given discharge was used. Depth at a set point in the flume, 3.25m upstream from the culvert inlet, was thereafter used as means of establishing the required discharge for each test. Additionally, velocities were checked using the ADV weekly or whenever changes to the test rig were made.

Once the required water level at the culvert inlet was established, the flow was allowed to stabilize and achieve a steady state before any testing was undertaken.

4.6. Test Debris Characteristics and Testing Methodology

The focus of the testing was on the influence of screen design on blockage potential. To reduce the impact of factors specifically relating to the debris, pieces of straight wooden dowel were used to represent woody debris with a simple geometry. Ten different debris lengths (Table 4.4) were used to assess blockage. This range of debris lengths was selected as field observations that suggest that, in general, channels with naturally eroding banks tend to be able to actively transport buoyant debris which is not more than half the channel width (Braudrick *et al.*, 1997) and consequently this condition was replicated in the flume by selecting a maximum debris length of 0.35m.

Table 4.4 Froude scaled debris for model and prototype

	Model (m)	**Prototype (m)**
Debris length (1)	0.025	0.083
Debris length (2)	0.050	0.167
Debris length (3)	0.075	0.250
Debris length (4)	0.100	0.333
Debris length (5)	0.150	0.500
Debris length (6)	0.200	0.667
Debris length (7)	0.275	0.917
Debris length (8)	0.300	1.000
Debris length (9)	0.325	1.083
Debris length (10)	0.350	1.167

For each assessment, each length of debris was tested 100 times to minimise the potential for sampling error, therefore 1000 debris passes (100 repetitions of 10 lengths) were made for each test case.

Individual pieces of dowel were introduced into the flow 5m upstream of the point of intersection of the screen and the water surface. The dowel pieces were dropped end on from a height of 0.25m, into the mid-channel. This technique was used as initial trials prior to testing had identified it as the method most likely to result in random initial orientation of the debris. During the initial trials which were undertaken to evaluate the methodology, it was found that dowel dropped end on into the channel entered the water vertically but then assumed various positions and orientations that appeared to be random. Some pieces tipped to travel immediately parallel to the flow direction, some tipped to travel immediately perpendicular to the flow direction, while others assumed an orientation between these extremes. Additionally, a number of pieces ‘bounced’ away from the midstream point of entry to travel either on the left hand side or right hand side of the channel. On occasions the dowel would very quickly reach the channel sides and become stuck against the sidewalls. These pieces of debris were not counted. While it is acknowledged that dropping all the debris mid-channel potentially resulted in more debris pieces being transported in the centre of the channel, any potential bias in blocking was considered to be not significant due to the observed variation in initial debris orientation. Once successfully introduced to the flow, each piece of debris was allowed to travel downstream independently. A piece of debris was considered to have blocked the screen if it bridged two or more bars (Figure 4.4), was balanced across a single bar (Figure 4.5), or was wedged between two bars or between the bars and either the sidewalls or headwall (Figure 4.6).

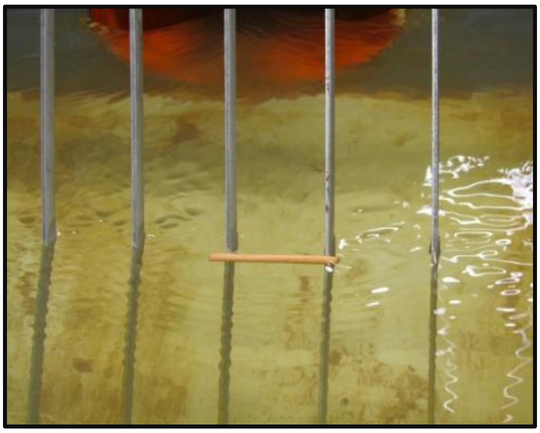
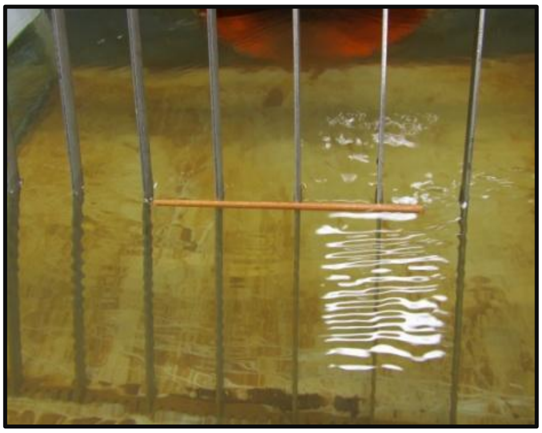

Figure 4.4 Debris bridged across screen bars

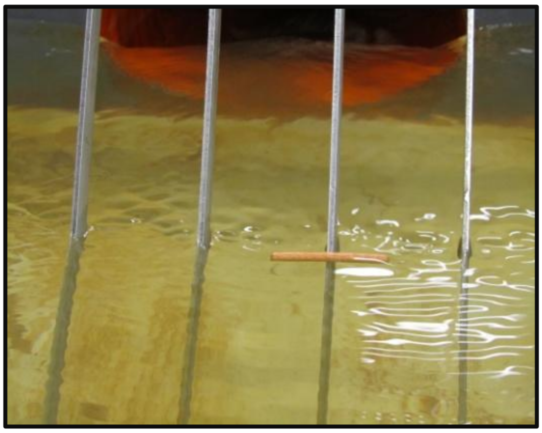

Figure 4.5 Balanced debris

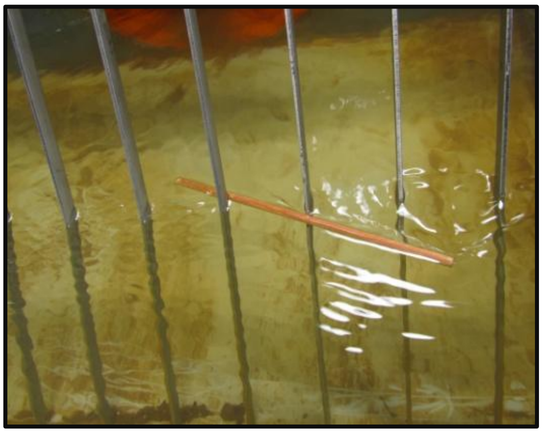

Figure 4.6 Wedged debris

Where a piece became blocked by the trash screen it was removed before the next piece arrived. The number of pieces of each length of debris that were blocked was recorded. A net placed across the flume downstream of the culvert outlet was used to retrieve debris pieces that passed through the screen. Properties of the dowel debris used during testing are given in Table 4.5.

Table 4.5 Properties of test debris

Material	Wawa wood (*Triplochiton sclerocylon*)
Density	380 kg/m^3
Diameter (m)	0.004

4.7. Potential Errors and Uncertainties

4.7.1. Scaling issues

Although the forces associated with surface tension and elastic compression are relatively small there may be some inherent error due to the scaling issues with physical properties of water such as density, surface tension and compressibility. The dowels used were selected as they were made from the lowest available density wood to minimise problems caused by scaling however, there may also be some errors associated with the scaling of the physical properties of the wood used for debris.

4.7.2. Measurement of velocity and discharge

Flow velocities were measured using a high-resolution acoustic doppler velocimeter (ADV); a side-looking, fixed stem Nortek Vectrino. The published accuracy of velocity readings using the Vectrino are ± 0.5% of measured value ± 1mm/s.

The cross sectional area was calculated as the depth of the water at the point of velocity sampling multiplied by the width of the flume (0.75m). Slight variations in the depth of the water over the width of the flume channel along with minor inaccuracies in determining the point of contact of the depth point gauge with the water surface will have resulted in potential errors in the calculated area. The potential inaccuracies in calculated area and measured velocities were minor and unlikely to have a significant impact on the final velocity and discharge values used during the analysis.

4.7.3. Selected test sample size

During testing each length of debris was tested 100 times to try and minimise sampling error. To assess whether 100 repetitions was an appropriate number of samples to use an initial test was undertaken for one bed slope, discharge, and screen angle. A trial run of 100 debris passes was undertaken for 3 debris lengths and 3 bar spacings and the results were then compared against the average value from a further nine sets of 100 debris passes to see if there was a significant difference between results for the percentages of debris blocked. For all bar spacings and debris lengths assessed there was no significant difference (at $p = 0.05$) between the value of percentage debris blocked during the trial run and the average of nine tests (Table 4.6). 100 repetitions was therefore considered to give a reliable value and suitable for the proposed testing. Full details of the sample size tests can be found in Table A.1 in Appendix A.

Table 4.6 Summary of sample size tests

Bar spacing (m)	Debris length (m)	Percentage of debris pieces blocked in trial run	Average percentage of debris pieces blocked from 9 test runs	T-stat	Critical t (p=0.05)	Significantly different
0.04	0.050	77	76.2	-2.101	2.306	No
0.04	0.200	30	30.1	0.197	2.306	No
0.04	0.325	30	29.0	-1.809	2.306	No
0.06	0.050	93	93.2	0.316	2.306	No
0.06	0.200	36	34.3	-2.163	2.306	No
0.06	0.325	32	32.1	0.155	2.306	No
0.10	0.050	96	96.3	0.632	2.306	No
0.10	0.200	52	52.6	1.512	2.306	No
0.10	0.325	44	42.8	-2.219	2.306	No

4.7.4. Testing plan and execution

A number of operational factors may have had an impact on the testing; these include slight variations in flow conditions during the duration of a testing session, changes in water temperature, changes in the efficiency of test execution during the course of a testing session, and the saturation levels of the wooden dowel. To minimise any errors resulting from these factors the order in which each bar spacing and each debris length was tested was selected at random, this ensured that the same bar spacing and debris length were not always tested at the same point during each session. In addition, the test sessions were not always started at the same time of day or on the same day of the week in order to minimise any potential background environmental influences such as changes in water temperature, power fluctuations, dowel saturation levels and tester effficiency. Ideally, the testing plan would have randomly selected the slope, angle and discharge as well as the bar spacing and debris length. However, due to the set up time required, each slope, angle and discharge combination was tested for all bar spacings and debris lengths before being changed to the next slope, angle and discharge combination. To minimise potential errors that may have resulted from fluctuations in the flow rate and pattern, on selection of the required discharge, conditions were allowed to stabilise for 15 minutes before any testing was undertaken. Fifteen minutes had been identified during pre-test trials as an appropriate length of time to establish stable conditions.

4.7.5. Use of dowel to represent debris

To minimise potential scaling issues with complex geometries, dowel was used to represent woody debris. The use of dowel to represent wooden debris was recognised as a simplification that may have resulted in considerable under estimates of blockage as they did not replicate the effect of root wads or branches which may have altered both debris transport (see Chapter 3) and passage through the screen. However, the use of dowels to represent woody debris has been considered a suitable approach for a number of studies into debris transport in rivers. This is because length and diameter or buoyant depth are considered the main characteristics influencing woody debris transport and accumulation with shape, texture and roughness being secondary factors (e.g. Cherry & Beschta, 1989; Van Sickle & Gregory, 1990; Braudrick & Grant, 2000, 2001; Wallerstein *et al*., 2001; Bocchiola *et al*., 2006a, 2006b). Although cylindrical dowel is not representative of more complex woody debris geometry, it does offer a reasonable representation of non-rooted, defoliated, cylindrical logs that may often occur in rivers as a result of wood harvesting and maintenance, or as a result of forest fires (Rulli *et al*., 2006; Rosso *et al*. 2007). In addition woody debris from coniferous sources typically has a cylindrical non-branching geometry. The use of natural twigs has also been used in some physical modelling studies (e.g. Lyn *et al*., 2003) and can offer a more realistic representation of debris. However, natural twigs were considered inappropriate for the planned testing as, although the use of complex geometries inherent in natural debris was felt to be a useful tool, particularly in qualitative studies, it presented a number of difficulties in clearly defining dimensions and in sourcing sufficient suitable material to allow model tests to be repeatable with the same debris characteristics. Importantly, the use of uniform debris made it easier to independently assess the influence of aspects of screen design on blockage and maintain the focus on screen structure and not debris type.

4.8. Chapter Summary

Scale models have an important role in the assessment and design of hydraulic structures. Modelling approaches can be based on mathematical or physical models. Mathematical models which include numerical and computational models allow simulation of a number of general conditions and a number of different packages are available for a variety of hydraulic processes. These include packages that can be used to model culvert and trash screen hydraulics although they are currently limited to representations of simple systems. Physical models, although potentially more expensive in cost and time than computational models, allow specific problems to be observed under controlled conditions. The results of physical modelling can be applied to prototype situations as long as there is appropriate similitude with the model.

The research detailed here used Froude Scale modelling to ensure similitude. A model culvert at 30 percent geometric scale was constructed in a flume which represented a straight water course. A variable configuration screen was constructed that could be placed at different positions upstream of the culvert inlet. A number of configurations were assessed using ten different lengths of dowel to represent woody debris. Each piece of debris was allowed to travel independently along an open channel towards a culvert protected by a trash screen and the percentage of debris pieces that became blocked by the screen was recorded.

A number of steps were taken in order to minimise potential errors including using 100 debris passes for each length and randomly selecting the order in which each bar spacing and debris length was tested. The resulting experimental uncertainties were not found to have a significant impact on the overall accuracy of the methodology.

Chapter 5

Results and Initial Analysis

5.1. Introduction

This chapter presents analyses of the results obtained from the experimental investigations into the influence of trash screen configuration on blocking potential. The methodology used to assess individual screen components under different discharges is described and the results obtained are presented. At the conclusion of each phase of testing the results are then analysed and conclusions are drawn.

5.2. The Influence of Bar Spacing, Screen Angle and Discharge

5.2.1. Overview

The objective of the first phase of testing was to assess the experimental model set-up while carrying out an initial investigation of the relationship between the degree of blockage, screen angle, bar spacing and discharge. A summary of the elements and conditions assessed during these initial tests are shown in Table 5.1.

Table 5.1 Screen elements assessed during initial testing

Number of angles assessed	Number of bar spacings assessed	Number of discharges assessed	Number of test cases	Number of debris passes made
3	7	3	63	63000

Three discharges, as detailed in Section 4.5, were used during the testing ($0.005m^3/s$, $0.021m^3/s$, $0.035m^3/s$).

The range of bar spacings tested (0.03m, 0.04m, 0.05m, 0.06m, 0.08m, 0.1m, 0.15m) was designed to represent prototypical values ranging from 0.1m to 0.5m (See Table 4.2). A prototype minimum of 0.1m was used as it lies just below the recommended maximum bar spacing for culvert access security screens (0.12m) (EA, 2009) and the maximum selected such that the screen would comprise a minimum of at least one bar across the culvert orifice.

The current recommendation for screen angles in the UK is between 45 and 60 degrees to facilitate maintenance and effective trash removal (EA, 2009). In the model three angles were tested, 45 and 60 degrees in order to replicate the extremes adopted for most prototypical screens in the UK and a lower angle of 30 degrees to determine as to what degree the construction of a prototypical screen with an angle outside the recommended range might compromise the screen function. An angle of 30 degrees was selected as it offered the opportunity for an increased screen area when compared to screens at 45 or 60 degrees fixed at the same point on the culvert headwall. Screen angles were measured from the channel bed (Figure 5.1).

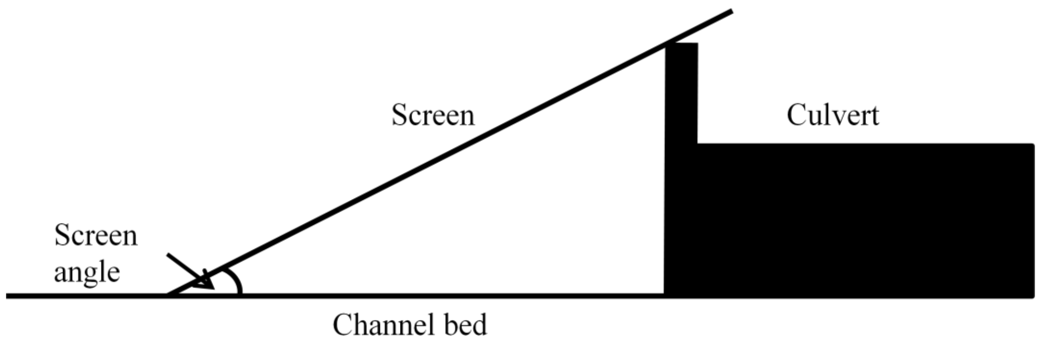

Figure 5.1 Screen angle

5.2.2. Results

Full details of the results obtained during the initial testing can be found in Table B.1, Appendix B.

The results are summarised in Figures 5.2 to 5.6 which show the percentage of pieces of debris blocked for each test case. Each test case represents a different combination of screen angle, bar spacing and discharge.

In the plots shown in Figures 5.2 to 5.4, the percentage debris blocked is shown as a contoured surface with bar spacing (S) on the x-axis and debris length (L) on the y-axis. The contoured surface represents the relationship of S and L with the percentage of debris pieces blocked (D). Interpolated isolines of equal D at 10 percent intervals are marked as black contour lines.

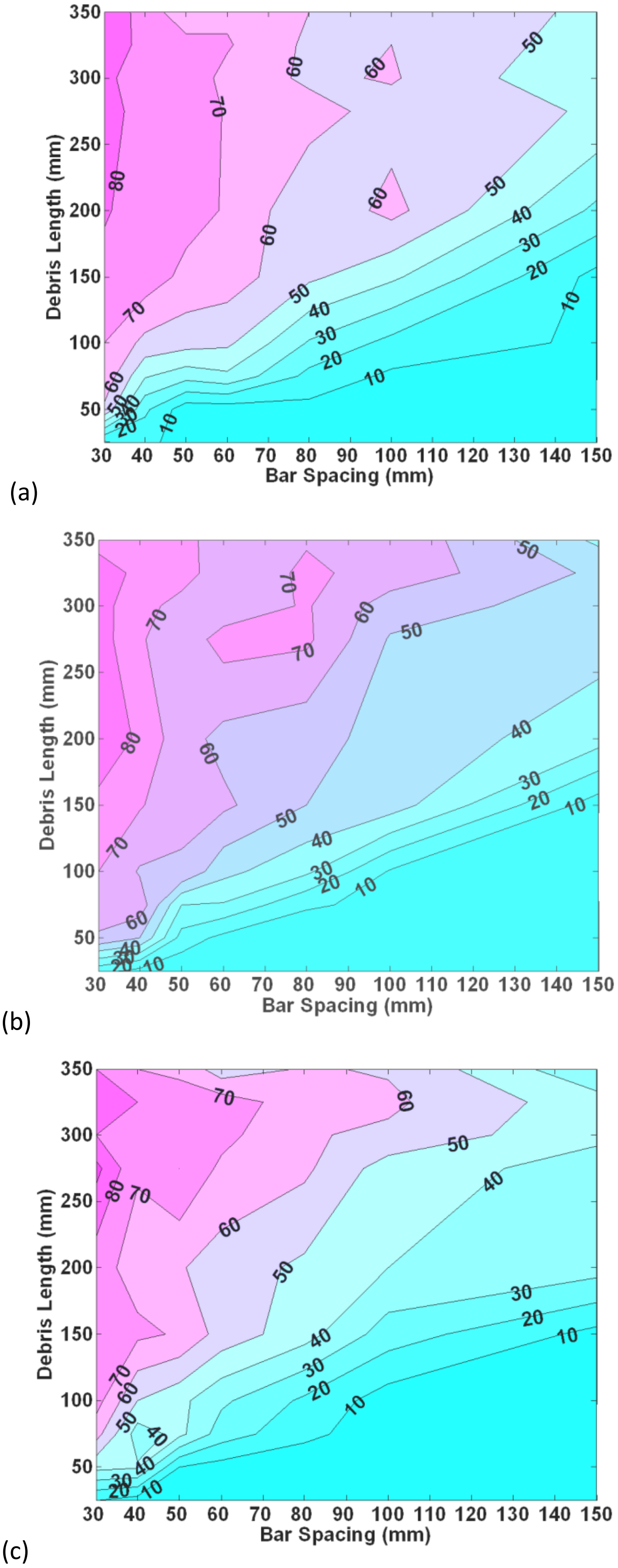

Figure 5.2 Contour plots showing percentage of debris pieces blocked at discharge of $0.005m^3/s$ for screen angles of (a) 30 degrees, (b) 45 degrees, (c) 60 degrees. Interpolated isolines of equal blockage at 10 percent intervals are marked as black contour lines.

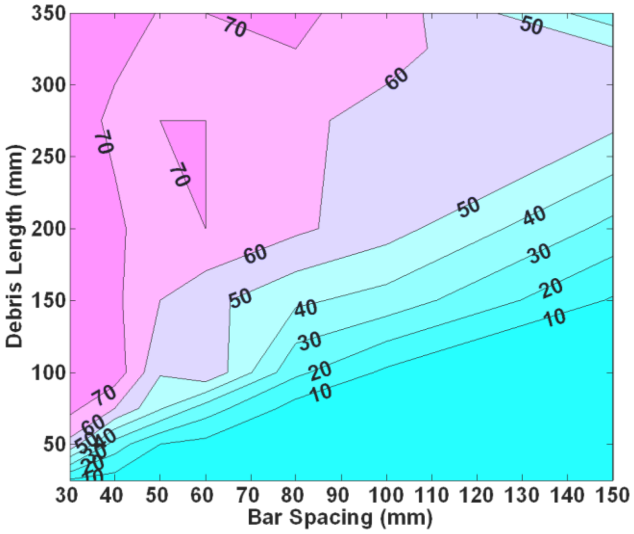

(a)

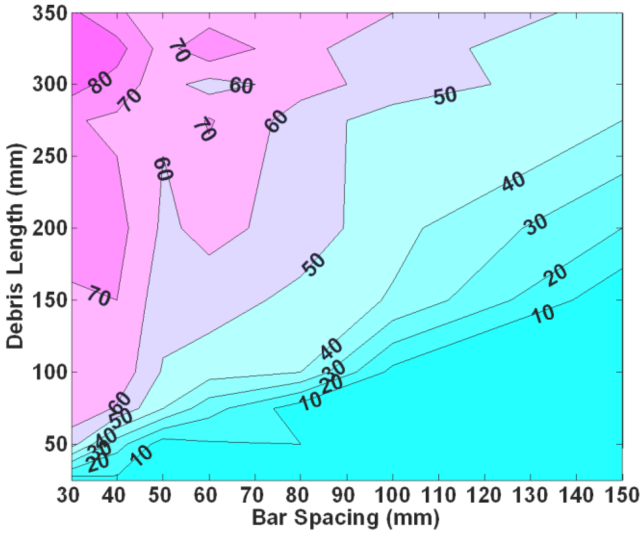

(b)

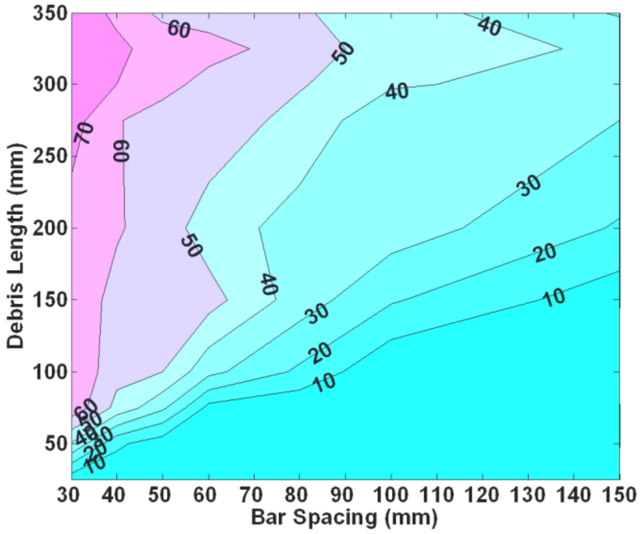

(c)

Figure 5.3 Contour plots showing percentage of debris pieces blocked at discharge of 0.021m^3/s for screen angles of (a) 30 degrees, (b) 45 degrees, (c) 60 degrees. Interpolated isolines of equal blockage at 10 percent intervals are marked as black contour lines.

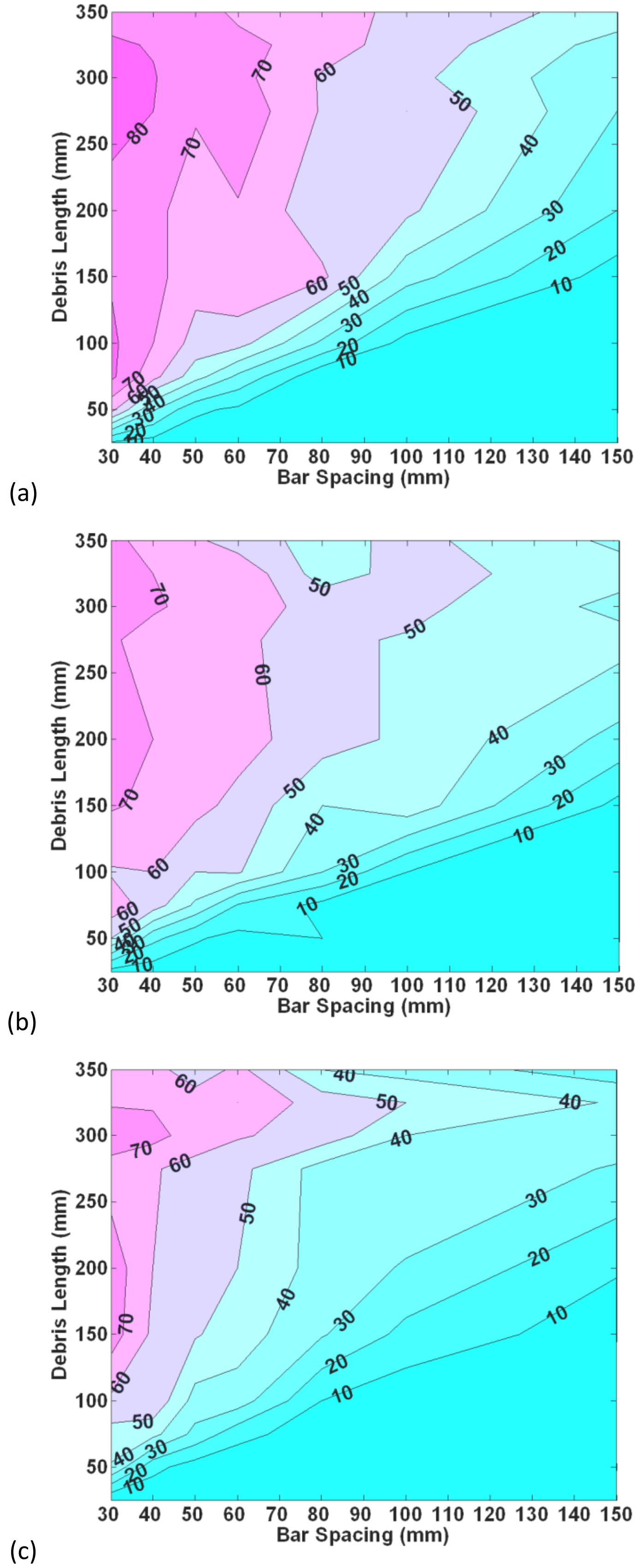

Figure 5.4 Contour plots showing percentage of debris pieces blocked at discharge of 0.035m^3/s for screen angles of (a) 30 degrees, (b) 45 degrees, (c) 60 degrees. Interpolated isolines of equal blockage at 10 percent intervals are marked as black contour lines.

The plots shown in Figures 5.2 to 5.4 show similar general patterns of blockage for all discharges and screen angles tested. However some plots show 'islands' of higher blockage in addition to the general trends (Figure 5.5).

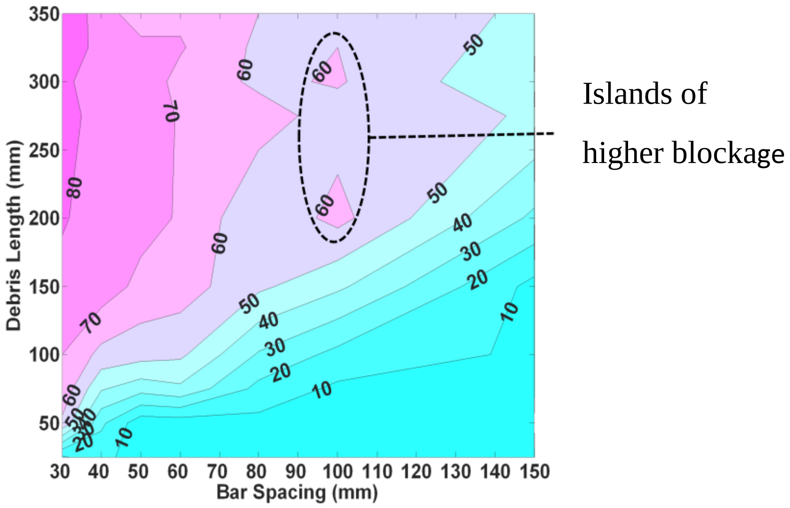

Figure 5.5 Example contour plot showing islands of higher blockage

These apparent areas of higher blockage generally do not represent significant increases in blockage for a particular debris length and bar spacing combination. They reflect a small difference of a few percent, for example from 59% to 61% but as the contours are at 10% intervals they appear in a different blockage zone. However, in some cases, an individual result did give a significantly higher blockage than the general trend, which contributed to the occurrence of the raised blockage islands. For example, a blockage rate of 74% was recorded for debris of length 275mm when bar spacing was 60mm, screen angle was 45 degrees and discharge was 0.005m3/s, one of the results underlying the plot shown in Figure 5.2b. This was approximately 10% higher than the general trend for these conditions. These 'outlier' results did not occur so frequently, or differ from the general trend by such amounts that they suggested there may be an unidentified underlying process at work or that the general trend was not an appropriate representation of the pattern of blockage. It is most likely that they represent the extremes of the inherent variation in the testing process.

As can be seen from Figures 5.2 to 5.4, under all conditions blockage increased as debris length increased and the percent blocked varied depending on the debris length to bar spacing ratio (L:S). Where L:S is approximately 2 or less, there appears to be a consistently almost linear relationship (Figure 5.6). Where L:S is greater than two, the relationship is much more variable and noticeably less dependent solely on debris length. At these ratios, orientation of the debris was observed to be much more significant in determining whether the pieces became trapped by the screen.

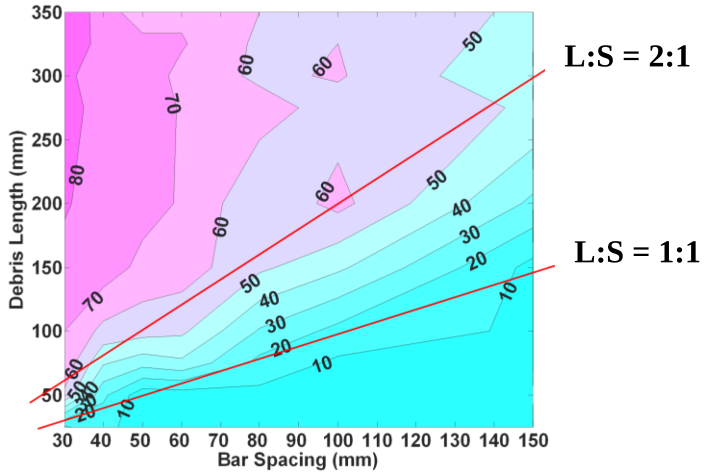

Figure 5.6 Example contour plot showing change in direction of trend with increasing debris length to bar spacing ratio (L:S).

One other noticeable feature of these plots is highlighted in Figure 5.7. The plots for screens at 60 degrees, and to a lesser extent for screens at other angles, show less blockage for a given bar spacing for debris lengths of 350mm than for lengths of 325mm. This reduced blockage for the longest debris lengths is not what was expected and is unlikely to reflect the start of a trend of reducing blockage with increasing length. The results may have been influenced by the 0.35m lengths having a greater tendency to enter the water parallel to the flow direction which would have facilitated their passage through the screen.

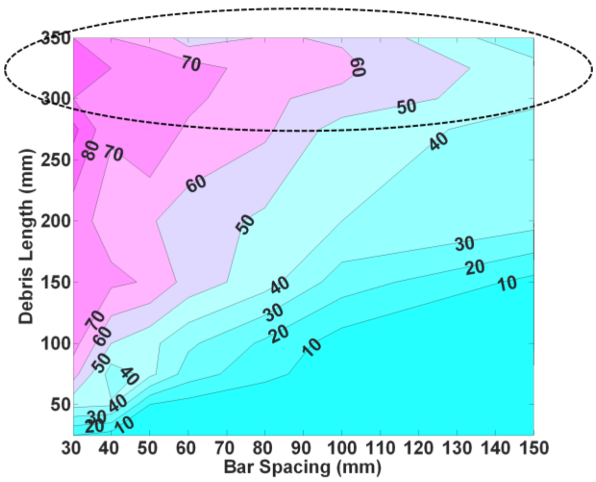

Figure 5.7 Example contour plot showing decrease in blockage for debris lengths greater than approximately 325mm.

The use of contour graphs offers a useful visualization tool for assessing independently the influence of bar spacing and debris length. However, as only one set of results can be easily visually represented on a single contour plot, to facilitate the comparison of results across all angles and discharges the percentage of debris pieces blocked were also assessed directly against the ratio of debris length to bar spacing (L:S) (Table 5.2) as this allows a direct visual comparison of the trends of blockage between different discharges or screen angles (see Figures 5.8 and 5.9).

Table 5.2 Debris length to bar spacing ratios used during testing

Bar spacing (S) (m)	**Debris element lengths (L) (m)**									
	0.025	**0.050**	**0.075**	**0.100**	**0.150**	**0.200**	**0.275**	**0.300**	**0.325**	**0.350**
	Test case (L:S)									
0.03	0.83	1.67	2.50	3.33	5.00	6.67	9.17	10.00	10.83	11.67
0.04	0.63	1.25	1.88	2.50	3.75	5.00	6.88	7.50	8.13	8.75
0.05	0.50	1.00	1.50	2.00	3.00	4.00	5.50	6.00	6.50	7.00
0.06	0.42	0.83	1.25	1.67	2.50	3.33	4.58	5.00	5.42	5.83
0.08	0.31	0.63	0.94	1.25	1.88	2.50	3.44	3.75	4.06	4.38
0.10	0.25	0.50	0.75	1.00	1.50	2.00	2.75	3.00	3.25	3.50
0.15	0.17	0.33	0.50	0.67	1.00	1.33	1.83	2.00	2.17	2.33

The plots in Figures 5.8 and 5.9 show clear relationships between the percentage of debris pieces blocked (D) and the debris length to bar spacing ratio. Using the R^2 regression coefficient as a measure of goodness of fit, these relationships were best fitted by logarithmic functions with high R^2 regression coefficients ranging from 0.85 to 0.90. The functions and R^2 regression coefficients associated with these graphs are detailed in Table 5.3.

A paired t-test analysis was undertaken to determine whether there was a statistically significant difference in the percentage of blockage found in different test cases and the results are summarised in Tables 5.4 and 5.5.

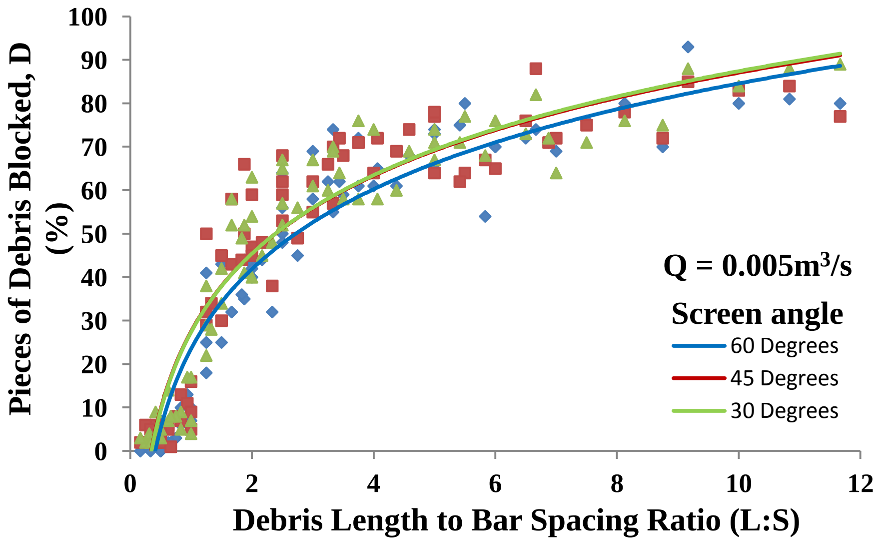

(a)

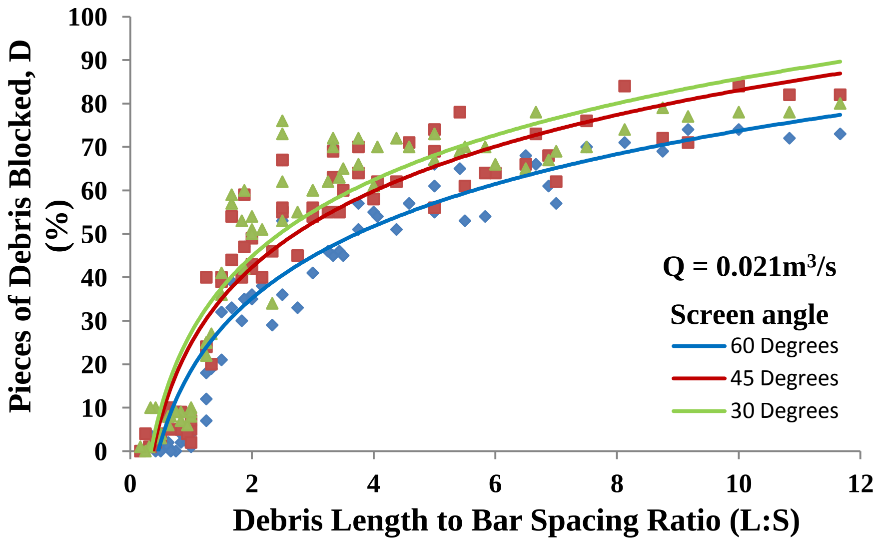

(b)

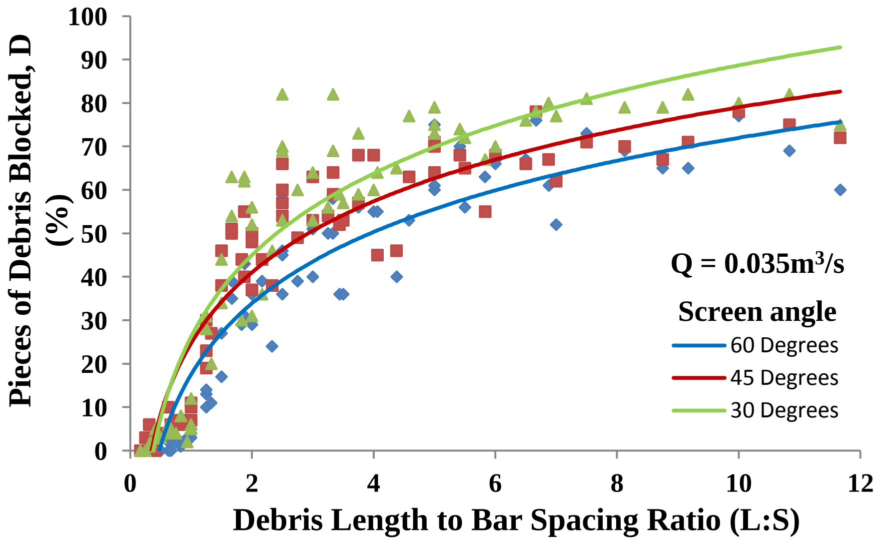

(c)

Figure 5.8 Graphs showing comparison of percentage of debris pieces blocked (D) at different screen angles when discharge is: (a) 0.005m^3/s, (b) 0.021m^3/s, (c) 0.035m^3/s. Each marker represents the percentage of 100 pieces of debris blocked.

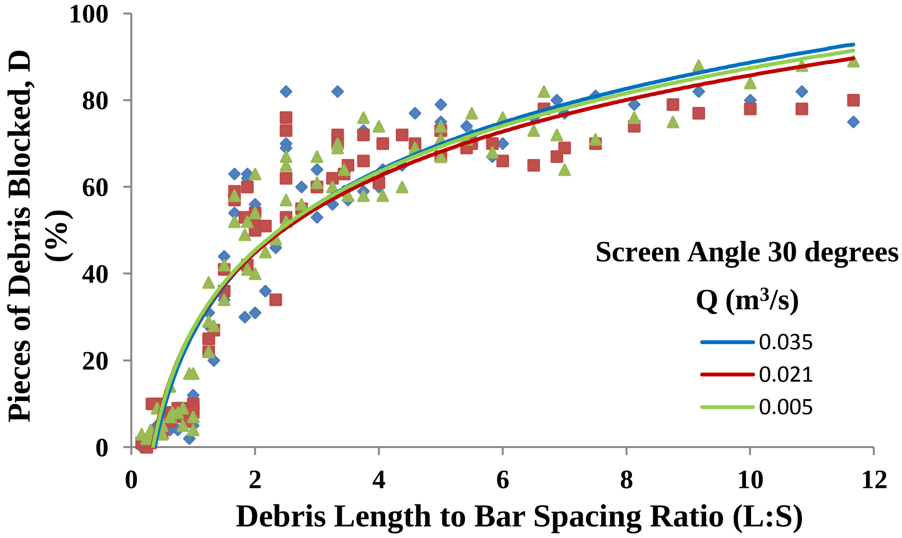

(a)

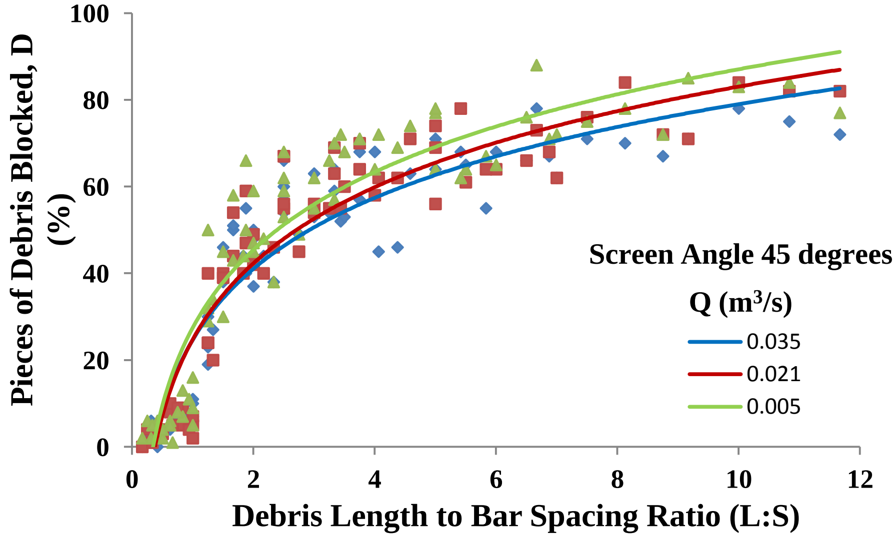

(b)

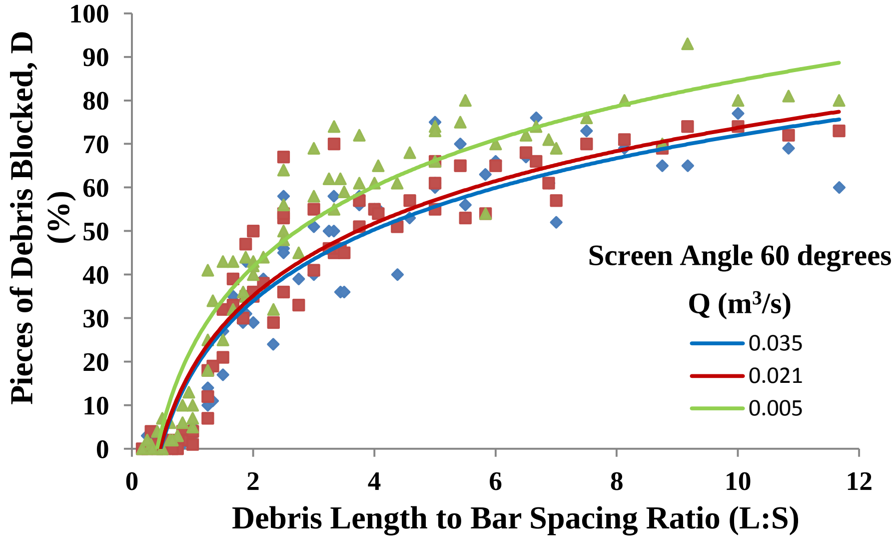

(c)

Figure 5.9 Graphs showing comparison of percentage of debris pieces blocked (D) for different discharges when screen angle is: (a) 30 degrees, (b) 45 degrees, (c) 60 degrees. Each marker represents the percentage of 100 pieces of debris blocked.

Table 5.3 Equations and corresponding R^2 regression coefficients for trends shown in Figures 5.8 and 5.9

Discharge (m^3/s)	Screen angle (degrees)	Trend function	R^2
0.005	30	D=26.09ln(L:S) + 27.31	0.89
0.005	45	D=25.88ln(L:S) + 27.46	0.87
0.005	60	D=26.54ln(L:S) + 23.45	0.90
0.021	30	D=25.40ln(L:S) + 27.21	0.86
0.021	45	D=25.31ln(L:S) + 24.76	0.87
0.021	60	D=23.96ln(L:S) + 18.55	0.87
0.035	30	D=27.14ln(L:S) + 26.16	0.85
0.035	45	D=23.61ln(L:S) + 24.65	0.87
0.035	60	D=23.66ln(L:S) + 17.51	0.86

Table 5.4 Paired t-test for comparison of different discharges. Critical t is1.99 (p=0.05).

Screen angle (degrees)	**Discharge 1 (m^3/s)**	**Discharge 2 (m^3/s)**	**t-stat**	**Significantly different**
30	0.005	0.021	0.73	No
30	0.005	0.035	0.36	No
30	0.021	0.035	-0.34	No
45	0.005	0.021	3.88	Yes
45	0.005	0.035	5.13	Yes
45	0.021	0.035	2.05	Yes
60	0.005	0.021	8.10	Yes
60	0.005	0.035	8.11	Yes
60	0.021	0.035	1.85	No

Table 5.5 Paired t-test for comparison of different angles. Critical t is 1.99 (p=0.05).

Discharge (m^3/s)	Screen angle 1 (degrees)	Screen angle 2 (degrees)	t-stat	Significantly different
0.005	30	45	0.02	No
0.005	30	60	3.94	Yes
0.005	45	60	3.92	Yes
0.021	30	45	3.53	Yes
0.021	30	60	11.09	Yes
0.021	45	60	9.78	Yes
0.035	30	45	4.64	Yes
0.035	30	60	10.28	Yes
0.035	45	60	8.44	Yes

The high R^2 regression coefficients for the plots shown in Figures 5.8 and 5.9 (see Table 5.3) suggest that the trends shown are a good fit to the experimental data. However, a noticeable feature of the experimental data is its asymptotic behaviour as L:S becomes large and this is perhaps not particularly well reflected in the selected trends which show a more sustained increase in blockage as L:S increases. Further experimental investigation looking at the same screen configurations with longer debris lengths would help to clarify blockage behaviour at higher ratios. Nonetheless, the trends represent the general blockage patterns found across all configurations assessed and can still offer a useful mechanism for comparison of performance between different configurations.

In addition to the general slight overestimation of blockage at high L:S, there are some other more specific deviations from the trends, a number of which are common to all the plots. A range of blockage percentages were recorded during testing for a single L:S. This is evident in all the plots and highlighted in Figure 5.10.

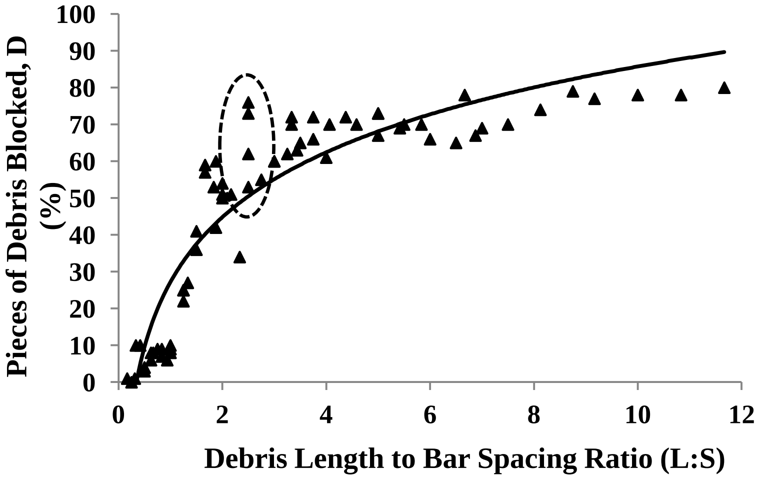

Figure 5.10 Example plot showing variation in blockage for a single debris length to bar spacing ratio.

It is particularly noticeable where L:S is 2.5 which is partly due to there being more debris length to bar spacing combinations that result in a 2.5:1 ratio. The higher percentages of blockage were recorded for the shorter debris lengths. This was found to be the general pattern where a range of blockage percentages were recorded for a single L:S greater than around 1.5.

Another feature of all the plots shown in Figures 5.8 and 5.9 is a group of results showing a percentage blocked noticeably above the general trend. As can be seen from the example plot shown in Figure 5.11 this group occurs where L:S is between 2 and 4. A number of the plots also show that the blockage recorded where L:S is large, greater than about 8, was generally lower than the general trend. The trend indicates a gradual increase in blockage as L:S increased. However, under some conditions the experimental data showed a drop in the percentage of blockage once L:S had reached 10. This is illustrated for an example plot in Figure 5.11. This reduction in blockage reflects the patterns shown in Figure 5.7 and as previously noted this apparent trend for increasingly reduced blockage at higher L:S is not what was expected and is unlikely to reflect what would generally happen.

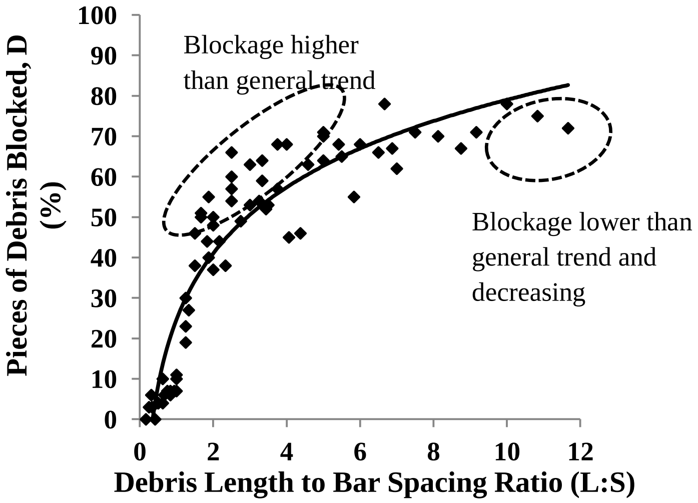

Figure 5.11 Example plot showing data clumping

5.2.3. Analysis

Bar Spacing

For all the screen angles and discharges assessed, as can be seen in Figures 5.8 and 5.9, there was a clear relationship between the percentage of debris pieces retained and the debris length to bar space ratio (L:S) whereby, as L:S increases more pieces of debris were likely to become blocked, a finding which is not unexpected. Using R^2 regression coefficients as a measure of goodness of fit, these relationships were best fitted by logarithmic functions and had high R^2 regression coefficients. The high R^2 values (0.85 to 0.90) indicate that the trends produced are a good fit to the test data. Where the ratio of debris length to bar spacing (L:S) is approximately 1.5 and less the major influencing factor was observed to be the length of clear space between the bars relative to the full length of the debris. Where L:S is greater than 1.5 the impact of the orientation of the debris on blockage was noticeably more significant resulting in greater variability in the amount of blockage that occurred. A number of factors can influence orientation including: debris length and buoyancy, position of the debris in the channel relative to the channel sides, initial orientation of the debris, flow depth and velocity, and flow patterns approaching and at the screen. During testing the longest lengths of debris had a greater tendency to align parallel with the flow direction and to travel mid-stream, a finding also noted by Lyn *et al*. (2003). Both of these factors facilitated the debris passage through the screen. This appeared to be due to the fact that longer lengths became aligned parallel to the flow direction more rapidly on their approach to the screen than shorter.

Screen Angle

Experiments were conducted for a range of screen angles (30, 45 and 60 degrees); the results of which are shown in Figure 5.8. Similar trends and goodness of fit were found to exist for the full range of discharges studied.

It is evident from these plots that the relationship between D and L:S varied with screen angle for all tested discharges. The difference in the predictive trends is quite small over the range of angles investigated particularly at low discharges. However, the plots show that higher screen angles resulted in consistently lower percentages of debris pieces blocked for any given value of L:S. The results from the paired t-test (Table 5.5) indicate that there was no significant difference in the results for screens of 30 degrees and 45 degrees when discharge was 0.005 m^3/s but all the other sets of results showed a statistically significant difference.

Observation of the test runs indicated that this effect may have been due to the fact that, at higher screen angles the bars intersected the water surface closer to the culvert inlet and were therefore closer to the zone of flow acceleration into the structure. This would have less impact at lower discharges. The zone of acceleration is important as debris elements which are initially randomly orientated tend towards aligning parallel with the flow as it accelerates and are therefore more likely to pass between the screen bars. In addition, at lower screen angles, a potentially higher bar surface area is likely to be in contact with the floating debris. As well as resulting in an increased area to trap the debris this also means the debris must overcome a greater resistance to move clear of the bars after initial contact. However, countering this, with the screen at 60 degrees which was the closest position to the culvert inlet, some of the larger pieces of debris initially cleared the screen with their leading end but then became jammed against the head wall as they rotated into the culvert entrance. The increased distance away from the head wall that resulted from lowering the screen angle to 45 or 30 degrees reduced the number of times this occurred.

Discharge

Experiments were conducted under a range of discharges. Figure 5.9 shows relationships between D and L:S for discharges of 0.005, 0.021 and 0.035 m^3/s at screen angles of 30, 45 and 60 degrees. It is evident from these results that, as discharge, and therefore approach flow velocity and depth increases, the proportion of debris pieces that became trapped at the screen falls. The blockage percentage at different discharges was not found to be significantly different when the screen angle was at 30 degrees (see Table 5.4). In addition no significant difference was found between the percentages of debris blocked for discharges of 0.021 and 0.035 m^3/s when the screen angle was 60 degrees. Two factors appear to be contributing to this. At higher flow velocities more pieces of debris had rotated to align parallel to the flow direction before they reached the screen, thereby facilitating their passage through the screen. Secondly, at lower flow rates, the debris had a greater tendency to reach a balance point across a single bar while at higher flows the debris may be initially stopped by a single bar but would rotate round the bar and clear the screen. At higher flows changes in flow paths due to the constriction of the flow as it entered the culvert was more noticeable.

5.2.4. Empirical relationship

From the analysis described in Sections 5.2.1 to 5.2.3, bar spacing, debris length, screen angle and discharge were identified as potential influencing factors in determining the amount of debris blocked. Regression analysis was used to establish an empirical relationship between these contributing factors and blockage potential. The hypothetical relationship can be formalized by

$$D = f\,(A, S, L, Q) \qquad (15)$$

Where D = percentage of debris pieces blocked (%), A = screen angle (degrees), S = bar spacing (m), L = debris length (m), and Q = discharge (m^3/s). A log transformation (logit) was used during the regression analysis to allow limits to be set on the dependent variable (D). As D represents the percentage of pieces blocked, the limits were set at 0 and 100. After transformation a stepwise multiple regression analysis was performed using a 95% probability significance limit. Output from the regression analysis can be found in Appendix E.

The R^2 value from the ANOVA analysis was used as a measure of goodness of fit. A quadratic function was found to provide the best solution (Equation 16).

$$\ln\left[\frac{(D)}{100-D}\right] = 0.0513+30.728L-64.303L^2-53.428S+115.236S^2-0.017A-8.823Q+56.441LS \quad (16)$$

The generated model had a high adjusted R^2 value, 0.87, indicating that it was a good fit to the experimental data and a high Prediction R^2 value, 0.87, indicating it had good predictive capabilities. Adjusted R^2 is a modification of R^2 that takes into account the number of terms in a model. Prediction R^2 indicates how well the model predicts responses for new observations. While the high adjusted R^2 values indicate the model is a good representation of the experimental data even allowing for the large number of terms, Equation 16 is perhaps overly cumbersome and some form of simplification that results in a reduction in the number of terms may be helpful to provide a more workable model (see Section 6.5). However the inclusion of all the terms contributing to the model can be justified by consideration of their theoretical impact on the ability of a screen to block debris. Debris length and bar spacing will have a major role in determining whether a piece of debris becomes blocked so their inclusion in the model along with a cross product that considers the impact of a combination of these two key terms is essential. Flow conditions will influence both how debris is transported to a screen and how likely it is to be forced through the screen therefore discharge, given that it contributes to different flow conditions, seems a reasonable inclusion at this stage. The inclusion of screen angle in the model is perhaps less obviously a key requirement. However, different screen angles can offer different surface areas of the screen both in terms of total area and area available for debris storage. In addition different screen angles can result in different flow patterns at the screen therefore screen angle could potentially influence blockage.

A plot of the percentage of debris pieces the model predicts will be blocked against the percentage recorded as blocked during the initial testing is shown in Figure 5.12.

Debris length (L), bar spacing (S), screen angle (A), and discharge (Q) were found to be significant predictive factors; all factors had p-values < 0.0001. Figures 5.13 to 5.16 show the individual contributions made by each element within the generated model.

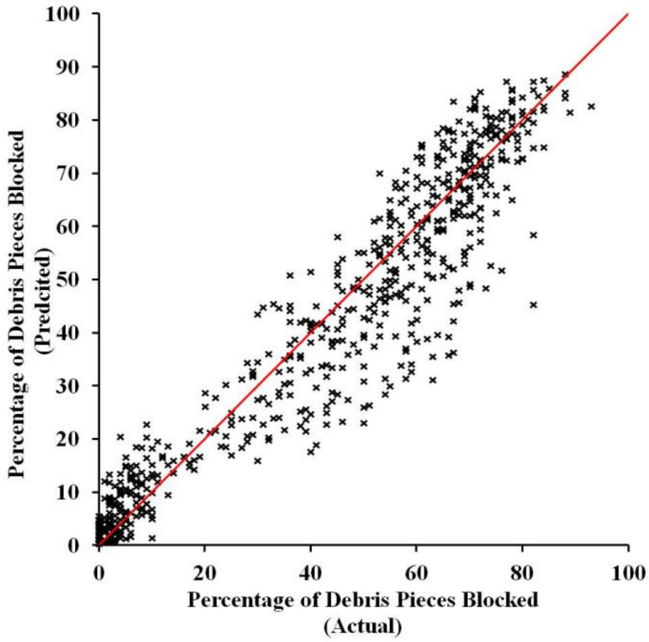

Figure 5.12 Modelled predicted blockage against actual debris pieces blocked during phase 1 testing. The position where actual equals predicted is shown by the red line.

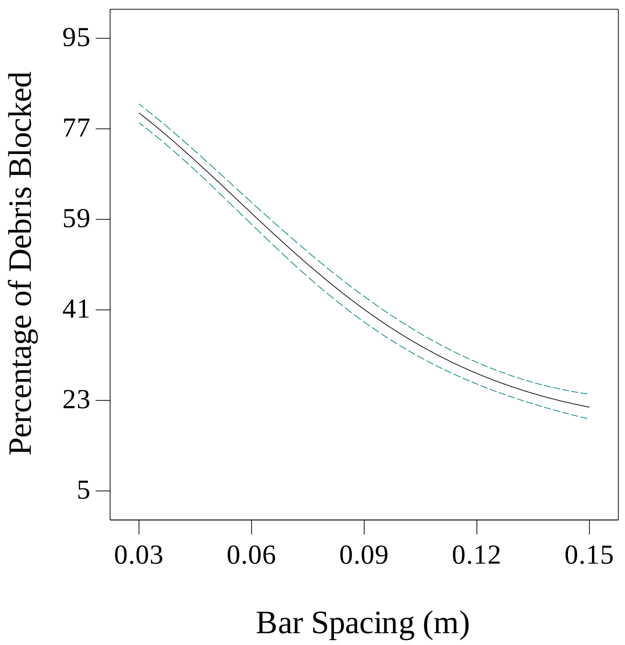

Figure 5.13 Influence of bar spacing on percentage blockage when screen angle = 45°, discharge = 0.021m^3/s, debris length = 0.18m. Similar trends were found for other tested angles, discharges and debris lengths. The dotted green lines show the 95% confidence interval.

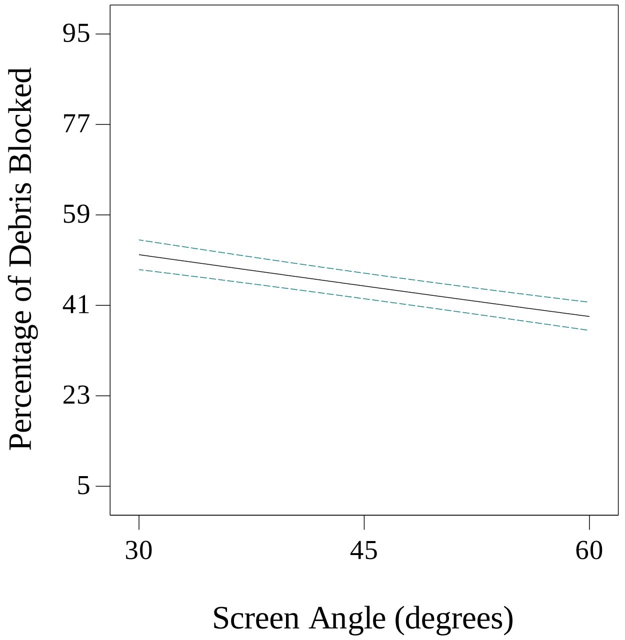

Figure 5.14 Influence of screen angle on percentage blockage when bar spacing = 0.08m, discharge = 0.021m^3/s, debris length = 0.18m. Similar trends were found for other tested bar spacings, discharges and debris lengths. The dotted green lines show the 95% confidence interval.

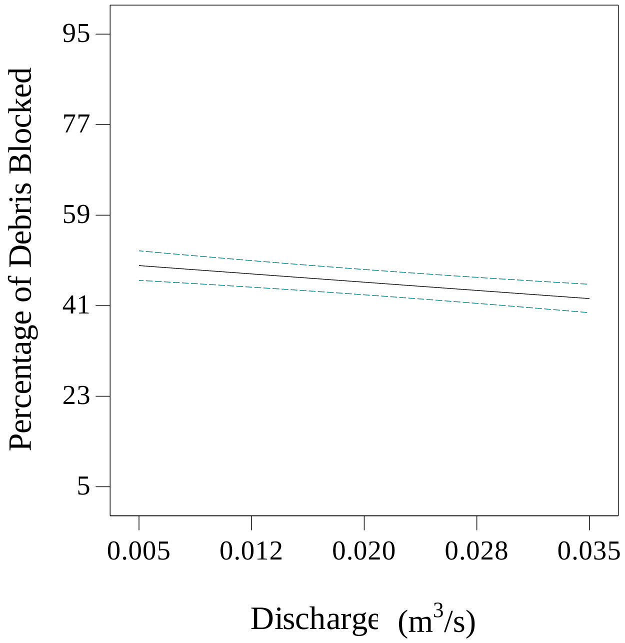

Figure 5.15 Influence of discharge on percentage blockage when screen angle = 45°, bar spacing = 0.08m, debris length = 0.18m. Similar trends were found for other tested angles, bar spacings and debris lengths. The dotted green lines show the 95% confidence interval.

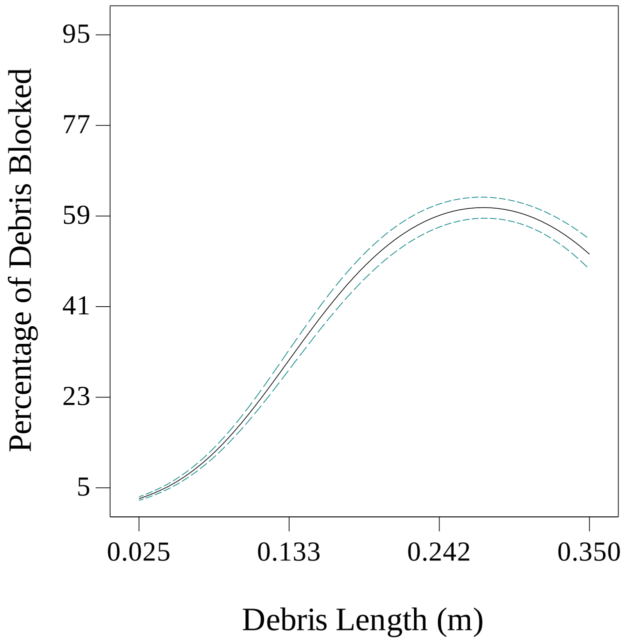

Figure 5.16 Influence of debris length on percentage blockage when screen angle = 45°, bar spacing = 0.08m, discharge = 0.021m^3/s. Similar trends were found for other tested screen angles, bar spacings and discharges. The dotted green lines show the 95% confidence interval.

As can be seen from Figure 5.13, as would be expected, less blockage occurs as bar spacing increases, this is reflected in the negative value for the bar spacing coefficient in the model. The influence of debris length is also in general as expected with blockage increasing as length increases as indicated by the positive bar spacing coefficient in the model. However Figure 5.16 shows that while there is an initial increase in blockage with increasing debris length, once a threshold length has been reached, blockage appears to decrease as length increases. As noted in Section 5.2.3 this may be in part due to larger pieces of debris being more likely to orientate parallel to the flow direction or it may be due to some other unidentified factor related to the experimental method. Alternatively it may just be natural variation in the results although the samples size should have minimised this. It is unlikely that the amount of blockage would continue to decrease as debris length increases as appears to be suggested by this trend. Both screen angle and discharge have negative coefficients in the generated model suggesting that blockage decreases as their values increase. The trend for screen angle is illustrated in Figure 5.14. However the results from the testing of the influence of screen angle may have been influenced by the position of the screen intersection with the water surface as well as the angle itself. If a screen is positioned so that the top of the screen is attached to the headwall, a screen of 60 degrees intersects the water surface closer to the culvert than a screen of 30 degrees (Figure 5.17). Further testing is required to determine the influence of screen angle independent of screen position (See Section 5.4).

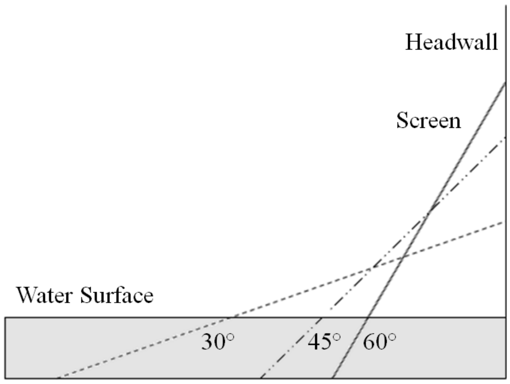

Figure 5.17 Diagram showing relative position of screens of different angles.

The slope of the trend for discharge (Figure 5.15) is very shallow suggesting that discharge does not greatly influence the percentage of debris blocked. However, as indicated by the negative coefficient, there is a slight decrease in blockage as discharge increases which may be the result of the lower flow velocities associated with lower discharges which do not as readily move pieces of balanced debris away from an obstacle once they have become initially trapped.

As a further measure of the contribution made by each of the individual elements, a sensitivity analysis was undertaken. The predicted blockage percentage (D) was calculated from the derived function for a mid value from the range tested (L=0.18m, S=0.08m, A=45 degrees, Q=0.021m^3/s, D = 45.6). Predicted blockage values were then calculated when one element was increased and then decreased by 25% of its initial value while the other element values remained unchanged. As can be seen from Figure 5.18, as would be expected debris length (L) and bar spacing (S) have a significant impact, screen angle (A) has less of an influence than these two while discharge (Q) has very little impact.

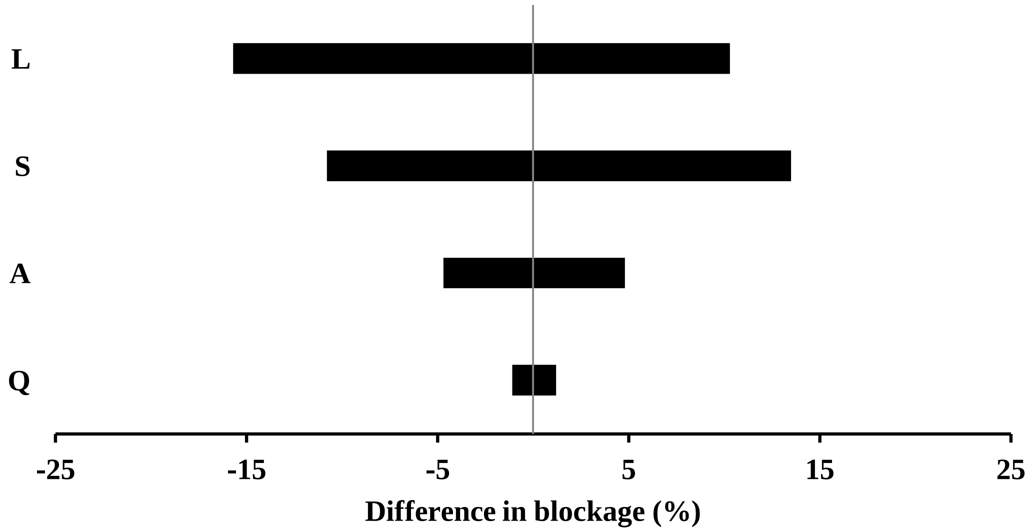

Figure 5.18 Sensitivity analysis for model generated from phase 1 testing showing change in predicted percentage of debris blocked when varying predictor variables by ±25%. L = Debris length, S=Bar spacing, A = Screen Angle, Q = Discharge

5.2.5. Recommendation for next step

Given the results from this initial investigation, it was concluded that some further analysis was required to gain a better understanding of the interaction of the screen and the flow conditions. Two further testing programs were undertaken. The first additional phase of testing considered changes in flow conditions due to increasing bed slope and is discussed in Section 5.3, the second additional phase assessed the influence of screen position relative to the culvert inlet and is discussed in Section 5.4.

5.3. The Influence of Bed Slope

5.3.1. Overview

This section presents and analyses the results obtained during a set of experimental investigations into how different flow conditions resulting from differing bed slopes influence blocking potential at trash screens. The objective of the second phase of testing was to determine whether the trends identified during the initial testing were applicable under different flow conditions and to identify whether different flow conditions resulting from changes in bed slope had an independent influence on blockage potential. A summary of the elements and conditions assessed during this second phase of testing are shown in Table 5.6.

Table 5.6 Elements assessed during the second phase of testing

Slopes assessed	Number of angles assessed	Number of bar spacings assessed	Number of discharges assessed	Number of test cases	Number of debris passes made
3	3	7	1	63	63000

As only one discharge was required for this phase of testing, the highest discharge used during the initial testing, 0.035m^3/s, was selected. During initial testing this was found to be the simplest of the discharges to repeat and stabilise. The bar spacings and screen angles tested were as described in Section 5.2 for the initial testing.

Testing was undertaken for two bed slopes steeper than the slope used in the initial testing and the results achieved were assessed along with the relevant results from the initial testing. The highest slope (0.016m/m) was selected because with a discharge of 0.035 m^3/s this was the steepest operating slope that ensured the culvert inlet did not become submerged.

Table 5.7 shows details of the slopes and flow conditions assessed.

Table 5.7 Slopes assessed during second phase of testing

Slope ID	Slope (m/m)	Discharge (m^3/s)	Depth averaged velocity (m/s)	Water depth (m)	Froude number
1	0.006	0.035	0.266	0.175	0.20
2	0.012	0.035	0.324	0.143	0.27
3	0.016	0.035	0.358	0.130	0.32

5.3.2. Results

Full details of the results obtained during the second phase of testing can be found in Table C.1, Appendix C.

The results are summarised in Figures 5.19 and 5.20 which show the percentage of pieces of debris blocked for each test case. Each test case represents a different combination of screen angle, bar spacing and slope. A paired t-test analysis was undertaken to determine any statistically significant difference in the percentage of blockage found for different slopes and the results are summarised in Table 5.8.

Table 5.8 Paired t-test for comparison of different slopes. Critical t is 1.99 (p=0.05).

Screen angle (degrees)	Slope A (m/m)	Slope B (m/m)	t-stat	Significantly different
30	0.0055	0.0120	-0.43	No
30	0.0055	0.0160	-1.48	No
30	0.0120	0.0160	-1.55	No
45	0.0055	0.0120	-2.04	Yes
45	0.0055	0.0160	-4.19	Yes
45	0.0120	0.0160	-2.60	Yes
60	0.0055	0.0120	-0.51	No
60	0.0055	0.0160	-4.15	Yes
60	0.0120	0.0160	-3.97	Yes

The plots shown in Figures 5.19 and 5.20 show the same general patterns of trends and outliers to those discussed in Section 5.2.2.

Figure 5.20 shows clear relationships between the percentage of debris pieces blocked (D) and the debris length to bar spacing ratio that follow similar trends for all slopes. In common with the results obtained from initial testing, those obtained for slopes two and three (0.012m/m, 0.016m/m) were also best fitted by logarithmic functions and had high R^2 regression coefficients ranging from 0.85 to 0.90. The functions and R^2 regression coefficients associated with the graphs shown in Figures 5.19 and 5.20 are detailed in Table 5.9.

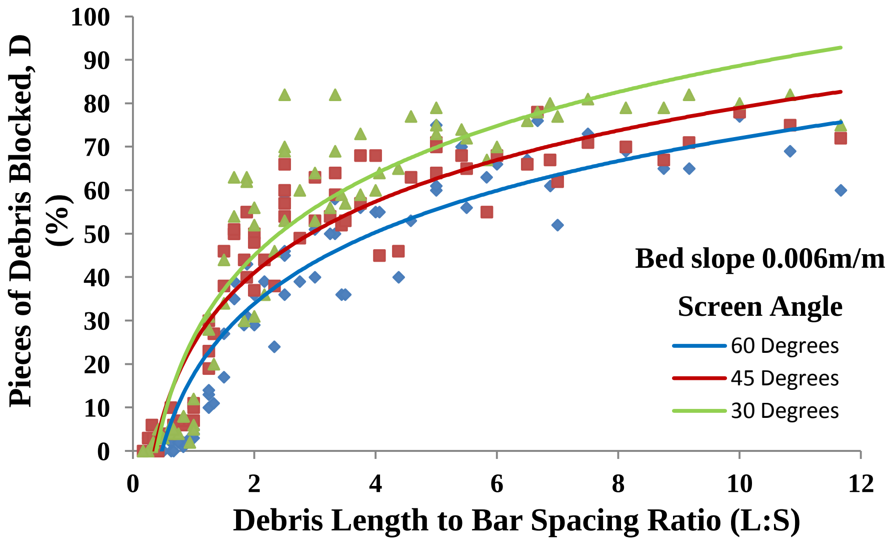

(a)

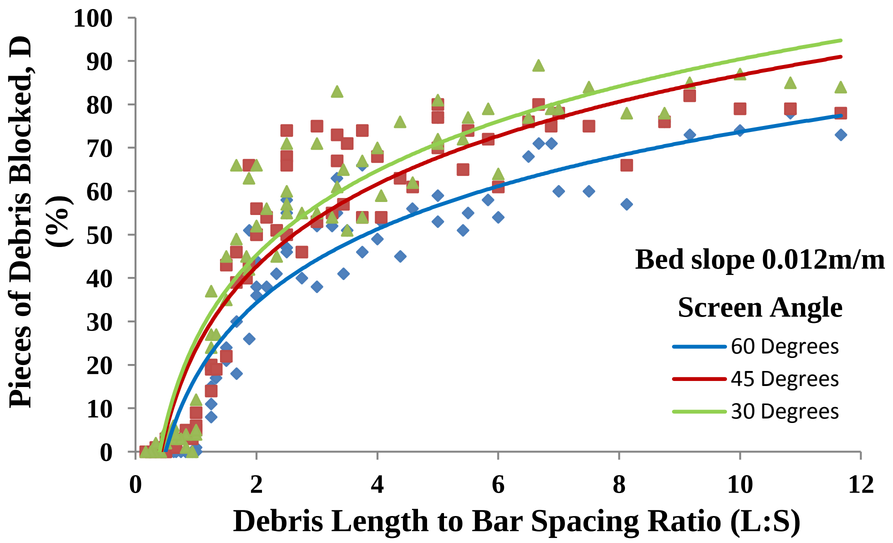

(b)

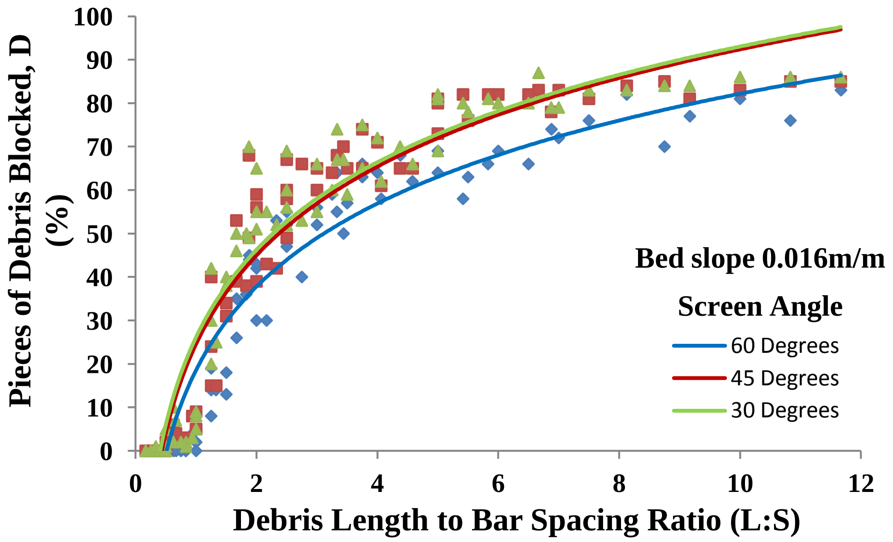

(c)

Figure 5.19 Graphs showing comparison of percentage of debris pieces blocked (D) for different screen angles when discharge is: 0.035m^3/s and bed slope is (a) 0.006m/m (b) 0.012m/m (c) 0.016m/m .

Each marker represents the percentage of 100 pieces of debris blocked.

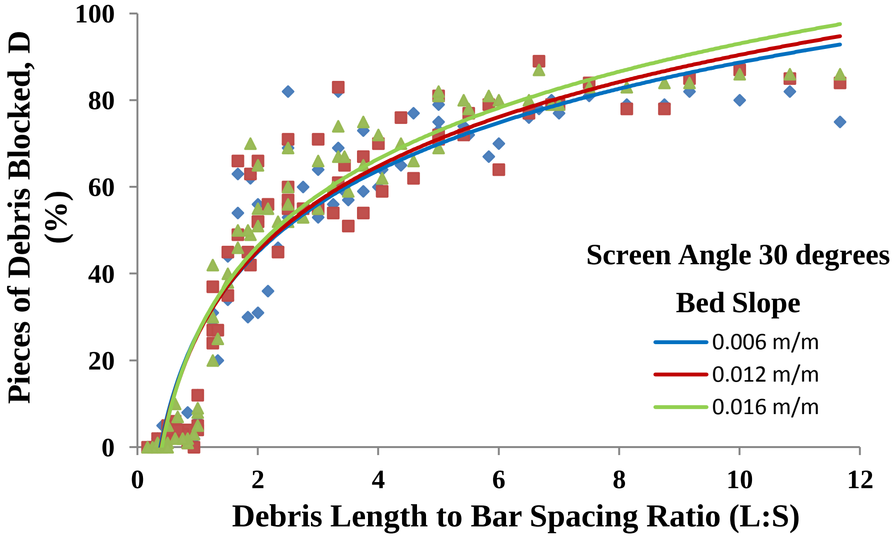

(a)

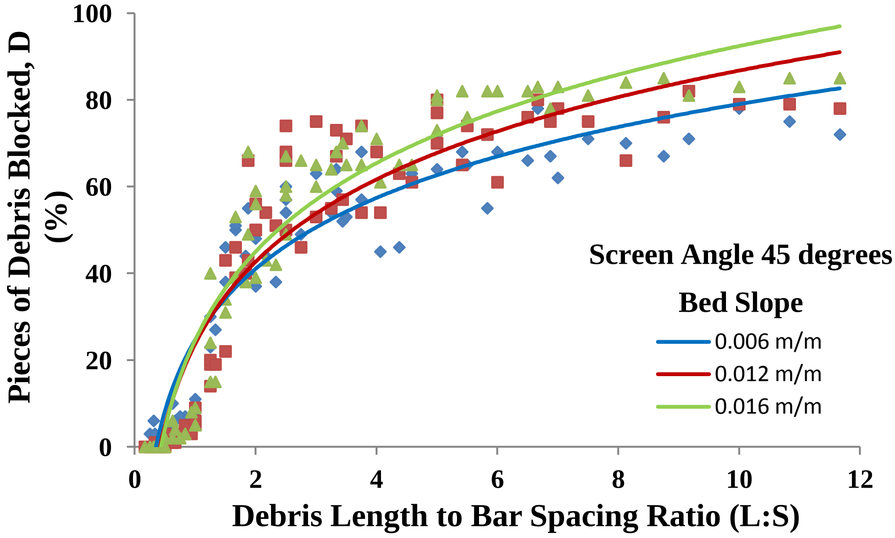

(b)

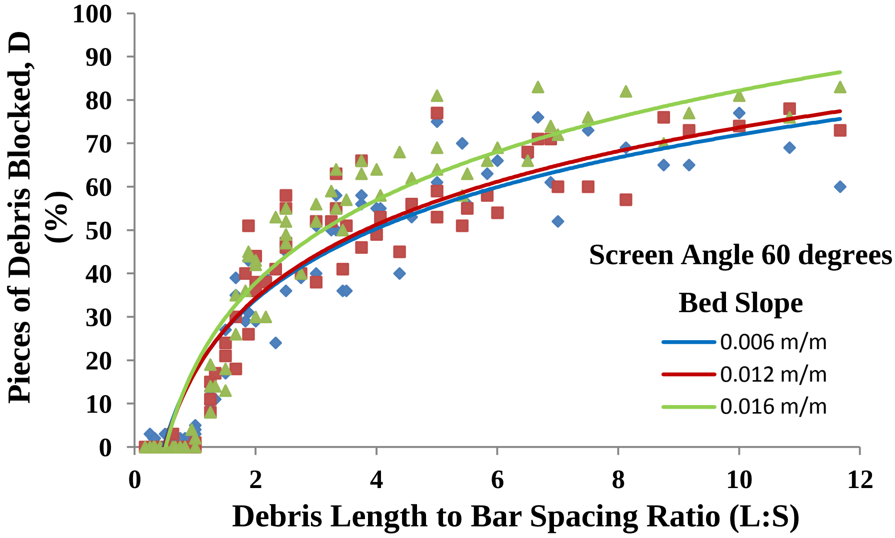

(c)

Figure 5.20 Graphs showing comparison of percentage of debris pieces blocked (D) for different bed slopes when discharge is 0.035m^3/s and screen angle is: (a) 30 degrees, (b) 45 degrees, (c) 60 degrees.

Each marker represents the percentage of 100 pieces of debris blocked.

Table 5.9 Equations and corresponding R^2 regression coefficients for trends shown in Figures 5.19 and 5.20

Discharge (m^3/s)	Bed slope (m/m)	Screen angle (degrees)	Trend function	R^2
0.035	0.006	30	D = 27.14ln(L:S) + 26.16	0.85
0.035	0.006	45	D = 23.60ln(L:S) + 24.65	0.87
0.035	0.006	60	D = 23.66ln(L:S) + 17.51	0.86
0.035	0.012	30	D = 28.04ln(L:S) + 25.85	0.87
0.035	0.012	45	D = 27.37ln(L:S) + 23.70	0.85
0.035	0.012	60	D = 24.45ln(L:S) + 17.34	0.86
0.035	0.016	30	D = 29.03ln(L:S) + 26.18	0.90
0.035	0.016	45	D = 29.44ln(L:S) + 24.59	0.89
0.035	0.016	60	D = 27.59ln(L:S) + 18.65	0.89

5.3.3. Analysis

As can be seen from Figures 5.19 and 5.20 the relationship between the percentage of debris pieces retained and the debris length to bar space ratio identified during the initial testing, outlined in Section 5.2, appears to be reproduced for all assessed slopes. While the general trends are similar for all slopes, there is a difference in the performance of different screen angles under different bed slopes. Figure 5.20a shows that the screen at 30 degrees showed almost no change in performance across all bed slopes and the results of the t-test (Table 5.8) indicate that the performance is not significantly different. However, the screen at 45 degrees showed an increasing tendency to block debris as the bed slope increases and the paired t-test results suggest there is a statistically significant difference between each slopes performance. A difference in performance is also apparent for a 60 degree screen although at this angle there does not appear to be a significant difference at the two lower slopes.

This change in performance under different flow conditions due to changes in bed slope may be the result of changes in the position of the screen relative to the maximum flow disturbance as the water is restricted at the culvert inlet. Increasing the bed slope increased the water depth immediately behind the headwall and reduced the depth to some degree further upstream. In addition, increasing the bed slope reduced the distance over which the most intense flow turbulence occurred. Therefore changing the slope may have resulted in the point of intersection of the screen with the water surface moving its position relative to the zone of maximum acceleration created by constriction at the culvert inlet. For example Figure 5.20(c) shows that most blockage occurs at a screen of 60 degrees where the bed slope is 0.016m/m. At this slope the point of intersection of the screen with the water surface may be situated upstream of the zone of acceleration while at the reduced bed slopes the screen still sits within the zone. Further research is necessary to clarify the role of screen position relative to inlet flow conditions(see Section 5.4).

5.3.4. Empirical Relationship

The analysis described in Section 5.2 identified bar spacing, debris length, screen angle and discharge as influencing factors in determining the amount of debris blocked. For the analysis described in this section an additional variable, bed slope, was considered while the discharge remained constant. A regression analysis was used to establish an empirical relationship between contributing factors and blockage potential. The hypothetical relationship can be formalized by

$$D = f(A, S, L, B) \tag{17}$$

Where D = percentage of debris pieces blocked (%), A = screen angle (degrees), S = bar spacing (m), L = debris length (m), and B = bed slope (m/m). A log transformation (logit) was used during the regression analysis to allow limits to be set on the dependent variable (D). As D represents the percentage of pieces blocked, the limits were set at 0 and 100. After transformation a stepwise multiple regression analysis was performed using a 95% probability significance limit. Output from the regression analysis can be found in Appendix F.

A quadratic function was found to provide the best solution (Equation 18).

$$\ln\left[\frac{(D)}{100\text{-}D}\right] = -0.176 + 33.742L - 71.394L^2 - 59.448S + 125.617S^2 - 0.018A + 68.936LS \quad (18)$$

While screen angle, debris length and bar spacing were again found to be significant predictive factors, bed slope (B), while considered as a potentially contributing function in the hypothetical relationship (Equation 17), was not found to be significant and is therefore not included in the model. Although the generated model had a high adjusted R^2 value, 0.85 indicating that it was a good fit to the test generated data and a high Prediction R^2 value, 0.84, indicating it had good predictive capabilities it was found to offer no improvement to the model generated from the initial testing (Equation 16). A plot of the percentage of debris pieces the model predicts will be blocked against the percentage actually blocked during testing is shown in Figure 5.21. This shows a similar pattern to that produced for the original model (see Section 5.2) but there is a noticeably greater variation between observed and predicted blockage.

As the model was found to offer no improvement to the original model no further sensitivity analysis was undertaken.

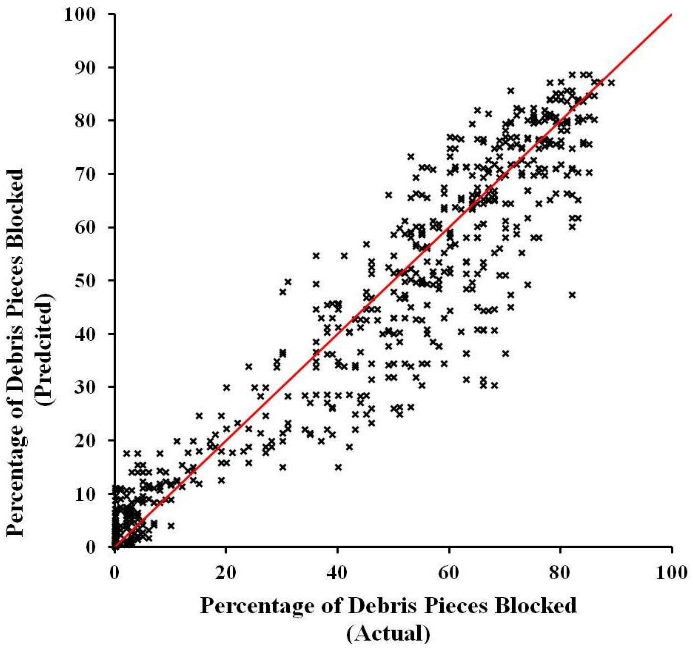

Figure 5.21 Modelled predicted blockage against actual debris pieces blocked during phase 2 testing. The position where actual equals predicted is shown by the red line.

5.4. The Influence of Screen Position Relative to Culvert Inlet

5.4.1. Overview

This section presents and analyses the results obtained during a set of experimental investigations into how the position of the trash screen relative to the culvert inlet influenced its blocking potential.

As a result of the findings of the initial testing which is detailed in Section 5.2, a follow up phase of testing was undertaken to investigate how the location of the trash screen relative to the entrance of the culvert influences potential blockage. Observations made during the initial testing suggested that as flow accelerates on nearing the culvert entrance it exerts forces on the debris that effect both its orientation relative to the flow direction and its potential for being pulled through the screen bars. Therefore, it appeared that under the experimental flow regime the location of the trash screen relative to the zone of flow acceleration which is generated as the watercourse is restricted to flow through the culvert may have influenced the amount of debris blocked by the screen.

In order to assess the influence of screen position two different assessments were undertaken:

1 An assessment of the blocking potential of screens at different angles that intersected the water surface at the same point upstream of the culvert inlet

2 An assessment of the blocking potential of a screen with an angle of 60 degrees at different positions upstream of the culvert inlet

A summary of the elements and conditions assessed during the third phase of testing are shown in Tables 5.10 and 5.11.

Table 5.10 Elements assessed during part 1 of the third phase of testing

Screen positions assessed	Number of angles assessed	Number of bar spacings assessed	Number of discharges assessed	Number of test cases	Number of debris passes made
1	3	7	1	21	21000

Table 5.11 Elements assessed during part 2 of the third phase of testing

Screen positions assessed	Number of angles assessed	Number of bar spacings assessed	Number of discharges assessed	Number of test cases	Number of debris passes made
4	1	7	1	28	28000

The bar spacings and bed slope tested were as described in Table 4.2 for the initial testing. As previously observed differences in blockage were more marked at higher discharges, the highest discharge used during the initial testing, 0.035m^3/s, was used during both parts of the screen position testing.

During assessment one, a single screen position was tested with screens of different angles (30, 45 and 60 degrees). The screens were placed so the point of intersection of the screen with the water surface was the same for all screen angles (see Figure 5.22). This differed from the approach used during the initial phase of testing (Section 5.2) where the top of the screens were fixed at a common point which resulted in them intersecting the water surface at different positions.

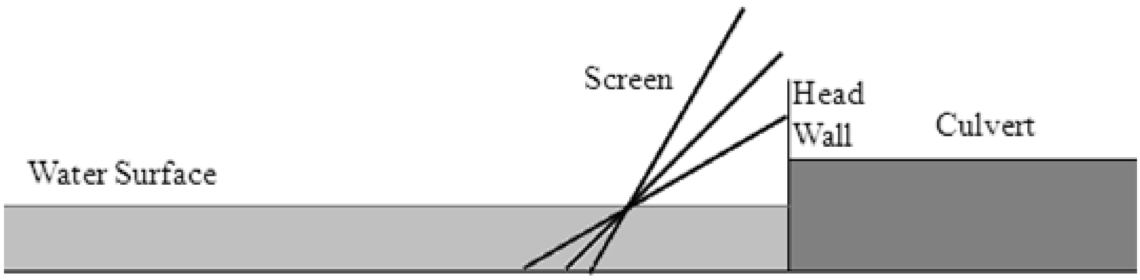

Figure 5.22 Schematic representation of screen positions used for the first assessment

During assessment two, four positions were tested for a screen at 60 degrees (Figure 5.20). An angle of 60 degrees was selected as this allowed testing of a position closer to the inlet than would have been possible with screens of 45 or 30 degrees while still allowing the screen to be positioned at any other point further upstream. Therefore a greater range of positions relative to the culvert inlet could be assessed. The distance upstream was measured from the culvert inlet to the point at which the screen intersected the water surface. Table 5.12 shows the screen positions assessed.

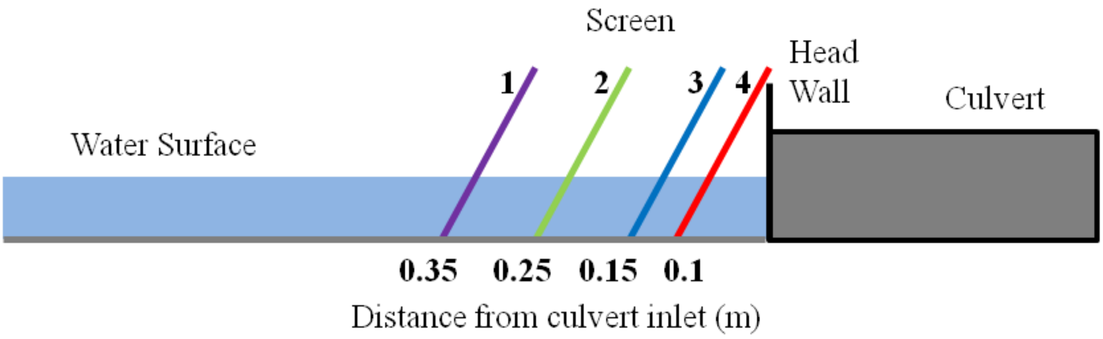

Figure 5.23 Schematic representation of screen positions used during second assessment

Table 5.12 Screen positions assessed during the third phase of testing

Position	Distance upstream from culvert inlet (m)
1	0.35
2	0.25
3	0.15
4	0.10

5.4.2. Results

Full details of the results obtained during the third phase of testing can be found in Tables D.1 and D.2, Appendix D.

The results from assessment one, testing a screen of different angles intersecting the water surface at the same position, are summarised in Figure 5.24. The functions and R^2 regression coefficients associated with these graphs are detailed in Table 5.13.

The results from assessment two, testing a screen of 60 degrees intersecting the water surface at different positions, are summarised in Figure 5.25. The functions and R^2 regression coefficients associated with these graphs are detailed in Table 5.14.

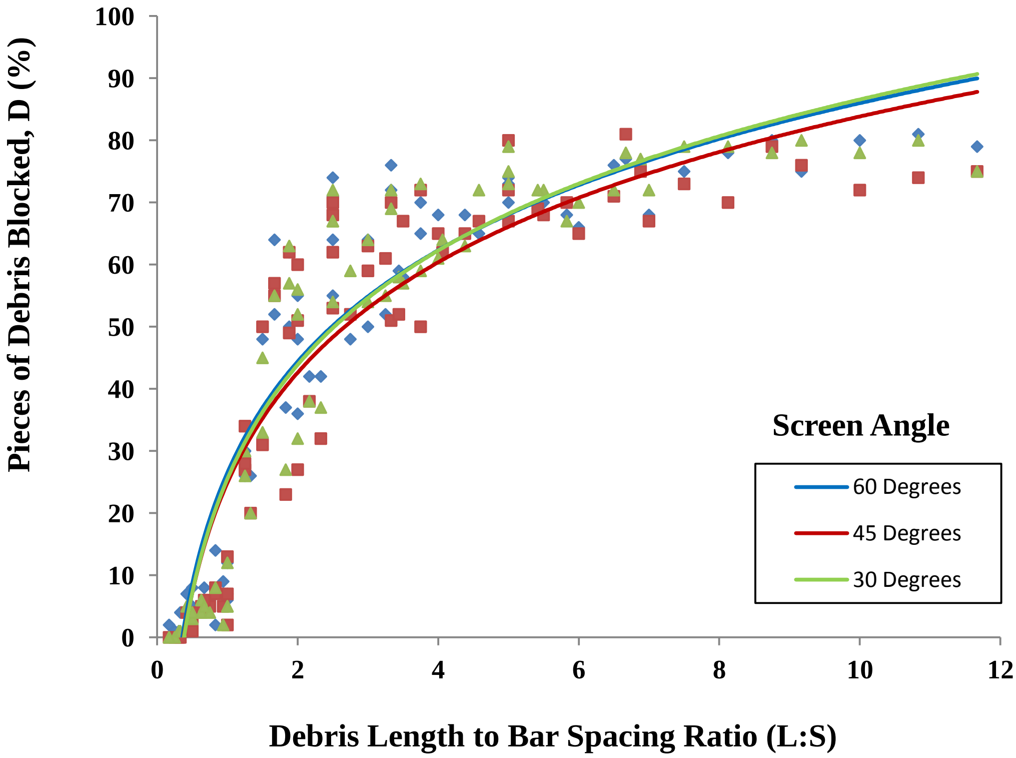

Figure 5.24 Graphs showing comparison of percentage of debris pieces blocked (D) at different screen angles when screens intersect the water surface at the same position. Each marker represents the percentage of 100 pieces of debris blocked.

Table 5.13 Equations and R^2 regression coefficients for in Figure 5.24

Screen angle (degrees)	Trend function	R^2
30	D = 26.54ln(L:S) + 24.46	0.87
45	D = 25.62ln(L:S) + 24.84	0.85
60	D = 25.84ln(L:S) + 26.48	0.87

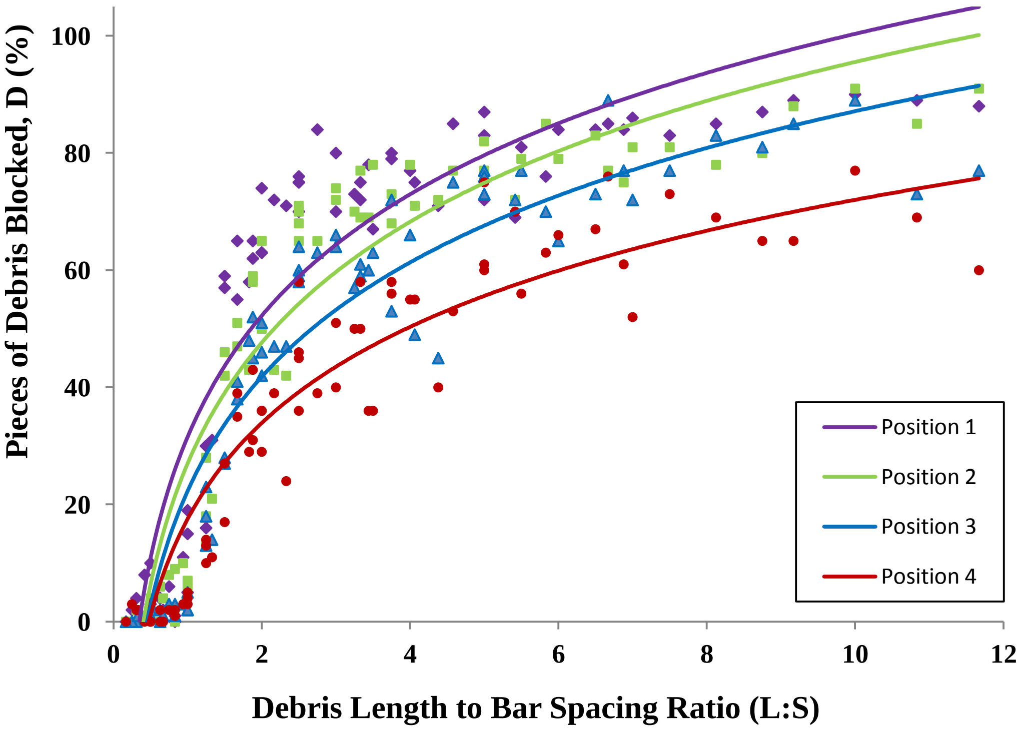

Figure 5.25 Plot showing comparison of percentage of debris pieces blocked (D) at different screen positions (screen angle 60°). Each marker represents the percentage of 100 pieces of debris blocked.

Table 5.14 Equations and corresponding R^2 regression coefficients for Figure 5.25

Screen position	Trend function	R^2
1	D = 29.87ln(L:S) + 31.53	0.85
2	D = 29.76ln(L:S) + 26.99	0.88
3	D = 28.16ln(L:S) + 22.28	0.88
4	D = 23.66ln(L:S) + 17.51	0.86

For both sets of results, paired t-test analysis was undertaken to determine whether there was a statistically significant difference between percentages of blockage found and the results are summarised in Tables 5.15 and 5.16.

Table 5.15 Paired t-test for comparison of different angles at a single position. Critical t is 1.99 (p=0.05).

Screen angle 1 (degrees)	Screen angle 2 (degrees)	t-stat	Significantly Different
30	45	-3.08	Yes
30	60	0.69	No
45	60	2.99	Yes

Table 5.16 Paired t-test for comparison of one angle at different positions. Critical t is 1.99 (p=0.05).

Distance from inlet (m)	Distance from inlet (m)	t-stat	Significantly different
0.35	0.25	5.00	Yes
0.35	0.15	-9.71	Yes
0.35	0.10	12.23	Yes
0.25	0.15	6.49	Yes
0.25	0.10	10.84	Yes
0.15	0.10	8.16	Yes

5.4.3. Analysis

Different Screen Angles at One Position

As can be seen from the results for assessment one (Figure 5.24), the difference found in the percentage of debris blocked by different screen angles when they intersected the water at the same position was relatively minor. However, while the results of the t-test (Table 5.15) showed no statistically significant difference between the results for the screen at 30 degrees and the screen at 60 degrees they did show a small but statistically significant difference between the screen at 45 degrees and both the other angles. This suggests that although screen angle may make a minor contribution to a screen's potential for blocking debris, the difference found in blockage for different screen angles during initial testing (Section 5.2) may have been influenced more by the position at which the screen intercepted the water surface than the actual screen angle. The nature of the influence of screen angle on blockage is still not clear from these findings.

One Screen Angle at Different Positions

The plot of the results of assessment two (Figure 5.25) shows that as the distance of the screen from the culvert inlet increased the percentage of debris pieces blocked also increased. The differences in these results were all found to be statistically significant (Table 5.16). The greatest increase in percentage blocked was found to occur between positions 3 and 4, with the least difference in blockage occurring between screens 1 and 2. The differences in blockage correspond to the differences in the measured mid stream flow velocity at the screen (Table 5.17). From Figure 5.26 it can be seen that as the flow approached the culvert inlet the midstream depth averaged velocity increased. At screen position 4, the closest position to the culvert inlet, the velocity was approximately 80 percent of the maximum velocity reached by the flow before entering the culvert, at position 1 the velocity was only approximately 50 percent of the maximum velocity. Although considerable constriction of the flow across the width of the channel was evident on approach to the culvert, flow constriction in the middle region of the channel was observed to be minimal and so only a longitudinal component of velocity was considered.

Table 5.17 Mid stream depth averaged velocities measured in the flume during phase three .

Screen Position	Depth averaged velocity at screen intersection with water surface (m/s)
1	0.249
2	0.270
3	0.340
4	0.407
2.25m upstream	0.232

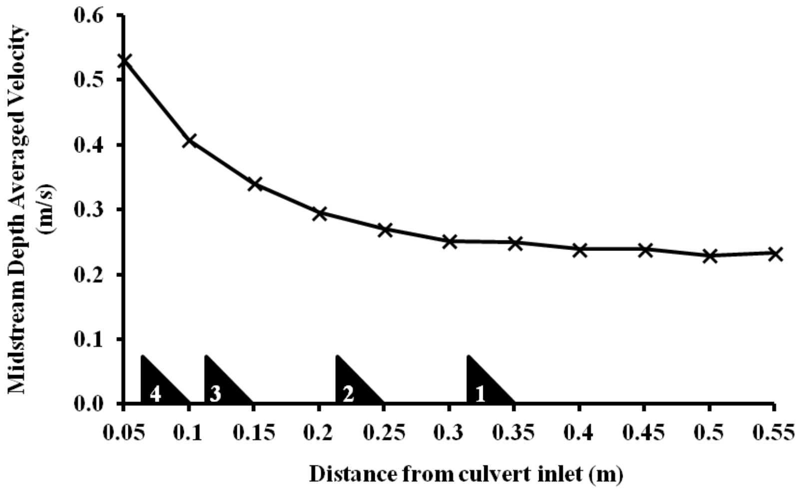

Figure 5.26 Plot of flume midstream depth averaged velocity and test screen position (◣).

Similar velocity patterns were found by Day (1997) who noted that a culvert exerts a major influence over longitudinal velocities for distances upstream approximately equivalent to the culverts diameter (Figure 5.27).

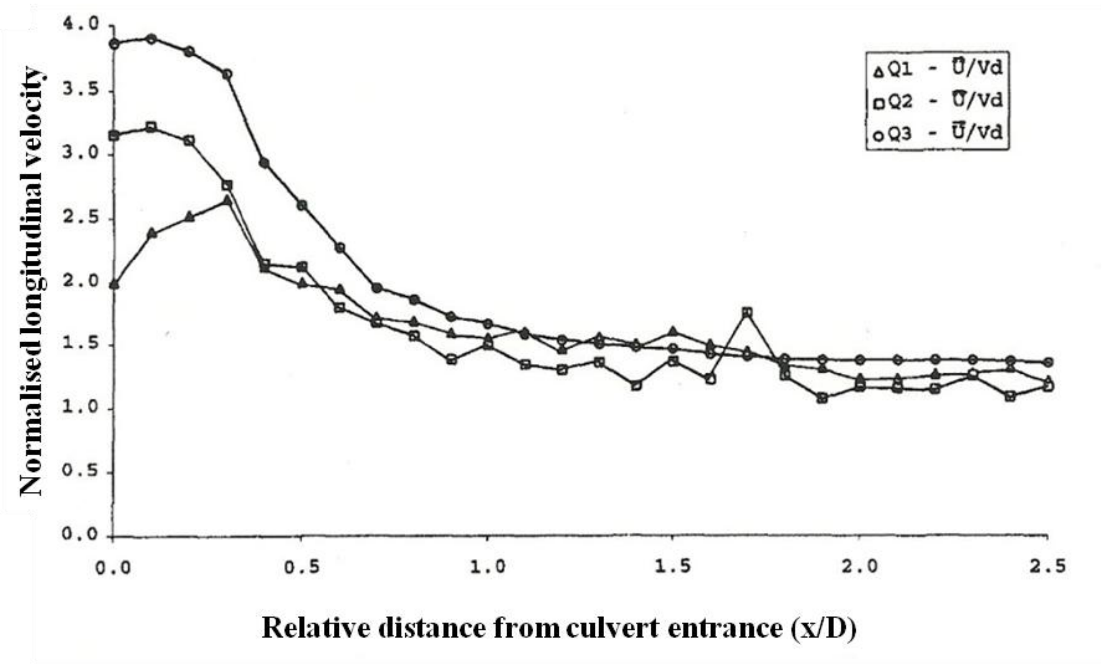

Figure 5.27 Variation of normalised longitudinal velocity with distance from culvert inlet: x = distance from culvert inlet (m), D= culvert diameter (m) (Q1 0.022m^3/s, Q2 0.03 m^3/s, Q3 0.04 m^3/s) (Day 1997, Figure 5(a))

As can be seen from Figure 5.26, at distances closer to the inlet than 0.3m which is the culvert diameter, the mid stream velocity started to increase significantly. Day (1997) studied surcharged culverts where the upstream water depth was greater than the culvert diameter and so in addition to the longitudinal velocities, changes in vertical velocity, which was influenced by headwater depth above the culvert, was also a major factor in his study.

As can be seen from the results shown in Figures 5.25 and 5.26, the greatest difference in blockage occurred where there was also the greatest difference in flow velocity suggesting that flow velocity has a major influence on blockage potential. These results are summarised in Figure 5.28 which shows the percentage of debris pieces blocked for all lengths and bar spacings against the relative mid stream velocity.

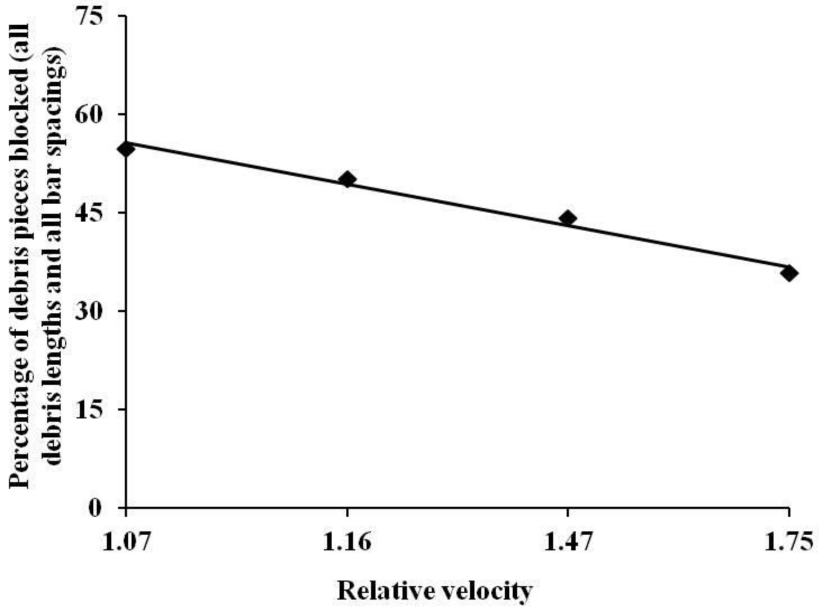

Figure 5.28Percentage of debris pieces blocked against relative velocity. Relative velocity was measured as the ratio of flow velocity at the point of screen intersection with the water surface to a base upstream flow velocity measured at a distance equal to three channel widths (2.25m) upstream of the culvert inlet.

5.4.4. Empirical relationship

From the analysis described in the previous section, in addition to bar spacing and debris length which had previously been identified as influencing factors (Section 5.2), screen position was also highlighted as potentially determining potential blockage. Only data gathered during assessment two, a screen of 60 degrees at different positions, was used for the development of an empirical relationship. The assessment of different angled screens at one position was the final assessment undertaken and took place after a minor alteration to the experimental test rig. During testing, water entered the flume via a stilling tank filled with a range of plastic baffles. The baffles were removed and then replaced during some development work on the flume which was undertaken before the final test. This resulted in a minor alteration in the flow direction on initially leaving the tank. Although this change, which only altered the flow pattern for the first few meters of the channel, will have had no impact on the analysis of the results of that individual assessment, the results were not used for this full empirical analysis to ensure no additional factors resulting from the changed inlet configuration influenced the results.

The hypothetical relationship can be formalized by

$$D = f(S, L, P_v) \tag{19}$$

Where D = percentage of debris pieces blocked (%), S = bar spacing (m), L = debris length (m), and P_v = relative velocity at screen position. As the major influence on blockage at the different screen positions appears to be flow velocity, P_v was calculated as the ratio of flow velocity at the point of screen intersection with the water surface to a base upstream flow velocity measured at a distance equal to three channel widths upstream of the culvert inlet.

Regression analysis was used to establish an empirical relationship between the identified contributing factors and blockage potential using the data gathered during assessment two.

A log transformation (logit) was used during the regression analysis to allow limits to be set on the dependent variable (D). As D represents the percentage of pieces blocked, the limits were set at 0 and 100. After transformation a stepwise multiple regression analysis was performed using a 95% probability significance limit (full statistics for the analysis can be found in Appendix G).

A cubic function was found to provide the best solution (Equation 20).

$$\ln\left[\frac{D}{100-D}\right] = -1.014 + 733.902L - 265.907L^2 + 273.786L^3 - 41.535S + 88.71S^2 \\ -15518P_v - 13.114LS + 478.182L^2S \tag{20}$$

The generated model had a high adjusted R^2 value, 0.90 indicating that it was a good fit to the test generated data and a high prediction R^2 value, 0.89, indicating it had good predictive capabilities. Debris length (L), bar spacing (S), and relative velocity at the screen position (P_v) were found to be significant predictive factors, all factors had p-values < 0.0001.

While the high adjusted R^2 value suggests the model is a good fit to the experimental data, despite the large number of terms in the equation, as for Equation 16 a simplification of the model may offer a more workable solution (see Section 6.5). A plot of the predicted debris blockage against the percentage actually blocked during testing is shown in Figure 5.29.

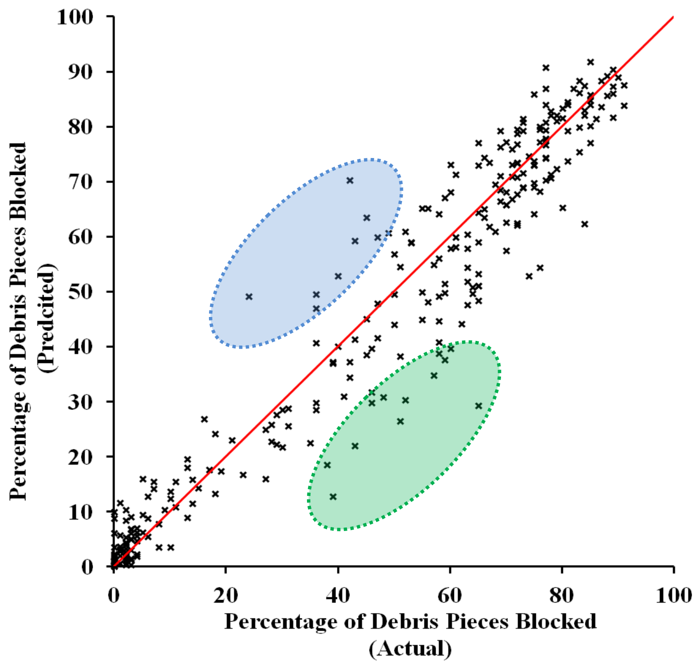

Figure 5.29 Modelled predicted blockage against actual debris pieces blocked during phase three testing. The red line indicates where predicted blockage equals actual blockage.

While the majority of the predicted results fall within an acceptable band, deviating from the actual results by 15% or less, the plot does show a number of outliers that fall some distance outwith that band. For example, two points are shown to significantly over estimate blockage: actual blockage 42%, estimated blockage 70% and actual blockage 24%, estimated blockage 49%. These results, and those in the same area on the plot (highlighted in blue), are for the largest debris lengths tested (0.35m) and this over estimate is consistent with the trends shown for results in Figure 5.25. The plot also shows a wider spread of estimates where actual percentages were between around

35 and 70%, with more precise estimates above and below these values. One noticeable group of underestimates is highlighted in green on Figure 5.29. These points refer to blockage recorded where the bar spacing was at its smallest (0.03 or 0.04m) and the debris lengths were also relatively small (0.05 or 0.075m). This is also reflected in position of the trend shown in Figure 5.25 where many of the data points fall above the trend where the debris length to bar spacing ratio is less than two.

Figures 5.30 to 5.32 show the individual contributions made by each of the identified driving elements within the generated model. As can be seen from Figure 5.30, less blockage occurs as bar spacing increases, this is reflected in the negative value for the bar spacing coefficient in the model. The influence of debris length (Figure 5.31) is also as expected with blockage increasing as length increases as indicated by the positive bar spacing coefficient in the model. While the results for both bar spacing and debris length agree in general with the findings of the initial testing (see Section 5.2) there is a marked difference in the influence of debris length once it reaches a certain threshold. In the model produced from the initial testing, while there is an initial increase in blockage with increasing debris length, once a threshold length has been reached blockage appears to decrease as length increases. The model produced from this later testing still shows an initial increase in blockage with increasing debris length. However, once above a threshold length, rather than blockage decreasing as length increases blockage continues to increase but at a much reduced rate. This is more representative of what was expected. This change from the original model may be partly due to an improved experimental technique; having identified a potential issue with the orientation of longer lengths being influenced by their tendency hit the channel bed on entry particular care was taken to minimise the number of times this occurred. Alternatively this may be due to the inclusion of results from screens some distance from the zone of flow acceleration. With the screen positioned some distance upstream from the inlet the debris spent less time travelling in the regions of flow at the higher velocities generated by flow constriction at the culvert. This may have resulted in fewer pieces of the longer length debris fully rotating to align parallel with the flow direction before reaching the screen. P_v has a negative coefficient in the generated model indicating that blockage decreases as its values increases. This is illustrated in Figure 5.32. Observation of the test runs suggests that the closer the screen is positioned to the zone of acceleration of flow as it constricts at the culvert inlet the greater likelihood that the debris will orient parallel to the flow direction which facilitates its passage through the screen. In addition debris that has become balanced on a bar is more likely to be pulled off by the drag forces of the flow.

As a further measure of the contribution made by each of the individual elements, a sensitivity analysis was undertaken to assess the impact of each of the contributing variables in the model. The predicted blockage percentage (D) was calculated from the derived function for a mid value from the range tested (L=0.18m, S=0.08m, P_v=1.35, D = 52.2). Predicted blockage values were then calculated when one element was increased and then decreased by 25% of its initial value while the other element values remained unchanged. As can be seen from Figure 5.33 all three assessed elements (L, S, P_v) have a significant impact.

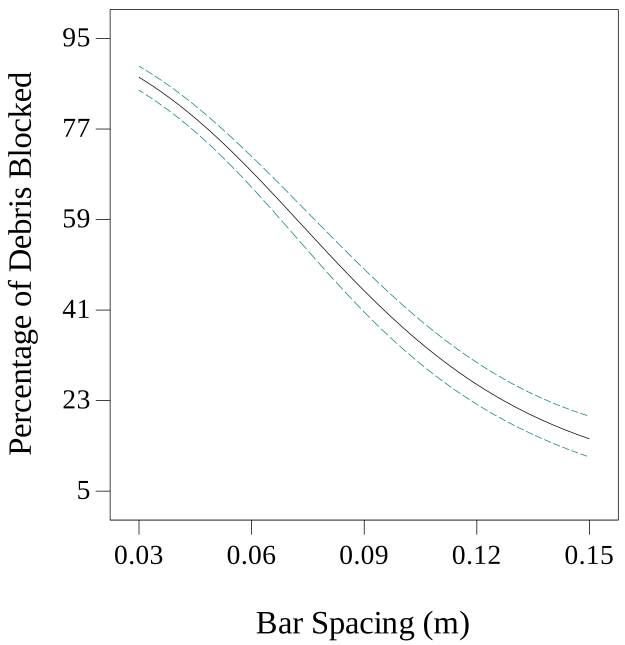

Figure 5.30 Influence of bar spacing on percentage blockage when screen position(relative velocity) = 1.35, debris length = 0.18m. Similar trends were found for other tested screen positions(relative velocity) and debris lengths. The dotted green lines show the 95% confidence interval.

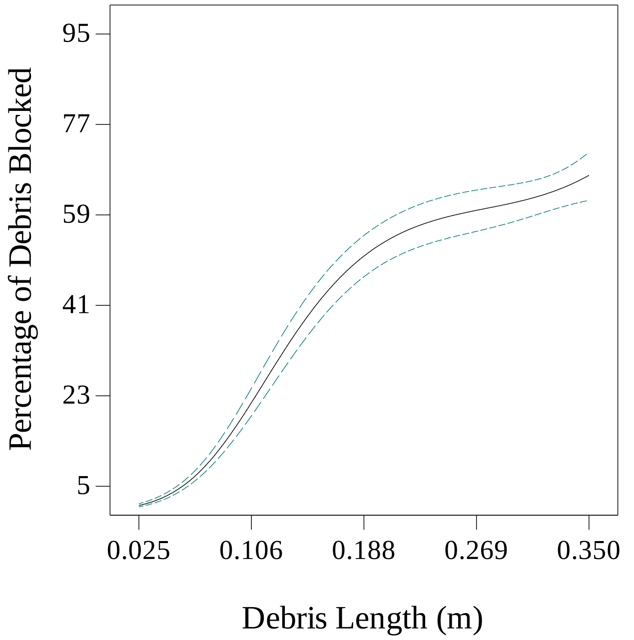

Figure 5.31 Influence of debris length on percentage blockage when bar spacing = 0.08m, screen position(relative velocity) = 1.35. Similar trends were found for other tested screen positions(relative velocity)and bar spacings. The dotted green lines show the 95% confidence interval.

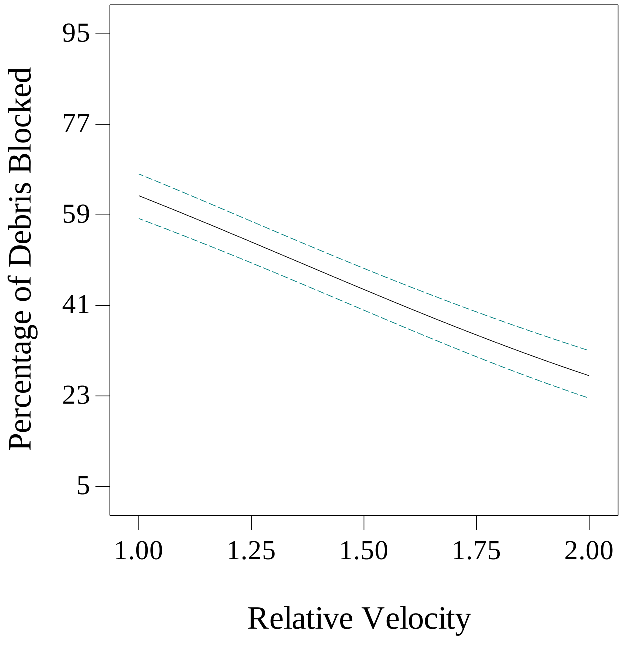

Figure 5.32 Influence of screen position (relative velocity) on percentage blockage when bar spacing = 0.08m, debris length = 0.18. Similar trends were found for other tested bar spacings and debris lengths. The dotted green lines show the 95% confidence interval.

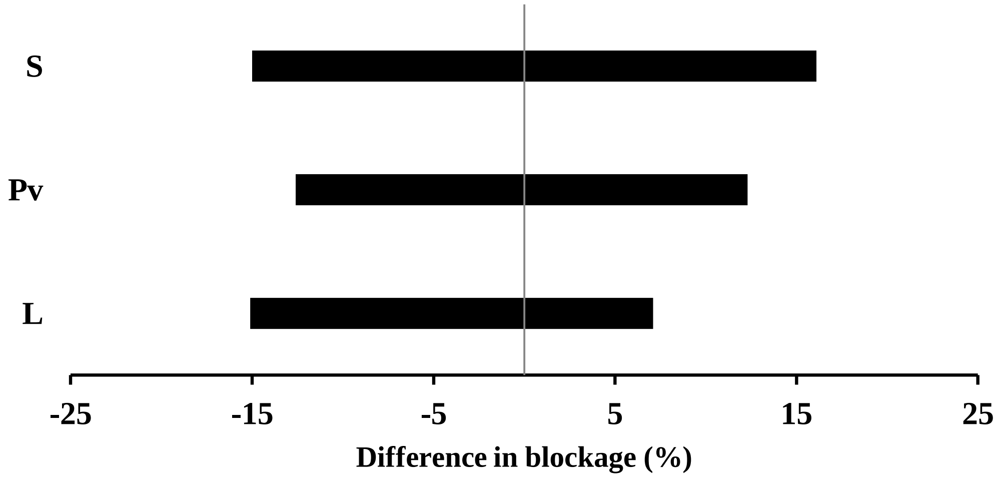

Figure 5.33 Sensitivity analysis for model generated from screen position testing showing change in predicted percentage of debris blocked when varying predictor variables by ±25%

L = Debris length, S=Bar spacing, P_v = Screen Position (relative velocity).

5.4.5. Recommendation for next step

The model was found to be statistically significant and all the terms found to actively contribute to the sensitivity of the model. However, this model was based only on the results gathered from the second assessment of the testing undertaken as a follow up to the initial testing; this only contained 280 values, a relatively limited data set. This model also did not take into account the influence of screen angle or discharge which, although not assessed during this second phase of testing, had been identified during the initial testing as being driving factors. An analysis covering all the elements assessed during the three phases of testing offers an opportunity to assess the impact of the identified driving factors (debris length, bar spacing, screen angle, discharge and screen position) with a significant data set. This more comprehensive analysis is detailed in Chapter 6.

5.5. Chapter Summary

Extensive experimental testing was undertaken under controlled laboratory conditions with the aim of assessing the extent to which screen geometry and position influence blockage at trash screens. The physical model constructed for the purpose of the testing proved to be robust and appropriate for the proposed analysis. Initial testing assessed a total of 63 different test cases: these involved seven bar spacings, three screen angles and three discharges. A total of 63,000 runs were made.

The use of contour plots was shown to be helpful in visualising the influence of bar spacing and debris length on blockage. However, logarithmic functions representing the relationship between the ratio of debris length to bar spacing and blockage offered a more practical tool for comparing blockage when a third component such as screen angle or discharge was assessed.

Blockage was shown to increase as the ratio of debris length to bar spacing increased. Blockage followed similar trends at all discharges tested but was greater at lower flow rates particularly where the ratio of debris length to bar spacing was high. Although fewer blockages occurred where the screen angle was high, it was noted that this result may have been influenced by the position of the screen relative to the culvert inlet as well as or rather than the angle of the screen itself.

For the initial phase of testing, regression analysis was used to establish a model defining blockage in terms of the contributing elements. A quadratic function was found to be the best fit (Equation 16). Sensitivity analysis was undertaken to assess the impact of the predictive factors and all the assessed factors were found to be statistically significant contributors to the model. Bar spacing, debris length and screen angle were shown to exert a major influence on blockage with discharge having only a minor impact.

As a result of the findings from the initial testing additional experimental testing was undertaken under controlled laboratory conditions with the aim of assessing the extent to which upstream bed slope influences blockage at trash screens. A total of 63 different test cases were assessed: these involved seven bar spacings, three screen angles and three bed slopes.

Blockage was shown to increase as the ratio of debris length to bar spacing increased for all bed slopes, this was consistent with the relationship defined for the initial phase of testing. While the blockage followed similar general trends for all slopes tested, the screen at 30 degrees showed consistent performance for all bed slopes but where the screen angle was 45 or 60 degrees more debris was blocked when the bed slope was greater. This may have been due to a change in the position of screen relative to the zone of rapid flow acceleration as the water surface profile and flow patterns were affected by the increasing build up of water behind the headwall as the slope increased.

As for the initial phase of testing, regression analysis was used to establish a model defining blockage in terms of the contributing elements and a quadratic function was found to be the best fit (Equation 18). Screen angle, debris length and bar spacing were again found to be significant predictive factors. Bed slope was not found to be significant and was therefore not included in the model. The model was not found to be an improvement on the model produced from initial testing so no further sensitivity analysis was undertaken.

A final phase of experimental testing was undertaken under controlled laboratory conditions with the aim of assessing the extent to which screen position influences blockage at trash screens. 49 different test cases were assessed: these involved seven bar spacing's, three screen angles and four different screen positions.

As for the initial testing, blockage was shown to increase as the ratio of debris length to bar spacing increased. Little difference in blockage was found for screens at different angles when they intersected the water surface at the same position. Blockage was shown to increase as the distance of the screen from the culvert inlet increased. The driving factor was found to be the screen position relative to the zone of flow acceleration created as the flow was constricted on approach to the culvert inlet. The amount of blockage decreased as the mid stream depth averaged velocity at the point at which the screen intersected the water surface increased relative to an average velocity measure upstream of the impacts on the flow created by the culvert inlet.

Regression analysis was again used to establish a model defining blockage in terms of the contributing elements. A cubic function offered the best fit (Equation 20). A sensitivity analysis was undertaken to assess the impact of the predictive factors and bar spacing, debris length and relative velocity at the screen position were all shown to exert a major influence on blockage.

The model was based on a limited data set and it was noted that a more comprehensive analysis would be possible by combining the results from all phases of testing rather than analysing each phase independently. This more comprehensive analysis is presented in Chapter 6.

Chapter 6

Development of an Empirical Model and End User Focused Tools for Blockage Estimation

6.1. Introduction

The analysis described in Section 5.2 identified bar spacing, debris length and screen angle as influencing factors in determining the amount of debris blocked at a screen. In addition, the relative velocity of mid-stream flow at the point the screen intersected the water surface was identified as a driving factor (see Section 5.4). This chapter uses the data gathered during both these phases of testing to establish empirical models defining blockage in terms of all the identified driving factors.

Two models are developed: the first uses the full data set to define blockage in terms of bar spacing, debris length, screen angle, discharge and relative velocity at the screen while the second model considers the overall percentage blockage for all debris lengths and defines blockage in terms of bar spacing, screen angle, discharge and relative velocity. This second approach was considered to be appropriate as while estimates of maximum debris length likely to be transported can be made based on channel width (see Section 4.6), in reality a mix of debris lengths is likely and therefore a model that does not require a fixed debris length as a parameter was felt to potentially offer a more practical solution.

6.2. Development of a Model with Debris Length as a Predictive Factor

Regression analysis was used to establish an empirical relationship between the contributing factors and blockage potential. The hypothetical relationship can be formalized by

$$D = f\,(A, S, L, Q, P_v) \tag{21}$$

Where D = percentage of debris pieces blocked (%), A = screen angle (degrees), S = bar spacing (m), L = debris length (m), Q = discharge (m^3/s), P_v = relative velocity at the screen position. The position (P_v) values were calculated as the ratio of flow velocity at the point of screen intersection with the water surface to a base upstream flow velocity measured at a distance equal to three channel widths upstream of the culvert inlet. Details of the measured velocities can be found in Table 5.17.

A log transformation (logit) was used during the regression analysis to allow limits to be set on the dependent variable (D). As D represents the percentage of pieces blocked, the limits were set at 0 and 100. After transformation a stepwise multiple regression analysis was performed using a 95% probability significance limit. Output from the regression analysis can be found in Appendix H.

A quadratic function was found to provide the best solution (Equation 22). While discharge was considered as a potentially contributing function in the hypothetical relationship (Equation 21), it was not found to be a statistically significant parameter and is therefore not included in the model.

$$\ln\left[\frac{(D)}{100\text{-}D}\right] = 0.034 + 32.350L - 67.896L^2 - 53.873S + 108.679S^2 + 0.013A - 1.249P_v + 61.956LS \quad (22)$$

The generated model had a high adjusted R^2 value, 0.87, indicating that it was a good fit to the test generated data and a high Prediction R^2 value, 0.86, indicating it had good predictive capabilities. A plot of the percentage of debris pieces the model predicts will be blocked against the percentage actually blocked during testing is shown in Figure 6.1.

Debris length (L), bar spacing (S), relative velocity at the screen (P_v) and screen angle (A) were found to be significant predictive factors; all factors had p-values < 0.0001. Figures 6.2 to 6.5 show the individual contributions made by each of these elements within the generated model.

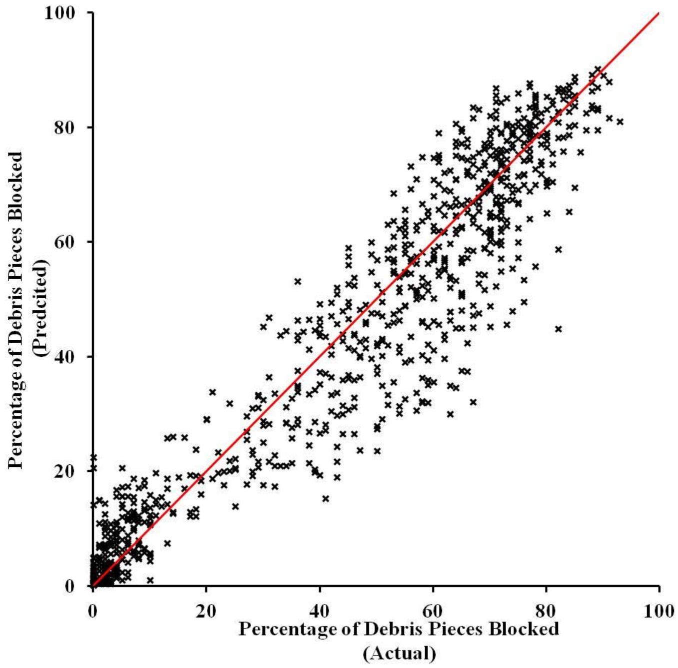

Figure 6.1 Blockage predicted by final model against actual debris pieces blocked. The position where actual equals predicted is shown by the red line.

Figure 6.2 shows that, as for the previous models, less blockage occurs as bar spacing increases, this is reflected in the negative value for the bar spacing coefficient in the model. Relative velocity also has a negative coefficient and exhibits an influence comparable with that identified during the analysis described in the previous chapter; blockage decreases as relative velocity increases (Figure 6.3). The influence of debris length (Figure 6.4) shows a similar trend to that generated from the initial analysis. While there is an initial increase in blockage with increasing debris length, once a threshold length has been reached blockage appears to decrease as length increases. In contrast to the empirical relationship derived from the initial analysis outlined in Section 5.2, which had a negative coefficient for screen angle suggesting blockage increases as angle decreases, this model has a positive coefficient for screen angle (Figure 6.5). This suggests that blockage will increase as the angle of the screen increases. However, as can be seen from the results of the sensitivity analysis (Figure 6.6) the percentage blockage predicted by the model is noticeably less sensitive to changes in the screen angle than to changes in any of the other driving variables. This is consistent with the observed data which suggests that all other factors being equal there is only a minor difference in blockage with different screen angles (see Section 5.4.1).

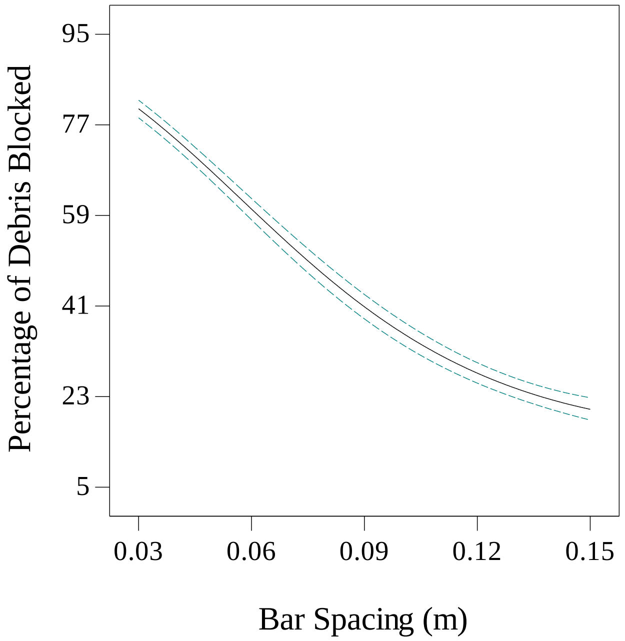

Figure 6.2 Influence of bar spacing on percentage blockage when screen angle = 45°, relative velocity = 1.35, debris length = 0.18m. Similar trends were found for other tested angles, relative velocities and debris lengths. The dotted green lines show the 95% confidence interval.

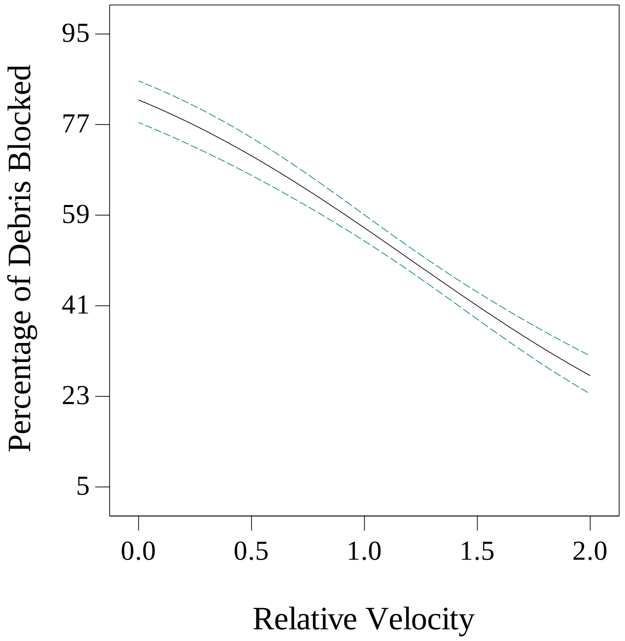

Figure 6.3 Influence of screen position (relative velocity) on percentage blockage when screen angle = 45°, bar spacing = 0.08m, debris length = 0.18m. Similar trends were found for other tested angles, spacings and debris lengths. The dotted green lines show the 95% confidence interval.

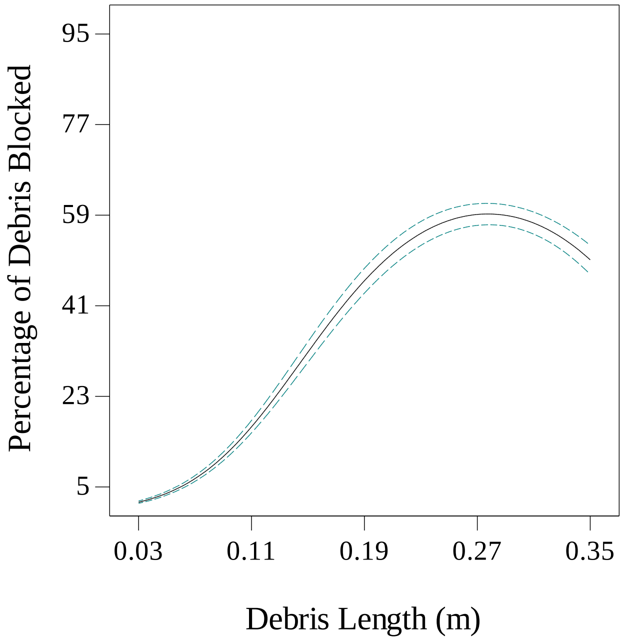

Figure 6.4 Influence of debris length on percentage blockage when screen angle = 45°, bar spacing = 0.08m, relative velocity = 1.35. Similar trends were found for other tested sceen angles, bar spacings and relative velocities. The dotted green lines show the 95% confidence interval.

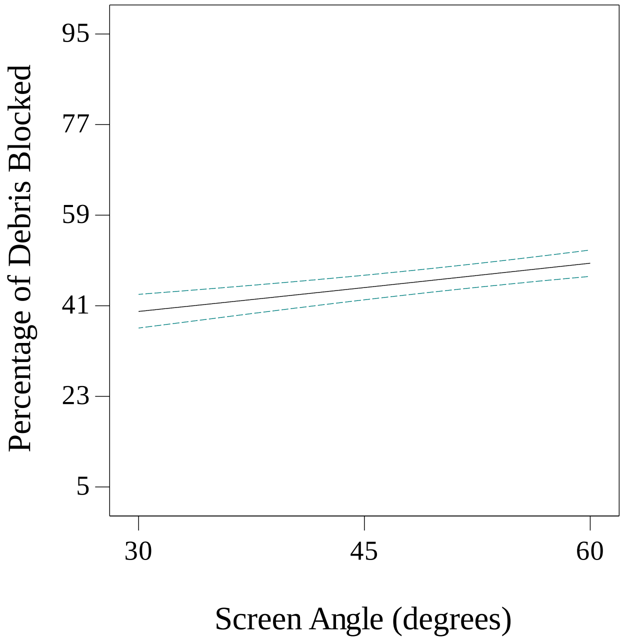

Figure 6.5 Influence of screen angle on percentage blockage when bar spacing = 0.08m, relative velocity = 1.35, debris length = 0.18m. Similar trends were found for other tested bar spacings, relative velocities and debris lengths. The dotted green lines show the 95% confidence interval.

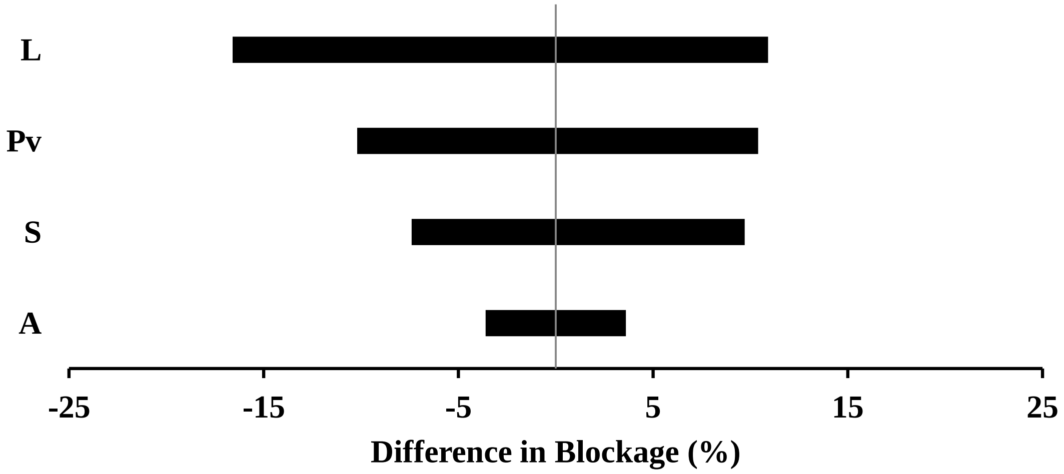

Figure 6.6 Sensitivity analyses for full data model showing change in predicted percentage of debris blocked when varying predictor variables by ±25%
L=Debris length, S=Bar spacing, P_v= Screen Position (relative velocity), A=Screen Angle

6.3. Development of a Model without Debris Length as a Predictive Factor

The model developed in the previous section included debris length as a driving factor in the estimation of potential percentage of blockage. While this comprehensive model can provide estimates where likely debris length is known or can be approximated based on channel width, in reality a mix of debris lengths is likely and therefore a model that does not require a known debris length as a parameter was felt to potentially offer a more practical solution.

The results from the testing outlined in Chapter 5 were used to determine the percentage of debris blocked for all debris lengths for each screen angle, bar spacing, discharge and screen position. These aggregated results were then assessed to determine whether the previously identified relationships for individual debris length were still evident for the aggregated data. The results of this assessment are illustrated in Figures 6.7 to 6.9 which show clear relationships between the percentage of debris pieces blocked (D) and the bar spacing. Figures 6.7 and 6.8 show the percentage of debris blocked at different bar spacings for a range of screen angles or discharges. These relationships were best fitted by logarithmic functions and had high R^2 regression coefficients ranging from 0.98 to 1.00. The functions and R^2 regression coefficients associated with these graphs are detailed in Table 6.1.

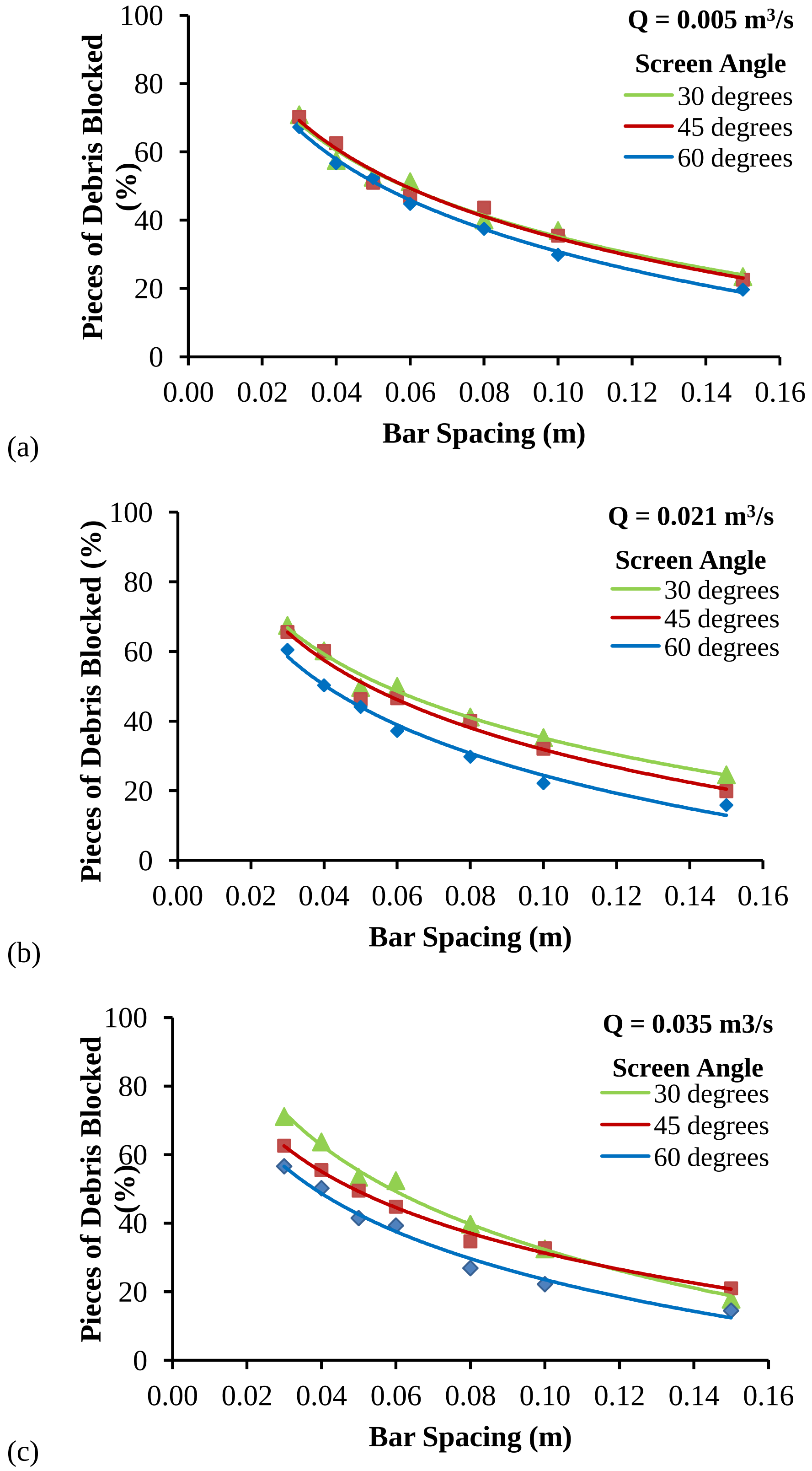

Figure 6.7 Graphs showing comparison of total percentage of debris pieces blocked (D) by different bar spacings (S) for all debris lengths at different screen angles when discharge is (a) 0.005m^3/s (b) 0.021m^3/s and (c) 0.035m 3/s

Each marker represents the percentage of 1000 pieces of debris blocked.

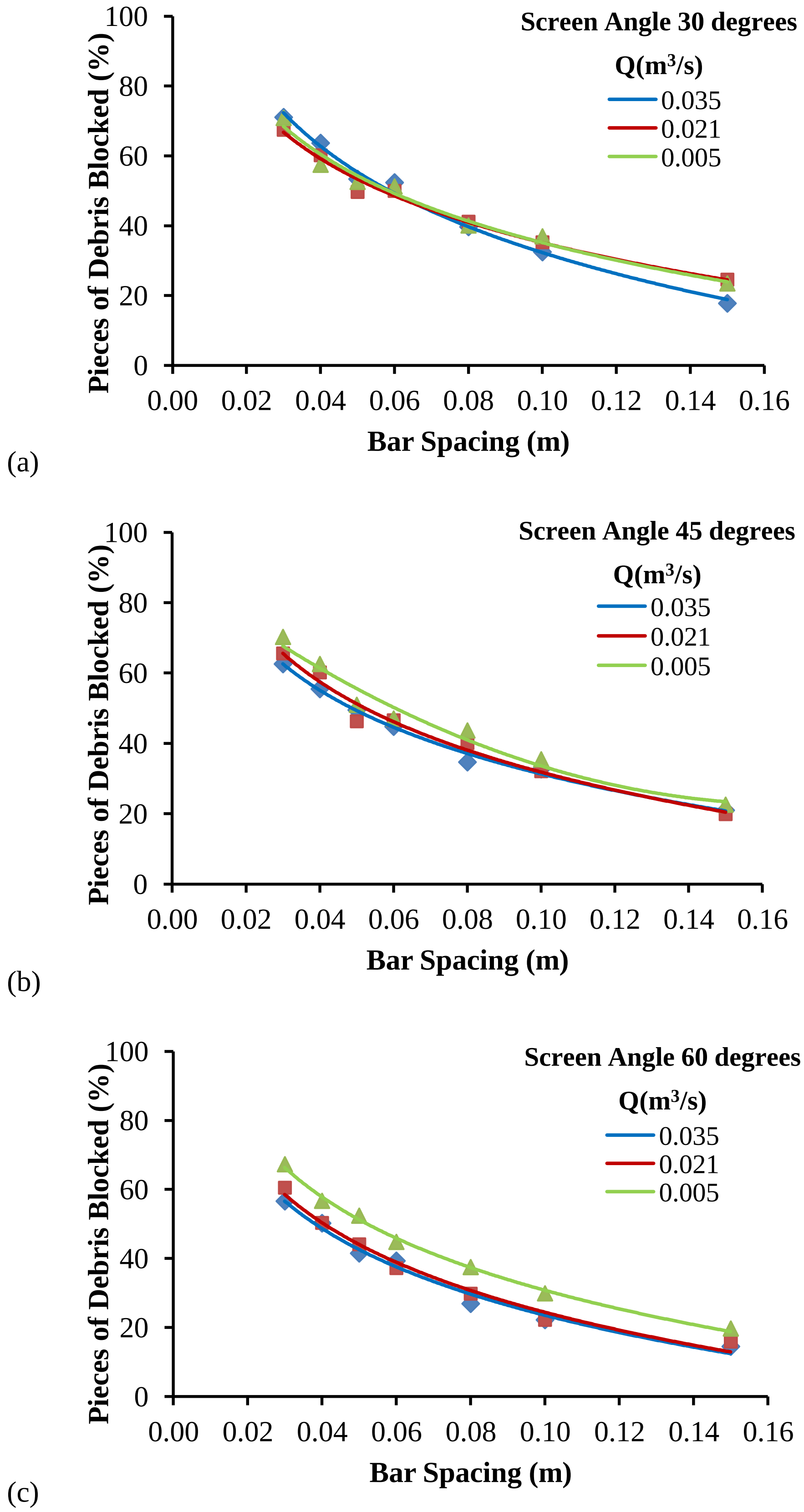

Figure 6.8 Graphs showing comparison of total percentage of debris pieces blocked (D) by different bar spacings (S) for all debris lengths at different discharges when screen angle is (a) 30 degrees (b) 45 degrees (c) 60 degrees
Each marker represents the percentage of 1000 pieces of debris blocked.

Table 6.1 Equations and corresponding R^2 regression coefficients for trends shown in Figures 6.7 and 6.8.

Discharge (m^3/s)	Screen angle (degrees)	Trend function	R^2
0.005	30	D = -27.64ln(S) - 28.50	0.98
0.005	45	D = -28.68ln(S) - 31.38	0.98
0.005	60	D = -29.54ln(S) - 37.23	1.00
0.021	30	D = -26.27ln(S) - 25.35	0.99
0.021	45	D = -28.03ln(S) - 32.72	0.98
0.021	60	D = -28.35ln(S) - 40.85	0.99
0.035	30	D = -33.25ln(S) - 44.27	0.99
0.035	45	D = -25.97ln(S) - 28.47	0.99
0.035	60	D = -27.45ln(S) - 39.64	0.99

The R^2 values of 0.98 to 1.0 are higher than those associated with the corresponding trends plotted for individual debris lengths, 0.85 to 0.89 (Table 5.3). This is likely to be due to the fact that plotting the aggregated results for all debris lengths against a single bar spacing has removed the variability that was evident when blockage was plotted against a debris length to bar spacing ratio (see for example Figure 5.6).

Figure 6.9 shows the percentage of debris blocked at different screen positions. These relationships were best fitted by quadratic functions and had high R^2 regression coefficients ranging from 0.97 to 0.99. The functions and R^2 regression coefficients associated with these graphs are detailed in Table 6.2.

Paired t-test analysis was undertaken to determine whether there was a statistically significant difference in the percentage of blockage found and the results are summarised in Tables 6.3 to 6.5.

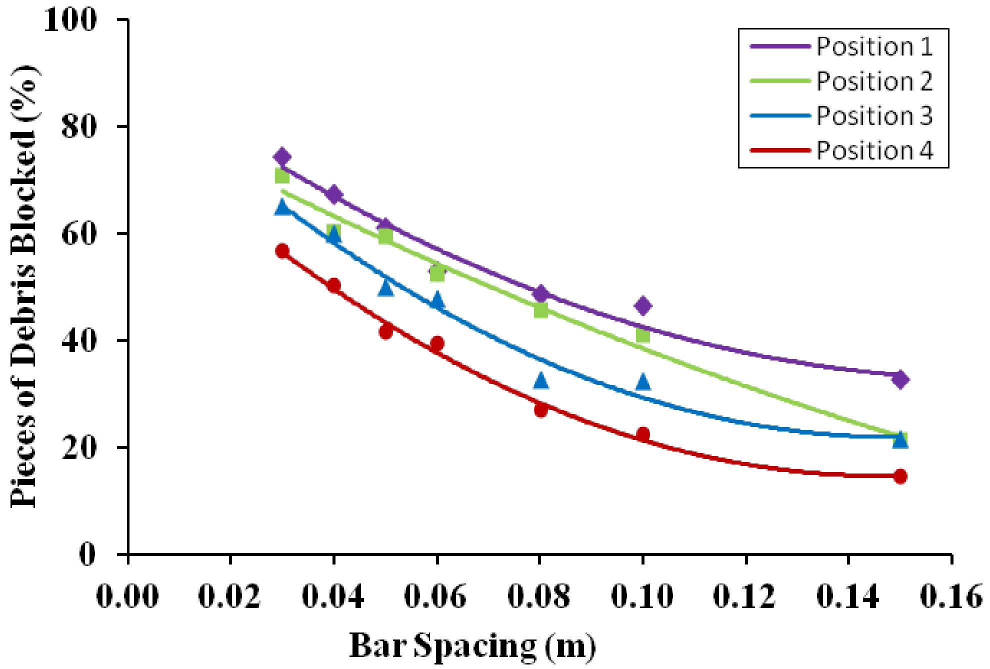

Figure 6.9 Plot showing comparison of percentage of debris pieces blocked (D) by different bar spacings (S)for all debris lengths at different screen positions (screen angle 60°). Each marker represents the percentage of 1000 pieces of debris blocked.

Table 6.2 Equations and corresponding R^2 regression coefficients for trends shown in Figure 6.9

Screen position	Trend function	R^2
1	$D = 2063.6S^2 - 695.88S + 91.43$	0.97
2	$D = 760.4S^2 - 519.78S + 82.81$	0.98
3	$D = 3055.7S^2 - 911.37S + 89.81$	0.98
4	$D = 3086.7S^2 - 904.18S + 80.82$	0.99

Table 6.3 Paired t-test for comparison of different discharges. Critical t is 2.45 (p=0.05).

Screen Angle (degrees)	**Discharge 1 (m^3/s)**	**Discharge 2 (m^3/s)**	**t-stat**	**Significantly different**
30	0.005	0.021	0.73	No
30	0.005	0.035	0.22	No
30	0.021	0.035	-0.19	No
45	0.005	0.021	5.68	Yes
45	0.005	0.035	3.75	Yes
45	0.021	0.035	1.19	No
60	0.005	0.021	12.13	Yes
60	0.005	0.035	8.50	Yes
60	0.021	0.035	1.60	No

Table 6.4 Paired t-test for comparison of different angles. Critical t is 2.45 (p=0.05).

Discharge (m^3/s)	**Screen angle 1 (degrees)**	**Screen angle 2 (degrees)**	**t-stat**	**Significantly different**
0.005	30	45	0.01	No
0.005	30	60	3.56	Yes
0.005	45	60	3.44	Yes
0.021	30	45	4.16	Yes
0.021	30	60	9.05	Yes
0.021	45	60	5.68	Yes
0.035	30	45	2.51	Yes
0.035	30	60	7.93	Yes
0.035	45	60	10.21	Yes

Table 6.5 Paired t-test for comparison of one angle at different positions. Critical t is 2.45 (p=0.05)

Distance from inlet (m)	Distance from inlet (m)	t-stat	Significantly different
0.35	0.25	3.37	Yes
0.35	0.15	7.52	Yes
0.35	0.10	14.69	Yes
0.25	0.15	3.31	Yes
0.25	0.10	8.18	Yes
0.15	0.10	14.59	Yes

The analysis detailed in Figures 6.1 to 6.9 and Tables 6.1 to 6.5 shows that the proposed approach of using summary data based on blockage for all debris length is valid as, in common with the findings for blockage of individual lengths, the summary data shows clear relationships between debris blockage and bar spacing that vary with screen angle, discharge and relative velocity at the screen position. Having identified this as an appropriate approach, regression analysis was used to establish an empirical relationship between the contributing factors and blockage potential. The hypothetical relationship can be formalized by

$$D = f(A, S, Q, P_v) \tag{23}$$

Where D = percentage of debris pieces blocked (%), A = screen angle (degrees), S = bar spacing (m), Q = discharge (m^3/s), P_v = relative velocity at screen position. The position (P_v) values were calculated as the ratio of flow velocity at the point of screen intersection with the water surface to a base upstream flow velocity measured at a distance equal to three channel widths upstream of the culvert inlet. Details of the measured velocities can be found in Table 5.17.

A log transformation (logit) was used during the regression analysis to allow limits to be set on the dependent variable (D). As D represents the percentage of pieces blocked, the limits were set at 0 and 100. After transformation a stepwise multiple regression analysis was performed using a 95% probability significance limit. Output from the regression analysis can be found in Appendix I.

A quadratic function was found to provide the best solution (Equation 24). While Q was considered as a potentially contributing function in the hypothetical relationship (Equation 23), it was not found to be statistically significant and is therefore not included in the generated model.

$$\ln\left[\frac{(D)}{100-D}\right] = 2.172 - 31.443S + 85.194S^2 + 0.012A - 0.975P_v \quad (24)$$

The generated model had a high adjusted R^2 value, 0.96 indicating that it was a very good fit to the test generated data and a similarly high Prediction R^2 value, 0.95, indicating it had good predictive capabilities. The R^2 values are higher for this model than for the model which included debris length as a predicting factor (Equation 22). When debris length was included the model performed better, in terms of predicting blockage, for some debris lengths than others; over estimating some and under estimating others. In particular, the model performed less well for the shortest and longest lengths. The aggregate model which does not include debris length as a parameter has evened out the over and under estimates therefore resulting in a better overall match to the experimental data.

A plot of the percentage of debris pieces the model predicts will be blocked against the percentage actually blocked during testing is shown in Figure 6.10.

Bar spacing (S), relative velocity (P_v) and screen angle (A) were found to be significant predictive factors; all factors had p-values < 0.0001. Figures 6.11 to 6.13 show the individual contributions made by each of these elements within the generated model.

As a further measure of the contribution made by each of the individual elements, a sensitivity analysis was undertaken. The predicted blockage percentage (D) was calculated from the derived function for a mid value from the range tested (S=0.08m, A=45 degrees, P_v=1.35, D = 36.2). Predicted blockage values were then calculated when one element was increased and then decreased by 25% of its initial value while the other element values remained unchanged. The results are shown in Figure 6.14.

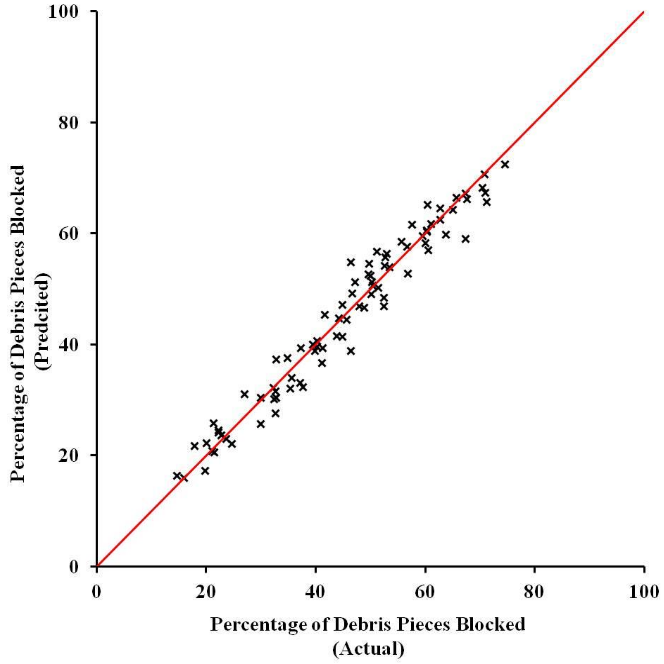

Figure 6.10 Blockage predicted by aggregate model against actual debris pieces blocked. The position where actual equals predicted is shown by the red line.

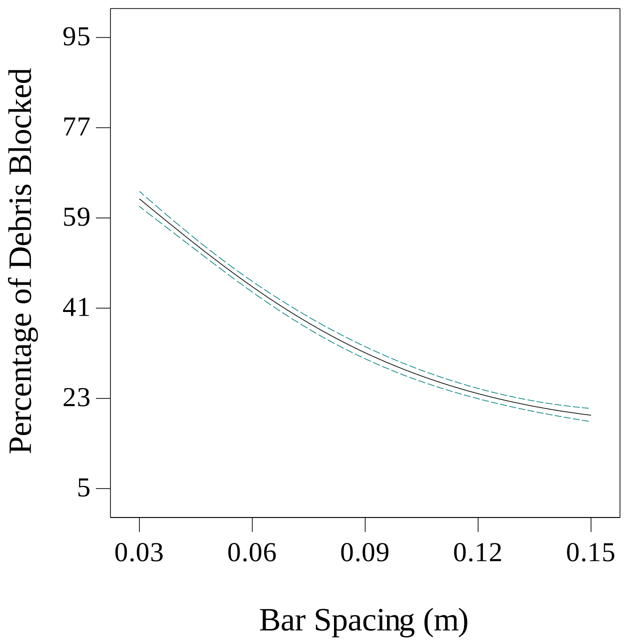

Figure 6.11 Influence of bar spacing on percentage blockage when screen angle = 45°, relative velocity = 1.35. Similar trends were found for other tested angles and relative velocities. The dotted green lines show the 95% confidence interval.

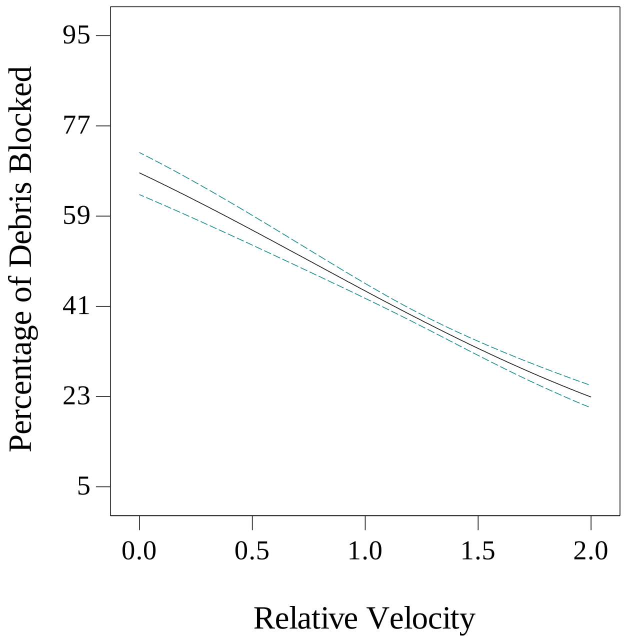

Figure 6.12 Influence of screen position (relative velocity) on percentage blockage when screen angle = 45°, bar spacing = 0.08m. Similar trends were found for other tested angles and spacings. The dotted green lines show the 95% confidence interval.

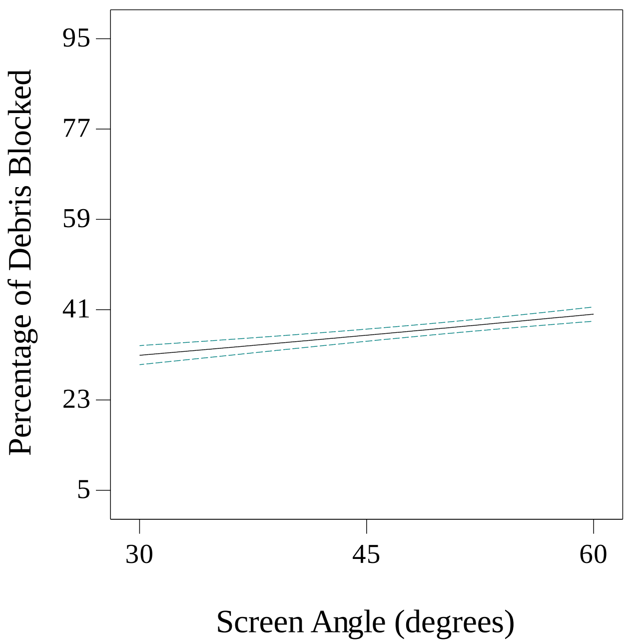

Figure 6.13 Influence of screen angle on percentage blockage when bar spacing = 0.08m, relative velocity = 1.35. Similar trends were found for other tested bar spacings and relative velocities. The dotted green lines show the 95% confidence interval.

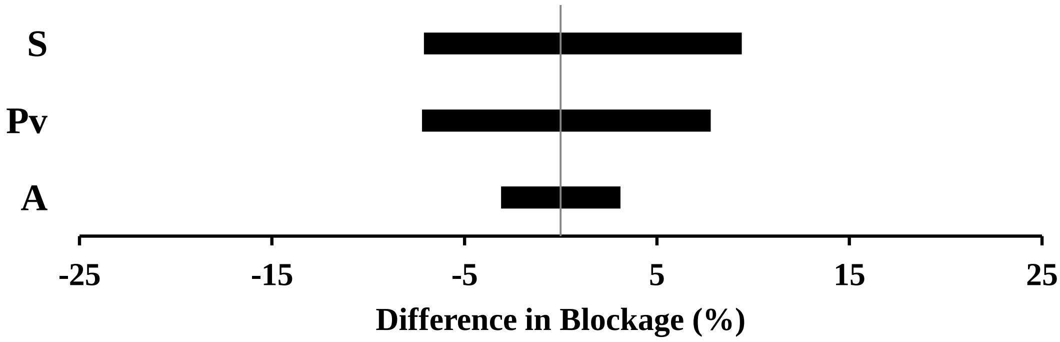

Figure 6.14 Sensitivity analysis for summary data model showing change in predicted percentage of debris blocked when varying predictor variables by ±25%

S=Bar spacing, P_v = Screen Position (relative velocity), A = Screen Angle.

Figures 6.11 and 6.12 show that, as for the previous models, less blockage occurs as bar spacing and relative velocity increase. This is reflected in the negative values for their coefficients in the model. The model has a positive coefficient for screen angle (Figure 6.13) indicating that blockage will increase as the angle of the screen increases. However, as was found in the analysis outlined in the previous section, the sensitivity analysis (Figure 6.14) shows that the percentage blockage predicted by the model is noticeably less sensitive to changes in the screen angle than to changes in any of the other driving variables.

6.4. Empirical Model Validation

To validate the generated models, both models were used to predict the percentage of blockage for the configurations used when assessing the performance of multiple screen angles at a single location (assessment one, Section 5.4) as the results from this test were not used in generation of the models and the test was geometrically similar to the tests used to provide data for the initial model generation. Figures 6.15 and 6.16 show the blockage predicted by the developed models against the actual blockage recorded for the test runs. The plots show similar patterns to those in the equivalent plots produced for the results on which the models were based (Figures 6.1 and 6.10). While the predicted blockages show some deviation from the actual blockages recorded during testing, the deviations exhibit a normal distribution with minimum and maximum differences within the limits of the deviations found for the results used to generate the models (see Figures 6.17 to 6.20).

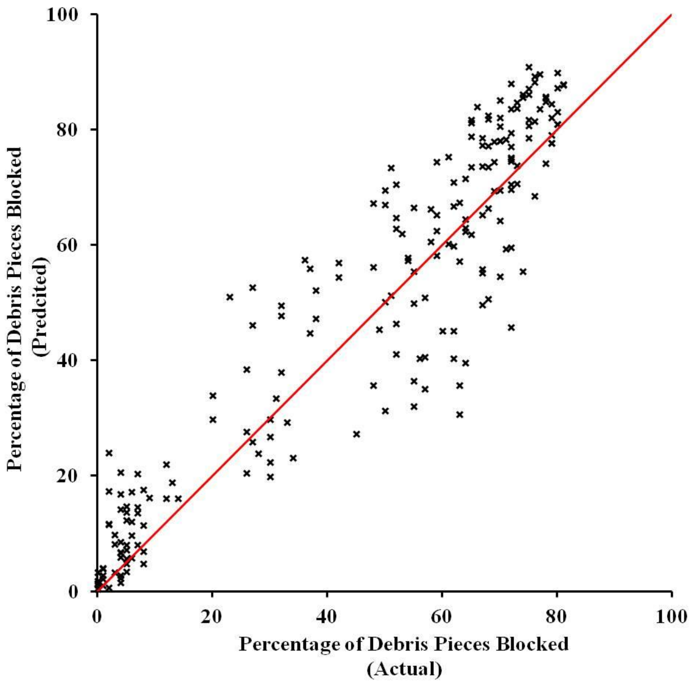

Figure 6.15 Blockage predicted by model against actual debris pieces blocked for validation data set. The position where actual equals predicted is shown by red line.

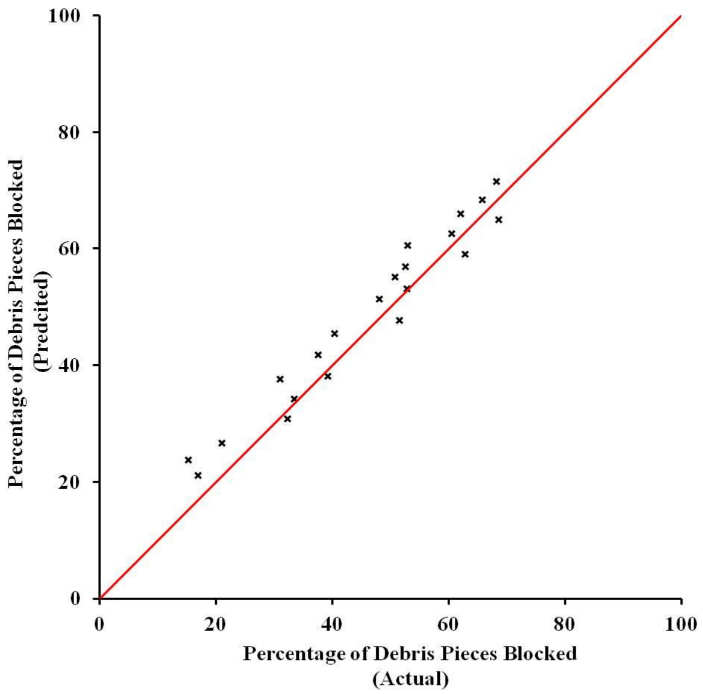

Figure 6.16 Blockage predicted by aggregate model against actual debris pieces blocked for validation data set. The position where actual equals predicted is shown by red line.

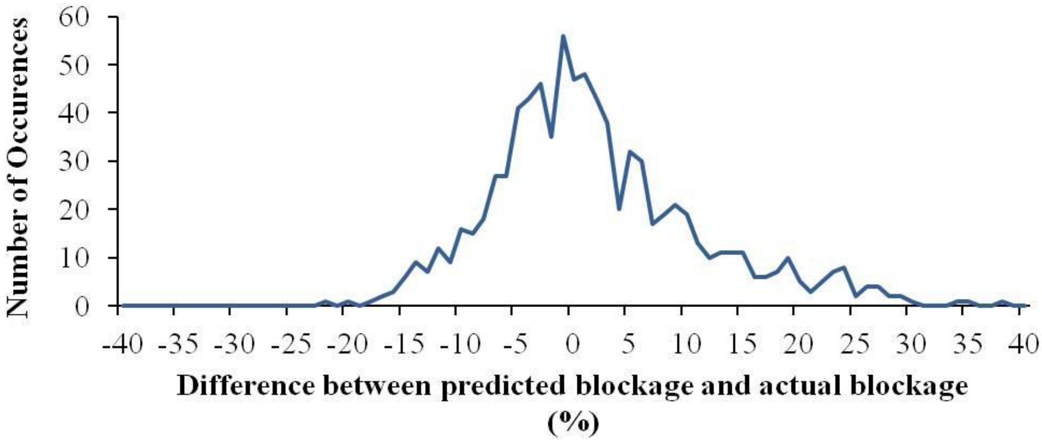

Figure 6.17 Distribution of deviation of predicted blockage from actual blockage for data used to generate full model

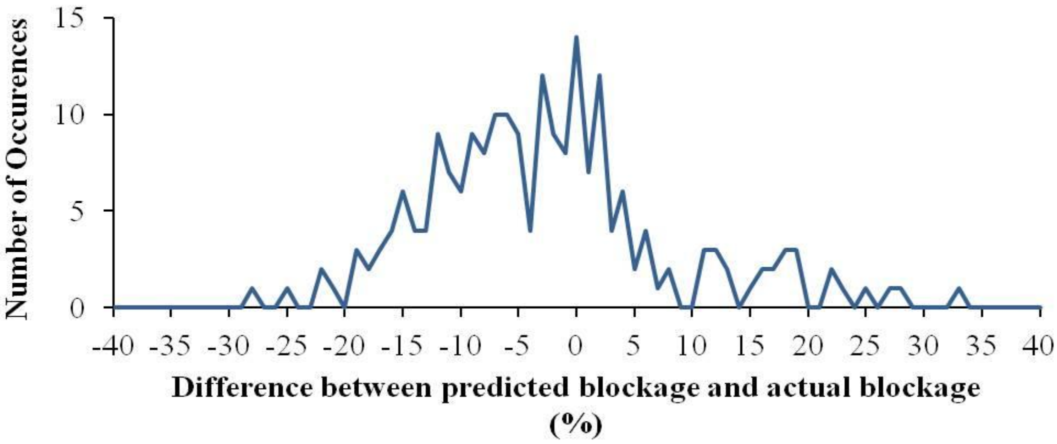

Figure 6.18 Distribution of deviation of predicted blockage from actual blockage for data used to validate full model

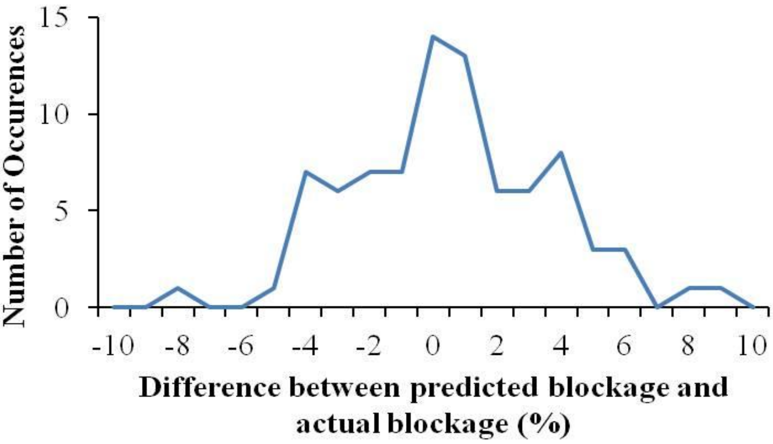

Figure 6.19 Distribution of deviation of predicted blockage from actual blockage for data used to generate aggregate model

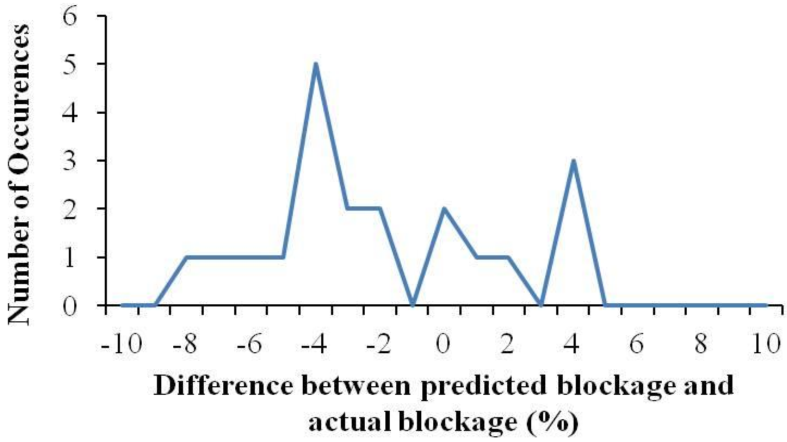

Figure 6.20 Distribution of deviation of predicted blockage from actual blockage for data used to validate aggregate model

6.5. Development of a Tool for Blockage Estimation

6.5.1. Overview

The previous sections in this chapter detailed the development of models that were the best fit to the generated empirical data. These models are useful for estimating likelihood of blockage where the parameters for screen angle, bar spacing, relative velocity and debris length fall within the minimum and maximum values used during testing. However, to provide a practical estimating tool that could be used for real field conditions, the models must also be capable of estimating blockage where the parameters fall out-with the tested limits.

To assess how the generated models performed, the models were tested using a range of debris lengths, bar spacings, screen angles and relative velocities that exceeded the maximum values used during the experimental phase. For all bar spacings, screen angles and relative velocities, estimated blockage was found to decrease as debris length increased once above a threshold length. This appears to be mainly due to the influence of debris length on the model as shown in Figure 5.16. This plot indicates that less blockage occurs at the longest debris lengths. As discussed in Chapter 5, a number of factors may have influenced this trend and it seems unlikely that blockage would continue to decrease as debris length relative to bar spacing increases. The empirically generated models (Equations 22 and 24) were not found to provide realistic estimates for values when the trends are extrapolated beyond the range of the test data, particularly where debris length is greater than the tested lengths. Therefore different models are required for an effective blockage estimation tool. Simplified linear models were thought to potentially offer a practical solution.

6.5.2. Development of simplified linear models

As detailed in Sections 6.2 and 6.3, quadratic functions were found to provide the best fit solutions to define the empirical relationship between contributing factors and blockage potential for the data generated from testing. However, to simplify the model, regression analysis was used to establish a linear relationship for the same data. As presented in Section 5.2.4, a log transformation (logit) was used during the regression analysis to allow limits of 0 and 100 to be set on the dependent variable (D). Output from the regression analysis can be found in Appendix J.

The generated linear models for both the full data set that included debris length as a parameter (Equation 25) and the aggregated data set without a debris length parameter (Equation 26) had relatively high adjusted R^2 values of 0.72 and 0.93 respectively. This indicates that they were a reasonably good fit to the test generated data. They also had relatively high Prediction R^2 values of 0.72 and 0.92 indicating they had good predictive capabilities. The R^2 values for the aggregated model was higher due to the fact that the model including debris length had a tendency to over predict blockage for some lengths and under predict for others. The model tends to over predict blockage to some degree where the debris length to bar spacing ratio is less than around 1.5 or greater than around 7 and under predict for ratios of between 2 and 4. By grouping all lengths together these balanced to give a more accurate estimate.

$$\ln\left[\frac{(D)}{100-D}\right] = -0.036 + 10.734L - 21.495S + 0.014A - 1.211P_v \qquad (25)$$

$$\ln\left[\frac{(D)}{100-D}\right] = 1.635 - 16.136S + 0.012A - 0.975P_v \qquad (26)$$

Plots of the percentage of debris pieces the linear models predict will be blocked against the percentage actually blocked during testing are shown in Figures 6.21 and 6.22.

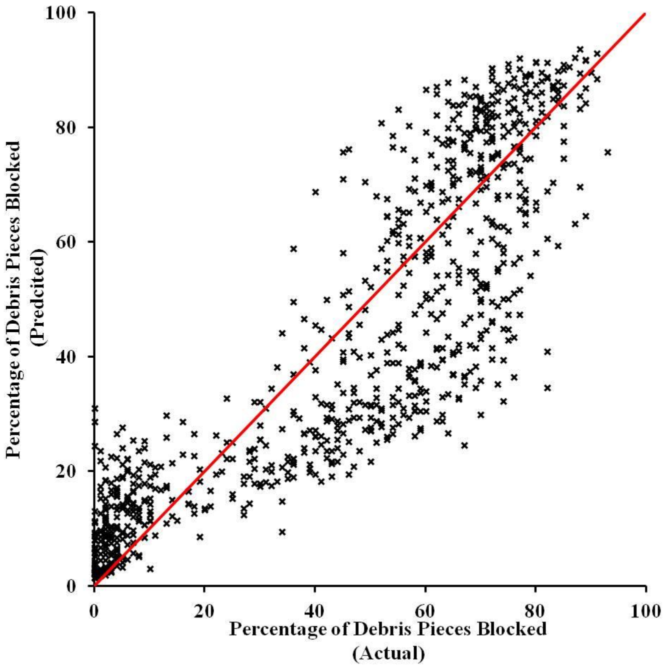

Figure 6.21 Blockage predicted by full linear model against actual debris pieces blocked. The position where actual equals predicted is shown by the red line.

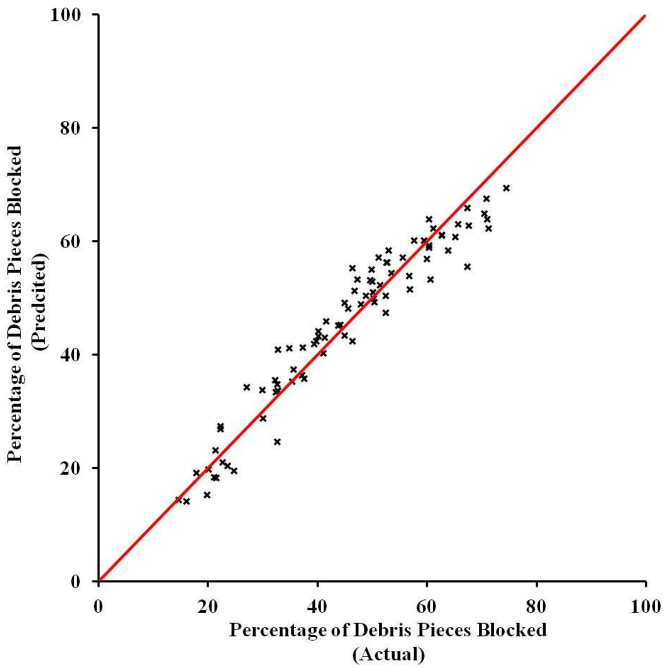

Figure 6.22 Blockage predicted by aggregated linear model against actual debris pieces blocked. The position where actual equals predicted is shown by the red line.

As highlighted in Figure 6.23, the linear model shows a generally greater deviation from the actual blockage recorded than was found for the estimates produced from the empirical model (Figure 6.1) and some noticeable groups where the differences are particularly high.

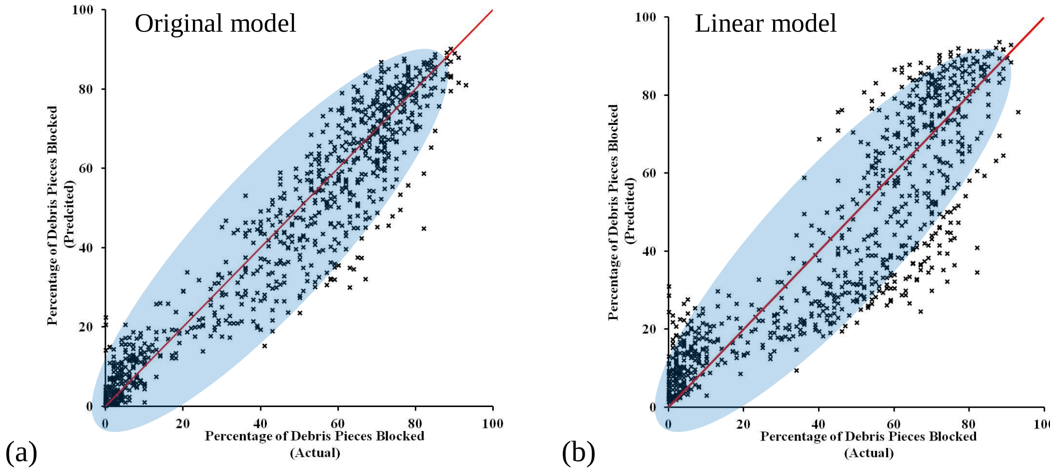

6.23 Comparison of model estimates produced by the (a) original empirical model (Figure 6.1) and (b) linear empirical model (Figure 6.21). The shaded areas are identical on each graph

In addition, the estimates of blockage produced using the linear model exhibit a different pattern of deviation from the actual blockage than the estimates produced from the full empirical model. While the estimates from the empirical model show an approximately even distribution of over and under estimates, with the exception of a few outliers; the estimates from the linear model show a greater degree of data clumping. For example, there are noticeable over estimates where the actual percentage blocked was less than 10 percent or over 80 percent, and a marked tendency to underestimate blockage where the actual blockage recorded was between around 60 and 80 percent.

In contrast, the estimates produced from the linear model that does not include debris length (Figure 6.22) show a similar pattern of distribution to those produced using the equivalent empirical model (Figure 6.10) with only a very slight general increase in deviation from the actual percentage recorded (Figure 6.24).

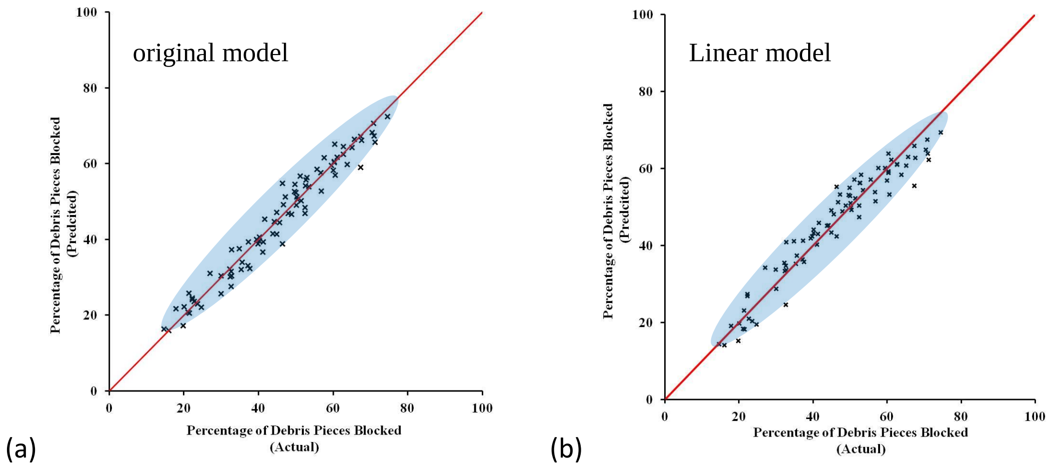

6.24 Comparison of aggregate model estimates of blockage against recorded blockage produced by the (a) original empirical model (Figure 6.10) and (b) linear empirical model (Figure 6.22). The shaded areas are identical on each graph.

For the linear model based on the full data set, debris length (L), bar spacing (S), relative velocity (P_v) and screen angle (A) were found to be significant predictive factors; all factors had p-values < 0.0001. Figures 6.25 to 6.28 show the individual contributions made by each of these elements within the generated model.

For the model based on the aggregated data set, bar spacing (S), relative velocity (P_v) and screen angle (A) were found to be significant predictive factors; all factors had p-values < 0.0001. Figures 6.29 to 6.31 show the individual contributions made by each of these elements within the generated model.

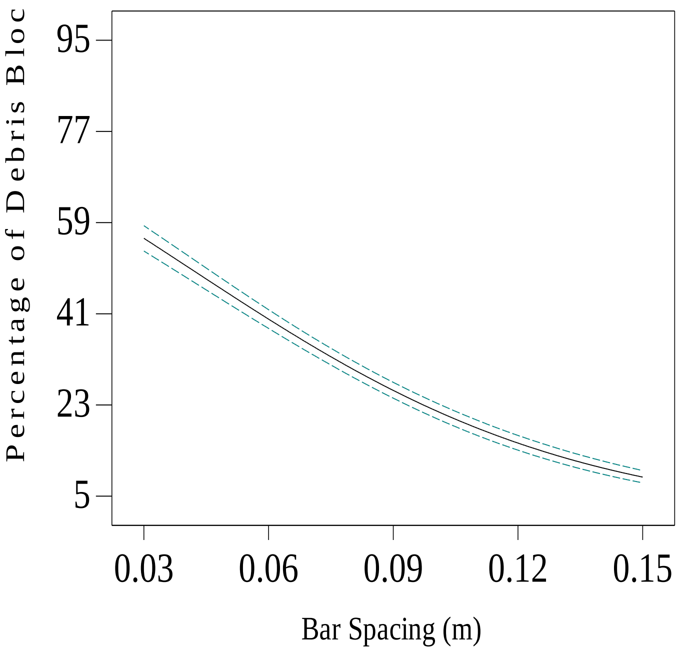

Figure 6.25 Influence of bar spacing on percentage blockage when screen angle = 45°, relative velocity = 1.35, debris length = 0.18m. Similar trends were found for other tested angles, relative velocities and debris lengths. The dotted green lines show the 95% confidence interval.

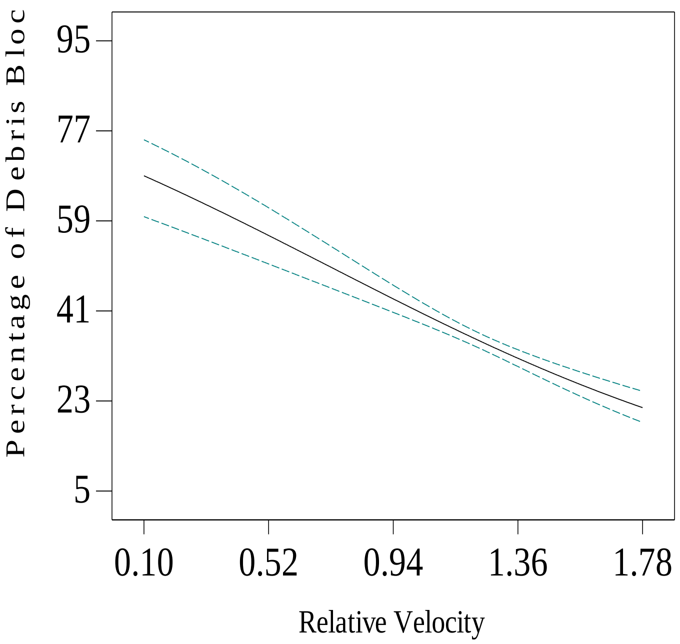

Figure 6.26 Influence of screen position (relative velocity) on percentage blockage when screen angle = 45°, bar spacing = 0.08m, debris length = 0.18m. Similar trends were found for other tested angles, spacings and debris lengths. The dotted green lines show the 95% confidence interval.

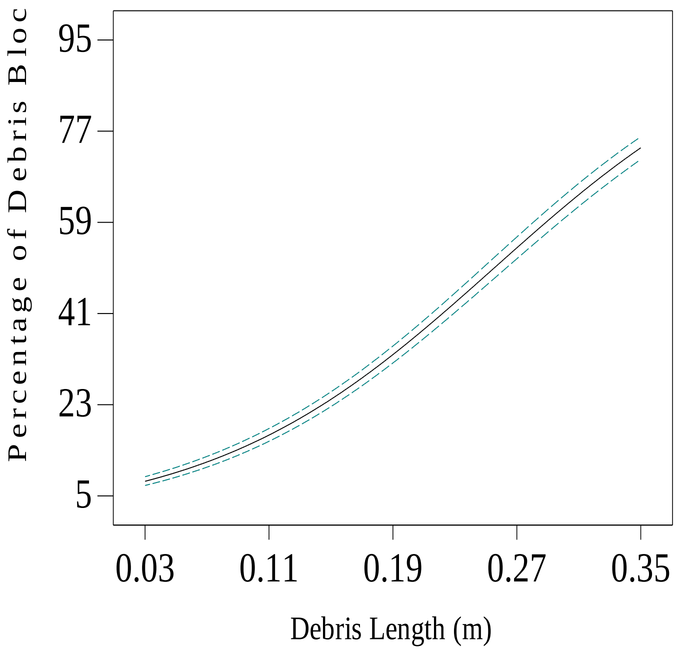

Figure 6.27 Influence of debris length on percentage blockage when screen angle = 45°, bar spacing = 0.08m, relative velocity = 1.35. Similar trends were found for other tested sceen angles, bar spacings and relative velocities. The dotted green lines show the 95% confidence interval.

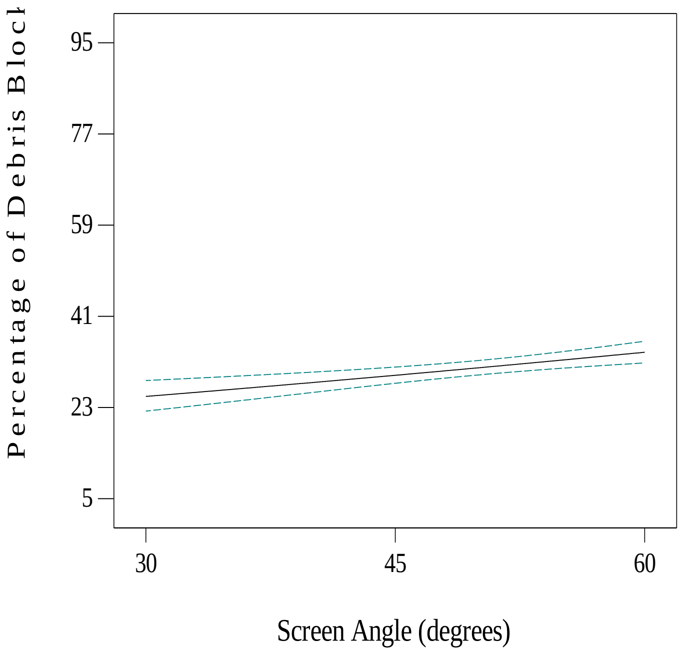

Figure 6.28 Influence of screen angle on percentage blockage when bar spacing = 0.08m, relative velocity = 1.35, debris length = 0.18m. Similar trends were found for other tested bar spacings, relative velocities and debris lengths. The dotted green lines show the 95% confidence interval.

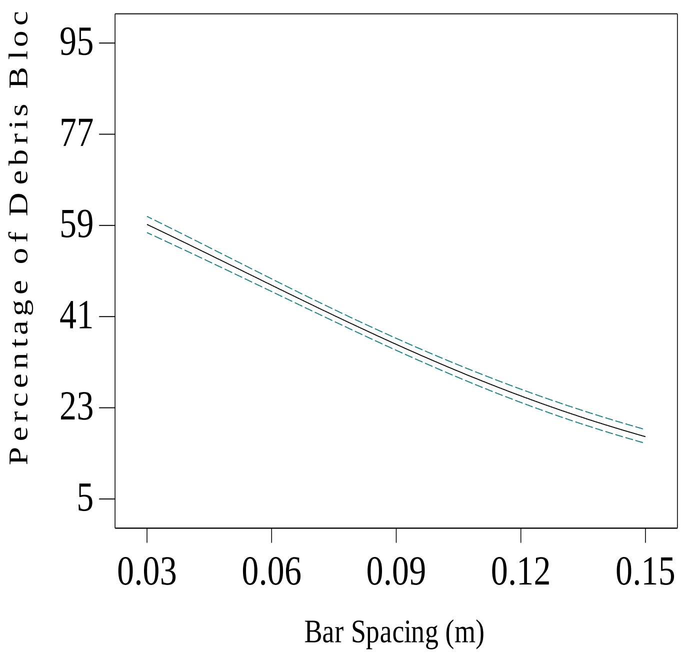

Figure 6.29Aggregate model: Influence of bar spacing on percentage blockage when screen angle = 45° and relative velocity = 1.35. Similar trends were found for other tested angles and relative velocities. The dotted green lines show the 95% confidence interval.

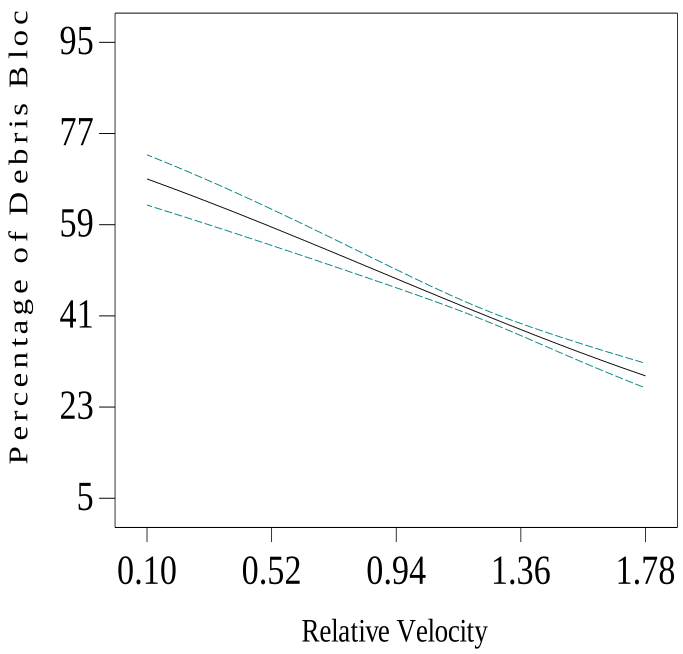

Figure 6.30 Aggregate model: Influence of screen position (relative velocity) on percentage blockage when screen angle = 45° and bar spacing = 0.08m. Similar trends were found for other tested angles and bar spacings. The dotted green lines show the 95% confidence interval.

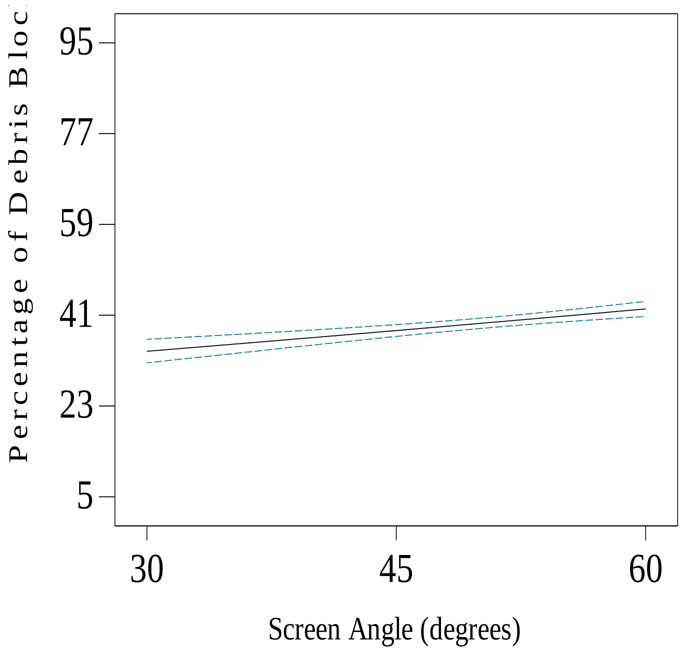

Figure 6.31 Aggregate model: Influence of screen angle on percentage blockage when bar spacing = 0.08m and relative velocity = 1.35. Similar trends were found for other tested bar spacings and relative velocities. The dotted green lines show the 95% confidence interval.

These plots show that the extent of the influence of individual parameters in the linear models is very similar to that shown by the contributing parameters for the more comprehensive models discussed in Chapter 5 and Sections 6.2 and 6.3.

Although not as precise as the best fit models described in Sections 6.2 and 6.3, the generated linear models (Equations 6.25 and 6.26) showed acceptable predictive capabilities.

While the model equations (Equations 25 and 26) can be used directly, the incorporation of the models into an end user focused tool offers a simple and accessible approach to estimating potential blockage at a screen.

6.5.3. Estimated blockage nomograph

Nomographs are used in a number of disciplines and historically were a key tool in engineering. A graphical approach is still commonly used for many engineering applications, including a number of standard calculation methods detailed in the current guidelines for trash screen design (EA, 2009). While the use of nomographs has in many cases been superseded by computer based tools, nomographs still offer a simple mechanism for visual expression of an equation that can allow more precise reading than the use of conventional graphs. In addition many engineers are familiar with this type of tool as they have been used to aid a number of calculations in civil engineering, including culvert design, and are suggested for use both within published standard guidelines (e.g. Amec, 2008; Lagasse *et al*., 2009, Schall *et al*., 2012) and by commercial product suppliers (e.g. Cretex, 2012).

Nomographs developed for the linear models described in Section 6.5.2 are shown in Figures 6.32 and 6.33. Figure 6.34 shows how the nomograph can be used to estimate blockage risk if the other values are known.

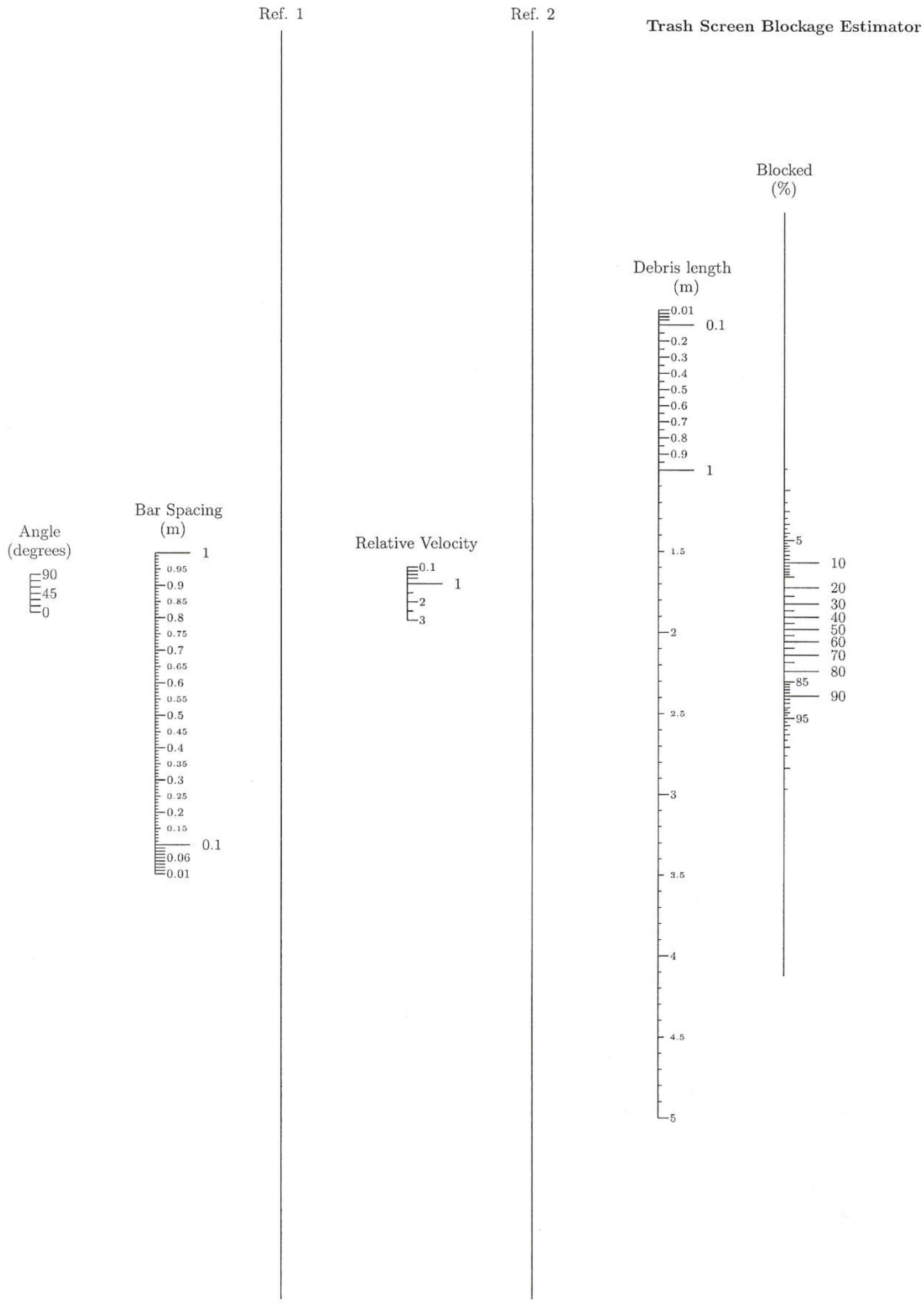

Figure 6.32 Trash screen blockage nomograph for use where debris length known

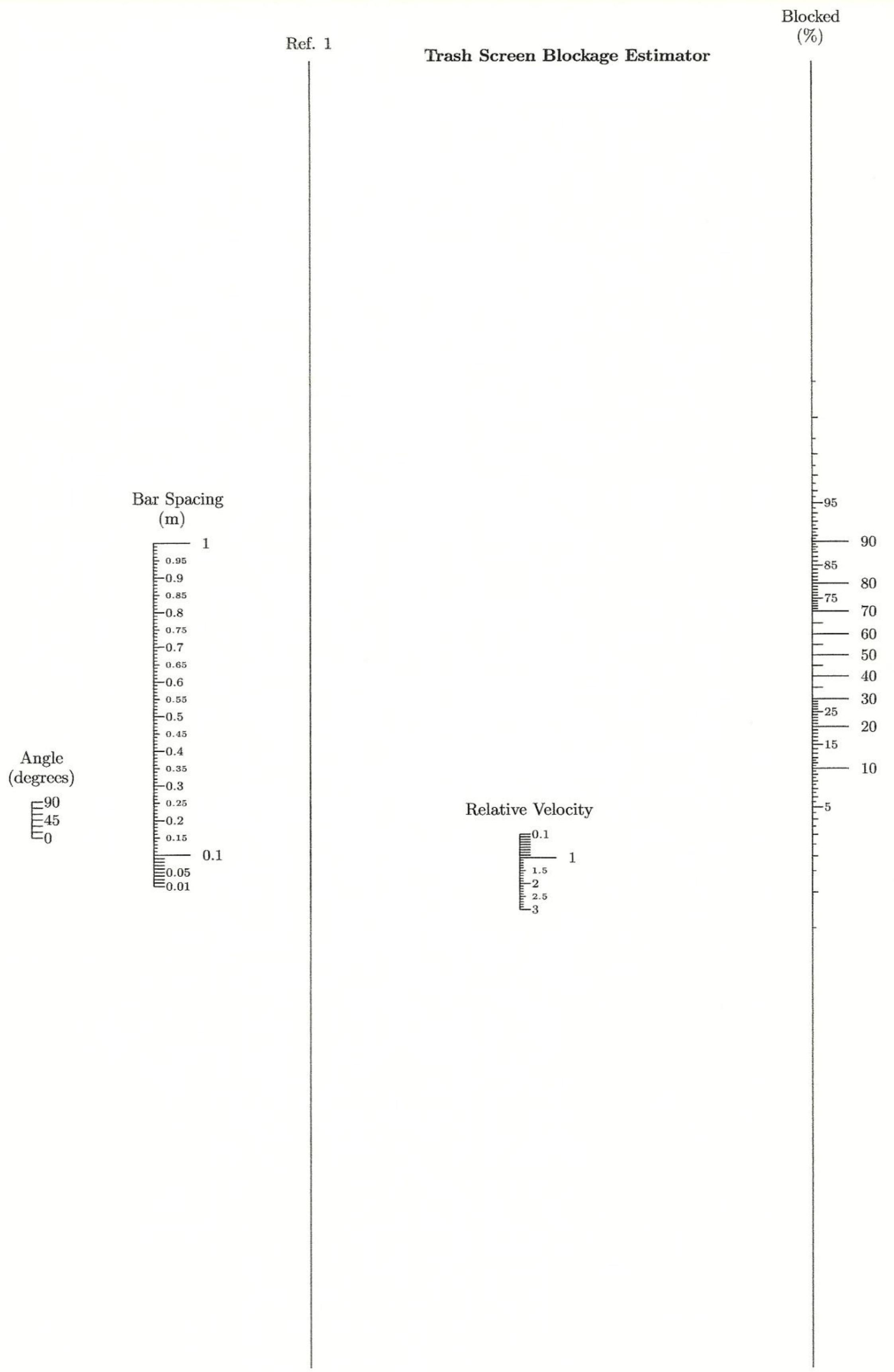

Figure 6.33 Trash screen blockage nomograph for use where debris length unknown

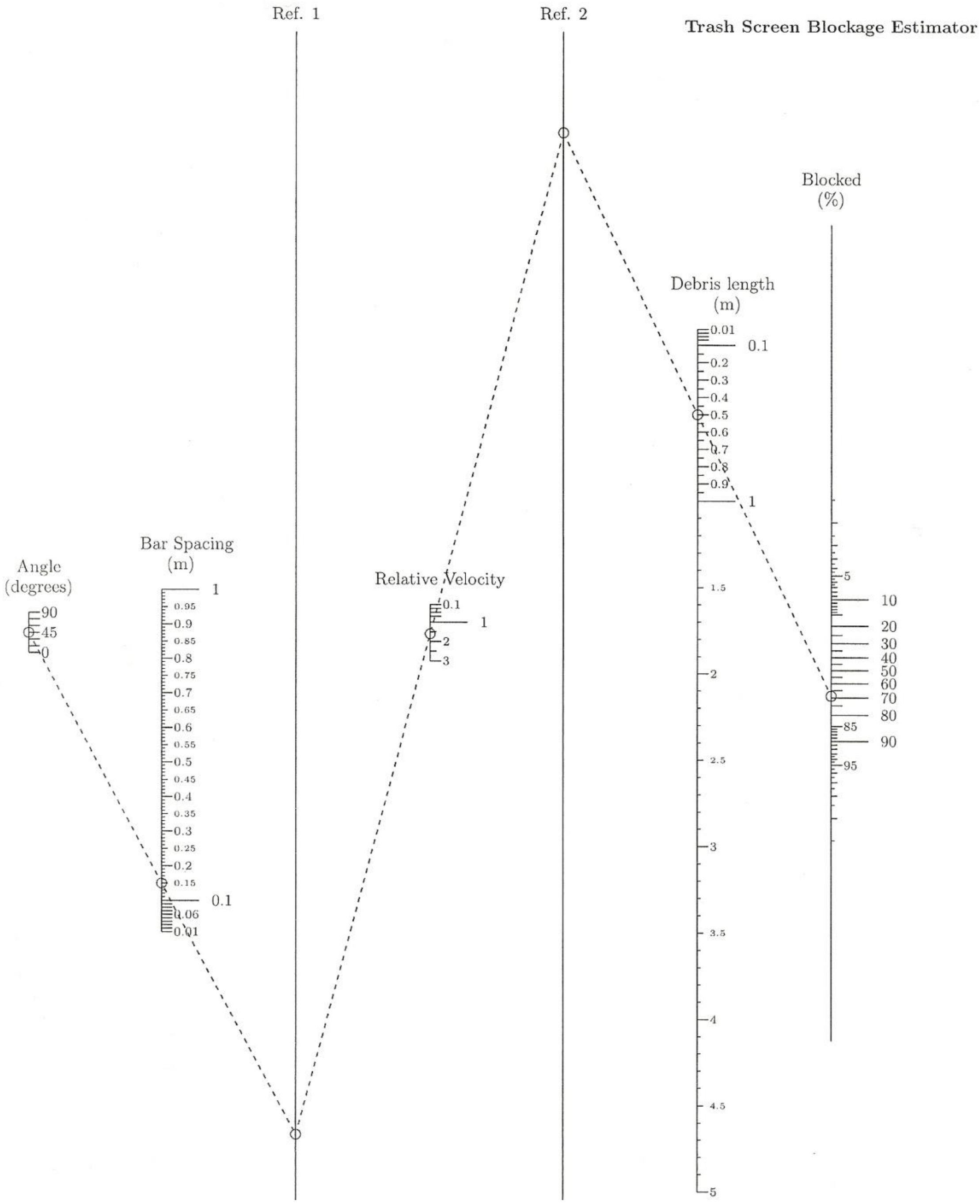

Figure 6.34 Trash screen blockage estimator with an isopleth showing estimated blockage for a screen angle of 45 degrees, bar spacing of 0.15m, a relative velocity of 1.6 and a debris length of 0.5m. The estimated percentage of debris that will become blocked is 70 percent.

6.5.4. Estimated blockage interactive spreadsheet

While the nomographs offer a simple graphical tool for blockage estimation, a computer based tool provides a consistently more precise estimate than is likely from manual reading from a scale which is required for use of the nomograph. In order to provide an accessible estimation tool that may be used on a number of platforms a macro driven Excel based spreadsheet was used to develop an estimation tool. The spreadsheet has a simple easy to use interface that allows the user to enter known parameters. It then calculates the estimated blockage based on either the full empirical model or the simplified linear model. The user may select which model to base the estimate on from the dropdown list. If a debris length is entered, the estimation is based on the full data models: if no debris length is entered the estimate is based on the aggregated data models. The user interface is shown in Figure 6.35. Estimates may be generated by using the up and down arrows associated with individual parameters or the values may be keyed in directly and the ‘Estimate’ button clicked to produce the calculated value.

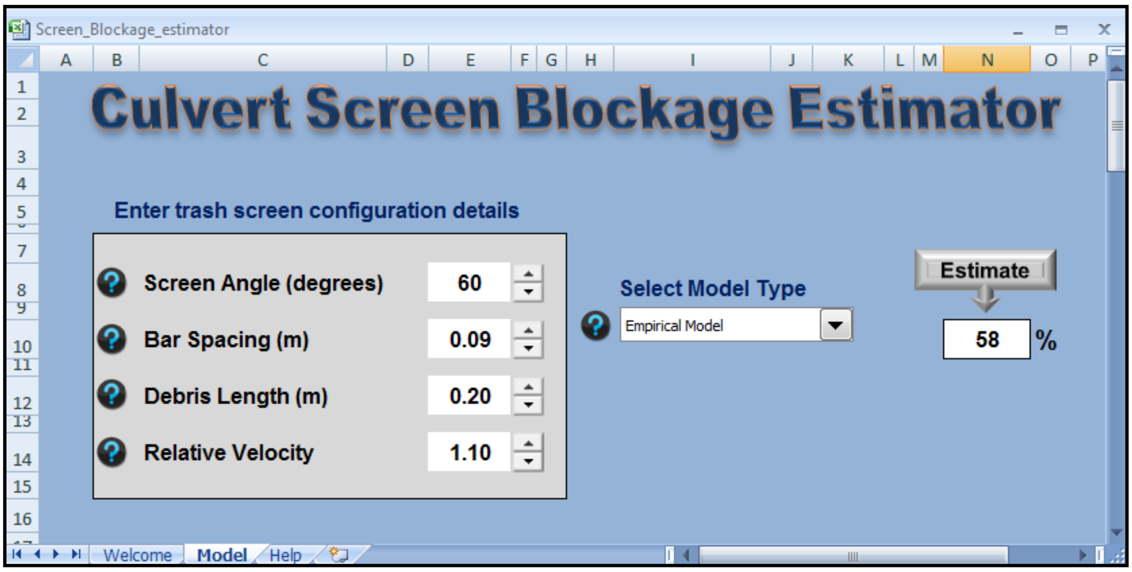

Figure 6.35 Interface to spreadsheet based Culvert Screen Blockage Estimator

Basic validation is carried out on entry of the known parameters and an appropriate error message is displayed if the entered values fall out-with the required ranges (see Figure 6.36). If the empirical model is selected and the entered parameters fall out-with the range of tested values then a warning message is displayed (see Figure 6.37).

The visual basic macros associated with the Blockage Estimator can be found in Appendix K.

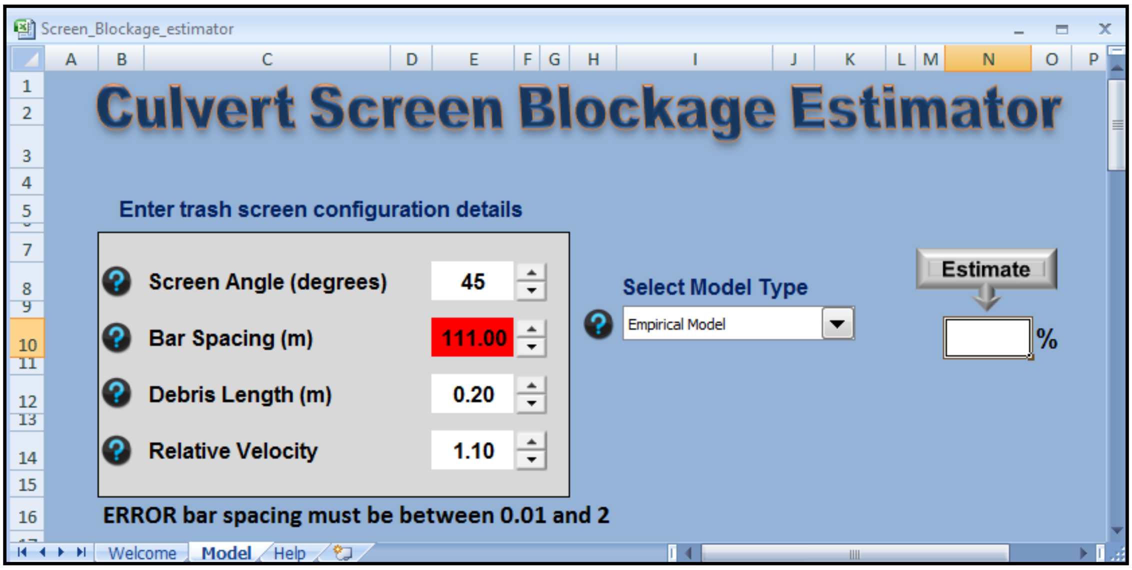

Figure 6.36 Interface to spreadsheet based Culvert Screen Blockage Estimator showing example error message displayed when incorrect parameter value entered

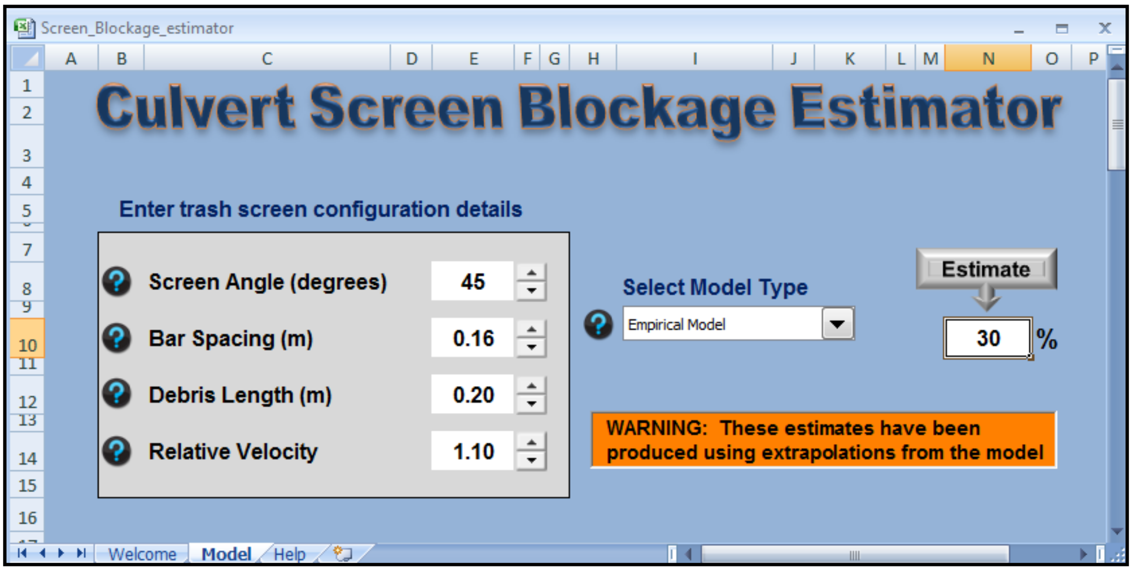

Figure 6.37 Interface to spreadsheet based Culvert Screen Blockage Estimator showing warning displayed when entered values fall outwith the range of values tested

6.5.5. Limitations of the tools

These estimation tools provide a user friendly method for using the model equations to estimate potential blockage. However, they are still limited by the accuracy of the models themselves and therefore must be used with caution. Further refinement and validation using laboratory and field based data is required to fully develop the underlying models into more accurate predictive tools. In addition these tools only consider a limited number of parameters; many other factors may also influence blockage potential and must be considered alongside the blockage potential of the screen geometry and position.

6.6. Dimensional analysis

As noted in Section 4.2, dimensional analysis has played a significant role in developing the use of models in hydraulic research. Dimensional analysis can provide information about the process under investigation by expressing it as a dimensionally correct equation (Novak et al., 2010). To express the models generated during this research as dimensionless relationships Buckinham's method was applied to the generated full empirical model (Equation 22). This generated an initial expression of the relationship as shown in Equation 27.

$$f\,(\mathrm{D, A, S, L, P_v}) = 0 \tag{27}$$

This expression contains five variables and one dimension, length, applicable to debris length (L) and bar spacing (S); Blockage (D), Screen angle (A) and Relative velocity at screen position (Pv) are dimesionless. Applying Buckinghams method, using S as a repeating variable, resulted in the formation of a relationship expressed in terms of four (dimensionless groups (Equation 28).

$$f\,(\mathrm{S^{a1}D, S^{a2}A, S^{a3}L, S^{a4}P_v}) = 0 \tag{28}$$

To achieve dimensionless variables the following values for the variable powers were applied: a1 = 0, a2 = 0, a3=-1, a4 =0 giving a final expression for blockage(D) as shown in Equation 29.

$$\mathrm{D} = f\,(\mathrm{A}, \tfrac{\mathrm{L}}{\mathrm{S}}, \mathrm{P_v}) \tag{29}$$

While dimensionless relationships may improve scalability and offer the potential for wider application of a model, the use of the debris length to bar spacing ratio (L:S) as a variable does not truly reflect the physical processes involved, as highlighted by the different pattern of blockage observed for identical L:S ratios for short and long lengths of debris (Section 5.2.2). Therefore, the generated dimensionless relationship (Equation 28) was not developed any further.

However, a number of other known variables may be included to produce an alternative dimensionless relationship. For example, Equation 30 shows a dimensionless relationship generated by including channel width (W_c) and screen width (W_s).

$$D = f\left(A, \frac{L}{W_c}, \frac{S}{W_s}, P_V\right) \tag{30}$$

Given that only single values of W_c and W_s were used throughout, the data collected do not give sufficient scope for the calibration of models of the type in Equation 30. Thus, further studies investigating different channel widths and screen widths may be beneficial in further refining the developed models.

6.7. Chapter Summary

This chapter used the data gathered during testing to establish empirical models defining blockage in terms of all the identified driving factors. Two empirical models were developed: the first defining blockage in terms of bar spacing, debris length, screen angle, discharge and relative velocity while the second model, based on an aggregated data set, defined blockage in terms of bar spacing, screen angle, discharge and relative velocity.

Regression analysis was used to establish an empirical relationship between the contributing factors and blockage potential. Quadratic functions were shown to offer the best fit with both models having high R^2 values.

The model based on the results for individual debris lengths identified debris length, bar spacing, screen position in terms of relative velocity, and screen angle as significant predicting factors. While blockage was found to increase as both bar spacing and relative velocity decreased, an increase in screen angle resulted in a slight increase in blockage. The influence of debris length was shown to be somewhat more complex:

initially an increase in debris length results in an increase in blockage but once a threshold length has been reached blockage appears to decrease as length increases.

The model based on the aggregated results, which provided a percentage of debris blocked for all debris lengths, identified bar spacing, screen position in terms of relative velocity, and screen angle as significant predicting factors. While blockage was found to increase as both bar spacing and relative velocity decreased an increase in screen angle resulted in a slight increase in blockage. A sensitivity analysis showed that the model was less sensitive to changes in screen area than to changes in the value of the other contributing parameters.

Results from testing that had not been used to generate the models were used for validation and plots of the predicted blockage generated by the models against the actual blockage recorded showed that the models could be used to produce reasonable estimates.

The chapter then detailed the generation of linear models from the test data. These simplified models were required as the best fit empirical models did not function particularly effectively when extrapolated out-with the range of data values tested. It was found that while these simplified models had reduced accuracy when compared to the best fit empirical models they still had a reasonable predictive capability.

The generated linear models were used as the basis for two end user focused tools: a nomograph and an interactive spreadsheet. These tools offer a simple and novel approach to estimating the likelihood of debris becoming blocked at a screen.

The generated models were used to develop dimensionless relationships. The use of the debris length to bar spacing ratio as an alternative to including these two variables independently was not considered to reflect the underlying observed behaviour. An alternative dimensionless relationship considering the additional variables of channel width and screen width was suggested as a potentially useful approach to further refining the developed models.

Chapter 7
Conclusions and Recommendations for Further Study

7.1. Overview

The research outlined in the preceding chapters set out to determine if aspects of trash screen geometry and location had an influence on potential blockage by debris. An experimental approach was taken, using a Froude scaled physical model to represent a generic prototype culvert.

To support the experimental analysis, a wide-ranging literature review was undertaken that covered the structure, use and maintenance of culverts and trash screens; water flow in culverted channels; trash screen hydraulics; sources of debris; mechanisms of debris transport and accumulation; and existing methods of debris control. In addition, the review also considered different modelling approaches used in hydraulic research.

This review was important in order to understand the fundamentals of culvert and trash screen design and hydraulics and also the potential flood risks associated with their installation and operation. The review clarified the current knowledge base supporting existing culvert and trash screen design and implementation guidelines and highlighted the need for experimental analysis and detailed investigation of how aspects of trash screen design, other than screen area, influence blockage potential.

The aim of this research was supported by four objectives:

1. The development of a physical model
2. The use of the constructed model to investigate blockage at a screen
3. The development of an empirical relationship
4. An assessment of the impact of the findings on current screen design guidelines

To meet the first objective, a Froude scaled physical model was developed and shown to be robust and appropriate for the required testing. The empirical approach to the research has resulted in the development of a novel methodology that can be used to assess the performance of various trash screen configurations and may also be adapted to assess different screen and inlet combinations.

The second and third objectives were met through an extensive series of tests which were undertaken to assess the influence of bar spacing, screen angle, debris length, discharge, bed slope and screen position relative to the culvert inlet. This research was the first major experimental assessment of trash screen performance in hydraulic conditions specific to a culvert inlet. In addition, the data set gathered was much more extensive than that gathered for previously reported studies of debris screen efficiency. The study by Padilla & Clark (2008) assessed 44 different screen configuration and discharge combinations while the assessment of screen efficiency undertaken by Xiang *et al*. (2009) considered only 32 different screen configuration and discharge combinations. The analysis reported in the preceding chapters was based on tests carried out on a total of 147 different trash screen configuration and discharge combinations and results for 147,000 pieces of debris were recorded. The resulting comprehensive data set was used to develop an empirical relationship that defines blockage potential in relation to individual contributing factors. The empirical results were then used as the basis for generating a simplified relationship that was used to develop end user focused tools for estimation of potential blockage. The potential impact of the findings of the research on current design guidelines is discussed in Section 7.3.

7.2. Main Findings

In addition to developing a novel methodology that allows comparison of the efficiency of different trash screen configurations, the research detailed in the preceding chapters has increased the scientific knowledge base surrounding the complex issue of debris blockage at trash screens. Current understanding has been extended through the use of an empirical approach that gathered an extensive data set and correlates the probability of debris becoming blocked at a trash screen with key contributing properties of the screen's design and installation. The resulting analysis facilitated the development of relationships that, once further refined and fully validated, may be used to help assess potential design options where a new culvert trash screen is required.

The main findings of the research were:

- The influence of bar spacing
  There is a clear relationship between the likelihood of a piece of debris being trapped by a screen and the debris length to bar spacing ratio (L:S): as L:S increases more pieces of debris are likely to become blocked (Section 5.2.3). While this finding is perhaps not unexpected the relationship was shown not to be linear but best represented by a logarithmic function. For small ratios, less than around 1.5, the controlling factor appeared to be simply whether the full length of the debris could pass through the gap between the bars. However, at

higher ratios in addition to the influence of the debris length to bar spacing ratio, the orientation of the debris had a noticeable influence. The passage of the debris through the screen varied depending on its orientation relative to the direction of flow and on its position within the channel, with pieces parallel to the direction of flow less likely to become trapped.

In all generated models, bar spacing was found to be a statistically significant factor in determining potential blockage.

- The influence of screen angle

  During the initial testing there was a relatively small but marked difference in blockage over the range of angles investigated, particularly at higher discharges (Section 5.2.3). Higher angle screens (measured from the channel bed) consistently resulted in a lower percentage of pieces of debris blocked for any given debris length to bar spacing ratio though these results may have been influenced heavily by the position of the screen relative to the culvert inlet. A screen at 60 degrees intersected the water surface closer to the culvert than a screen at 30 degrees.

  When screen performance was assessed for different angled screens that intersected the water surface at the same position, only a very minor difference in performance was noted (Section 5.4.3). However, screen angle was found to be a statistically significant parameter in both of the generated empirical models (Equations 22 and 24) although it had much less influence on the estimated blockage generated than the other parameters (see Sections 6.2 and 6.3). In both models the coefficient while small is positive, indicating that blockage increases as screen angle increases. While this contradicts the findings from the initial testing it matches the findings of Wallerstein and Arthur (2011) who also reported that blockage increased as angle increased. Their findings were based on a set of field data gathered from functioning trash screens.

- The influence of discharge

  The results from the empirical analysis show that as discharge increased, the proportion of debris pieces trapped by the screen fell slightly (Section 5.2.3). At the higher flow velocities associated with higher discharges, more debris rotated to align parallel to the flow direction facilitating passage through the screen. In addition, at lower flow rates, debris had a greater tendency to remain balanced across a single bar.

Empirical analysis of the initial testing indicated discharge was a contributing factor although had it substantially less influence than the other driving parameters (see Section 5.2.4). However, the final generated best fit empirical models do not include discharge as it was not found to be statistically significant.

- The influence of bed slope

  The relationships identified between the debris length to bar spacing ratio and blockage appear to be valid regardless of the bed slope (Section 5.3.3). A statistically significant difference in screen performance for some bed slopes was found during testing with screens at 45 and 60 degrees but was not apparent for screens at 30 degrees. This change in performance under different flow conditions due to changes in bed slope appears to be due to a combination of the change in the position of the screen relative to the area of rapid flow acceleration created as the water is constricted at the culvert inlet, and changing water depths at the screen resulting from flow build up at the headwall. Bed slope was not found to be a statistically significant contributing factor to potential blockage at the screen (Section 5.3.4). This confirms an observation by Wallerstein and Arthur (2012) based on field data who noted that that upstream bed slope appeared to exert no significant influence on potential load delivery. Therefore it appears that bed slope exerts no noticeable impact on debris blockage at a trash screen.

- The influence of screen position

  The mid-stream depth averaged flow velocity within the channel was shown to increase as it approached the culvert inlet (Figure 5.21). This acceleration in flow exerts forces on the debris that affect both its orientation relative to the flow direction and its potential for being pulled through the screen bars. Therefore, the position of the screen relative to the area of flow acceleration will have a significant impact on its blocking capability. This was reflected in the results which showed that as the distance of the screen from the culvert inlet increased the percentage of debris pieces blocked also increased (Section 5.4.3). The relative velocity at the point the screen intersects the water surface was considered to be an appropriate reflection of the screens position and was included as a potential contributing factor in the empirical analysis. In all generated models, the relative velocity at the screens position was found to be one of the most significant influencing factors in determining the likelihood that debris would become blocked.

- Development of a predictive tool

  While quadratic functions were found to provide the best fit for the empirical data (Sections 6.2 and 6.3), simplified linear models were generated which although not as accurate as the best fit models, showed acceptable predictive capabilities where extrapolations from the tested parameter ranges were required (Section 6.5.2).

  The linear models were used to produce two end user focused tools, a nomograph and an interactive spreadsheet, to provide novel, simple and accessible approaches for estimating potential blockage at a screen. The nomograph provides a simple graphical mechanism for visualising and using the model (Section 6.5.3) while the interactive spreadsheet (Section 6.5.4) allows for estimation based on either the best fit empirical or simplified linear models.

7.3. Practical Implications for Trash Screen Design and Implementation

Positioning the screen a distance upstream from the culvert inlet is often considered a practical approach to allow horizontal working platforms to be positioned between the headwall and screen for ease of maintenance or to increase the available surface area of the screen. However, given the findings from this research, this approach may increase the likelihood of the screen becoming blocked. While it is acknowledged that many factors can influence potential blockage, all other things being equal, a screen with a smaller overall area positioned closer to the culvert inlet may offer a reduced potential for blockage therefore reducing any flood risk associated with the installation of a screen.

Current guidelines (EA, 2009) recommend that a comprehensive hydraulic analysis should be undertaken in order to determine optimum trash screen design. This analysis would be enhanced by an assessment of potential blockage at any planned trash screen. While the models generated from the empirical data gathered during this research require further development and validation before they can provide direct estimates of blockage, it may be worth noting within the guidelines that the position of the screen within the zone of flow acceleration has a significant influence on blockage potential. Any hydraulic modelling of potential screen designs undertaken during the design phase could then consider position relative to the culvert inlet along with all other design aspects.

A recent study has focused on developing a process to rank culverts in terms of their blockage potential as a mechanism for optimising operation and maintenance regimes (Wallerstein & Arthur, 2012). Although not considered as part of the research detailed in the preceding chapters, it should be possible to use the developed models to highlight high risk or low risk existing screens in terms of potential blockage for that screen design. This could then be incorporated as an additional factor in the decision tool developed in that study.

7.4. Recommendations for Future Work

The research to date has highlighted a number of areas relating to screen performance that would benefit from further investigation. These research requirements can be grouped into four main areas:

1. Further analysis and validation of tested components
2. Testing of additional factors
3. Further consideration of debris
4. Analysis of patterns of blockage

7.4.1. Further analysis and validation of tested components

While the derived models were validated against a small data set (Section 6.4), the use of a larger data set derived from a different experimental set up or from field based data would be beneficial to help assess the applicability of the derived models to more general conditions.

As discussed in Section 7.2, the influence of screen angle is still somewhat unclear. The results used for data analysis were gathered using only three different screen angles with approximately 50% of the results from testing using a single screen angle (60 degrees).

A more comprehensive experimental analysis of the influence of screen angle assessing a greater number of screen angles and testing all angles under different flow conditions may help clarify the role screen angle plays in debris blockage.

7.4.2. Testing of additional factors

The research identified screen components that influenced blockage potential. However a number of other aspects of screen geometry may also influence blockage potential and the test rig could be adapted to assess their performance. These include: the presence and positioning of cross bar supports; bar shape and material; the design of working platforms; the angle of the screen relative to the flow direction; the shape of the screen (e.g. straight slope or parabolic curve).

One of the major findings of the research is the influence of relative flow velocity on blockage potential therefore there is a need to assess screen performance in different flow environments such as: different flow patterns caused by different diameter culverts relative to channel width; changes in flow due to the influence of wingwalls or other inlet features; flow patterns caused by the shape of the upstream channel including upstream bends or natural or artificial obstacles. An assessment of how varying flow velocities and patterns across the channel width, caused by the inlet and screen structure, influence debris orientation may be particularly useful.

In addition, the research to date has only considered culvert operation under routine operating conditions. There is a need to look at the performance of trash screens under more extreme flows that represent flood conditions.

7.4.3. Further consideration of debris

The research to date has focused specifically on screen performance and therefore the use of dowel to represent debris was appropriate to eliminate the influence of factors related to the variable nature of debris. However, natural debris has a much more complex geometry and the use of more representative debris including root wads and leaves should be considered.

Another simplification used in the research to date was debris was always introduced to the water at the midpoint of the channel. While this approach was taken in order to retain focus on screen performance as it removed an additional variable from the analysis, in natural environments debris may enter the watercourse across the full channel width. An investigation of how point of entry affects debris transport and potential deposition at a screen would be useful.

Non-floating debris can play a significant role in blockage at trash screens (e.g. Abt *et al*., 1992). A similar experimental approach to that outlined in the preceding chapters could be used to investigate the transport, deposition and accumulation of non-floating debris.

7.4.4. Analysis of patterns of blockage

Although for the purposes of this study balanced, bridged and wedged debris were treated the same and classed as blocked, there is a fundamental difference in the potential blocking capabilities of these situations. For example, debris bridged across two or more bars can provide a possible starter log for the formation of jams. In a study looking at the transport of debris in the presence of obstacles, Bocchiola *et al.* (2006b) report that qualitative experimental results showed that when a moving dowel made contact with a bridging log, the bridging log generally remained in place and tended to lead to the formation of a jam. In contrast, when a moving dowel makes contact with a balanced log, the balancing log may or may not be swept away, depending on the size and momentum of the moving dowel. Therefore further analysis of blocking patterns looking at the type of blocking that occurred would be beneficial in gaining a more detailed understanding of the blockage process.

The research to date focused on the trapping of an initial piece of debris but there is also a need to look at cumulative debris build up on a screen. A number of factors could be investigated including: the stability of debris accumulations under different flow conditions; the hydraulic impact of different percentages and locations of blockage; which aspects of screen design complicate clearance once blocked.

References

Abbe, T.B. & Montgomery, D.R., 1996. Large woody debris jams, channel hydraulics and habitat formation in large rivers. *Regulated rivers: research & management*, **12(2-3),** pp201-221.

Abt, S.R., Brisbane, T.E., Frick, D.M. & Mcknight, C.A., 1992. Trash rack blockage in supercritical flow. *Journal of Hydraulic Engineering*. **118(12)**, pp1692-1696.

Acreman, M. (Ed), 1999. The hydrology of the UK. A study of change. Oxon, Routledge.

Allred-Coonrod, J.E., 1994. Safety grates in supercritical channels. *Journal of Irrigation and Drainage Engineering*, **120(1)**, pp218-224.

Antón, A., Elosegi, A., García-Arberas, L., Díez, J. Rallo, A., 2011. Restoration of dead wood in Basque stream channels: effects on brown trout population. *Ecology of Freshwater Fish*, **20(3)**, pp461-471.

AMEC, 2008. Knox County Tennessee Stormwater Management Manual, Volume 2: Technical guidance, prepared by Amec Earth & Environmental, Inc. [online], http://www.knoxcounty.org/stormwater/pdfs/vol2/7-3%20Culvert%20Design.pdf, [Accessed 26/12/2012].

Andreoli, A., Comiti, F. & Lenzi, M.A., 2007. Characteristics, distribution and geomorphic role of large woody debris in a mountain stream of the Chilean Andes. *Earth Surface Processes and Landforms*, **32(11)**, pp1675–1692.

Andrew, F.J., 1951. *The head-discharge relationship for wire screens in plane and cylindrical forms*. International Pacific Salmon Fisheries Commission, New Westminster, British Columbia, Canada. in Tsikata, J.M., Katopodis, C. & Tachie, M.F., 2009. Experimental study of turbulent flow near model trashracks. *Journal of Hydraulic Research*, **47(2)**, pp275-280.

ASCE, 1942. Hydraulic Models. The American Society of Civil Engineers Manual of Practice, 25. New York, American Society of Civil Engineers.

Aquaveo, 2012. WMS:HY-8 Broken Back Culverts. [online], http://www.xmswiki.com/xms/WMS:HY-8_Broken_Back_Culverts, [Accessed 03/09/2012].

Baillie, B.R. & Davies, T.R., 2002. Influence of large woody debris on channel morphology in native forest and pine plantation streams in the Nelson region, New Zealand. *New Zealand Journal of Marine and Freshwater Research*, **36(4)**, pp763–774.

Baines, W.D. & Peterson, E.G., 1951. An investigation of flow through screens. *Transactions of the American Society of Mechanical Engineers*, **73**, pp467-480, in Tsikata, J.M., Katopodis, C. & Tachie, M.F., 2009. Experimental study of turbulent flow near model trashracks. *Journal of Hydraulic Research*, **47(2)**, pp275-280.

Balkham, M., Fosbeary, C., Kitchen, A. & Rickard, C., 2010. Culvert design and operation guide, London, Construction and Industry Research and Information Association.

Benn, J.R., Mantz, P., Lamb, R., Riddell, R. & Nalluri, C., 2004. Afflux at bridges and culverts, Review of current knowledge and practice. Defra/Environment Agency Flood and Coastal Defence R&D Programme, Technical Report W5A-061/TR1.

Beschta, R.L & Robison, E.G., 1990. Characteristics of coarse wood debris for several coastal streams of southeast Alaska, USA. *Canadian Journal of Fisheries and Aquatic Sciences*, **47(9)**, pp1684-1693.

Bilby, R.E. & Ward, J.W., 1989. Changes in characteristics and function of woody debris with increasing size of streams in Western Washington. *Transactions of the American Fisheries Society*, **118**, pp368-378.

Bocchiola, D., Catalano, F., Menduni, G. & Passoni, G., 2002. An analytical–numerical approach to the hydraulics of floating debris in river channels. *Journal of Hydrology*, **269(1)**, pp65–78.

Bocchiola, D., Rulli, M.C. & Rosso, R., 2006a. Flume experiments on wood entrainment in rivers. *Advances in Water Resources,* **29(8)**, pp1182-1195.

Bocchiola, D., Rulli, M.C. & Rosso, R., 2006b. Transport of large woody debris in the presence of obstacles. *Geomorphology,* **76(1)**, pp166-178.

Bocchiola, D., Rulli, M.C. & Rosso, R., 2008. A flume experiment on the formation of wood jams in rivers. *Water Resources Research*, **44(2)**, W02408, doi:10.1029/2006WR005846.

Bradley, J.B., Richards, D.L. & Bahner, C.D., 2005. Debris Control Structures Evaluation and Countermeasures. U.S. Department of Transportation, Federal Highway Administration. Hydraulic Engineering Circular No. 9, Third Edition. [online], http://www.fhwa.dot.gov/engineering/hydraulics/pubs/04016/hec09.pdf, [Accessed 30/11/2009].

Braudrick, C.A. & Grant, G.E., 2000. When do logs move in rivers?. *Water Resources Research*, **36(2)**, pp571-583.

Braudrick, C.A. & Grant, G.E., 2001. Transport and deposition of large woody debris in streams: a flume experiment. *Geomorphology*, **41(4)**, pp263-283.

Braudrick, C.A., Grant G.E., Ishikawa, Y. & Ikeda, H., 1997. Dynamics of wood transport in streams: A flume experiment. *Earth Surface Processes and Landforms*, **22(7)**, pp669-683.

Buckingham, E., 1915. Model experiments and the forms of empirical equations, *Transactions of the American Society of Mechanical Engineers*, **37**, pp263-292.

Chadwick, A., Morfett, J. & Borthwick, M., 2004. Hydraulics in Civil and Environmental Engineering. Fourth Edition. Spon Press, London.

Cherry, J. & Beschta, R.L., 1989. Course woody debris and channel morphology: a flume study. *Water Resources Bulletin*, **25(5)**, pp1031-1036.

CIWEM, 2010. De-Culverting of Watercourses. CIWEM policy position statement. [online], http://www.ciwem.org/policy/policies/de-culverting_of_watercourses.asp, [Accessed 15/02/2010].

Clark, S. P., Tsikata, J. M. & Haresign, M., 2010. Experimental study of energy loss through submerged trashracks. *Journal of Hydraulic Research*, **48(1)**, pp113-118.

Clevenger, A.P., Chruszcz, B. & Gunson, K., 2001. Drainage culverts as habitat linkages and factors affecting passage by mammals. *Journal of Applied Ecology*, **38(6)**, pp1340–1349.

Comiti, F., Andreoli, A., Lenzi, M.A. & Mao, L., 2006. Spatial density and characteristics of woody debris in five mountain rivers of the Dolomites (Italian Alps). *Geomorphology*, **78(1-2)**, pp44–63.

Cretex, 2012. Cretex Concrete products. Culvert Nomograph - Horizontal Elliptical Concrete Pipe Culverts with Inlet Control. [online], http://www.iowaconcrete.com/node/767, [Accessed 26/12/2012].

Dasika, B., 1995. New Approach to Design of Culverts. *Journal of Irrigation and Drainage Engineering*, **121(3)**, p261.

Davis, C.V., 1952. Handbook of Applied Hydraulics, McGraw-Hill Book Co., Inc., New York, N.Y.

Dawson, R.J., Speight, L., Hall, J.W., Djordjevic, S., Savic, D. & Leandro, J., 2008. Attribution of flood risk in urban areas. *Journal of Hydroinformatics*, **10(4),** pp275-288.

Day, R.A., 1997. Preliminary observations of turbulent flow at culvert inlets. *Journal of Hydraulic Engineering*, **123(2)**, pp116-124.

DEFRA, 2004. *Making space for water – developing a new Government strategy for flood and coastal erosion management in England.* [online], http://www.defra.gov.uk/environ/fcd/policy/strategy.htm, [Accessed 18/05/2009].

DEFRA, 2006. Flood and Coastal Defence Appraisal Guidance (FCDPAG3) Economic Appraisal. Supplementary Note to Operating Authorities – Climate Change impacts. London, Defra. [online], http://www.defra.gov.uk/environment/flooding/documents/policy/guidance/fcdpag/fcd3climate.pdf, [Accessed 11/08/2010].

Diehl, T.H., 1997. Potential drift accumulations at bridges. U.S. Department of Transportation, Federal Highway Administration, Research and Development, Publication No. FHWA-RD-97-028. [online], http://tn.water.usgs.gov/pubs/FHWA-RD-97-028/tablecon.htm, [Accessed 22/09/2010].

Diehl, T.H. & Bryan. B.A., 1993. Supply of large woody debris in a stream channel, in Shen, H.W., Su, S.T. & Wen, F. (eds.), 1993, Proceedings of Hydraulic Engineering '93 Conference, San Francisco. American Society of Civil Engineers, **1**, pp1055-1060.

Dodd Jr., C.K., Barichivich, W.J. & Smith, L.L., 2004. Effectiveness of a barrier wall and culverts in reducing wildlife mortality on a heavily travelled highway in Florida. *Biological Conservation*, **118,** pp619–631.

EA, 2009. Trash and Security Screen Guide. Bristol, Environment Agency.

EA, 2010. Environment Agency Fluvial Design Guide. [online], http://evidence.environment-agency.gov.uk/FCERM/en/FluvialDesignGuide/Chapter7.aspx?pagenum=4, [Accessed 20/9/2012].

Elder, J. W., 1959. Steady flow through non-uniform gauzes of arbitrary shape. *Journal of Fluid Mechanics*, **5**, pp355-368, in Tsikata, J.M., Katopodis, C. & Tachie, M.F., 2009. Experimental study of turbulent flow near model trashracks. *Journal of Hydraulic Research*, **47(2)**, pp275-280.

Elmore, A.J. &, Kaushal, S.S., 2008. Disappearing headwaters: patterns of stream burial due to urbanization. *Frontiers in Ecology and the Environment*, **6(6),** pp308–312.

Engel, P. & Lau, Y.L., 1981. Hydraulic model study of large culvert inlet gratings. Natural Water Resources Institute, Environment Canada, Ontario, Canada.

Ettema, R., Arndt, R., Roberts, P. & Wahl, T. (eds), 2000. Hydraulic Modeling: Concepts and Practice (ASCE Manual and Reports on Engineering Practice No. 97). Reston, Virginia, American Society of Civil Engineers.

EU, 2000. Directive 2000/60/EC of the European Parliament and of the Council of 23 October 2000 establishing a framework for Community action in the field of water policy. [online], http://circa.europa.eu/Public/irc/env/wfd/library?l=/framework_directive/legislative_texts/wfd_en_pdf/_EN_1.0_&a=d, [Accessed 25/01/2010].

EU, 2007. DIRECTIVE 2007/60/EC OF THE EUROPEAN PARLIAMENT AND OF THE COUNCIL of 23 October 2007 on the assessment and management of flood risks. [online], http://eur-lex.europa.eu/LexUriServ/site/en/oj/2007/l_288/l_28820071106en00270034.pdf, [accessed 25/01/2010].

Evans, E., Ashley, R., Hall, J., Penning-Rowsell, E., Saul, A., Sayers, P., Thorne, C. & Watkinson, A., 2004a. *Future Flooding: Executive Summary*. London, Office of Science and Technology.

Evans, E., Ashley, R., Hall, J., Penning-Rowsell, E., Saul, A., Sayers, P., Thorne, C. & Watkinson, A., 2004b. *Foresight Future Flooding. Scientific Summary: Volume I Future risks and their drivers.* London, Office of Science and Technology.

FCSCP, 2002. A Water Quality and Stream Habitat Protection Manual for County Road Maintenance in Northwestern California Watersheds. Administrative Draft, Prepared for the Five Counties Salmon Conservation Program. [online], http://www.5counties.org/PDF_Files/Roads%20Manual/5C%20Roads%20Manual.pdf, [Accessed 26/09/2010].

FEMA, 1998. Federal Emergency Management Agency: Costs and benefits of natural hazard mitigation, Washington DC, Federal Emergency Management Agency. [online], http://www.fema.gov/pdf/library/haz_cost.pdf, [Accessed 03/06/2009].

FEMA, 2001. Federal Emergency Management Agency: Flood Hazard Mitigation Handbook for Public Facilities. [online], http://www.conservationtech.com/FEMA-WEB/FEMA-subweb-flood/index.htm, [Accessed 22/10/2012].

FEMA, 2009. Federal Emergency Management Agency: Environmental Assessment for City of Peabody, Goldthwaite Brook Flood Mitigation Project, Peabody, Massachusetts. [online], http://www.fema.gov/library/viewRecord.do?id=3850, [Accessed 29/09/2010].

Fetherston, K.L., Naiman, R.J. & Bilby, R.E., 1995. Large woody debris, physical process, and riparian forest development in montane river networks of the Pacific Northwest. *Geomorphology*, **13,** pp133-144.

Floodsite, 2009. Integrated flood risk analysis and management methodologies. Evaluating flood damages: guidance and recommendations on principles and methods. Executive summary. Report T09-07-03. [online], http://www.floodsite.net/html/partner_area/project_docs/T09_07_03_Evaluating_Flood_Damages_ExecSum_v2_2_p01.pdf, [Accessed 31/09/2009].

Foresight, 2006. Foresight project in flood and coastal defence. [online], http://www.foresight.gov.uk/OurWork/CompletedProjects/Flood/Unknown/Projectsummary.asp, [Accessed 24/07/09].

French, R.H., 1985. Open-channel Hydraulics, New York, McGraw-Hill.

Freuchie Flood Action Group, 2011. Pensioner Dies in Flood. Freuchie Flood Action Group, Working to Prevent Future Flooding in Freuchie. [online], http://www.floodaction.org.uk/blog/tag/culvert/, [Accessed 26/01/2012].

FSSSWG, 2008. Stream Simulation: An Ecological Approach to Providing Passage for Aquatic Organisms at Road-Stream Crossings. Forest Service Stream-Simulation Working Group, U.S. Department of Agriculture. [online], http://stream.fs.fed.us/fishxing/publications/PDFs/AOP_PDFs/08771801.pdf, [Accessed 23/10/2010].

Gilbert, G.K., 1914. Transportation of debris by running water, US Geological Survey Professional Paper **86**.

Gippel, C.J., 1995. Environmental Hydraulics of large woody debris in streams and rivers. *Journal of Environmental Engineering*, **121(5)**, pp388-395.

Golding, B.W., 2009. Uncertainty propagation in a London Flood simulation. *Journal of Flood Risk Management*, **2(1)**, pp2–15.

Gomi, T., Sidle, R.C., Noguchi, S., Negishi, J.N., Nik, A.R. & Sasaki, S., 2006. Sediment and wood accumulations in humid tropical headwater streams: Effects of logging and riparian buffers. *Forest Ecology and Management*, **224(1-2)**, pp166–175.

Gregory, K.J. & Davis, R.J., 1992. Coarse woody debris in stream channels in relation to river channel management in woodland areas, *Regulated Rivers: Research and Management*, **7**, pp117–136.

Groffman, P.M., Boulware, N.J., Zipperer, W.C., Pouyat, R.V., Band, L.E. & Colosimo, M. F., 2002. Soil nitrogen cycling processes in urban riparian zones. *Environmental Science & Technology,* **36(21),** pp 4547–4552.

Gurnell, M., Piégay, H., Swanson, F.J. & Gregory, S.V., 2002. Large wood and fluvial processes. *Freshwater Biology*, **47(4)**, pp601–619.

Habersack, H., Piégay, H. & Rinaldi, M. (Eds), 2007. Gravel Bed Rivers 6 - From Process Understanding to River Restoration, Elsevier, Amsterdam, pp359–381.

Haga, H., Kumagai, T., Otsuki, K. & Ogawa, S., 2002. Transport and retention of coarse woody debris in mountain streams: an in situ field experiment of log transport and a field survey of coarse woody debris distribution. *Water Resources Research*, **38(8)**, pp1029–1044.

Hager, W.H. & Del Giudice, G., 1998. Generalized Culvert Design Diagram. *Journal of Irrigation and Drainage Engineering*, **124(5)**, pp271-274.

Haines-Young, R. & Potschin, M., 2008. England's Terrestrial Ecosystem Services and the Rationale for an Ecosystem Approach. Full technical report, DEFRA Project Code NR0107.

Hall, J.W., Meadowcroft, I.C., Sayers, P.B. & Bramley, M.E., 2003. Integrated Flood Risk Management In England and Wales. *Natural Hazards Review,* **4(3),** pp126-135.

Hall, J.W., Sayers, P.B. & Dawson, R.J., 2005. National-scale Assessment of Current and Future Flood Risk in England and Wales. *Natural Hazards,* **36(102),** pp147–164.

Hall, P., 2007. Urban Land, Housing, and Transportation: The Global Challenge. *Global Urban Development,* **3**. [online], http://www.globalurban.org/GUDMag07Vol3Iss1/Hall.htm, [Accessed 11/01/2011].

HEC, 2006. CONCEPTUAL DESIGN GUIDELINES, Application of Engineered Logjams. Prepared for the Scottish Environmental Protection Agency by Herrera Environmental Consultants, Inc. Seattle, Washington.

Hershey, R.W., 2009. Streamflow Measurement. Third Edition. Abingdon, Taylor & Francis.

HMSO, 1936. Public Health Act, 1936. [online], http://www.legislation.gov.uk/ukpga/1936/49/pdfs/ukpga_19360049_en.pdf, [Accessed 28/9/2011].

HMSO, 1994. *Biodiversity: the UK Action Plan*, 1994. (Cm 2428). London, HMSO.

Ho, J., Hanna, L., Mefford, B. & Coonrod, J., 2006. Numerical Modeling Study for Fish Screen at River Intake Channel. In Randall Graham, P.E., (ed), Proceedings of the 2006 World Environmental and Water Resources Congress, May 21-25, 2006, Omaha, Nebraska.

Hogan, D.L., 1987. The influence of large organic debris on channel recovery in the Queen Charlotte Islands, British Columbia, Canada. Pages 345-353 in Erosion and Sedimentation in the Pacific Rim. IAHS Publication No. 165. International Association of Hydrological Sciences, Washington, DC.

Homes and Communities Agency, 2012. Hexham Flood Trail: A beautiful walk that turns flood defences into a community resource. [online], http://www.homesandcommunities.co.uk/hexham-flood-trail, [Accessed 24/9/2012].

Hotchkiss, R.H., Flanagan, P.J. & Donahoo, K., 2003. Hydraulic jumps in broken-back culverts. *Transportation Research Record: Journal of the Transportation Research Board*, **1851(1)**, pp35-44.

Hotchkiss, R.H., Thiele, E.A., Nelson, E.J. & Thompson, P.L., 2008. Culvert hydraulics: comparison of current computer models and recommended improvements. *Transportation Research Record: Journal of the Transportation Research Board*, **2060(1)**, pp141-149.

HR Wallingford, 2009. Reducing uncertainty in estimation of flood levels. [online], http://www.river-conveyance.net/index.html#software, [accessed 18/10/2012].

Hughes, S.A., 1993. Physical Models and Laboratory Techniques in Coastal Engineering, Singapore, World Scientific.

Humphrey, J. & Bailey, S., 2012. Managing deadwood in forests and woodlands. Forestry Commission Practice Guide. Forestry Commission, Edinburgh.

Hydro-Logic, 2007. Supply of a Trash Screen monitoring and flood warning system. [online], http://www.hydro-logic.co.uk/HL/grille-monitoring-in-the-scottish-borders, [Accessed 23/09/2010].

Hydrothane Systems, 2011. Hydrothane: the first non-metallic trashrack. [online], http://www.hydrothane.com, [Accessed 18/1/2011].

Hygelund, B. & Manga, M., 2003. Field measurement of drag coefficients for model large woody debris. *Geomorphology*, **51(1)**, pp175–185.

ICE, 2001. Learning to live with rivers. Final report of the Institution of Civil Engineers Presidential Commission to review the technical aspects of flood risk management in England and Wales. London, ICE. [online], http://www.ice.org.uk/rtfpdf/ICEFlooding.pdf, [Accessed 04/06/2009].

ISU, 2009. Iowa Stormwater Management Manual. Iowa State University, Institute for Transportation. [online], http://www.intrans.iastate.edu/pubs/stormwater/index.cfm, [Accessed 28/07/2010].

Johnson, P.A. & Brown, E.R., 2000. Stream Assessment for Multicell Culvert Use. *Journal of Hydraulic Engineering*, **126(5)**, pp381-386.

Johnson, S.L., Swanson, F.J., Grant, G.E. & Wondzell, S.M., 2000. Riparian forest disturbances by a mountain flood – the influence of floated wood. *Hydrological Processes*, **14(16-17)**, pp3031–3050.

Katopodis, C., Ead, S.A., Standen, G. & Rajaratnum, N., 2005. Structure of flow upstream of vertical angled screens in open channels. *Journal of Hydraulic Engineering*, **131(4)**, pp294-305.

Kaushal, S.S., Groffman, P.M., Band, L.E., Shields, C.A., Morgan, R.P., Palmer, M.A., Belt, K.T., Swan, C.M., Findlay, S.E.G. & Fisher, G.T., 2008. Interaction between urbanization and climate variability amplifies watershed nitrate export in Maryland. *Environmental Science & Technology*, **42(16),** pp 872–5878.

Kells, J., 2008. Hydraulic performance of damaged-end corrugated steel pipe culverts. *Canadian Journal of Civil Engineering*, **35(9)**, pp918-24.

Kosicki, A.J. & Davis, S.R., 2001. Consideration of Stream Morphology in Culvert and Bridge Design. *Transportation Research Record: Journal of the Transportation Research Board*, **1743**, pp57-59.

Lagasse, P.F., Clopper, P.E., Pagán-Ortiz, J.E., Zevenbergen, L.W., Arneson, L.A., Schall, J.D., Girard, L.G., 2009. U.S. Department of Transportation, Federal Highway Administration. Hydraulic Engineering Circular No. 23. Bridge Scour and Stream Instability countermeasures, Experience, Selection and Design Guidance. Volumes 1 and 2, Third Edition. [online], ,http://www.fhwa.dot.gov/engineering/hydraulics/pubs/09112/page00.cfm, [Accessed 27/12/2012].

Laws, E.M. & Livesey, J.L., 1978. Flow through screens. *Annual Review of Fluid Mechanics*, **10**, pp247-266.

Lemon, D.D., Wittinger, R.J., Cattie, W.W. & Emmert, R., 1999. Measuring the effect of fish diversion screens on turbine efficiency with acoustic scintillation flow meter at unit 5, McNary Dam. *Proceedings of the International Conference on Hydropower*, ASCE Waterpower '99, Las Vegas, NV. [online], http://www.aqflow.com/reports/mcnary-WaterPower99.pdf, [accessed 18/10/2012].

Lyn, D.A., Cooper, T., Yi, Y., Sinha, R. & Rao, A.R., 2003. Debris Accumulation at Bridge Crossings: Laboratory and Field Studies. Indiana Department of Transportation report FHWA/IN/JTRP-2003/10. Springfield, National Technical Information Service.

Macdonald, J.I. & Davies, P.E., 2007. Improving the upstream passage of two Galaxiid fish species through a pipe culvert. *Fisheries Management and Ecology*, **14(3)**, pp221–230.

Magenis, S.E., 1988. Trash screens on culverts in urban areas. *Journal of the Chartered Institution of Water and Environmental Management*, **2(5)**, pp476-484.

Manga, M., & Kirchner, J.W., 2000. Stress partitioning in streams by large woody debris. *Water Resources Research*, **36(8)**, pp2373–2379.

Manners, R.B. & Doyle, M.W., 2008. A mechanistic model of woody debris jam evolution and its application to wood-based restoration and management. *River Research and Applications*, **24(8)**, pp1104–1123.

Manners, R.B., Doyle, M.W. & Small, M.J., 2007. Structure and hydraulics of natural woody debris jams. *Water Resources Research*, **43(6)**, pp1-17.

Manning, A.D., Cunningham, R.B. & Lindenmayer, D.B., 2013. Bringing forward the benefits of coarse woody debris in ecosystem recovery under different levels of grazing and vegetation density. *Biological Conservation*, **157**, pp204-214.

Mansell, M.G., 2003. Rural and Urban Hydrology. London, Thomas Telford Ltd.

Marcus, W.A., Marston, R.A., Colvard, C.R., Gray, R.D., 2002. Mapping the spatial and temporal distributions of large woody debris in streams of the Greater Yellowstone Ecosystem, USA. *Geomorphology*, **44(3)**, pp323–335.

Martinson, B., 2010. Designs That Hold Water: Sustainable drainage systems (SUDS) explained - pt1. A film from the Environment Agency, SEPA and the Institution of Civil Engineers on the need for, practice and outcomes of Sustainable Urban Drainage Systems (SUDS). [online], http://www.youtube.com/watch?v=QAOQDRIp6uo, [Accessed 23/8/2012].

Mays, L.W., Walker, M.E., Bennet, M.S. & Arbuckle, R.P., 1983. *Hydraulic Performance of Culverts with Safety Grates.* Federal Highways Administration Report FHWA/TX-82/55T301-1F. Springfield, National Technical Information Service.

Mazzorana, B., Hübl, J., Zischg, A. & Largiader, A., 2011. Modelling woody material transport and deposition in alpine rivers. *Natural Hazards*, **56(2)**, pp425–449.

Mccarthy, J., 2008. Gosford council neglect in road culvert deaths. Newcastle Herald. [online], http://www.theherald.com.au/news/local/news/general/gosford-council-neglect-in-road-culvert-deaths/1276637.aspx?storypage=1, [Accessed 18/1/2011].

Melville, B.W. & Dongol, D.M., 1992. Bridge pier scour with debris accumulation. *Journal of Hydraulic Engineering*, **118(9)**, pp1306-1310.

Messner, F. & Meyer, V., 2005. Flood damage, vulnerability and risk perception—challenges for flood damage research. UFZ discussion paper 13/2005. [online], http://www.floodsite.net/html/partner_area/project_docs/DP_13-05_Flood_damage_and_vulnerability _Messner_Meyer_2005.pdf, [Accessed 13/05/2009].

Metcalf and Eddy, Inc., 1972. *Wastewater Engineering*, New York, McGraw-Hill Book Co.

Meusburger, H., Volkart, P. & Minor, H-E., 2001. A new improved formula for calculating trashrack losses. *Proceedings of the XXIX IAHR Congress*, Beijing, September 16-21, 2001.

Millennium Ecosystem Assessment, 2005. *Ecosystems and Human Well-being: Synthesis.* Island Press, Washington, DC.

Ministry for the Environment, 2004. Culvert and Bridge Construction. Guidelines for Farmers. Wellington, New Zealand, Ministry for the Environment.[online], http://www.mfe.govt.nz/publications/land/culvert-bridge-oct04/culvert-bridge-oct04.pdf, [Accessed 16/1/2013].

Molinas, A. & Mommandi, A., 2009. Development of New Corrosion/Abrasion Guidelines for Selection of Culvert Pipe Materials Colorado Department of Transportation Report No. CDOT-2009-11. [online], http://www.coloradodot.info/programs/research/pdfs/2009/culvetrpipes.pdf, [Accessed10/09/2010].

Moore, I.D., 2008. Pipe rehabilitation: effect of damage to existing pipes and design of pipe repairs. Trenchless Australia 2008, 7th National ASTT National Conference and Exhibition, 2-5 March.

Mott, N., 2010. Large Woody Debris National Demonstration Project, River Churnet, Tittesworth Water, Staffordshire. [online], http://www.staffs-wildlife.org.uk/files/documents/393.pdf, [Accessed 13/12/2012].

Mott, R. L., 2006. Applied fluid mechanics, Sixth Edition. Jurong, Prentice Hall.

Montes, J.S., 1997. Irrotational flow and real fluid effects under planar sluice gates. *Journal of Hydraulic Engineering*, **123(3)**, pp219-232.

Murphy, G., 1950. *Similitude in Engineering.* New York, Ronald Press.

Nakamura, F. & Swanson, F.J., 1994. Distribution of coarse woody debris in mountain streams, Western Cascade Range, Oregon. *Canadian Journal of Forest Research*, **24(12)**, pp2395-2405.

Nislow, K.H., Hudy, M., Letcher, B.H. & Smith, E.P., 2011. Variation in local abundance and species richness of stream fishes in relation to dispersal barriers: implications for management and conservation. *Freshwater Biology*. **56(10)**, pp2135-2144.

Normann, J.M., Houghtalen, R.J. & Johnston, W.J., 2001. Hydraulic Design of Highway Culverts, Second Edition. Federal Highways Administration Report FHWA-NHI-01-020. [online], http://isddc.dot.gov/OLPFiles/FHWA/015808.pdf, [Accessed 10/08/2010].

Novak, P., Guinot, V., Jeffrey, A. & Reeve, D. E., 2010. Hydraulic Modelling – an Introduction. Principles, methods and applications. Abingdon, Spon Press.

Novak, P., Moffat, A.I.B, Nalluri, C. & Narayanan, R., 2001. Hydraulic Structures. Third Edition. London, Spon Press.

OFWAT, 2002. Flooding from sewers – a way forward: Consultation. [online], www.ofwat.gov.uk, [Accessed 16/05/2009].

Osborn, J.F., 1968. Rectangular-Bar Trashrack and Baffle Headlosses. *Journal of the Power Division, Proceedings of the American Society of Civil Engineers*, **94**, pp111-123.

Ott, R.F., Boersma, E. & Strong, J., 1987. Innovative intake protects both aquatic life and turbine equipment. in B.W. Clowes, (ed.), Waterpower 87: *Proceedings of the International Conference on Hydrology*. Portland, OR. August. 19-21, 1987.

Padilla, R. & Clark, K., 2008. Debris Rack: Debris Capture and Fish Passage, Bay-Delta Office Memorandum, California Department of Water Resources. [online], http://baydeltaoffice.water.ca.gov/ndelta/fishery/documents/DWR_memo_031008UCD_TDF_Debris%20rack%20study.pdf, [Accessed 19/09/2010].

Pagliara, S. & Carnacina, I., 2010. Temporal scour evolution at bridge piers: effect of wood debris roughness and porosity. *Journal of Hydraulic Research*, **48(1)**, pp3-13.

Peakall, J., Ashworth, P. & Best, J., 1996. Physical Modelling in Fluvial Geomorphology: Principles, Applications and Unresolved Issues. In: The Scientific Nature of Geomorphology: *Proceedings of the 27th Binghamton Symposium in Geomorphology*, 27 – 29 September, 1996.

Pelinsky, A. 2012. New study uncovers how animals in Maryland use underground highway culverts. University of Maryland center for Environmental Science. [online], http://www.umces.edu/al/project/new-study-uncovers-how-animals-maryland-use-underground-highway-culverts, [Accessed 12/9/2012].

Penning-Rowsell, E.C. & Green, C., 2000. New insights into the appraisal of flood-alleviation benefits: (1) Flood damage and flood loss information. *Journal of the Chartered Institution of Water Engineers*, **14**, pp347–353.

Perham, R.E., 1987. Floating debris control: a literature review. U.S. Army Cold Regions Res. Lab., Hanover, N.H., 13. In Abt, S.R., Brisbane, T.E., Frick, D.M. & Mcknight, C.A., 1992. Trash rack blockage in supercritical flow. *Journal of Hydraulic Engineering*. **118**, pp1692-1696.

Perrin, J. Jr. & Jhaveri, C.S., 2004. The Economic Costs of Culvert Failures. Transportation Research Board Annual Meeting 2004. [online], http://www.concrete-pipe.org/research/economiccosts.pdf, [Accessed 08/03/2010].

Pickett, S.T.A., Cadenasso, M.L., Grove. J.M., Boone, C., Groffman, P., Irwin, E., Kaushal, S.S., Marshall, V., Mcgrath, B.P., Nilon, C., Pouyat, R.V., Szlavecz, K., Troy, A. & Warren, P., 2011. Urban ecological systems: Scientific foundations and a decade of progress. *Journal of Environmental Management,* **92(3)**, pp331-362.

Pilgrim, D.H., (ed), 1987. *Australian Rainfall & Runoff - A Guide to Flood Estimation*, Institution of Engineers, Australia, Barton, ACT.

Pizzuto, J., Moglen, G., Palmer, M.A. & Nelson, K., 2008. Two model scenarios illustrating the effects of land use and climate change on gravel riverbeds of suburban Maryland, U.S.A., in Habersack, H., Piégay, H. & Rinaldi, M. (Eds), 2007. Gravel Bed Rivers 6 - From Process Understanding to River Restoration, Elsevier, Amsterdam, pp. 359–381.

Pitt, M., 2008. The Pitt Review: Learning lessons from the 2007 floods. Cabinet Office, 284668/1207. [online], http://archive.cabinetoffice.gov.uk/pittreview/_/media/assets/www.cabinetoffice.gov.uk/flooding_review/pitt_review_full%20pdf.pdf, [Accessed 14/05/2009].

POST, 2011. Natural Flood Management. POSTnote 396, Parliamentary Office of Science and Technology. [online], www.parliament.uk/briefing-papers/POST-PN-396.pdf, [Accessed 30/01/2012].

Rees, M., Roe, J.H. & Georges, A., 2009. Life in the suburbs: Behavior and survival of a freshwater turtle in response to drought and urbanization. *Biological Conservation*, **142(12)**, pp3172–3181.

Reihsen, G., 1964. Debris Control Structures. U.S. Department of Transportation, Federal Highway Administration. Hydraulic Engineering Circular No. 9. Springfield, National Technical Information Service.

Reihsen, G. & Harrison, L. J., 1971. Debris Control Structures Evaluation and Countermeasures. U.S. Department of Transportation, Federal Highway Administration. Hydraulic Engineering Circular No. 9, Second Edition. Springfield, National Technical Information Service.

Reynolds, O., 1887. On certain laws relating to the regime of rivers and estuaries, and on the possibility of experiments on a small scale. A Report of the British Association, in Reynolds, O., 1901. *Papers on Mechanical and Physical Subjects*, **11**, Cambridge University Press pp326-335.

Rigby, E.H., Boyd, M.J., Roso, S., Silveri, P. & Davis, A., 2002. Causes and effects of culvert blockage during large storms. Global Solutions for Urban Drainage, *Proceedings of 9th International Conference on Urban Drainage*, Sept. 8-13, 2002, Portland, Oregon.

River Restoration Centre, 2012. River Quaggy at Sutcliffe Park. Techniques: Re-meandering, backwater creation, de-culverting. [online], http://www.therrc.co.uk/case_studies/sutcliffe%20park.pdf, [Accessed 3/9/2012].

RSSB, 2004. Rail Safety & Standards Board. Scour and Flood Risk at Railway Structures. [online], http://www.rssb.co.uk/pdf/reports/research/impact%20of%20scour%20and%20flood%20risk%20on%20railway%20structures.pdf, [Accessed 02/03/2010].

Roach, W.J., Heffernan, J.B., Grimm, N.B., Arrowsmith, J.R., Eisinger, C. & Rychener, T., 2008. Unintended consequences of urbanization for aquatic ecosystems: a case study from the Arizona desert. *BioScience*, **58(8),** pp715–727.

Robinson, M., Boardmann, J., Evans, R., Heppell, K., Packman, J., Leeks, G., 2000. Urban development, in: Acreman, M. (Ed), 1999. The hydrology of the UK. A study of change. Oxon, Routledge.

RoSPA, 2002. UK Drowning Statistics – 2002. [online], http://www.rospa.com/leisuresafety/Info/WaterSafety/statistics/2002-chart.pdf, [Accessed 18/1/2011].

Rosso, R., Rulli, M.C.& Bocchiola, D., 2007. Transient catchments hydrology after wildfires in a Mediterranean watershed: runoff, sediment and woody debris. *Hydrology and Earth Systems Science*, **11(1)**, pp125–40.

Rulli, M.C., Bozzi, S., Spada, M., Bocchiola, D. & Rosso, R., 2006. Rainfall simulations on a fire disturbed Mediterranean area. *Journal of Hydrology*, **327(3)**, pp323–38.

Samuels, P.G., 2004. Defra/Environment Agency Flood and Coastal Defence R&D Programme, Afflux at bridges and culverts. Review of current knowledge and practice, Annex 2: Hydraulic Model Implementation of Bridge and Culvert Afflux and Blockage R&D Project Record W5A-061/PR2.

Schall, J.D., Richardson, E.V. & Morris, J.L., 2008. Introduction to Highway Hydraulics, Hydraulic Design Series No. 4, Federal Highways Administration Report No. FHWA NHI-08-090 (HDS-4)**,** National Technical Information Service, Springfield, Virginia.

Schall, J.D., Thompson, P.L., Zerges, S.M., Kilgore, R.T. & Morris, J.L., 2012. Hydraulic Design Of Highway Culverts. Third Edition. Federal Highways Administration Report No.FHWA-HIF-12-026, HDS 5.

Shields, F.D. Jr. & Alonso, C.V., 2012. Assessment of flow forces on large wood in rivers, *Water Resources Research*, **48(4)**, W04516, doi:10.1029/2011WR011547.

Scottish Executive, 2000. River Crossings and Migratory Fish: Design Guidance. A Consultation Paper. [online], http://www.scotland.gov.uk/consultations/transport/rcmf-00.asp, [Accessed 3/09/2010].

Scottish Executive, 2004. SCOTTISH PLANNING POLICY 7: PLANNING and FLOODING. Edinburgh, Crown Copyright.

Scottish Government, 2009. Flood Risk Management (Scotland) Act 2009. [online], http://www.opsi.gov.uk/legislation/scotland/acts2009/pdf/asp_20090006_en.pdf, [accessed 10/09/2010].

Seo, J.I. & Nakamura, F., 2009. Scale-dependent controls upon the fluvial export of large wood from river catchments. *Earth Surface Processes and Landforms*, **34(6)**, pp786–800.

Seo, J.I., Nakamura, F., Nakano, D., Ichiyanagi, H. & Chin, K.W., 2008. Factors controlling the fluvial export of large woody debris, and its contribution to organic carbon budgets at watershed scales. *Water Resources Research*, **44(4)**, W04428, doi:10.1029/2007WR006453.

SEPA, 2005. SEPA Position Statement to support the implementation of the Water Environment (Controlled Activities) (Scotland) Regulations 2005: CULVERTING OF WATERCOURSES.

SEPA, 2008. Construction of River Crossings. Engineering in the Water Environment Good Practice Guide. First edition. Scottish Environment Protection Agency document WAT-SG-25. [online], http://www.sepa.org.uk/water/water_regulation/guidance/engineering.aspx, [Accessed 10/08/2012].

SEPA, 2010. Construction of River Crossings. Engineering in the Water Environment Good Practice Guide. Second edition. Scottish Environment Protection Agency document SG-25 GpG. [online], http://www.sepa.org.uk/water/water_regulation/guidance/engineering.aspx, [Accessed 10/08/2012].

SEPA, 2011. The National Flood Risk Assessment. December 2011.

SEPA, 2012a. Flood Risk Management Planning in Scotland: Arrangements for 2012 – 2016. February 2012. SEPA, Stirling.

SEPA, 2012b. Fly Tipping. [online], http://www.sepa.org.uk/waste/waste_regulation/fly-tipping.aspx, [Accessed 9/10/2012].

Shields, D.F. & Gippel, C.J., 1995. Prediction of effects of woody debris removal on flow resistance. *Journal of Hydraulic Engineering*, **121(4)**, pp341–354.

Smith, R.D. & Maltby, E., 2003. *Using the Ecosystem Approach to Implement the Convention on Biological Diversity: Key Issues and Case Studies*. IUCN, Cambridge, UK.

Stefan, H. & Fu, A., 1978. Headloss characteristics of six profile-wire screen panels. *Report No. 175*, St. Anthony Falls Hydr. Lab., University of Minnesota, Minneapolis, Minnesota.

Sterling Jones, J., Kerenyi, K. & Stein, S., 2006. *Effects of inlet geometry on hydraulic performance of box culverts*. Federal Highway Administration Report FHWA-HRT-06-138. [online], http://www.fhwa.dot.gov/engineering/hydraulics/pubs/06138/index.cfm, [Accessed 10/08/2010].

Stevenson, C., Kopeinig, T., Feurich, R. & Boubée, J., 2008. Culvert barrel design to facilitate the upstream passage of small fish. National Institute of Water & Atmospheric Research Ltd Client Report: HAM2008-046.

Strong, J.J. & Ott, R.F., 1988. Intake screens for small hydro plants. *Hydro Review*, **7(5)**, in Xiang, F., Kavvas, L. M., Zhiqiang, C., Bandeh, H., Ohara, N., Kim, S., Jang, S., Churchwell, R., 2009. Experimental study of debris capture efficiency of trash racks. *Journal of Hydro-environment Research*, **3**, pp138-147.

Structure Guard, 2011. Trash Racks and Screens. [online], http://www.poweronline.com/product.mvc/Trash-Racks-and-Screens-0001,[Accessed 18/1/2011].

Swanson, F.J., Lienkaemper, G.W. & Sedell, J.R., 1975. History, physical effects, and management implications of large organic debris in Western Oregon streams. Paper presented at the workshop on logging debris in streams, Oregon State University, Corvallis, September, 9-10, 1975. [online], http://www.fs.fed.us/pnw/pubs/pnw_gtr056.pdf, [Accessed 23/09/2010].

Taylor, G.I., 1944. *Air resistance of a flat plate of very porous material*. Reports and Memoranda No. 2236, British Aeronautical Research Council in Tsikata, J.M., Katopodis, C. & Tachie, M.F., 2009. Experimental study of turbulent flow near model trashracks. *Journal of Hydraulic Research*, **47(2)**, pp275-280.

Taylor, G.I. & Batchelor, G. K., 1949. The effect of wire gauze on small disturbances in a uniform stream. *Quarterly Journal of Mechanics and Applied Mathematics*, **2(1)**, pp1-29, in Tsikata, J.M., Katopodis, C. & Tachie, M.F., 2009. Experimental study of turbulent flow near model trashracks. *Journal of Hydraulic Research*, **47(2)**, pp275-280.

Taylor, G.I. & Davies, R. M., 1944. *The aerodynamics of porous sheets*. Reports and Memoranda No. 2237, British Aeronautical Research Council, in Tsikata, J.M., Katopodis, C. & Tachie, M.F., 2009. Experimental study of turbulent flow near model trashracks. *Journal of Hydraulic Research*, **47(2)**, pp275-280.

Teo, F.Y., Falconer, R.A. & Lin, B., 2011. Hydrodynamics of urban floodplains with vehicle blockages at bridges. Proceedings of the 3rd International Conference on Managing Rivers in the 21st Century: Sustainable Solutions for Global Crisis of Flooding, Pollution and Water Scarcity. 6th-9th December 2011, Penang, Malaysia.

Thomas, H. & Nisbet, T.R., 2012. Modelling the hydraulic impact of reintroducing large woody debris into watercourses. *Journal of Flood Risk Management*, **5**, pp164–174.

Thomson, J., 1879. Flow round river bends. *Proceedings of the Institute of Mechanical Engineers*, pp.456-460.

Tsikata, J.M., Katopodis, C. & Tachie, M.F., 2009. Experimental study of turbulent flow near model trashracks. *Journal of Hydraulic Research*, **47(2)**, pp275-280.

TSO, 2004. The design manual for roads and bridges, Volume 4 Geotechnics and Drainage, Section 2 Drainage, Part 7 ha107/04, Design of outfall and culvert details. London, The Stationary Office Ltd.

TSO, 2005. The Water Environment (Controlled Activities) (Scotland) Regulations 2005. London, The Stationary Office Ltd.

TSO, 2010. Flood and Water Management Act 2010. London, The Stationary Office Ltd.

TxDOT, 2012. Hydraulic Design Manual. Texas Department of Transportation. [online], http://onlinemanuals.txdot.gov/txdotmanuals/hyd/index.htm, [Accessed 14/1/2013].

UKWIR, 2004. Climate change and the hydraulic design of sewerage systems. UK Water Industry Research Project CL10. [online], http://www.ukwir.org/content/default.asp?PageId=38194, [Accessed 19/05/2009].

Van Sickle, J. & Gregory, S.V., 1990. Modeling inputs of large woody debris to streams from falling trees. *Canadian Journal of Forest Research*, **20(10),** pp1593-1601.

Vassalos, D., 1999. Physical modelling and similitude of marine structures. *Ocean Engineering*, **26(2)**, pp111-123.

Wahl, T.L., 1992. Trash control structures and equipment: a literature review and survey of Bureau of Reclamation experience. Report R-92-05. Bureau of Reclamation, Denver, US.

Wahl, T.L. & Einhellig, R.F., 2000. Laboratory testing and numerical modelling of Coanda-effect screens. 2000 Joint Conference on Water Resources Engineering and Water Resources Planning & Management, July 30 - August 2, 2000, Minneapolis, Minnesota. [online], http://www.usbr.gov/pmts/hydraulics_lab/pubs/PAP/PAP-0841.pdf, [accessed 18/10/2012].

Walesh, S., 1989. Urban surface water management. New York, Wiley.

Wallerstein, N.P., 2010. Predicting and Managing Flood Risk Associated with Debris at Structures. Flood Risk Management Research Consortium, Seventh Annual Assembly, Heriot-Watt University, 12-15th July 2010.

Wallerstein, N.P., Alonso, C.V., Bennet, S.J. & Thorne, C.R., 2001. Distorted Froude-scaled flume analysis of large woody debris. *Earth Surface Processes and Landforms*, **26(12)**, pp1265-1283.

Wallerstein, N.P. & Arthur, S., 2011. Development of decision support tools to aid with prediction and reduction of blockage risks caused by debris at culverts. *Proceedings of the 3rd International Conference on Managing Rivers in the 21st Century:* Sustainable Solutions for Global Crisis of Flooding, Pollution and Water Scarcity, 6th-9th December 2011, Penang, Malaysia.

Wallerstein, N.P. & Arthur, S., 2012. Improved methods for predicting trash delivery to culverts protected by trash screens. *Journal of Flood Risk Management*, **5(1),** pp23-36.

Wallerstein, N.P. & Thorne, C.R., 2004. Influence of large woody debris on morphological evolution of incised, sand-bed channels. *Geomorphology*, **57(1)**, pp53–73.

Wallerstein, N.P., Thorne, C.R. & Abt, S.R., 1997. *Debris control at Hydraulic Structures in Selected areas of the United States and Europe*. US Army Corps of Engineers report CHL-94-4. [online], http://chl.erdc.usace.army.mil/Media/7/5/6/CHL-CR-97-4.pdf, [Accessed 20/09/2010].

Walsh, C.J., Fletcher, T.D. & Ladson, A.R., 2005a. Stream restoration in urban catchments through redesigning stormwater systems: looking to the catchment to save the stream. *Journal of the North American Benthological Society*, **24(3),** pp690–705.

Walsh, C.J., Roy, A.H., Feminella, J.W., Cottingham, P.D. Groffman, P.M. & Morgan, R.P., 2005b. The urban stream syndrome: current knowledge and the search for a cure. *Journal of the North American Benthological Society*, **24(3)**, pp706–723.

Webb, A.A. & Erskine, W.D. 2003. Distribution, recruitment, and geomorphic significance of large woody debris in an alluvial forest stream: Tonghi Creek, southeastern Australia. *Geomorphology*, **51(1)**, pp109–126.

Webb, B., Marshall, B., Czarnomski, S. & Tilley, N., 2006. *Fly-tipping: causes, incentives and solutions*. London, Jill Dando Institute of Crime Science, UCL.

Weeks, W., Barthelmess, A., Rigby, E., Witheridge, G. & Adamson, R., 2009. Australian Rainfall And Runoff Revision Project 11: Blockage of Hydraulic Structures Stage 1 Report, [online], http://www.ncwe.org.au/arr/Website_links/ARR_Project_11_Stage1_report_Final.pdf, [Accessed 23/09/2010].

Weeks, W., Witheridge, G., Rigby, E., Barthelmess, A., G. O'loughlin, 2012. Australian Rainfall and Runoff Revision, Project 11: Blockage of Hydraulic Structures, Report P11/S2/007.

Weisman, R.N., 1989. Model study of safety grating for culvert inlet. *Journal of Transportation Engineering*, **115**, pp130-138.

Werritty, A., Houston, D., Ball, T., Tavendale, A. & Black, A., 2007. *Exploring the social impacts of flood risk and flooding in Scotland*. Edinburgh, Crown Copyright.

Wild, T.C., Bernet, J.F., Westling, E.L., Lerner, D.N., 2011. Deculverting: reviewing the evidence on the 'daylighting' and restoration of culverted rivers. *Water and Environment Journal*, **25(3)**, pp412–421.

Winter, M.G., Heald, A.P., Parsons, J.A., Spence, D., Macgregor, F. & Shackman, L. 2008. Scottish Road Network Landslides Study: Implementation. Landslide Events. [online], http://www.transportscotland.gov.uk/strategy-and-research/publications-and-consultations/j10107-05.htm, [Accessed 22/10/2012].

Wohl, E., Cenderelli, D.A., Dwire, K.A., Ryan-Burkett, S.E., Young, M.K. & Fausch, K.D., 2010. Large in-stream wood studies: A call for common metrics. *Earth Surface Processes and Landforms*, **35(5)**, pp618–625.

Xiang, F., Kavvas, L.M., Zhiqiang, C., Bandeh, H., Ohara, N., Kim, S., Jang, S. & Churchwell, R., 2009. Experimental study of debris capture efficiency of trash racks. *Journal of Hydro-environment Research*, **3(3)**, pp138-147.

Yanes, M., Velasco, J.M. & Suárez, F., 1995. Permeability of roads and railways to vertebrates: the importance of culverts. *Biological Conservation*, **71(3)**, pp217–222.

Yeh, H.H., 1989. Free-surface flow through screen. *Journal of Hydraulic Engineering*, **115(10)**, pp1371-1385.

Young, W.J., 1991. Flume study of the hydraulic effects of large woody debris in lowland rivers. *Regulated Rivers: Research and Management*, **6(3)**, pp203-211.

Zevenbergen, C., Veerbeek, W., Gersonius, B. & Van Herk, S., 2008. Challenges in urban flood management: travelling across spatial and temporal scales. *Journal of Flood Risk Management*, **1(2)**, 81–88.

Appendix A – Results from Sample Size Test

Table A.1 Results from sample size testing

Run ID	Screen Angle (Degrees)	Discharge (m^3/s)	Bar Spacing (m)	Debris Length (m)	Percentage of Debris Pieces Blocked
SSB40D501	45	0.035	0.04	0.050	77
SSB40D502	45	0.035	0.04	0.050	75
SSB40D503	45	0.035	0.04	0.050	77
SSB40D504	45	0.035	0.04	0.050	78
SSB40D505	45	0.035	0.04	0.050	75
SSB40D506	45	0.035	0.04	0.050	76
SSB40D507	45	0.035	0.04	0.050	76
SSB40D508	45	0.035	0.04	0.050	74
SSB40D509	45	0.035	0.04	0.050	77
SSB40D5010	45	0.035	0.04	0.050	77
SSB40D2001	45	0.035	0.04	0.200	30
SSB40D2002	45	0.035	0.04	0.200	29
SSB40D2003	45	0.035	0.04	0.200	28
SSB40D2004	45	0.035	0.04	0.200	30
SSB40D2005	45	0.035	0.04	0.200	30
SSB40D2006	45	0.035	0.04	0.200	30
SSB40D2007	45	0.035	0.04	0.200	33
SSB40D2008	45	0.035	0.04	0.200	32
SSB40D2009	45	0.035	0.04	0.200	31
SSB40D20010	45	0.035	0.04	0.200	28
SSB40D3251	45	0.035	0.04	0.325	30
SSB40D3252	45	0.035	0.04	0.325	31
SSB40D3253	45	0.035	0.04	0.325	27
SSB40D3254	45	0.035	0.04	0.325	28
SSB40D3255	45	0.035	0.04	0.325	31
SSB40D3256	45	0.035	0.04	0.325	28
SSB40D3257	45	0.035	0.04	0.325	29
SSB40D3258	45	0.035	0.04	0.325	29
SSB40D3259	45	0.035	0.04	0.325	31
SSB40D32510	45	0.035	0.04	0.325	27
SSB60D501	45	0.035	0.06	0.050	93
SSB60D502	45	0.035	0.06	0.050	91
SSB60D503	45	0.035	0.06	0.050	91

Run ID	Screen Angle (Degrees)	Discharge (m^3/s)	Bar Spacing (m)	Debris Length (m)	Percentage of Debris Pieces Blocked
SSB60D504	45	0.035	0.06	0.050	96
SSB60D505	45	0.035	0.06	0.050	95
SSB60D506	45	0.035	0.06	0.050	93
SSB60D507	45	0.035	0.06	0.050	91
SSB60D508	45	0.035	0.06	0.050	96
SSB60D509	45	0.035	0.06	0.050	94
SSB60D5010	45	0.035	0.06	0.050	92
SSB60D2001	45	0.035	0.06	0.200	36
SSB60D2002	45	0.035	0.06	0.200	32
SSB60D2003	45	0.035	0.06	0.200	32
SSB60D2004	45	0.035	0.06	0.200	32
SSB60D2005	45	0.035	0.06	0.200	36
SSB60D2006	45	0.035	0.06	0.200	36
SSB60D2007	45	0.035	0.06	0.200	35
SSB60D2008	45	0.035	0.06	0.200	37
SSB60D2009	45	0.035	0.06	0.200	30
SSB60D20010	45	0.035	0.06	0.200	37
SSB60D3251	45	0.035	0.06	0.325	32
SSB60D3252	45	0.035	0.06	0.325	32
SSB60D3253	45	0.035	0.06	0.325	32
SSB60D3254	45	0.035	0.06	0.325	32
SSB60D3255	45	0.035	0.06	0.325	36
SSB60D3256	45	0.035	0.06	0.325	31
SSB60D3257	45	0.035	0.06	0.325	35
SSB60D3258	45	0.035	0.06	0.325	31
SSB60D3259	45	0.035	0.06	0.325	31
SSB60D32510	45	0.035	0.06	0.325	29
SSB100D501	45	0.035	0.10	0.050	96
SSB100D502	45	0.035	0.10	0.050	99
SSB100D503	45	0.035	0.10	0.050	94
SSB100D504	45	0.035	0.10	0.050	95
SSB100D505	45	0.035	0.10	0.050	97
SSB100D506	45	0.035	0.10	0.050	98
SSB100D507	45	0.035	0.10	0.050	96
SSB100D508	45	0.035	0.10	0.050	96

Run ID	**Screen Angle (Degrees)**	**Discharge (m^3/s)**	**Bar Spacing (m)**	**Debris Length (m)**	**Percentage of Debris Pieces Blocked**
SSB100D509	45	0.035	0.10	0.050	95
SSB100D5010	45	0.035	0.10	0.050	97
SSB100D2001	45	0.035	0.10	0.200	52
SSB100D2002	45	0.035	0.10	0.200	52
SSB100D2003	45	0.035	0.10	0.200	51
SSB100D2004	45	0.035	0.10	0.200	54
SSB100D2005	45	0.035	0.10	0.200	51
SSB100D2006	45	0.035	0.10	0.200	52
SSB100D2007	45	0.035	0.10	0.200	52
SSB100D2008	45	0.035	0.10	0.200	54
SSB100D2009	45	0.035	0.10	0.200	54
SSB100D20010	45	0.035	0.10	0.200	54
SSB100D3251	45	0.035	0.10	0.325	44
SSB100D3252	45	0.035	0.10	0.325	41
SSB100D3253	45	0.035	0.10	0.325	40
SSB100D3254	45	0.035	0.10	0.325	41
SSB100D3255	45	0.035	0.10	0.325	45
SSB100D3256	45	0.035	0.10	0.325	43
SSB100D3257	45	0.035	0.10	0.325	44
SSB100D3258	45	0.035	0.10	0.325	43
SSB100D3259	45	0.035	0.10	0.325	42
SSB100D32510	45	0.035	0.10	0.325	45

Appendix B – Results from Initial Testing

Table B.1 Results from initial testing

Run ID	Rack Angle (Degrees)	Bar Spacing (mm)	Discharge (m^3/s)	Debris Length (mm)	Ratio of debris length to bar spacing	Passed Through	Blocked
T1S1P0A30B30QHD25	30	30	0.035	25	0.83	92	8
T1S1P0A30B30QHD50	30	30	0.035	50	1.67	37	63
T1S1P0A30B30QHD75	30	30	0.035	75	2.50	18	82
T1S1P0A30B30QHD100	30	30	0.035	100	3.33	18	82
T1S1P0A30B30QHD150	30	30	0.035	150	5.00	21	79
T1S1P0A30B30QHD200	30	30	0.035	200	6.67	22	78
T1S1P0A30B30QHD275	30	30	0.035	275	9.17	18	82
T1S1P0A30B30QHD300	30	30	0.035	300	10.00	20	80
T1S1P0A30B30QHD325	30	30	0.035	325	10.83	18	82
T1S1P0A30B30QHD350	30	30	0.035	350	11.67	25	75
T1S1P0A30B40QHD25	30	40	0.035	25	0.63	94	6
T1S1P0A30B40QHD50	30	40	0.035	50	1.25	69	31
T1S1P0A30B40QHD75	30	40	0.035	75	1.88	37	63
T1S1P0A30B40QHD100	30	40	0.035	100	2.50	30	70
T1S1P0A30B40QHD150	30	40	0.035	150	3.75	27	73
T1S1P0A30B40QHD200	30	40	0.035	200	5.00	25	75
T1S1P0A30B40QHD275	30	40	0.035	275	6.88	20	80
T1S1P0A30B40QHD300	30	40	0.035	300	7.50	19	81
T1S1P0A30B40QHD325	30	40	0.035	325	8.13	21	79
T1S1P0A30B40QHD350	30	40	0.035	350	8.75	21	79
T1S1P0A30B50QHD25	30	50	0.035	25	0.50	97	3
T1S1P0A30B50QHD50	30	50	0.035	50	1.00	88	12
T1S1P0A30B50QHD75	30	50	0.035	75	1.50	56	44
T1S1P0A30B50QHD100	30	50	0.035	100	2.00	44	56
T1S1P0A30B50QHD150	30	50	0.035	150	3.00	36	64
T1S1P0A30B50QHD200	30	50	0.035	200	4.00	40	60
T1S1P0A30B50QHD275	30	50	0.035	275	5.50	28	72
T1S1P0A30B50QHD300	30	50	0.035	300	6.00	30	70
T1S1P0A30B50QHD325	30	50	0.035	325	6.50	24	76
T1S1P0A30B50QHD350	30	50	0.035	350	7.00	23	77
T1S1P0A30B60QHD25	30	60	0.035	25	0.42	95	5
T1S1P0A30B60QHD50	30	60	0.035	50	0.83	92	8
T1S1P0A30B60QHD75	30	60	0.035	75	1.25	72	28

Appendix B

Run ID	Rack Angle (Degrees)	Bar Spacing (mm)	Discharge (m^3/s)	Debris Length (mm)	Ratio of debris length to bar spacing	Passed Through	Blocked
T1S1P0A30B60QHD100	30	60	0.035	100	1.67	46	54
T1S1P0A30B60QHD150	30	60	0.035	150	2.50	31	69
T1S1P0A30B60QHD200	30	60	0.035	200	3.33	31	69
T1S1P0A30B60QHD275	30	60	0.035	275	4.58	23	77
T1S1P0A30B60QHD300	30	60	0.035	300	5.00	27	73
T1S1P0A30B60QHD325	30	60	0.035	325	5.42	26	74
T1S1P0A30B60QHD350	30	60	0.035	350	5.83	33	67
T1S1P0A30B80QHD25	30	80	0.035	25	0.31	99	1
T1S1P0A30B80QHD50	30	80	0.035	50	0.63	96	4
T1S1P0A30B80QHD75	30	80	0.035	75	0.94	98	2
T1S1P0A30B80QHD100	30	80	0.035	100	1.25	72	28
T1S1P0A30B80QHD150	30	80	0.035	150	1.88	38	62
T1S1P0A30B80QHD200	30	80	0.035	200	2.50	47	53
T1S1P0A30B80QHD275	30	80	0.035	275	3.44	41	59
T1S1P0A30B80QHD300	30	80	0.035	300	3.75	41	59
T1S1P0A30B80QHD325	30	80	0.035	325	4.06	36	64
T1S1P0A30B80QHD350	30	80	0.035	350	4.38	35	65
T1S1P0A30B100QHD25	30	100	0.035	25	0.25	100	0
T1S1P0A30B100QHD50	30	100	0.035	50	0.50	97	3
T1S1P0A30B100QHD75	30	100	0.035	75	0.75	96	4
T1S1P0A30B100QHD100	30	100	0.035	100	1.00	94	6
T1S1P0A30B100QHD150	30	100	0.035	150	1.50	66	34
T1S1P0A30B100QHD200	30	100	0.035	200	2.00	48	52
T1S1P0A30B100QHD275	30	100	0.035	275	2.75	40	60
T1S1P0A30B100QHD300	30	100	0.035	300	3.00	47	53
T1S1P0A30B100QHD325	30	100	0.035	325	3.25	44	56
T1S1P0A30B100QHD350	30	100	0.035	350	3.50	43	57
T1S1P0A30B150QHD25	30	150	0.035	25	0.17	100	0
T1S1P0A30B150QHD50	30	150	0.035	50	0.33	98	2
T1S1P0A30B150QHD75	30	150	0.035	75	0.50	97	3
T1S1P0A30B150QHD100	30	150	0.035	100	0.67	95	5
T1S1P0A30B150QHD150	30	150	0.035	150	1.00	95	5
T1S1P0A30B150QHD200	30	150	0.035	200	1.33	80	20
T1S1P0A30B150QHD275	30	150	0.035	275	1.83	70	30
T1S1P0A30B150QHD300	30	150	0.035	300	2.00	69	31
T1S1P0A30B150QHD325	30	150	0.035	325	2.17	64	36

Run ID	Rack Angle (Degrees)	Bar Spacing (mm)	Discharge (m^3/s)	Debris Length (mm)	Ratio of debris length to bar spacing	Passed Through	Blocked
T1S1P0A30B150QHD350	30	150	0.035	350	2.33	54	46
T1S1P0A45B30QHD25	45	30	0.035	25	0.83	94	6
T1S1P0A45B30QHD50	45	30	0.035	50	1.67	50	50
T1S1P0A45B30QHD75	45	30	0.035	75	2.50	34	66
T1S1P0A45B30QHD100	45	30	0.035	100	3.33	41	59
T1S1P0A45B30QHD150	45	30	0.035	150	5.00	29	71
T1S1P0A45B30QHD200	45	30	0.035	200	6.67	22	78
T1S1P0A45B30QHD275	45	30	0.035	275	9.17	29	71
T1S1P0A45B30QHD300	45	30	0.035	300	10.00	22	78
T1S1P0A45B30QHD325	45	30	0.035	325	10.83	25	75
T1S1P0A45B30QHD350	45	30	0.035	350	11.67	28	72
T1S1P0A45B40QHD25	45	40	0.035	25	0.63	96	4
T1S1P0A45B40QHD50	45	40	0.035	50	1.25	77	23
T1S1P0A45B40QHD75	45	40	0.035	75	1.88	45	55
T1S1P0A45B40QHD100	45	40	0.035	100	2.50	40	60
T1S1P0A45B40QHD150	45	40	0.035	150	3.75	32	68
T1S1P0A45B40QHD200	45	40	0.035	200	5.00	30	70
T1S1P0A45B40QHD275	45	40	0.035	275	6.88	33	67
T1S1P0A45B40QHD300	45	40	0.035	300	7.50	29	71
T1S1P0A45B40QHD325	45	40	0.035	325	8.13	30	70
T1S1P0A45B40QHD350	45	40	0.035	350	8.75	33	67
T1S1P0A45B50QHD25	45	50	0.035	25	0.50	96	4
T1S1P0A45B50QHD50	45	50	0.035	50	1.00	89	11
T1S1P0A45B50QHD75	45	50	0.035	75	1.50	62	38
T1S1P0A45B50QHD100	45	50	0.035	100	2.00	50	50
T1S1P0A45B50QHD150	45	50	0.035	150	3.00	37	63
T1S1P0A45B50QHD200	45	50	0.035	200	4.00	32	68
T1S1P0A45B50QHD275	45	50	0.035	275	5.50	35	65
T1S1P0A45B50QHD300	45	50	0.035	300	6.00	32	68
T1S1P0A45B50QHD325	45	50	0.035	325	6.50	34	66
T1S1P0A45B50QHD350	45	50	0.035	350	7.00	38	62
T1S1P0A45B60QHD25	45	60	0.035	25	0.42	100	0
T1S1P0A45B60QHD50	45	60	0.035	50	0.83	93	7
T1S1P0A45B60QHD75	45	60	0.035	75	1.25	81	19
T1S1P0A45B60QHD100	45	60	0.035	100	1.67	49	51
T1S1P0A45B60QHD150	45	60	0.035	150	2.50	43	57

Appendix B

Run ID	Rack Angle (Degrees)	Bar Spacing (mm)	Discharge (m^3/s)	Debris Length (mm)	Ratio of debris length to bar spacing	Passed Through	Blocked
T1S1P0A45B60QHD200	45	60	0.035	200	3.33	36	64
T1S1P0A45B60QHD275	45	60	0.035	275	4.58	37	63
T1S1P0A45B60QHD300	45	60	0.035	300	5.00	36	64
T1S1P0A45B60QHD325	45	60	0.035	325	5.42	32	68
T1S1P0A45B60QHD350	45	60	0.035	350	5.83	45	55
T1S1P0A45B80QHD25	45	80	0.035	25	0.31	94	6
T1S1P0A45B80QHD50	45	80	0.035	50	0.63	90	10
T1S1P0A45B80QHD75	45	80	0.035	75	0.94	93	7
T1S1P0A45B80QHD100	45	80	0.035	100	1.25	70	30
T1S1P0A45B80QHD150	45	80	0.035	150	1.88	60	40
T1S1P0A45B80QHD200	45	80	0.035	200	2.50	46	54
T1S1P0A45B80QHD275	45	80	0.035	275	3.44	48	52
T1S1P0A45B80QHD300	45	80	0.035	300	3.75	43	57
T1S1P0A45B80QHD325	45	80	0.035	325	4.06	55	45
T1S1P0A45B80QHD350	45	80	0.035	350	4.38	54	46
T1S1P0A45B100QHD25	45	100	0.035	25	0.25	97	3
T1S1P0A45B100QHD50	45	100	0.035	50	0.50	96	4
T1S1P0A45B100QHD75	45	100	0.035	75	0.75	93	7
T1S1P0A45B100QHD100	45	100	0.035	100	1.00	90	10
T1S1P0A45B100QHD150	45	100	0.035	150	1.50	54	46
T1S1P0A45B100QHD200	45	100	0.035	200	2.00	52	48
T1S1P0A45B100QHD275	45	100	0.035	275	2.75	51	49
T1S1P0A45B100QHD300	45	100	0.035	300	3.00	47	53
T1S1P0A45B100QHD325	45	100	0.035	325	3.25	44	54
T1S1P0A45B100QHD350	45	100	0.035	350	3.50	47	53
T1S1P0A45B150QHD25	45	150	0.035	25	0.17	100	0
T1S1P0A45B150QHD50	45	150	0.035	50	0.33	97	3
T1S1P0A45B150QHD75	45	150	0.035	75	0.50	96	4
T1S1P0A45B150QHD100	45	150	0.035	100	0.67	94	6
T1S1P0A45B150QHD150	45	150	0.035	150	1.00	93	7
T1S1P0A45B150QHD200	45	150	0.035	200	1.33	73	27
T1S1P0A45B150QHD275	45	150	0.035	275	1.83	56	44
T1S1P0A45B150QHD300	45	150	0.035	300	2.00	63	37
T1S1P0A45B150QHD325	45	150	0.035	325	2.17	56	44
T1S1P0A45B150QHD350	45	150	0.035	350	2.33	62	38
T1S1P0A60B30QHD25	60	30	0.035	25	0.83	99	1

Run ID	Rack Angle (Degrees)	Bar Spacing (mm)	Discharge (m^3/s)	Debris Length (mm)	Ratio of debris length to bar spacing	Passed Through	Blocked
T1S1P0A60B30QHD50	60	30	0.035	50	1.67	61	39
T1S1P0A60B30QHD75	60	30	0.035	75	2.5	54	46
T1S1P0A60B30QHD100	60	30	0.035	100	3.33	42	58
T1S1P0A60B30QHD150	60	30	0.035	150	5	25	75
T1S1P0A60B30QHD200	60	30	0.035	200	6.67	24	76
T1S1P0A60B30QHD275	60	30	0.035	275	9.17	35	65
T1S1P0A60B30QHD300	60	30	0.035	300	10.00	23	77
T1S1P0A60B30QHD325	60	30	0.035	325	10.83	31	69
T1S1P0A60B30QHD350	60	30	0.035	350	11.67	40	60
T1S1P0A60B40QHD25	60	40	0.035	25	0.63	98	2
T1S1P0A60B40QHD50	60	40	0.035	50	1.25	87	13
T1S1P0A60B40QHD75	60	40	0.035	75	1.88	57	43
T1S1P0A60B40QHD100	60	40	0.035	100	2.5	42	58
T1S1P0A60B40QHD150	60	40	0.035	150	3.75	42	58
T1S1P0A60B40QHD200	60	40	0.035	200	5	40	60
T1S1P0A60B40QHD275	60	40	0.035	275	6.88	39	61
T1S1P0A60B40QHD300	60	40	0.035	300	7.50	27	73
T1S1P0A60B40QHD325	60	40	0.035	325	8.13	31	69
T1S1P0A60B40QHD350	60	40	0.035	350	8.75	35	65
T1S1P0A60B50QHD25	60	50	0.035	25	0.5	100	0
T1S1P0A60B50QHD50	60	50	0.035	50	1	95	5
T1S1P0A60B50QHD75	60	50	0.035	75	1.5	73	27
T1S1P0A60B50QHD100	60	50	0.035	100	2	64	36
T1S1P0A60B50QHD150	60	50	0.035	150	3	49	51
T1S1P0A60B50QHD200	60	50	0.035	200	4	45	55
T1S1P0A60B50QHD275	60	50	0.035	275	5.5	44	56
T1S1P0A60B50QHD300	60	50	0.035	300	6.00	34	66
T1S1P0A60B50QHD325	60	50	0.035	325	6.50	33	67
T1S1P0A60B50QHD350	60	50	0.035	350	7	48	52
T1S1P0A60B60QHD25	60	60	0.035	25	0.42	100	0
T1S1P0A60B60QHD50	60	60	0.035	50	0.83	98	2
T1S1P0A60B60QHD75	60	60	0.035	75	1.25	86	14
T1S1P0A60B60QHD100	60	60	0.035	100	1.67	65	35
T1S1P0A60B60QHD150	60	60	0.035	150	2.5	55	45
T1S1P0A60B60QHD200	60	60	0.035	200	3.33	50	50
T1S1P0A60B60QHD275	60	60	0.035	275	4.58	47	53

Run ID	Rack Angle (Degrees)	Bar Spacing (mm)	Discharge (m^3/s)	Debris Length (mm)	Ratio of debris length to bar spacing	Passed Through	Blocked
T1S1P0A60B60QHD300	60	60	0.035	300	5.00	39	61
T1S1P0A60B60QHD325	60	60	0.035	325	5.42	30	70
T1S1P0A60B60QHD350	60	60	0.035	350	5.83	37	63
T1S1P0A60B80QHD25	60	80	0.035	25	0.31	98	2
T1S1P0A60B80QHD50	60	80	0.035	50	0.63	100	0
T1S1P0A60B80QHD75	60	80	0.035	75	0.94	97	3
T1S1P0A60B80QHD100	60	80	0.035	100	1.25	90	10
T1S1P0A60B80QHD150	60	80	0.035	150	1.88	69	31
T1S1P0A60B80QHD200	60	80	0.035	200	2.5	64	36
T1S1P0A60B80QHD275	60	80	0.035	275	3.44	64	36
T1S1P0A60B80QHD300	60	80	0.035	300	3.75	44	56
T1S1P0A60B80QHD325	60	80	0.035	325	4.06	45	55
T1S1P0A60B80QHD350	60	80	0.035	350	4.38	60	40
T1S1P0A60B100QHD25	60	100	0.035	25	0.25	97	3
T1S1P0A60B100QHD50	60	100	0.035	50	0.5	97	3
T1S1P0A60B100QHD75	60	100	0.035	75	0.75	98	2
T1S1P0A60B100QHD100	60	100	0.035	100	1	97	3
T1S1P0A60B100QHD150	60	100	0.035	150	1.5	83	17
T1S1P0A60B100QHD200	60	100	0.035	200	2	71	29
T1S1P0A60B100QHD275	60	100	0.035	275	2.75	61	39
T1S1P0A60B100QHD300	60	100	0.035	300	3.00	60	40
T1S1P0A60B100QHD325	60	100	0.035	325	3.25	50	50
T1S1P0A60B100QHD350	60	100	0.035	350	3.5	64	36
T1S1P0A60B150QHD25	60	150	0.035	25	0.17	100	0
T1S1P0A60B150QHD50	60	150	0.035	50	0.33	98	2
T1S1P0A60B150QHD75	60	150	0.035	75	0.5	100	0
T1S1P0A60B150QHD100	60	150	0.035	100	0.67	100	0
T1S1P0A60B150QHD150	60	150	0.035	150	1	96	4
T1S1P0A60B150QHD200	60	150	0.035	200	1.33	89	11
T1S1P0A60B150QHD275	60	150	0.035	275	1.83	71	29
T1S1P0A60B150QHD300	60	150	0.035	300	2.00	64	36
T1S1P0A60B150QHD325	60	150	0.035	325	2.17	61	39
T1S1P0A60B150QHD350	60	150	0.035	350	2.33	76	24
T1S1P0A30B30QLD25	30	30	0.005	25	0.83	91	9
T1S1P0A30B30QLD50	30	30	0.005	50	1.67	42	58
T1S1P0A30B30QLD75	30	30	0.005	75	2.50	33	67

Run ID	Rack Angle (Degrees)	Bar Spacing (mm)	Discharge (m^3/s)	Debris Length (mm)	Ratio of debris length to bar spacing	Passed Through	Blocked
T1S1P0A30B30QLD100	30	30	0.005	100	3.33	30	70
T1S1P0A30B30QLD150	30	30	0.005	150	5.00	26	74
T1S1P0A30B30QLD200	30	30	0.005	200	6.67	18	82
T1S1P0A30B30QLD275	30	30	0.005	275	9.17	12	88
T1S1P0A30B30QLD300	30	30	0.005	300	10.00	16	84
T1S1P0A30B30QLD325	30	30	0.005	325	10.83	12	88
T1S1P0A30B30QLD350	30	30	0.005	350	11.67	11	89
T1S1P0A30B40QLD25	30	40	0.005	25	0.63	86	14
T1S1P0A30B40QLD50	30	40	0.005	50	1.25	78	22
T1S1P0A30B40QLD75	30	40	0.005	75	1.88	59	41
T1S1P0A30B40QLD100	30	40	0.005	100	2.50	43	57
T1S1P0A30B40QLD150	30	40	0.005	150	3.75	24	76
T1S1P0A30B40QLD200	30	40	0.005	200	5.00	29	71
T1S1P0A30B40QLD275	30	40	0.005	275	6.88	28	72
T1S1P0A30B40QLD300	30	40	0.005	300	7.50	29	71
T1S1P0A30B40QLD325	30	40	0.005	325	8.13	24	76
T1S1P0A30B40QLD350	30	40	0.005	350	8.75	25	75
T1S1P0A30B50QLD25	30	50	0.005	25	0.50	97	3
T1S1P0A30B50QLD50	30	50	0.005	50	1.00	96	4
T1S1P0A30B50QLD75	30	50	0.005	75	1.50	66	34
T1S1P0A30B50QLD100	30	50	0.005	100	2.00	46	54
T1S1P0A30B50QLD150	30	50	0.005	150	3.00	33	67
T1S1P0A30B50QLD200	30	50	0.005	200	4.00	26	74
T1S1P0A30B50QLD275	30	50	0.005	275	5.50	23	77
T1S1P0A30B50QLD300	30	50	0.005	300	6.00	24	76
T1S1P0A30B50QLD325	30	50	0.005	325	6.50	27	73
T1S1P0A30B50QLD350	30	50	0.005	350	7.00	36	64
T1S1P0A30B60QLD25	30	60	0.005	25	0.42	91	9
T1S1P0A30B60QLD50	30	60	0.005	50	0.83	95	5
T1S1P0A30B60QLD75	30	60	0.005	75	1.25	62	38
T1S1P0A30B60QLD100	30	60	0.005	100	1.67	48	52
T1S1P0A30B60QLD150	30	60	0.005	150	2.50	35	65
T1S1P0A30B60QLD200	30	60	0.005	200	3.33	31	69
T1S1P0A30B60QLD275	30	60	0.005	275	4.58	31	69
T1S1P0A30B60QLD300	30	60	0.005	300	5.00	33	67
T1S1P0A30B60QLD325	30	60	0.005	325	5.42	29	71

Appendix B

Run ID	Rack Angle (Degrees)	Bar Spacing (mm)	Discharge (m^3/s)	Debris Length (mm)	Ratio of debris length to bar spacing	Passed Through	Blocked
T1S1P0A30B60QLD350	30	60	0.005	350	5.83	32	68
T1S1P0A30B80QLD25	30	80	0.005	25	0.31	96	4
T1S1P0A30B80QLD50	30	80	0.005	50	0.63	93	7
T1S1P0A30B80QLD75	30	80	0.005	75	0.94	83	17
T1S1P0A30B80QLD100	30	80	0.005	100	1.25	71	29
T1S1P0A30B80QLD150	30	80	0.005	150	1.88	48	52
T1S1P0A30B80QLD200	30	80	0.005	200	2.50	48	52
T1S1P0A30B80QLD275	30	80	0.005	275	3.44	36	64
T1S1P0A30B80QLD300	30	80	0.005	300	3.75	42	58
T1S1P0A30B80QLD325	30	80	0.005	325	4.06	42	58
T1S1P0A30B80QLD350	30	80	0.005	350	4.38	40	60
T1S1P0A30B100QLD25	30	100	0.005	25	0.25	98	2
T1S1P0A30B100QLD50	30	100	0.005	50	0.50	97	3
T1S1P0A30B100QLD75	30	100	0.005	75	0.75	92	8
T1S1P0A30B100QLD100	30	100	0.005	100	1.00	83	17
T1S1P0A30B100QLD150	30	100	0.005	150	1.50	58	42
T1S1P0A30B100QLD200	30	100	0.005	200	2.00	37	63
T1S1P0A30B100QLD275	30	100	0.005	275	2.75	44	56
T1S1P0A30B100QLD300	30	100	0.005	300	3.00	39	61
T1S1P0A30B100QLD325	30	100	0.005	325	3.25	40	60
T1S1P0A30B100QLD350	30	100	0.005	350	3.50	42	58
T1S1P0A30B150QLD25	30	150	0.005	25	0.17	97	3
T1S1P0A30B150QLD50	30	150	0.005	50	0.33	98	2
T1S1P0A30B150QLD75	30	150	0.005	75	0.50	95	5
T1S1P0A30B150QLD100	30	150	0.005	100	0.67	92	8
T1S1P0A30B150QLD150	30	150	0.005	150	1.00	93	7
T1S1P0A30B150QLD200	30	150	0.005	200	1.33	72	28
T1S1P0A30B150QLD275	30	150	0.005	275	1.83	51	49
T1S1P0A30B150QLD300	30	150	0.005	300	2.00	60	40
T1S1P0A30B150QLD325	30	150	0.005	325	2.17	55	45
T1S1P0A30B150QLD350	30	150	0.005	350	2.33	52	48
T1S1P0A45B30QLD25	45	30	0.005	25	0.83	87	13
T1S1P0A45B30QLD50	45	30	0.005	50	1.67	42	58
T1S1P0A45B30QLD75	45	30	0.005	75	2.50	32	68
T1S1P0A45B30QLD100	45	30	0.005	100	3.33	30	70
T1S1P0A45B30QLD150	45	30	0.005	150	5.00	23	77

Appendix B

Run ID	Rack Angle (Degrees)	Bar Spacing (mm)	Discharge (m^3/s)	Debris Length (mm)	Ratio of debris length to bar spacing	Passed Through	Blocked
T1S1P0A45B30QLD200	45	30	0.005	200	6.67	14	88
T1S1P0A45B30QLD275	45	30	0.005	275	9.17	15	85
T1S1P0A45B30QLD300	45	30	0.005	300	10.00	18	83
T1S1P0A45B30QLD325	45	30	0.005	325	10.83	16	84
T1S1P0A45B30QLD350	45	30	0.005	350	11.67	23	77
T1S1P0A45B40QLD25	45	40	0.005	25	0.63	89	6
T1S1P0A45B40QLD50	45	40	0.005	50	1.25	80	50
T1S1P0A45B40QLD75	45	40	0.005	75	1.88	47	66
T1S1P0A45B40QLD100	45	40	0.005	100	2.50	27	59
T1S1P0A45B40QLD150	45	40	0.005	150	3.75	31	71
T1S1P0A45B40QLD200	45	40	0.005	200	5.00	28	78
T1S1P0A45B40QLD275	45	40	0.005	275	6.88	31	71
T1S1P0A45B40QLD300	45	40	0.005	300	7.50	24	75
T1S1P0A45B40QLD325	45	40	0.005	325	8.13	16	78
T1S1P0A45B40QLD350	45	40	0.005	350	8.75	14	72
T1S1P0A45B50QLD25	45	50	0.005	25	0.50	98	2
T1S1P0A45B50QLD50	45	50	0.005	50	1.00	84	16
T1S1P0A45B50QLD75	45	50	0.005	75	1.50	70	30
T1S1P0A45B50QLD100	45	50	0.005	100	2.00	41	59
T1S1P0A45B50QLD150	45	50	0.005	150	3.00	38	62
T1S1P0A45B50QLD200	45	50	0.005	200	4.00	36	64
T1S1P0A45B50QLD275	45	50	0.005	275	5.50	36	64
T1S1P0A45B50QLD300	45	50	0.005	300	6.00	36	65
T1S1P0A45B50QLD325	45	50	0.005	325	6.50	24	76
T1S1P0A45B50QLD350	45	50	0.005	350	7.00	28	72
T1S1P0A45B60QLD25	45	60	0.005	25	0.42	94	6
T1S1P0A45B60QLD50	45	60	0.005	50	0.83	93	7
T1S1P0A45B60QLD75	45	60	0.005	75	1.25	71	29
T1S1P0A45B60QLD100	45	60	0.005	100	1.67	57	43
T1S1P0A45B60QLD150	45	60	0.005	150	2.50	38	62
T1S1P0A45B60QLD200	45	60	0.005	200	3.33	43	57
T1S1P0A45B60QLD275	45	60	0.005	275	4.58	26	74
T1S1P0A45B60QLD300	45	60	0.005	300	5.00	36	64
T1S1P0A45B60QLD325	45	60	0.005	325	5.42	38	62
T1S1P0A45B60QLD350	45	60	0.005	350	5.83	33	67
T1S1P0A45B80QLD25	45	80	0.005	25	0.31	98	2

Appendix B

Run ID	Rack Angle (Degrees)	Bar Spacing (mm)	Discharge (m^3/s)	Debris Length (mm)	Ratio of debris length to bar spacing	Passed Through	Blocked
T1S1P0A45B80QLD50	45	80	0.005	50	0.63	95	5
T1S1P0A45B80QLD75	45	80	0.005	75	0.94	89	11
T1S1P0A45B80QLD100	45	80	0.005	100	1.25	68	32
T1S1P0A45B80QLD150	45	80	0.005	150	1.88	50	50
T1S1P0A45B80QLD200	45	80	0.005	200	2.50	47	53
T1S1P0A45B80QLD275	45	80	0.005	275	3.44	28	72
T1S1P0A45B80QLD300	45	80	0.005	300	3.75	29	71
T1S1P0A45B80QLD325	45	80	0.005	325	4.06	28	72
T1S1P0A45B80QLD350	45	80	0.005	350	4.38	31	69
T1S1P0A45B100QLD25	45	100	0.005	25	0.25	94	6
T1S1P0A45B100QLD50	45	100	0.005	50	0.50	98	2
T1S1P0A45B100QLD75	45	100	0.005	75	0.75	92	8
T1S1P0A45B100QLD100	45	100	0.005	100	1.00	91	9
T1S1P0A45B100QLD150	45	100	0.005	150	1.50	55	45
T1S1P0A45B100QLD200	45	100	0.005	200	2.00	53	47
T1S1P0A45B100QLD275	45	100	0.005	275	2.75	51	49
T1S1P0A45B100QLD300	45	100	0.005	300	3.00	45	55
T1S1P0A45B100QLD325	45	100	0.005	325	3.25	34	66
T1S1P0A45B100QLD350	45	100	0.005	350	3.50	32	68
T1S1P0A45B150QLD25	45	150	0.005	25	0.17	98	2
T1S1P0A45B150QLD50	45	150	0.005	50	0.33	95	5
T1S1P0A45B150QLD75	45	150	0.005	75	0.50	96	4
T1S1P0A45B150QLD100	45	150	0.005	100	0.67	99	1
T1S1P0A45B150QLD150	45	150	0.005	150	1.00	95	5
T1S1P0A45B150QLD200	45	150	0.005	200	1.33	66	34
T1S1P0A45B150QLD275	45	150	0.005	275	1.83	56	44
T1S1P0A45B150QLD300	45	150	0.005	300	2.00	55	45
T1S1P0A45B150QLD325	45	150	0.005	325	2.17	52	48
T1S1P0A45B150QLD350	45	150	0.005	350	2.33	62	38
T1S1P0A60B30QLD25	60	30	0.005	25	0.83	90	10
T1S1P0A60B30QLD50	60	30	0.005	50	1.67	57	43
T1S1P0A60B30QLD75	60	30	0.005	75	2.50	36	64
T1S1P0A60B30QLD100	60	30	0.005	100	3.33	26	74
T1S1P0A60B30QLD150	60	30	0.005	150	5.00	26	74
T1S1P0A60B30QLD200	60	30	0.005	200	6.67	26	74
T1S1P0A60B30QLD275	60	30	0.005	275	9.17	7	93

Run ID	Rack Angle (Degrees)	Bar Spacing (mm)	Discharge (m^3/s)	Debris Length (mm)	Ratio of debris length to bar spacing	Passed Through	Blocked
T1S1P0A60B30QLD300	60	30	0.005	300	10.00	20	80
T1S1P0A60B30QLD325	60	30	0.005	325	10.83	19	81
T1S1P0A60B30QLD350	60	30	0.005	350	11.67	20	80
T1S1P0A60B40QLD25	60	40	0.005	25	0.63	94	6
T1S1P0A60B40QLD50	60	40	0.005	50	1.25	59	41
T1S1P0A60B40QLD75	60	40	0.005	75	1.88	65	35
T1S1P0A60B40QLD100	60	40	0.005	100	2.50	50	50
T1S1P0A60B40QLD150	60	40	0.005	150	3.75	28	72
T1S1P0A60B40QLD200	60	40	0.005	200	5.00	34	66
T1S1P0A60B40QLD275	60	40	0.005	275	6.88	29	71
T1S1P0A60B40QLD300	60	40	0.005	300	7.50	24	76
T1S1P0A60B40QLD325	60	40	0.005	325	8.13	20	80
T1S1P0A60B40QLD350	60	40	0.005	350	8.75	30	70
T1S1P0A60B50QLD25	60	50	0.005	25	0.50	93	7
T1S1P0A60B50QLD50	60	50	0.005	50	1.00	90	10
T1S1P0A60B50QLD75	60	50	0.005	75	1.50	57	43
T1S1P0A60B50QLD100	60	50	0.005	100	2.00	57	43
T1S1P0A60B50QLD150	60	50	0.005	150	3.00	31	69
T1S1P0A60B50QLD200	60	50	0.005	200	4.00	39	61
T1S1P0A60B50QLD275	60	50	0.005	275	5.50	20	80
T1S1P0A60B50QLD300	60	50	0.005	300	6.00	30	70
T1S1P0A60B50QLD325	60	50	0.005	325	6.50	28	72
T1S1P0A60B50QLD350	60	50	0.005	350	7.00	31	69
T1S1P0A60B60QLD25	60	60	0.005	25	0.42	96	4
T1S1P0A60B60QLD50	60	60	0.005	50	0.83	94	6
T1S1P0A60B60QLD75	60	60	0.005	75	1.25	75	25
T1S1P0A60B60QLD100	60	60	0.005	100	1.67	68	32
T1S1P0A60B60QLD150	60	60	0.005	150	2.50	44	56
T1S1P0A60B60QLD200	60	60	0.005	200	3.33	45	55
T1S1P0A60B60QLD275	60	60	0.005	275	4.58	32	68
T1S1P0A60B60QLD300	60	60	0.005	300	5.00	27	73
T1S1P0A60B60QLD325	60	60	0.005	325	5.42	25	75
T1S1P0A60B60QLD350	60	60	0.005	350	5.83	46	54
T1S1P0A60B80QLD25	60	80	0.005	25	0.31	99	1
T1S1P0A60B80QLD50	60	80	0.005	50	0.63	98	2
T1S1P0A60B80QLD75	60	80	0.005	75	0.94	87	13

Appendix B

Run ID	Rack Angle (Degrees)	Bar Spacing (mm)	Discharge (m^3/s)	Debris Length (mm)	Ratio of debris length to bar spacing	Passed Through	Blocked
T1S1P0A60B80QLD100	60	80	0.005	100	1.25	82	18
T1S1P0A60B80QLD150	60	80	0.005	150	1.88	56	44
T1S1P0A60B80QLD200	60	80	0.005	200	2.50	52	48
T1S1P0A60B80QLD275	60	80	0.005	275	3.44	38	62
T1S1P0A60B80QLD300	60	80	0.005	300	3.75	39	61
T1S1P0A60B80QLD325	60	80	0.005	325	4.06	35	65
T1S1P0A60B80QLD350	60	80	0.005	350	4.38	40	61
T1S1P0A60B100QLD25	60	100	0.005	25	0.25	98	2
T1S1P0A60B100QLD50	60	100	0.005	50	0.50	100	0
T1S1P0A60B100QLD75	60	100	0.005	75	0.75	97	3
T1S1P0A60B100QLD100	60	100	0.005	100	1.00	95	5
T1S1P0A60B100QLD150	60	100	0.005	150	1.50	75	25
T1S1P0A60B100QLD200	60	100	0.005	200	2.00	60	40
T1S1P0A60B100QLD275	60	100	0.005	275	2.75	55	45
T1S1P0A60B100QLD300	60	100	0.005	300	3.00	42	58
T1S1P0A60B100QLD325	60	100	0.005	325	3.25	38	62
T1S1P0A60B100QLD350	60	100	0.005	350	3.50	41	59
T1S1P0A60B150QLD25	60	150	0.005	25	0.17	100	0
T1S1P0A60B150QLD50	60	150	0.005	50	0.33	100	0
T1S1P0A60B150QLD75	60	150	0.005	75	0.50	100	0
T1S1P0A60B150QLD100	60	150	0.005	100	0.67	98	2
T1S1P0A60B150QLD150	60	150	0.005	150	1.00	93	7
T1S1P0A60B150QLD200	60	150	0.005	200	1.33	66	34
T1S1P0A60B150QLD275	60	150	0.005	275	1.83	64	36
T1S1P0A60B150QLD300	60	150	0.005	300	2.00	58	42
T1S1P0A60B150QLD325	60	150	0.005	325	2.17	56	44
T1S1P0A60B150QLD350	60	150	0.005	350	2.33	68	32
T1S2P4A30B30QMD25	30	30	0.021	25	0.83	91	9
T1S1P0A30B30QMD50	30	30	0.021	50	1.67	43	57
T1S1P0A30B30QMD75	30	30	0.021	75	2.50	27	73
T1S1P0A30B30QMD100	30	30	0.021	100	3.33	28	72
T1S1P0A30B30QMD150	30	30	0.021	150	5.00	27	73
T1S1P0A30B30QMD200	30	30	0.021	200	6.67	22	78
T1S1P0A30B30QMD275	30	30	0.021	275	9.17	23	77
T1S1P0A30B30QMD300	30	30	0.021	300	10.00	22	78
T1S1P0A30B30QMD325	30	30	0.021	325	10.83	22	78

Run ID	Rack Angle (Degrees)	Bar Spacing (mm)	Discharge (m^3/s)	Debris Length (mm)	Ratio of debris length to bar spacing	Passed Through	Blocked
T1S1P0A30B30QMD350	30	30	0.021	350	11.67	20	80
T1S1P0A30B40QMD25	30	40	0.021	25	0.63	94	6
T1S1P0A30B40QMD50	30	40	0.021	50	1.25	75	25
T1S1P0A30B40QMD75	30	40	0.021	75	1.88	40	60
T1S1P0A30B40QMD100	30	40	0.021	100	2.50	24	76
T1S1P0A30B40QMD150	30	40	0.021	150	3.75	28	72
T1S1P0A30B40QMD200	30	40	0.021	200	5.00	27	73
T1S1P0A30B40QMD275	30	40	0.021	275	6.88	33	67
T1S1P0A30B40QMD300	30	40	0.021	300	7.50	30	70
T1S1P0A30B40QMD325	30	40	0.021	325	8.13	26	74
T1S1P0A30B40QMD350	30	40	0.021	350	8.75	21	79
T1S1P0A30B50QMD25	30	50	0.021	25	0.50	96	4
T1S1P0A30B50QMD50	30	50	0.021	50	1.00	90	10
T1S1P0A30B50QMD75	30	50	0.021	75	1.50	59	41
T1S1P0A30B50QMD100	30	50	0.021	100	2.00	49	51
T1S1P0A30B50QMD150	30	50	0.021	150	3.00	40	60
T1S1P0A30B50QMD200	30	50	0.021	200	4.00	39	61
T1S1P0A30B50QMD275	30	50	0.021	275	5.50	30	70
T1S1P0A30B50QMD300	30	50	0.021	300	6.00	34	66
T1S1P0A30B50QMD325	30	50	0.021	325	6.50	35	65
T1S1P0A30B50QMD350	30	50	0.021	350	7.00	31	69
T1S1P0A30B60QMD25	30	60	0.021	25	0.42	90	10
T1S1P0A30B60QMD50	30	60	0.021	50	0.83	93	7
T1S1P0A30B60QMD75	30	60	0.021	75	1.25	75	25
T1S1P0A30B60QMD100	30	60	0.021	100	1.67	41	59
T1S1P0A30B60QMD150	30	60	0.021	150	2.50	47	53
T1S1P0A30B60QMD200	30	60	0.021	200	3.33	30	70
T1S1P0A30B60QMD275	30	60	0.021	275	4.58	30	70
T1S1P0A30B60QMD300	30	60	0.021	300	5.00	33	67
T1S1P0A30B60QMD325	30	60	0.021	325	5.42	31	69
T1S1P0A30B60QMD350	30	60	0.021	350	5.83	30	70
T1S1P0A30B80QMD25	30	80	0.021	25	0.31	99	1
T1S1P0A30B80QMD50	30	80	0.021	50	0.63	92	8
T1S1P0A30B80QMD75	30	80	0.021	75	0.94	94	6
T1S1P0A30B80QMD100	30	80	0.021	100	1.25	78	22
T1S1P0A30B80QMD150	30	80	0.021	150	1.88	58	42

Appendix B

Run ID	Rack Angle (Degrees)	Bar Spacing (mm)	Discharge (m^3/s)	Debris Length (mm)	Ratio of debris length to bar spacing	Passed Through	Blocked
T1S1P0A30B80QMD200	30	80	0.021	200	2.50	38	62
T1S1P0A30B80QMD275	30	80	0.021	275	3.44	37	63
T1S1P0A30B80QMD300	30	80	0.021	300	3.75	34	66
T1S1P0A30B80QMD325	30	80	0.021	325	4.06	30	70
T1S1P0A30B80QMD350	30	80	0.021	350	4.38	28	72
T1S1P0A30B100QMD25	30	100	0.021	25	0.25	100	0
T1S1P0A30B100QMD50	30	100	0.021	50	0.50	96	4
T1S1P0A30B100QMD75	30	100	0.021	75	0.75	91	9
T1S1P0A30B100QMD100	30	100	0.021	100	1.00	92	8
T1S1P0A30B100QMD150	30	100	0.021	150	1.50	64	36
T1S1P0A30B100QMD200	30	100	0.021	200	2.00	46	54
T1S1P0A30B100QMD275	30	100	0.021	275	2.75	45	55
T1S1P0A30B100QMD300	30	100	0.021	300	3.00	40	60
T1S1P0A30B100QMD325	30	100	0.021	325	3.25	38	62
T1S1P0A30B100QMD350	30	100	0.021	350	3.50	35	65
T1S1P0A30B150QMD25	30	150	0.021	25	0.17	99	1
T1S1P0A30B150QMD50	30	150	0.021	50	0.33	90	10
T1S1P0A30B150QMD75	30	150	0.021	75	0.50	97	3
T1S1P0A30B150QMD100	30	150	0.021	100	0.67	92	8
T1S1P0A30B150QMD150	30	150	0.021	150	1.00	91	9
T1S1P0A30B150QMD200	30	150	0.021	200	1.33	73	27
T1S1P0A30B150QMD275	30	150	0.021	275	1.83	47	53
T1S1P0A30B150QMD300	30	150	0.021	300	2.00	50	50
T1S1P0A30B150QMD325	30	150	0.021	325	2.17	49	51
T1S1P0A30B150QMD350	30	150	0.021	350	2.33	66	34
T1S1P0A45B30QMD25	45	30	0.021	25	0.83	95	5
T1S1P0A45B30QMD50	45	30	0.021	50	1.67	46	54
T1S1P0A45B30QMD75	45	30	0.021	75	2.50	33	67
T1S1P0A45B30QMD100	45	30	0.021	100	3.33	31	69
T1S1P0A45B30QMD150	45	30	0.021	150	5.00	31	69
T1S1P0A45B30QMD200	45	30	0.021	200	6.67	27	73
T1S1P0A45B30QMD275	45	30	0.021	275	9.17	29	71
T1S1P0A45B30QMD300	45	30	0.021	300	10.00	16	84
T1S1P0A45B30QMD325	45	30	0.021	325	10.83	18	82
T1S1P0A45B30QMD350	45	30	0.021	350	11.67	18	82
T1S1P0A45B40QMD25	45	40	0.021	25	0.63	92	8

Run ID	Rack Angle (Degrees)	Bar Spacing (mm)	Discharge (m^3/s)	Debris Length (mm)	Ratio of debris length to bar spacing	Passed Through	Blocked
T1S1P0A45B40QMD50	45	40	0.021	50	1.25	76	24
T1S1P0A45B40QMD75	45	40	0.021	75	1.88	41	59
T1S1P0A45B40QMD100	45	40	0.021	100	2.50	33	67
T1S1P0A45B40QMD150	45	40	0.021	150	3.75	30	70
T1S1P0A45B40QMD200	45	40	0.021	200	5.00	26	74
T1S1P0A45B40QMD275	45	40	0.021	275	6.88	32	68
T1S1P0A45B40QMD300	45	40	0.021	300	7.50	24	76
T1S1P0A45B40QMD325	45	40	0.021	325	8.13	16	84
T1S1P0A45B40QMD350	45	40	0.021	350	8.75	28	72
T1S1P0A45B50QMD25	45	50	0.021	25	0.50	96	4
T1S1P0A45B50QMD50	45	50	0.021	50	1.00	95	5
T1S1P0A45B50QMD75	45	50	0.021	75	1.50	60	40
T1S1P0A45B50QMD100	45	50	0.021	100	2.00	51	49
T1S1P0A45B50QMD150	45	50	0.021	150	3.00	46	54
T1S1P0A45B50QMD200	45	50	0.021	200	4.00	42	58
T1S1P0A45B50QMD275	45	50	0.021	275	5.50	39	61
T1S1P0A45B50QMD300	45	50	0.021	300	6.00	36	64
T1S1P0A45B50QMD325	45	50	0.021	325	6.50	34	66
T1S1P0A45B50QMD350	45	50	0.021	350	7.00	38	62
T1S1P0A45B60QMD25	45	60	0.021	25	0.42	98	2
T1S1P0A45B60QMD50	45	60	0.021	50	0.83	91	9
T1S1P0A45B60QMD75	45	60	0.021	75	1.25	76	24
T1S1P0A45B60QMD100	45	60	0.021	100	1.67	56	44
T1S1P0A45B60QMD150	45	60	0.021	150	2.50	45	55
T1S1P0A45B60QMD200	45	60	0.021	200	3.33	37	63
T1S1P0A45B60QMD275	45	60	0.021	275	4.58	29	71
T1S1P0A45B60QMD300	45	60	0.021	300	5.00	44	56
T1S1P0A45B60QMD325	45	60	0.021	325	5.42	22	78
T1S1P0A45B60QMD350	45	60	0.021	350	5.83	36	64
T1S1P0A45B80QMD25	45	80	0.021	25	0.31	99	1
T1S1P0A45B80QMD50	45	80	0.021	50	0.63	90	10
T1S1P0A45B80QMD75	45	80	0.021	75	0.94	96	4
T1S1P0A45B80QMD100	45	80	0.021	100	1.25	60	40
T1S1P0A45B80QMD150	45	80	0.021	150	1.88	53	47
T1S1P0A45B80QMD200	45	80	0.021	200	2.50	44	56
T1S1P0A45B80QMD275	45	80	0.021	275	3.44	45	55

Run ID	Rack Angle (Degrees)	Bar Spacing (mm)	Discharge (m^3/s)	Debris Length (mm)	Ratio of debris length to bar spacing	Passed Through	Blocked
T1S1P0A45B80QMD300	45	80	0.021	300	3.75	36	64
T1S1P0A45B80QMD325	45	80	0.021	325	4.06	38	62
T1S1P0A45B80QMD350	45	80	0.021	350	4.38	38	62
T1S1P0A45B100QMD25	45	100	0.021	25	0.25	96	4
T1S1P0A45B100QMD50	45	100	0.021	50	0.50	97	3
T1S1P0A45B100QMD75	45	100	0.021	75	0.75	91	9
T1S1P0A45B100QMD100	45	100	0.021	100	1.00	93	7
T1S1P0A45B100QMD150	45	100	0.021	150	1.50	61	39
T1S1P0A45B100QMD200	45	100	0.021	200	2.00	57	43
T1S1P0A45B100QMD275	45	100	0.021	275	2.75	55	45
T1S1P0A45B100QMD300	45	100	0.021	300	3.00	44	56
T1S1P0A45B100QMD325	45	100	0.021	325	3.25	45	55
T1S1P0A45B100QMD350	45	100	0.021	350	3.50	40	60
T1S1P0A45B150QMD25	45	150	0.021	25	0.17	100	0
T1S1P0A45B150QMD50	45	150	0.021	50	0.33	99	1
T1S1P0A45B150QMD75	45	150	0.021	75	0.50	97	3
T1S1P0A45B150QMD100	45	150	0.021	100	0.67	95	5
T1S1P0A45B150QMD150	45	150	0.021	150	1.00	98	2
T1S1P0A45B150QMD200	45	150	0.021	200	1.33	80	20
T1S1P0A45B150QMD275	45	150	0.021	275	1.83	60	40
T1S1P0A45B150QMD300	45	150	0.021	300	2.00	58	42
T1S1P0A45B150QMD325	45	150	0.021	325	2.17	60	40
T1S1P0A45B150QMD350	45	150	0.021	350	2.33	54	46
T1S1P0A60B30QMD25	60	30	0.021	25	0.83	96	4
T1S1P0A60B30QMD50	60	30	0.021	50	1.67	61	39
T1S1P0A60B30QMD75	60	30	0.021	75	2.50	33	67
T1S1P0A60B30QMD100	60	30	0.021	100	3.33	30	70
T1S1P0A60B30QMD150	60	30	0.021	150	5.00	34	66
T1S1P0A60B30QMD200	60	30	0.021	200	6.67	34	66
T1S1P0A60B30QMD275	60	30	0.021	275	9.17	26	74
T1S1P0A60B30QMD300	60	30	0.021	300	10.00	26	74
T1S1P0A60B30QMD325	60	30	0.021	325	10.83	28	72
T1S1P0A60B30QMD350	60	30	0.021	350	11.67	27	73
T1S1P0A60B40QMD25	60	40	0.021	25	0.63	98	2
T1S1P0A60B40QMD50	60	40	0.021	50	1.25	88	12
T1S1P0A60B40QMD75	60	40	0.021	75	1.88	53	47

Run ID	Rack Angle (Degrees)	Bar Spacing (mm)	Discharge (m^3/s)	Debris Length (mm)	Ratio of debris length to bar spacing	Passed Through	Blocked
T1S1P0A60B40QMD100	60	40	0.021	100	2.50	47	53
T1S1P0A60B40QMD150	60	40	0.021	150	3.75	43	57
T1S1P0A60B40QMD200	60	40	0.021	200	5.00	39	61
T1S1P0A60B40QMD275	60	40	0.021	275	6.88	39	61
T1S1P0A60B40QMD300	60	40	0.021	300	7.50	30	70
T1S1P0A60B40QMD325	60	40	0.021	325	8.13	29	71
T1S1P0A60B40QMD350	60	40	0.021	350	8.75	31	69
T1S1P0A60B50QMD25	60	50	0.021	25	0.50	98	2
T1S1P0A60B50QMD50	60	50	0.021	50	1.00	96	4
T1S1P0A60B50QMD75	60	50	0.021	75	1.50	68	32
T1S1P0A60B50QMD100	60	50	0.021	100	2.00	50	50
T1S1P0A60B50QMD150	60	50	0.021	150	3.00	45	55
T1S1P0A60B50QMD200	60	50	0.021	200	4.00	45	55
T1S1P0A60B50QMD275	60	50	0.021	275	5.50	47	53
T1S1P0A60B50QMD300	60	50	0.021	300	6.00	35	65
T1S1P0A60B50QMD325	60	50	0.021	325	6.50	32	68
T1S1P0A60B50QMD350	60	50	0.021	350	7.00	43	57
T1S1P0A60B60QMD25	60	60	0.021	25	0.42	100	0
T1S1P0A60B60QMD50	60	60	0.021	50	0.83	98	2
T1S1P0A60B60QMD75	60	60	0.021	75	1.25	93	7
T1S1P0A60B60QMD100	60	60	0.021	100	1.67	67	33
T1S1P0A60B60QMD150	60	60	0.021	150	2.50	46	54
T1S1P0A60B60QMD200	60	60	0.021	200	3.33	55	45
T1S1P0A60B60QMD275	60	60	0.021	275	4.58	43	57
T1S1P0A60B60QMD300	60	60	0.021	300	5.00	45	55
T1S1P0A60B60QMD325	60	60	0.021	325	5.42	35	65
T1S1P0A60B60QMD350	60	60	0.021	350	5.83	46	54
T1S1P0A60B80QMD25	60	80	0.021	25	0.31	96	4
T1S1P0A60B80QMD50	60	80	0.021	50	0.63	99	1
T1S1P0A60B80QMD75	60	80	0.021	75	0.94	98	2
T1S1P0A60B80QMD100	60	80	0.021	100	1.25	82	18
T1S1P0A60B80QMD150	60	80	0.021	150	1.88	65	35
T1S1P0A60B80QMD200	60	80	0.021	200	2.50	64	36
T1S1P0A60B80QMD275	60	80	0.021	275	3.44	54	46
T1S1P0A60B80QMD300	60	80	0.021	300	3.75	49	51
T1S1P0A60B80QMD325	60	80	0.021	325	4.06	46	54

Appendix B

Run ID	Rack Angle (Degrees)	Bar Spacing (mm)	Discharge (m^3/s)	Debris Length (mm)	Ratio of debris length to bar spacing	Passed Through	Blocked
T1S1P0A60B80QMD350	60	80	0.021	350	4.38	49	51
T1S1P0A60B100QMD25	60	100	0.021	25	0.25	100	0
T1S1P0A60B100QMD50	60	100	0.021	50	0.50	100	0
T1S1P0A60B100QMD75	60	100	0.021	75	0.75	100	0
T1S1P0A60B100QMD100	60	100	0.021	100	1.00	99	1
T1S1P0A60B100QMD150	60	100	0.021	150	1.50	79	21
T1S1P0A60B100QMD200	60	100	0.021	200	2.00	65	35
T1S1P0A60B100QMD275	60	100	0.021	275	2.75	67	33
T1S1P0A60B100QMD300	60	100	0.021	300	3.00	59	41
T1S1P0A60B100QMD325	60	100	0.021	325	3.25	54	46
T1S1P0A60B100QMD350	60	100	0.021	350	3.50	55	45
T1S1P0A60B150QMD25	60	150	0.021	25	0.17	100	0
T1S1P0A60B150QMD50	60	150	0.021	50	0.33	99	1
T1S1P0A60B150QMD75	60	150	0.021	75	0.50	98	2
T1S1P0A60B150QMD100	60	150	0.021	100	0.67	100	0
T1S1P0A60B150QMD150	60	150	0.021	150	1.00	96	4
T1S1P0A60B150QMD200	60	150	0.021	200	1.33	81	19
T1S1P0A60B150QMD275	60	150	0.021	275	1.83	70	30
T1S1P0A60B150QMD300	60	150	0.021	300	2.00	64	36
T1S1P0A60B150QMD325	60	150	0.021	325	2.17	62	38
T1S1P0A60B150QMD350	60	150	0.021	350	2.33	71	29

Appendix C – Results from Test Phase 2

Table C.1 Results from flow conditions testing

Run ID	Rack Angle (Degrees)	Bar Spacing (mm))	Discharge (m^3/s)	Slope	Debris Length (mm)	Ratio of debris Length to bar spacing	Passed Through	Blocked
T2S2P0A30B30QHD25	30	30	0.035	2	25	0.83	96	4
T2S2P0A30B30QHD50	30	30	0.035	2	50	1.67	34	66
T2S2P0A30B30QHD75	30	30	0.035	2	75	2.50	29	71
T2S2P0A30B30QHD100	30	30	0.035	2	100	3.33	17	83
T2S2P0A30B30QHD150	30	30	0.035	2	150	5.00	19	81
T2S2P0A30B30QHD200	30	30	0.035	2	200	6.67	11	89
T2S2P0A30B30QHD275	30	30	0.035	2	275	9.17	15	85
T2S2P0A30B30QHD300	30	30	0.035	2	300	10.00	13	87
T2S2P0A30B30QHD325	30	30	0.035	2	325	10.83	15	85
T2S2P0A30B30QHD350	30	30	0.035	2	350	11.67	16	84
T2S2P0A30B40QHD25	30	40	0.035	2	25	0.63	94	6
T2S2P0A30B40QHD50	30	40	0.035	2	50	1.25	76	24
T2S2P0A30B40QHD75	30	40	0.035	2	75	1.88	37	63
T2S2P0A30B40QHD100	30	40	0.035	2	100	2.50	43	57
T2S2P0A30B40QHD150	30	40	0.035	2	150	3.75	33	67
T2S2P0A30B40QHD200	30	40	0.035	2	200	5.00	28	72
T2S2P0A30B40QHD275	30	40	0.035	2	275	6.88	21	79
T2S2P0A30B40QHD300	30	40	0.035	2	300	7.50	16	84
T2S2P0A30B40QHD325	30	40	0.035	2	325	8.13	22	78
T2S2P0A30B40QHD350	30	40	0.035	2	350	8.75	22	78
T2S2P0A30B50QHD25	30	50	0.035	2	25	0.50	98	2
T2S2P0A30B50QHD50	30	50	0.035	2	50	1.00	96	4
T2S2P0A30B50QHD75	30	50	0.035	2	75	1.50	65	35
T2S2P0A30B50QHD100	30	50	0.035	2	100	2.00	34	66
T2S2P0A30B50QHD150	30	50	0.035	2	150	3.00	29	71
T2S2P0A30B50QHD200	30	50	0.035	2	200	4.00	30	70
T2S2P0A30B50QHD275	30	50	0.035	2	275	5.50	23	77
T2S2P0A30B50QHD300	30	50	0.035	2	300	6.00	36	64
T2S2P0A30B50QHD325	30	50	0.035	2	325	6.50	23	77
T2S2P0A30B50QHD350	30	50	0.035	2	350	7.00	21	79
T2S2P0A30B60QHD25	30	60	0.035	2	25	0.42	100	0
T2S2P0A30B60QHD50	30	60	0.035	2	50	0.83	99	1
T2S2P0A30B60QHD75	30	60	0.035	2	75	1.25	63	37

Run ID	Rack Angle (Degrees)	Bar Spacing (mm))	Discharge (m^3/s)	Slope	Debris Length (mm)	Ratio of debris Length to bar spacing	Passed Through	Blocked
T2S2P0A30B60QHD100	30	60	0.035	2	100	1.67	51	49
T2S2P0A30B60QHD150	30	60	0.035	2	150	2.50	45	55
T2S2P0A30B60QHD200	30	60	0.035	2	200	3.33	39	61
T2S2P0A30B60QHD275	30	60	0.035	2	275	4.58	38	62
T2S2P0A30B60QHD300	30	60	0.035	2	300	5.00	29	71
T2S2P0A30B60QHD325	30	60	0.035	2	325	5.42	28	72
T2S2P0A30B60QHD350	30	60	0.035	2	350	5.83	21	79
T2S2P0A30B80QHD25	30	80	0.035	2	25	0.31	100	0
T2S2P0A30B80QHD50	30	80	0.035	2	50	0.63	97	3
T2S2P0A30B80QHD75	30	80	0.035	2	75	0.94	100	0
T2S2P0A30B80QHD100	30	80	0.035	2	100	1.25	73	27
T2S2P0A30B80QHD150	30	80	0.035	2	150	1.88	58	42
T2S2P0A30B80QHD200	30	80	0.035	2	200	2.50	40	60
T2S2P0A30B80QHD275	30	80	0.035	2	275	3.44	35	65
T2S2P0A30B80QHD300	30	80	0.035	2	300	3.75	46	54
T2S2P0A30B80QHD325	30	80	0.035	2	325	4.06	41	59
T2S2P0A30B80QHD350	30	80	0.035	2	350	4.38	24	76
T2S2P0A30B100QHD25	30	100	0.035	2	25	0.25	100	0
T2S2P0A30B100QHD50	30	100	0.035	2	50	0.50	95	5
T2S2P0A30B100QHD75	30	100	0.035	2	75	0.75	97	3
T2S2P0A30B100QHD100	30	100	0.035	2	100	1.00	88	12
T2S2P0A30B100QHD150	30	100	0.035	2	150	1.50	55	45
T2S2P0A30B100QHD200	30	100	0.035	2	200	2.00	48	52
T2S2P0A30B100QHD275	30	100	0.035	2	275	2.75	45	55
T2S2P0A30B100QHD300	30	100	0.035	2	300	3.00	45	55
T2S2P0A30B100QHD325	30	100	0.035	2	325	3.25	46	54
T2S2P0A30B100QHD350	30	100	0.035	2	350	3.50	49	51
T2S2P0A30B150QHD25	30	150	0.035	2	25	0.17	100	0
T2S2P0A30B150QHD50	30	150	0.035	2	50	0.33	98	2
T2S2P0A30B150QHD75	30	150	0.035	2	75	0.50	96	4
T2S2P0A30B150QHD100	30	150	0.035	2	100	0.67	96	4
T2S2P0A30B150QHD150	30	150	0.035	2	150	1.00	95	5
T2S2P0A30B150QHD200	30	150	0.035	2	200	1.33	73	27
T2S2P0A30B150QHD275	30	150	0.035	2	275	1.83	55	45
T2S2P0A30B150QHD300	30	150	0.035	2	300	2.00	48	52
T2S2P0A30B150QHD325	30	150	0.035	2	325	2.17	44	56

Appendix C

Run ID	Rack Angle (Degrees)	Bar Spacing (mm))	Discharge (m^3/s)	Slope	Debris Length (mm)	Ratio of debris Length to bar spacing	Passed Through	Blocked
T2S2P0A30B150QHD350	30	150	0.035	2	350	2.33	55	45
T2S2P0A45B30QHD25	45	30	0.035	2	25	0.83	96	4
T2S2P0A45B30QHD50	45	30	0.035	2	50	1.67	54	46
T2S2P0A45B30QHD75	45	30	0.035	2	75	2.50	32	68
T2S2P0A45B30QHD100	45	30	0.035	2	100	3.33	27	73
T2S2P0A45B30QHD150	45	30	0.035	2	150	5.00	23	77
T2S2P0A45B30QHD200	45	30	0.035	2	200	6.67	20	80
T2S2P0A45B30QHD275	45	30	0.035	2	275	9.17	18	82
T2S2P0A45B30QHD300	45	30	0.035	2	300	10.00	21	79
T2S2P0A45B30QHD325	45	30	0.035	2	325	10.83	21	79
T2S2P0A45B30QHD350	45	30	0.035	2	350	11.67	22	78
T2S2P0A45B40QHD25	45	40	0.035	2	25	0.63	99	1
T2S2P0A45B40QHD50	45	40	0.035	2	50	1.25	81	19
T2S2P0A45B40QHD75	45	40	0.035	2	75	1.88	34	66
T2S2P0A45B40QHD100	45	40	0.035	2	100	2.50	34	66
T2S2P0A45B40QHD150	45	40	0.035	2	150	3.75	26	74
T2S2P0A45B40QHD200	45	40	0.035	2	200	5.00	20	80
T2S2P0A45B40QHD275	45	40	0.035	2	275	6.88	25	75
T2S2P0A45B40QHD300	45	40	0.035	2	300	7.50	25	75
T2S2P0A45B40QHD325	45	40	0.035	2	325	8.13	34	66
T2S2P0A45B40QHD350	45	40	0.035	2	350	8.75	24	76
T2S2P0A45B50QHD25	45	50	0.035	2	25	0.50	100	0
T2S2P0A45B50QHD50	45	50	0.035	2	50	1.00	95	5
T2S2P0A45B50QHD75	45	50	0.035	2	75	1.50	57	43
T2S2P0A45B50QHD100	45	50	0.035	2	100	2.00	44	56
T2S2P0A45B50QHD150	45	50	0.035	2	150	3.00	25	75
T2S2P0A45B50QHD200	45	50	0.035	2	200	4.00	32	68
T2S2P0A45B50QHD275	45	50	0.035	2	275	5.50	26	74
T2S2P0A45B50QHD300	45	50	0.035	2	300	6.00	39	61
T2S2P0A45B50QHD325	45	50	0.035	2	325	6.50	24	76
T2S2P0A45B50QHD350	45	50	0.035	2	350	7.00	22	78
T2S2P0A45B60QHD25	45	60	0.035	2	25	0.42	100	0
T2S2P0A45B60QHD50	45	60	0.035	2	50	0.83	95	5
T2S2P0A45B60QHD75	45	60	0.035	2	75	1.25	80	20
T2S2P0A45B60QHD100	45	60	0.035	2	100	1.67	61	39
T2S2P0A45B60QHD150	45	60	0.035	2	150	2.50	26	74

Run ID	Rack Angle (Degrees)	Bar Spacing (mm))	Discharge (m^3/s)	Slope	Debris Length (mm)	Ratio of debris Length to bar spacing	Passed Through	Blocked
T2S2P0A45B60QHD200	45	60	0.035	2	200	3.33	33	67
T2S2P0A45B60QHD275	45	60	0.035	2	275	4.58	39	61
T2S2P0A45B60QHD300	45	60	0.035	2	300	5.00	30	70
T2S2P0A45B60QHD325	45	60	0.035	2	325	5.42	35	65
T2S2P0A45B60QHD350	45	60	0.035	2	350	5.83	28	72
T2S2P0A45B80QHD25	45	80	0.035	2	25	0.31	100	0
T2S2P0A45B80QHD50	45	80	0.035	2	50	0.63	99	1
T2S2P0A45B80QHD75	45	80	0.035	2	75	0.94	97	3
T2S2P0A45B80QHD100	45	80	0.035	2	100	1.25	86	14
T2S2P0A45B80QHD150	45	80	0.035	2	150	1.88	57	43
T2S2P0A45B80QHD200	45	80	0.035	2	200	2.50	50	50
T2S2P0A45B80QHD275	45	80	0.035	2	275	3.44	43	57
T2S2P0A45B80QHD300	45	80	0.035	2	300	3.75	46	54
T2S2P0A45B80QHD325	45	80	0.035	2	325	4.06	46	54
T2S2P0A45B80QHD350	45	80	0.035	2	350	4.38	37	63
T2S2P0A45B100QHD25	45	100	0.035	2	25	0.25	100	0
T2S2P0A45B100QHD50	45	100	0.035	2	50	0.50	100	0
T2S2P0A45B100QHD75	45	100	0.035	2	75	0.75	97	3
T2S2P0A45B100QHD100	45	100	0.035	2	100	1.00	91	9
T2S2P0A45B100QHD150	45	100	0.035	2	150	1.50	78	22
T2S2P0A45B100QHD200	45	100	0.035	2	200	2.00	50	50
T2S2P0A45B100QHD275	45	100	0.035	2	275	2.75	54	46
T2S2P0A45B100QHD300	45	100	0.035	2	300	3.00	47	53
T2S2P0A45B100QHD325	45	100	0.035	2	325	3.25	45	55
T2S2P0A45B100QHD350	45	100	0.035	2	350	3.50	29	71
T2S2P0A45B150QHD25	45	150	0.035	2	25	0.17	100	0
T2S2P0A45B150QHD50	45	150	0.035	2	50	0.33	99	1
T2S2P0A45B150QHD75	45	150	0.035	2	75	0.50	97	3
T2S2P0A45B150QHD100	45	150	0.035	2	100	0.67	99	1
T2S2P0A45B150QHD150	45	150	0.035	2	150	1.00	94	6
T2S2P0A45B150QHD200	45	150	0.035	2	200	1.33	81	19
T2S2P0A45B150QHD275	45	150	0.035	2	275	1.83	60	40
T2S2P0A45B150QHD300	45	150	0.035	2	300	2.00	50	50
T2S2P0A45B150QHD325	45	150	0.035	2	325	2.17	46	54
T2S2P0A45B150QHD350	45	150	0.035	2	350	2.33	49	51
T2S2P0A60B30QHD25	60	30	0.035	2	25	0.83	100	0

Run ID	Rack Angle (Degrees)	Bar Spacing (mm))	Discharge (m^3/s)	Slope	Debris Length (mm)	Ratio of debris Length to bar spacing	Passed Through	Blocked
T2S2P0A60B30QHD50	60	30	0.035	2	50	1.67	82	18
T2S2P0A60B30QHD75	60	30	0.035	2	75	2.5	45	55
T2S2P0A60B30QHD100	60	30	0.035	2	100	3.33	37	63
T2S2P0A60B30QHD150	60	30	0.035	2	150	5.00	23	77
T2S2P0A60B30QHD200	60	30	0.035	2	200	6.67	29	71
T2S2P0A60B30QHD275	60	30	0.035	2	275	9.17	27	73
T2S2P0A60B30QHD300	60	30	0.035	2	300	10.00	26	74
T2S2P0A60B30QHD325	60	30	0.035	2	325	10.83	22	78
T2S2P0A60B30QHD350	60	30	0.035	2	350	11.67	27	73
T2S2P0A60B40QHD25	60	40	0.035	2	25	0.63	100	0
T2S2P0A60B40QHD50	60	40	0.035	2	50	1.25	92	8
T2S2P0A60B40QHD75	60	40	0.035	2	75	1.88	49	51
T2S2P0A60B40QHD100	60	40	0.035	2	100	2.50	42	58
T2S2P0A60B40QHD150	60	40	0.035	2	150	3.75	34	66
T2S2P0A60B40QHD200	60	40	0.035	2	200	5.00	47	53
T2S2P0A60B40QHD275	60	40	0.035	2	275	6.88	29	71
T2S2P0A60B40QHD300	60	40	0.035	2	300	7.50	40	60
T2S2P0A60B40QHD325	60	40	0.035	2	325	8.13	43	57
T2S2P0A60B40QHD350	60	40	0.035	2	350	8.75	24	76
T2S2P0A60B50QHD25	60	50	0.035	2	25	0.50	100	0
T2S2P0A60B50QHD50	60	50	0.035	2	50	1.00	100	0
T2S2P0A60B50QHD75	60	50	0.035	2	75	1.5	79	21
T2S2P0A60B50QHD100	60	50	0.035	2	100	2.00	62	38
T2S2P0A60B50QHD150	60	50	0.035	2	150	3.00	48	52
T2S2P0A60B50QHD200	60	50	0.035	2	200	4.00	51	49
T2S2P0A60B50QHD275	60	50	0.035	2	275	5.5	45	55
T2S2P0A60B50QHD300	60	50	0.035	2	300	6.00	46	54
T2S2P0A60B50QHD325	60	50	0.035	2	325	6.50	32	68
T2S2P0A60B50QHD350	60	50	0.035	2	350	7.00	40	60
T2S2P0A60B60QHD25	60	60	0.035	2	25	0.42	100	0
T2S2P0A60B60QHD50	60	60	0.035	2	50	0.83	100	0
T2S2P0A60B60QHD75	60	60	0.035	2	75	1.25	89	11
T2S2P0A60B60QHD100	60	60	0.035	2	100	1.67	70	30
T2S2P0A60B60QHD150	60	60	0.035	2	150	2.50	53	47
T2S2P0A60B60QHD200	60	60	0.035	2	200	3.33	45	55
T2S2P0A60B60QHD275	60	60	0.035	2	275	4.58	44	56

Run ID	Rack Angle (Degrees)	Bar Spacing (mm))	Discharge (m^3/s)	Slope	Debris Length (mm)	Ratio of debris Length to bar spacing	Passed Through	Blocked
T2S2P0A60B60QHD300	60	60	0.035	2	300	5.00	41	59
T2S2P0A60B60QHD325	60	60	0.035	2	325	5.42	49	51
T2S2P0A60B60QHD350	60	60	0.035	2	350	5.83	42	58
T2S2P0A60B80QHD25	60	80	0.035	2	25	0.31	100	0
T2S2P0A60B80QHD50	60	80	0.035	2	50	0.63	97	3
T2S2P0A60B80QHD75	60	80	0.035	2	75	0.94	100	0
T2S2P0A60B80QHD100	60	80	0.035	2	100	1.25	85	15
T2S2P0A60B80QHD150	60	80	0.035	2	150	1.88	74	26
T2S2P0A60B80QHD200	60	80	0.035	2	200	2.50	54	46
T2S2P0A60B80QHD275	60	80	0.035	2	275	3.44	59	41
T2S2P0A60B80QHD300	60	80	0.035	2	300	3.75	54	46
T2S2P0A60B80QHD325	60	80	0.035	2	325	4.06	47	53
T2S2P0A60B80QHD350	60	80	0.035	2	350	4.38	55	45
T2S2P0A60B100QHD25	60	100	0.035	2	25	0.25	100	0
T2S2P0A60B100QHD50	60	100	0.035	2	50	0.50	100	0
T2S2P0A60B100QHD75	60	100	0.035	2	75	0.75	100	0
T2S2P0A60B100QHD100	60	100	0.035	2	100	1.00	99	1
T2S2P0A60B100QHD150	60	100	0.035	2	150	1.5	76	24
T2S2P0A60B100QHD200	60	100	0.035	2	200	2.00	64	36
T2S2P0A60B100QHD275	60	100	0.035	2	275	2.75	60	40
T2S2P0A60B100QHD300	60	100	0.035	2	300	3.00	62	38
T2S2P0A60B100QHD325	60	100	0.035	2	325	3.25	48	52
T2S2P0A60B100QHD350	60	100	0.035	2	350	3.50	49	51
T2S2P0A60B150QHD25	60	150	0.035	2	25	0.17	100	0
T2S2P0A60B150QHD50	60	150	0.035	2	50	0.33	100	0
T2S2P0A60B150QHD75	60	150	0.035	2	75	0.50	100	0
T2S2P0A60B150QHD100	60	150	0.035	2	100	0.67	100	0
T2S2P0A60B150QHD150	60	150	0.035	2	150	1.00	100	0
T2S2P0A60B150QHD200	60	150	0.035	2	200	1.33	83	17
T2S2P0A60B150QHD275	60	150	0.035	2	275	1.83	60	40
T2S2P0A60B150QHD300	60	150	0.035	2	300	2.00	56	44
T2S2P0A60B150QHD325	60	150	0.035	2	325	2.17	62	38
T2S2P0A60B150QHD350	60	150	0.035	2	350	2.33	59	41
T2S3P0A30B30QHD25	30	30	0.035	3	25	0.83	98	2
T2S3P0A30B30QHD50	30	30	0.035	3	50	1.67	54	46
T2S3P0A30B30QHD75	30	30	0.035	3	75	2.50	48	52

Run ID	Rack Angle (Degrees)	Bar Spacing (mm))	Discharge (m^3/s)	Slope	Debris Length (mm)	Ratio of debris Length to bar spacing	Passed Through	Blocked
T2S3P0A30B30QHD100	30	30	0.035	3	100	3.33	26	74
T2S3P0A30B30QHD150	30	30	0.035	3	150	5.00	19	81
T2S3P0A30B30QHD200	30	30	0.035	3	200	6.67	13	87
T2S3P0A30B30QHD275	30	30	0.035	3	275	9.17	16	84
T2S3P0A30B30QHD300	30	30	0.035	3	300	10.00	14	86
T2S3P0A30B30QHD325	30	30	0.035	3	325	10.83	14	86
T2S3P0A30B30QHD350	30	30	0.035	3	350	11.67	14	86
T2S3P0A30B40QHD25	30	40	0.035	3	25	0.63	90	10
T2S3P0A30B40QHD50	30	40	0.035	3	50	1.25	80	20
T2S3P0A30B40QHD75	30	40	0.035	3	75	1.88	30	70
T2S3P0A30B40QHD100	30	40	0.035	3	100	2.50	31	69
T2S3P0A30B40QHD150	30	40	0.035	3	150	3.75	25	75
T2S3P0A30B40QHD200	30	40	0.035	3	200	5.00	18	82
T2S3P0A30B40QHD275	30	40	0.035	3	275	6.88	21	79
T2S3P0A30B40QHD300	30	40	0.035	3	300	7.50	17	83
T2S3P0A30B40QHD325	30	40	0.035	3	325	8.13	17	83
T2S3P0A30B40QHD350	30	40	0.035	3	350	8.75	16	84
T2S3P0A30B50QHD25	30	50	0.035	3	25	0.50	99	1
T2S3P0A30B50QHD50	30	50	0.035	3	50	1.00	95	5
T2S3P0A30B50QHD75	30	50	0.035	3	75	1.50	62	38
T2S3P0A30B50QHD100	30	50	0.035	3	100	2.00	35	65
T2S3P0A30B50QHD150	30	50	0.035	3	150	3.00	34	66
T2S3P0A30B50QHD200	30	50	0.035	3	200	4.00	28	72
T2S3P0A30B50QHD275	30	50	0.035	3	275	5.50	22	78
T2S3P0A30B50QHD300	30	50	0.035	3	300	6.00	20	80
T2S3P0A30B50QHD325	30	50	0.035	3	325	6.50	20	80
T2S3P0A30B50QHD350	30	50	0.035	3	350	7.00	21	79
T2S3P0A30B60QHD25	30	60	0.035	3	25	0.42	100	0
T2S3P0A30B60QHD50	30	60	0.035	3	50	0.83	99	1
T2S3P0A30B60QHD75	30	60	0.035	3	75	1.25	70	30
T2S3P0A30B60QHD100	30	60	0.035	3	100	1.67	50	50
T2S3P0A30B60QHD150	30	60	0.035	3	150	2.50	44	56
T2S3P0A30B60QHD200	30	60	0.035	3	200	3.33	33	67
T2S3P0A30B60QHD275	30	60	0.035	3	275	4.58	34	66
T2S3P0A30B60QHD300	30	60	0.035	3	300	5.00	31	69
T2S3P0A30B60QHD325	30	60	0.035	3	325	5.42	20	80

Run ID	Rack Angle (Degrees)	Bar Spacing (mm))	Discharge (m^3/s)	Slope	Debris Length (mm)	Ratio of debris Length to bar spacing	Passed Through	Blocked
T2S3P0A30B60QHD350	30	60	0.035	3	350	5.83	19	81
T2S3P0A30B80QHD25	30	80	0.035	3	25	0.31	100	0
T2S3P0A30B80QHD50	30	80	0.035	3	50	0.63	98	2
T2S3P0A30B80QHD75	30	80	0.035	3	75	0.94	97	3
T2S3P0A30B80QHD100	30	80	0.035	3	100	1.25	58	42
T2S3P0A30B80QHD150	30	80	0.035	3	150	1.88	51	49
T2S3P0A30B80QHD200	30	80	0.035	3	200	2.50	40	60
T2S3P0A30B80QHD275	30	80	0.035	3	275	3.44	33	67
T2S3P0A30B80QHD300	30	80	0.035	3	300	3.75	35	65
T2S3P0A30B80QHD325	30	80	0.035	3	325	4.06	38	62
T2S3P0A30B80QHD350	30	80	0.035	3	350	4.38	30	70
T2S3P0A30B100QHD25	30	100	0.035	3	25	0.25	100	0
T2S3P0A30B100QHD50	30	100	0.035	3	50	0.50	100	0
T2S3P0A30B100QHD75	30	100	0.035	3	75	0.75	98	2
T2S3P0A30B100QHD100	30	100	0.035	3	100	1.00	92	8
T2S3P0A30B100QHD150	30	100	0.035	3	150	1.50	60	40
T2S3P0A30B100QHD200	30	100	0.035	3	200	2.00	49	51
T2S3P0A30B100QHD275	30	100	0.035	3	275	2.75	47	53
T2S3P0A30B100QHD300	30	100	0.035	3	300	3.00	45	55
T2S3P0A30B100QHD325	30	100	0.035	3	325	3.25	40	60
T2S3P0A30B100QHD350	30	100	0.035	3	350	3.50	41	59
T2S3P0A30B150QHD25	30	150	0.035	3	25	0.17	100	0
T2S3P0A30B150QHD50	30	150	0.035	3	50	0.33	99	1
T2S3P0A30B150QHD75	30	150	0.035	3	75	0.50	95	5
T2S3P0A30B150QHD100	30	150	0.035	3	100	0.67	93	7
T2S3P0A30B150QHD150	30	150	0.035	3	150	1.00	91	9
T2S3P0A30B150QHD200	30	150	0.035	3	200	1.33	75	25
T2S3P0A30B150QHD275	30	150	0.035	3	275	1.83	50	50
T2S3P0A30B150QHD300	30	150	0.035	3	300	2.00	45	55
T2S3P0A30B150QHD325	30	150	0.035	3	325	2.17	45	55
T2S3P0A30B150QHD350	30	150	0.035	3	350	2.33	48	52
T2S3P0A45B30QHD25	45	30	0.035	3	25	0.83	97	3
T2S3P0A45B30QHD50	45	30	0.035	3	50	1.67	61	39
T2S3P0A45B30QHD75	45	30	0.035	3	75	2.50	51	49
T2S3P0A45B30QHD100	45	30	0.035	3	100	3.33	32	68
T2S3P0A45B30QHD150	45	30	0.035	3	150	5.00	20	80

Run ID	Rack Angle (Degrees)	Bar Spacing (mm))	Discharge (m^3/s)	Slope	Debris Length (mm)	Ratio of debris Length to bar spacing	Passed Through	Blocked
T2S3P0A45B30QHD200	45	30	0.035	3	200	6.67	17	83
T2S3P0A45B30QHD275	45	30	0.035	3	275	9.17	19	81
T2S3P0A45B30QHD300	45	30	0.035	3	300	10.00	17	83
T2S3P0A45B30QHD325	45	30	0.035	3	325	10.83	15	85
T2S3P0A45B30QHD350	45	30	0.035	3	350	11.67	15	85
T2S3P0A45B40QHD25	45	40	0.035	3	25	0.63	94	6
T2S3P0A45B40QHD50	45	40	0.035	3	50	1.25	85	15
T2S3P0A45B40QHD75	45	40	0.035	3	75	1.88	32	68
T2S3P0A45B40QHD100	45	40	0.035	3	100	2.50	33	67
T2S3P0A45B40QHD150	45	40	0.035	3	150	3.75	26	74
T2S3P0A45B40QHD200	45	40	0.035	3	200	5.00	19	81
T2S3P0A45B40QHD275	45	40	0.035	3	275	6.88	22	78
T2S3P0A45B40QHD300	45	40	0.035	3	300	7.50	19	81
T2S3P0A45B40QHD325	45	40	0.035	3	325	8.13	16	84
T2S3P0A45B40QHD350	45	40	0.035	3	350	8.75	15	85
T2S3P0A45B50QHD25	45	50	0.035	3	25	0.50	98	2
T2S3P0A45B50QHD50	45	50	0.035	3	50	1.00	91	9
T2S3P0A45B50QHD75	45	50	0.035	3	75	1.50	66	34
T2S3P0A45B50QHD100	45	50	0.035	3	100	2.00	41	59
T2S3P0A45B50QHD150	45	50	0.035	3	150	3.00	35	65
T2S3P0A45B50QHD200	45	50	0.035	3	200	4.00	29	71
T2S3P0A45B50QHD275	45	50	0.035	3	275	5.50	24	76
T2S3P0A45B50QHD300	45	50	0.035	3	300	6.00	18	82
T2S3P0A45B50QHD325	45	50	0.035	3	325	6.50	18	82
T2S3P0A45B50QHD350	45	50	0.035	3	350	7.00	17	83
T2S3P0A45B60QHD25	45	60	0.035	3	25	0.42	100	0
T2S3P0A45B60QHD50	45	60	0.035	3	50	0.83	97	3
T2S3P0A45B60QHD75	45	60	0.035	3	75	1.25	76	24
T2S3P0A45B60QHD100	45	60	0.035	3	100	1.67	47	53
T2S3P0A45B60QHD150	45	60	0.035	3	150	2.50	42	58
T2S3P0A45B60QHD200	45	60	0.035	3	200	3.33	32	68
T2S3P0A45B60QHD275	45	60	0.035	3	275	4.58	35	65
T2S3P0A45B60QHD300	45	60	0.035	3	300	5.00	27	73
T2S3P0A45B60QHD325	45	60	0.035	3	325	5.42	18	82
T2S3P0A45B60QHD350	45	60	0.035	3	350	5.83	18	82
T2S3P0A45B80QHD25	45	80	0.035	3	25	0.31	100	0

Run ID	Rack Angle (Degrees)	Bar Spacing (mm))	Discharge (m^3/s)	Slope	Debris Length (mm)	Ratio of debris Length to bar spacing	Passed Through	Blocked
T2S3P0A45B80QHD50	45	80	0.035	3	50	0.63	98	2
T2S3P0A45B80QHD75	45	80	0.035	3	75	0.94	92	8
T2S3P0A45B80QHD100	45	80	0.035	3	100	1.25	60	40
T2S3P0A45B80QHD150	45	80	0.035	3	150	1.88	51	49
T2S3P0A45B80QHD200	45	80	0.035	3	200	2.50	40	60
T2S3P0A45B80QHD275	45	80	0.035	3	275	3.44	30	70
T2S3P0A45B80QHD300	45	80	0.035	3	300	3.75	35	65
T2S3P0A45B80QHD325	45	80	0.035	3	325	4.06	39	61
T2S3P0A45B80QHD350	45	80	0.035	3	350	4.38	35	65
T2S3P0A45B100QHD25	45	100	0.035	3	25	0.25	100	0
T2S3P0A45B100QHD50	45	100	0.035	3	50	0.50	100	0
T2S3P0A45B100QHD75	45	100	0.035	3	75	0.75	98	2
T2S3P0A45B100QHD100	45	100	0.035	3	100	1.00	95	5
T2S3P0A45B100QHD150	45	100	0.035	3	150	1.50	69	31
T2S3P0A45B100QHD200	45	100	0.035	3	200	2.00	44	56
T2S3P0A45B100QHD275	45	100	0.035	3	275	2.75	34	66
T2S3P0A45B100QHD300	45	100	0.035	3	300	3.00	40	60
T2S3P0A45B100QHD325	45	100	0.035	3	325	3.25	36	64
T2S3P0A45B100QHD350	45	100	0.035	3	350	3.50	35	65
T2S3P0A45B150QHD25	45	150	0.035	3	25	0.17	100	0
T2S3P0A45B150QHD50	45	150	0.035	3	50	0.33	100	0
T2S3P0A45B150QHD75	45	150	0.035	3	75	0.50	100	0
T2S3P0A45B150QHD100	45	150	0.035	3	100	0.67	96	4
T2S3P0A45B150QHD150	45	150	0.035	3	150	1.00	95	5
T2S3P0A45B150QHD200	45	150	0.035	3	200	1.33	85	15
T2S3P0A45B150QHD275	45	150	0.035	3	275	1.83	62	38
T2S3P0A45B150QHD300	45	150	0.035	3	300	2.00	61	39
T2S3P0A45B150QHD325	45	150	0.035	3	325	2.17	57	43
T2S3P0A45B150QHD350	45	150	0.035	3	350	2.33	58	42
T2S3P0A60B30QHD25	60	30	0.035	3	25	0.83	100	0
T2S3P0A60B30QHD50	60	30	0.035	3	50	1.67	65	35
T2S3P0A60B30QHD75	60	30	0.035	3	75	2.5	48	52
T2S3P0A60B30QHD100	60	30	0.035	3	100	3.33	36	64
T2S3P0A60B30QHD150	60	30	0.035	3	150	5	19	81
T2S3P0A60B30QHD200	60	30	0.035	3	200	6.67	17	83
T2S3P0A60B30QHD275	60	30	0.035	3	275	9.17	23	77

Appendix C

Run ID	Rack Angle (Degrees)	Bar Spacing (mm))	Discharge (m^3/s)	Slope	Debris Length (mm)	Ratio of debris Length to bar spacing	Passed Through	Blocked
T2S3P0A60B30QHD300	60	30	0.035	3	300	10.00	19	81
T2S3P0A60B30QHD325	60	30	0.035	3	325	10.83	24	76
T2S3P0A60B30QHD350	60	30	0.035	3	350	11.67	17	83
T2S3P0A60B40QHD25	60	40	0.035	3	25	0.63	100	0
T2S3P0A60B40QHD50	60	40	0.035	3	50	1.25	86	14
T2S3P0A60B40QHD75	60	40	0.035	3	75	1.88	55	45
T2S3P0A60B40QHD100	60	40	0.035	3	100	2.5	51	49
T2S3P0A60B40QHD150	60	40	0.035	3	150	3.75	34	66
T2S3P0A60B40QHD200	60	40	0.035	3	200	5	31	69
T2S3P0A60B40QHD275	60	40	0.035	3	275	6.88	26	74
T2S3P0A60B40QHD300	60	40	0.035	3	300	7.50	24	76
T2S3P0A60B40QHD325	60	40	0.035	3	325	8.13	18	82
T2S3P0A60B40QHD350	60	40	0.035	3	350	8.75	30	70
T2S3P0A60B50QHD25	60	50	0.035	3	25	0.5	100	0
T2S3P0A60B50QHD50	60	50	0.035	3	50	1	98	2
T2S3P0A60B50QHD75	60	50	0.035	3	75	1.5	87	13
T2S3P0A60B50QHD100	60	50	0.035	3	100	2	58	42
T2S3P0A60B50QHD150	60	50	0.035	3	150	3	48	52
T2S3P0A60B50QHD200	60	50	0.035	3	200	4	36	64
T2S3P0A60B50QHD275	60	50	0.035	3	275	5.5	37	63
T2S3P0A60B50QHD300	60	50	0.035	3	300	6.00	31	69
T2S3P0A60B50QHD325	60	50	0.035	3	325	6.50	34	66
T2S3P0A60B50QHD350	60	50	0.035	3	350	7	28	72
T2S3P0A60B60QHD25	60	60	0.035	3	25	0.42	100	0
T2S3P0A60B60QHD50	60	60	0.035	3	50	0.83	100	0
T2S3P0A60B60QHD75	60	60	0.035	3	75	1.25	81	19
T2S3P0A60B60QHD100	60	60	0.035	3	100	1.67	74	26
T2S3P0A60B60QHD150	60	60	0.035	3	150	2.5	45	55
T2S3P0A60B60QHD200	60	60	0.035	3	200	3.33	45	55
T2S3P0A60B60QHD275	60	60	0.035	3	275	4.58	38	62
T2S3P0A60B60QHD300	60	60	0.035	3	300	5.00	36	64
T2S3P0A60B60QHD325	60	60	0.035	3	325	5.42	42	58
T2S3P0A60B60QHD350	60	60	0.035	3	350	5.83	34	66
T2S3P0A60B80QHD25	60	80	0.035	3	25	0.31	100	0
T2S3P0A60B80QHD50	60	80	0.035	3	50	0.63	100	0
T2S3P0A60B80QHD75	60	80	0.035	3	75	0.94	96	4

Run ID	Rack Angle (Degrees)	Bar Spacing (mm))	Discharge (m^3/s)	Slope	Debris Length (mm)	Ratio of debris Length to bar spacing	Passed Through	Blocked
T2S3P0A60B80QHD100	60	80	0.035	3	100	1.25	92	8
T2S3P0A60B80QHD150	60	80	0.035	3	150	1.88	56	44
T2S3P0A60B80QHD200	60	80	0.035	3	200	2.5	53	47
T2S3P0A60B80QHD275	60	80	0.035	3	275	3.44	50	50
T2S3P0A60B80QHD300	60	80	0.035	3	300	3.75	37	63
T2S3P0A60B80QHD325	60	80	0.035	3	325	4.06	42	58
T2S3P0A60B80QHD350	60	80	0.035	3	350	4.38	32	68
T2S3P0A60B100QHD25	60	100	0.035	3	25	0.25	100	0
T2S3P0A60B100QHD50	60	100	0.035	3	50	0.5	100	0
T2S3P0A60B100QHD75	60	100	0.035	3	75	0.75	100	0
T2S3P0A60B100QHD100	60	100	0.035	3	100	1	98	2
T2S3P0A60B100QHD150	60	100	0.035	3	150	1.5	82	18
T2S3P0A60B100QHD200	60	100	0.035	3	200	2	57	43
T2S3P0A60B100QHD275	60	100	0.035	3	275	2.75	60	40
T2S3P0A60B100QHD300	60	100	0.035	3	300	3.00	44	56
T2S3P0A60B100QHD325	60	100	0.035	3	325	3.25	41	59
T2S3P0A60B100QHD350	60	100	0.035	3	350	3.5	43	57
T2S3P0A60B150QHD25	60	150	0.035	3	25	0.17	100	0
T2S3P0A60B150QHD50	60	150	0.035	3	50	0.33	100	0
T2S3P0A60B150QHD75	60	150	0.035	3	75	0.5	100	0
T2S3P0A60B150QHD100	60	150	0.035	3	100	0.67	100	0
T2S3P0A60B150QHD150	60	150	0.035	3	150	1	100	0
T2S3P0A60B150QHD200	60	150	0.035	3	200	1.33	86	14
T2S3P0A60B150QHD275	60	150	0.035	3	275	1.83	64	36
T2S3P0A60B150QHD300	60	150	0.035	3	300	2.00	70	30
T2S3P0A60B150QHD325	60	150	0.035	3	325	2.17	70	30
T2S3P0A60B150QHD350	60	150	0.035	3	350	2.33	47	53

Appendix D – Results from Test Phase 3

Table D.1 Results from screen position testing part 1

Run ID	Rack Angle (Degrees)	Bar Spacing (mm)	Discharge (m^3/s)	Screen Pos.	Debris Length (mm)	Ratio of debris length to bar spacing	Passed Through	Blocked
T3S1P1A60B30QHD025	60	30	0.035	1	25	0.83	100	0
T3S1P1A60B30QHD050	60	30	0.035	1	50	1.67	35	65
T3S1P1A60B30QHD075	60	30	0.035	1	75	2.50	24	76
T3S1P1A60B30QHD100	60	30	0.035	1	100	3.33	25	75
T3S1P1A60B30QHD150	60	30	0.035	1	150	5.00	13	87
T3S1P1A60B30QHD200	60	30	0.035	1	200	6.67	15	85
T3S1P1A60B30QHD275	60	30	0.035	1	275	9.17	11	89
T3S1P1A60B30QHD300	60	30	0.035	1	300	10.00	10	90
T3S1P1A60B30QHD325	60	30	0.035	1	325	10.83	11	89
T3S1P1A60B30QHD350	60	30	0.035	1	350	11.67	12	88
T3S1P1A60B40QHD025	60	40	0.035	1	25	0.63	96	4
T3S1P1A60B40QHD050	60	40	0.035	1	50	1.25	70	30
T3S1P1A60B40QHD075	60	40	0.035	1	75	1.88	38	62
T3S1P1A60B40QHD100	60	40	0.035	1	100	2.50	25	75
T3S1P1A60B40QHD150	60	40	0.035	1	150	3.75	20	80
T3S1P1A60B40QHD200	60	40	0.035	1	200	5.00	17	83
T3S1P1A60B40QHD275	60	40	0.035	1	275	6.88	16	84
T3S1P1A60B40QHD300	60	40	0.035	1	300	7.50	17	83
T3S1P1A60B40QHD325	60	40	0.035	1	325	8.13	15	85
T3S1P1A60B40QHD350	60	40	0.035	1	350	8.75	13	87
T3S1P1A60B50QHD025	60	50	0.035	1	25	0.50	97	3
T3S1P1A60B50QHD050	60	50	0.035	1	50	1.00	95	5
T3S1P1A60B50QHD075	60	50	0.035	1	75	1.50	43	57
T3S1P1A60B50QHD100	60	50	0.035	1	100	2.00	37	63
T3S1P1A60B50QHD150	60	50	0.035	1	150	3.00	30	70
T3S1P1A60B50QHD200	60	50	0.035	1	200	4.00	23	77
T3S1P1A60B50QHD275	60	50	0.035	1	275	5.50	19	81
T3S1P1A60B50QHD300	60	50	0.035	1	300	6.00	16	84
T3S1P1A60B50QHD325	60	50	0.035	1	325	6.50	16	84
T3S1P1A60B50QHD350	60	50	0.035	1	350	7.00	14	86

Appendix D

Run ID	Rack Angle (Degrees)	Bar Spacing (mm)	Discharge (m^3/s)	Screen Pos.	Debris Length (mm)	Ratio of debris length to bar spacing	Passed Through	Blocked
T3S1P1A60B60QHD025	60	60	0.035	1	25	0.42	92	8
T3S1P1A60B60QHD050	60	60	0.035	1	50	0.83	99	1
T3S1P1A60B60QHD075	60	60	0.035	1	75	1.25	84	16
T3S1P1A60B60QHD100	60	60	0.035	1	100	1.67	45	55
T3S1P1A60B60QHD150	60	60	0.035	1	150	2.50	25	75
T3S1P1A60B60QHD200	60	60	0.035	1	200	3.33	28	72
T3S1P1A60B60QHD275	60	60	0.035	1	275	4.58	15	85
T3S1P1A60B60QHD300	60	60	0.035	1	300	5.00	28	72
T3S1P1A60B60QHD325	60	60	0.035	1	325	5.42	31	69
T3S1P1A60B60QHD350	60	60	0.035	1	350	5.83	24	76
T3S1P1A60B80QHD025	60	80	0.035	1	25	0.31	96	4
T3S1P1A60B80QHD050	60	80	0.035	1	50	0.63	96	4
T3S1P1A60B80QHD075	60	80	0.035	1	75	0.94	89	11
T3S1P1A60B80QHD100	60	80	0.035	1	100	1.25	70	30
T3S1P1A60B80QHD150	60	80	0.035	1	150	1.88	35	65
T3S1P1A60B80QHD200	60	80	0.035	1	200	2.50	30	70
T3S1P1A60B80QHD275	60	80	0.035	1	275	3.44	22	78
T3S1P1A60B80QHD300	60	80	0.035	1	300	3.75	21	79
T3S1P1A60B80QHD325	60	80	0.035	1	325	4.06	25	75
T3S1P1A60B80QHD350	60	80	0.035	1	350	4.38	29	71
T3S1P1A60B100QHD025	60	100	0.035	1	25	0.25	98	2
T3S1P1A60B100QHD050	60	100	0.035	1	50	0.50	90	10
T3S1P1A60B100QHD075	60	100	0.035	1	75	0.75	94	6
T3S1P1A60B100QHD100	60	100	0.035	1	100	1.00	81	19
T3S1P1A60B100QHD150	60	100	0.035	1	150	1.50	41	59
T3S1P1A60B100QHD200	60	100	0.035	1	200	2.00	37	63
T3S1P1A60B100QHD275	60	100	0.035	1	275	2.75	16	84
T3S1P1A60B100QHD300	60	100	0.035	1	300	3.00	20	80
T3S1P1A60B100QHD325	60	100	0.035	1	325	3.25	27	73
T3S1P1A60B100QHD350	60	100	0.035	1	350	3.50	33	67
T3S1P1A60B150QHD025	60	150	0.035	1	25	0.17	100	0
T3S1P1A60B150QHD050	60	150	0.035	1	50	0.33	100	0
T3S1P1A60B150QHD075	60	150	0.035	1	75	0.50	98	2

Appendix D

Run ID	Rack Angle (Degrees)	Bar Spacing (mm)	Discharge (m^3/s)	Screen Pos.	Debris Length (mm)	Ratio of debris length to bar spacing	Passed Through	Blocked
T3S1P1A60B150QHD100	60	150	0.035	1	100	0.67	98	2
T3S1P1A60B150QHD150	60	150	0.035	1	150	1.00	85	15
T3S1P1A60B150QHD200	60	150	0.035	1	200	1.33	69	31
T3S1P1A60B150QHD275	60	150	0.035	1	275	1.83	42	58
T3S1P1A60B150QHD300	60	150	0.035	1	300	2.00	26	74
T3S1P1A60B150QHD325	60	150	0.035	1	325	2.17	28	72
T3S1P1A60B150QHD350	60	150	0.035	1	350	2.33	29	71
T3S1P2A60B30QHD025	60	30	0.035	2	25	0.83	100	0
T3S1P2A60B30QHD050	60	30	0.035	2	50	1.67	49	51
T3S1P2A60B30QHD075	60	30	0.035	2	75	2.50	35	65
T3S1P2A60B30QHD100	60	30	0.035	2	100	3.33	23	77
T3S1P2A60B30QHD150	60	30	0.035	2	150	5.00	18	82
T3S1P2A60B30QHD200	60	30	0.035	2	200	6.67	23	77
T3S1P2A60B30QHD275	60	30	0.035	2	275	9.17	12	88
T3S1P2A60B30QHD300	60	30	0.035	2	300	10.00	9	91
T3S1P2A60B30QHD325	60	30	0.035	2	325	10.83	15	85
T3S1P2A60B30QHD350	60	30	0.035	2	350	11.67	9	91
T3S1P2A60B40QHD025	60	40	0.035	2	25	0.63	100	0
T3S1P2A60B40QHD050	60	40	0.035	2	50	1.25	87	13
T3S1P2A60B40QHD075	60	40	0.035	2	75	1.88	42	58
T3S1P2A60B40QHD100	60	40	0.035	2	100	2.50	32	68
T3S1P2A60B40QHD150	60	40	0.035	2	150	3.75	27	73
T3S1P2A60B40QHD200	60	40	0.035	2	200	5.00	23	77
T3S1P2A60B40QHD275	60	40	0.035	2	275	6.88	25	75
T3S1P2A60B40QHD300	60	40	0.035	2	300	7.50	19	81
T3S1P2A60B40QHD325	60	40	0.035	2	325	8.13	22	78
T3S1P2A60B40QHD350	60	40	0.035	2	350	8.75	20	80
T3S1P2A60B50QHD025	60	50	0.035	2	25	0.50	98	2
T3S1P2A60B50QHD050	60	50	0.035	2	50	1.00	93	7
T3S1P2A60B50QHD075	60	50	0.035	2	75	1.50	54	46
T3S1P2A60B50QHD100	60	50	0.035	2	100	2.00	35	65
T3S1P2A60B50QHD150	60	50	0.035	2	150	3.00	26	74
T3S1P2A60B50QHD200	60	50	0.035	2	200	4.00	22	78

Run ID	Rack Angle (Degrees)	Bar Spacing (mm)	Discharge (m^3/s)	Screen Pos.	Debris Length (mm)	Ratio of debris length to bar spacing	Passed Through	Blocked
T3S1P2A60B50QHD275	60	50	0.035	2	275	5.50	21	79
T3S1P2A60B50QHD300	60	50	0.035	2	300	6.00	21	79
T3S1P2A60B50QHD325	60	50	0.035	2	325	6.50	17	83
T3S1P2A60B50QHD350	60	50	0.035	2	350	7.00	19	81
T3S1P2A60B60QHD025	60	60	0.035	2	25	0.42	99	1
T3S1P2A60B60QHD050	60	60	0.035	2	50	0.83	91	9
T3S1P2A60B60QHD075	60	60	0.035	2	75	1.25	82	18
T3S1P2A60B60QHD100	60	60	0.035	2	100	1.67	53	47
T3S1P2A60B60QHD150	60	60	0.035	2	150	2.50	29	71
T3S1P2A60B60QHD200	60	60	0.035	2	200	3.33	31	69
T3S1P2A60B60QHD275	60	60	0.035	2	275	4.58	23	77
T3S1P2A60B60QHD300	60	60	0.035	2	300	5.00	24	76
T3S1P2A60B60QHD325	60	60	0.035	2	325	5.42	28	72
T3S1P2A60B60QHD350	60	60	0.035	2	350	5.83	15	85
T3S1P2A60B80QHD025	60	80	0.035	2	25	0.31	98	2
T3S1P2A60B80QHD050	60	80	0.035	2	50	0.63	94	6
T3S1P2A60B80QHD075	60	80	0.035	2	75	0.94	90	10
T3S1P2A60B80QHD100	60	80	0.035	2	100	1.25	72	28
T3S1P2A60B80QHD150	60	80	0.035	2	150	1.88	41	59
T3S1P2A60B80QHD200	60	80	0.035	2	200	2.50	30	70
T3S1P2A60B80QHD275	60	80	0.035	2	275	3.44	31	69
T3S1P2A60B80QHD300	60	80	0.035	2	300	3.75	32	68
T3S1P2A60B80QHD325	60	80	0.035	2	325	4.06	29	71
T3S1P2A60B80QHD350	60	80	0.035	2	350	4.38	28	72
T3S1P2A60B100QHD025	60	100	0.035	2	25	0.25	100	0
T3S1P2A60B100QHD050	60	100	0.035	2	50	0.50	97	3
T3S1P2A60B100QHD075	60	100	0.035	2	75	0.75	92	8
T3S1P2A60B100QHD100	60	100	0.035	2	100	1.00	93	7
T3S1P2A60B100QHD150	60	100	0.035	2	150	1.50	58	42
T3S1P2A60B100QHD200	60	100	0.035	2	200	2.00	35	65
T3S1P2A60B100QHD275	60	100	0.035	2	275	2.75	35	65
T3S1P2A60B100QHD300	60	100	0.035	2	300	3.00	28	72
T3S1P2A60B100QHD325	60	100	0.035	2	325	3.25	30	70

Run ID	Rack Angle (Degrees)	Bar Spacing (mm)	Discharge (m^3/s)	Screen Pos.	Debris Length (mm)	Ratio of debris length to bar spacing	Passed Through	Blocked
T3S1P2A60B100QHD350	60	100	0.035	2	350	3.50	22	78
T3S1P2A60B150QHD025	60	150	0.035	2	25	0.17	100	0
T3S1P2A60B150QHD050	60	150	0.035	2	50	0.33	100	0
T3S1P2A60B150QHD075	60	150	0.035	2	75	0.50	96	4
T3S1P2A60B150QHD100	60	150	0.035	2	100	0.67	96	4
T3S1P2A60B150QHD150	60	150	0.035	2	150	1.00	94	6
T3S1P2A60B150QHD200	60	150	0.035	2	200	1.33	79	21
T3S1P2A60B150QHD275	60	150	0.035	2	275	1.83	57	43
T3S1P2A60B150QHD300	60	150	0.035	2	300	2.00	50	50
T3S1P2A60B150QHD325	60	150	0.035	2	325	2.17	57	43
T3S1P2A60B150QHD350	60	150	0.035	2	350	2.33	58	42
T3S1P3A60B30QHD025	60	30	0.035	3	25	0.83	99	1
T3S1P3A60B30QHD050	60	30	0.035	3	50	1.67	62	38
T3S1P3A60B30QHD075	60	30	0.035	3	75	2.50	40	60
T3S1P3A60B30QHD100	60	30	0.035	3	100	3.33	39	61
T3S1P3A60B30QHD150	60	30	0.035	3	150	5.00	23	77
T3S1P3A60B30QHD200	60	30	0.035	3	200	6.67	11	89
T3S1P3A60B30QHD275	60	30	0.035	3	275	9.17	15	85
T3S1P3A60B30QHD300	60	30	0.035	3	300	10.00	11	89
T3S1P3A60B30QHD325	60	30	0.035	3	325	10.83	27	73
T3S1P3A60B30QHD350	60	30	0.035	3	350	11.67	23	77
T3S1P3A60B40QHD025	60	40	0.035	3	25	0.63	98	2
T3S1P3A60B40QHD050	60	40	0.035	3	50	1.25	82	18
T3S1P3A60B40QHD075	60	40	0.035	3	75	1.88	48	52
T3S1P3A60B40QHD100	60	40	0.035	3	100	2.50	36	64
T3S1P3A60B40QHD150	60	40	0.035	3	150	3.75	28	72
T3S1P3A60B40QHD200	60	40	0.035	3	200	5.00	27	73
T3S1P3A60B40QHD275	60	40	0.035	3	275	6.88	23	77
T3S1P3A60B40QHD300	60	40	0.035	3	300	7.50	23	77
T3S1P3A60B40QHD325	60	40	0.035	3	325	8.13	17	83
T3S1P3A60B40QHD350	60	40	0.035	3	350	8.75	19	81
T3S1P3A60B50QHD025	60	50	0.035	3	25	0.50	99	1
T3S1P3A60B50QHD050	60	50	0.035	3	50	1.00	95	5

Run ID	Rack Angle (Degrees)	Bar Spacing (mm)	Discharge (m^3/s)	Screen Pos.	Debris Length (mm)	Ratio of debris length to bar spacing	Passed Through	Blocked
T3S1P3A60B50QHD075	60	50	0.035	3	75	1.50	72	28
T3S1P3A60B50QHD100	60	50	0.035	3	100	2.00	54	46
T3S1P3A60B50QHD150	60	50	0.035	3	150	3.00	34	66
T3S1P3A60B50QHD200	60	50	0.035	3	200	4.00	34	66
T3S1P3A60B50QHD275	60	50	0.035	3	275	5.50	23	77
T3S1P3A60B50QHD300	60	50	0.035	3	300	6.00	35	65
T3S1P3A60B50QHD325	60	50	0.035	3	325	6.50	27	73
T3S1P3A60B50QHD350	60	50	0.035	3	350	7.00	28	72
T3S1P3A60B60QHD025	60	60	0.035	3	25	0.42	99	1
T3S1P3A60B60QHD050	60	60	0.035	3	50	0.83	97	3
T3S1P3A60B60QHD075	60	60	0.035	3	75	1.25	77	23
T3S1P3A60B60QHD100	60	60	0.035	3	100	1.67	59	41
T3S1P3A60B60QHD150	60	60	0.035	3	150	2.50	42	58
T3S1P3A60B60QHD200	60	60	0.035	3	200	3.33	41	59
T3S1P3A60B60QHD275	60	60	0.035	3	275	4.58	25	75
T3S1P3A60B60QHD300	60	60	0.035	3	300	5.00	24	76
T3S1P3A60B60QHD325	60	60	0.035	3	325	5.42	28	72
T3S1P3A60B60QHD350	60	60	0.035	3	350	5.83	30	70
T3S1P3A60B80QHD025	60	80	0.035	3	25	0.31	100	0
T3S1P3A60B80QHD050	60	80	0.035	3	50	0.63	100	0
T3S1P3A60B80QHD075	60	80	0.035	3	75	0.94	97	3
T3S1P3A60B80QHD100	60	80	0.035	3	100	1.25	87	13
T3S1P3A60B80QHD150	60	80	0.035	3	150	1.88	55	45
T3S1P3A60B80QHD200	60	80	0.035	3	200	2.50	41	59
T3S1P3A60B80QHD275	60	80	0.035	3	275	3.44	40	60
T3S1P3A60B80QHD300	60	80	0.035	3	300	3.75	47	53
T3S1P3A60B80QHD325	60	80	0.035	3	325	4.06	51	49
T3S1P3A60B80QHD350	60	80	0.035	3	350	4.38	55	45
T3S1P3A60B100QHD025	60	100	0.035	3	25	0.25	100	0
T3S1P3A60B100QHD050	60	100	0.035	3	50	0.50	98	2
T3S1P3A60B100QHD075	60	100	0.035	3	75	0.75	97	3
T3S1P3A60B100QHD100	60	100	0.035	3	100	1.00	98	2
T3S1P3A60B100QHD150	60	100	0.035	3	150	1.50	73	27

Appendix D

Run ID	Rack Angle (Degrees)	Bar Spacing (mm)	Discharge (m^3/s)	Screen Pos.	Debris Length (mm)	Ratio of debris length to bar spacing	Passed Through	Blocked
T3S1P3A60B100QHD200	60	100	0.035	3	200	2.00	58	42
T3S1P3A60B100QHD275	60	100	0.035	3	275	2.75	37	63
T3S1P3A60B100QHD300	60	100	0.035	3	300	3.00	36	64
T3S1P3A60B100QHD325	60	100	0.035	3	325	3.25	43	57
T3S1P3A60B100QHD350	60	100	0.035	3	350	3.50	37	63
T3S1P3A60B150QHD025	60	150	0.035	3	25	0.17	100	0
T3S1P3A60B150QHD050	60	150	0.035	3	50	0.33	99	1
T3S1P3A60B150QHD075	60	150	0.035	3	75	0.50	97	3
T3S1P3A60B150QHD100	60	150	0.035	3	100	0.67	99	1
T3S1P3A60B150QHD150	60	150	0.035	3	150	1.00	98	2
T3S1P3A60B150QHD200	60	150	0.035	3	200	1.33	86	14
T3S1P3A60B150QHD275	60	150	0.035	3	275	1.83	52	48
T3S1P3A60B150QHD300	60	150	0.035	3	300	2.00	49	51
T3S1P3A60B150QHD325	60	150	0.035	3	325	2.17	53	47
T3S1P3A60B150QHD350	60	150	0.035	3	350	2.33	53	47
T3S1P4A60B30QHD025	60	30	0.035	4	25	0.83	99	1
T3S1P4A60B30QHD050	60	30	0.035	4	50	1.67	61	39
T3S1P4A60B30QHD075	60	30	0.035	4	75	2.50	54	46
T3S1P4A60B30QHD100	60	30	0.035	4	100	3.33	42	58
T3S1P4A60B30QHD150	60	30	0.035	4	150	5.00	25	75
T3S1P4A60B30QHD200	60	30	0.035	4	200	6.67	24	76
T3S1P4A60B30QHD275	60	30	0.035	4	275	9.17	35	65
T3S1P4A60B30QHD300	60	30	0.035	4	300	10.00	23	77
T3S1P4A60B30QHD325	60	30	0.035	4	325	10.83	31	69
T3S1P4A60B30QHD350	60	30	0.035	4	350	11.67	40	60
T3S1P4A60B40QHD025	60	40	0.035	4	25	0.63	98	2
T3S1P4A60B40QHD050	60	40	0.035	4	50	1.25	87	13
T3S1P4A60B40QHD075	60	40	0.035	4	75	1.88	57	43
T3S1P4A60B40QHD100	60	40	0.035	4	100	2.50	42	58
T3S1P4A60B40QHD150	60	40	0.035	4	150	3.75	42	58
T3S1P4A60B40QHD200	60	40	0.035	4	200	5.00	40	60
T3S1P4A60B40QHD275	60	40	0.035	4	275	6.88	39	61
T3S1P4A60B40QHD300	60	40	0.035	4	300	7.50	27	73

Run ID	Rack Angle (Degrees)	Bar Spacing (mm)	Discharge (m^3/s)	Screen Pos.	Debris Length (mm)	Ratio of debris length to bar spacing	Passed Through	Blocked
T3S1P4A60B40QHD325	60	40	0.035	4	325	8.13	31	69
T3S1P4A60B40QHD350	60	40	0.035	4	350	8.75	35	65
T3S1P4A60B50QHD025	60	50	0.035	4	25	0.50	100	0
T3S1P4A60B50QHD050	60	50	0.035	4	50	1.00	95	5
T3S1P4A60B50QHD075	60	50	0.035	4	75	1.50	73	27
T3S1P4A60B50QHD100	60	50	0.035	4	100	2.00	64	36
T3S1P4A60B50QHD150	60	50	0.035	4	150	3.00	49	51
T3S1P4A60B50QHD200	60	50	0.035	4	200	4.00	45	55
T3S1P4A60B50QHD275	60	50	0.035	4	275	5.50	44	56
T3S1P4A60B50QHD300	60	50	0.035	4	300	6.00	34	66
T3S1P4A60B50QHD325	60	50	0.035	4	325	6.50	33	67
T3S1P4A60B50QHD350	60	50	0.035	4	350	7.00	48	52
T3S1P4A60B60QHD025	60	60	0.035	4	25	0.42	100	0
T3S1P4A60B60QHD050	60	60	0.035	4	50	0.83	98	2
T3S1P4A60B60QHD075	60	60	0.035	4	75	1.25	86	14
T3S1P4A60B60QHD100	60	60	0.035	4	100	1.67	65	35
T3S1P4A60B60QHD150	60	60	0.035	4	150	2.50	55	45
T3S1P4A60B60QHD200	60	60	0.035	4	200	3.33	50	50
T3S1P4A60B60QHD275	60	60	0.035	4	275	4.58	47	53
T3S1P4A60B60QHD300	60	60	0.035	4	300	5.00	39	61
T3S1P4A60B60QHD325	60	60	0.035	4	325	5.42	30	70
T3S1P4A60B60QHD350	60	60	0.035	4	350	5.83	37	63
T3S1P4A60B80QHD025	60	80	0.035	4	25	0.31	98	2
T3S1P4A60B80QHD050	60	80	0.035	4	50	0.63	100	0
T3S1P4A60B80QHD075	60	80	0.035	4	75	0.94	97	3
T3S1P4A60B80QHD100	60	80	0.035	4	100	1.25	90	10
T3S1P4A60B80QHD150	60	80	0.035	4	150	1.88	69	31
T3S1P4A60B80QHD200	60	80	0.035	4	200	2.50	64	36
T3S1P4A60B80QHD275	60	80	0.035	4	275	3.44	64	36
T3S1P4A60B80QHD300	60	80	0.035	4	300	3.75	44	56
T3S1P4A60B80QHD325	60	80	0.035	4	325	4.06	45	55
T3S1P4A60B80QHD350	60	80	0.035	4	350	4.38	60	40
T3S1P4A60B100QHD025	60	100	0.035	4	25	0.25	97	3

Appendix D

Run ID	Rack Angle (Degrees)	Bar Spacing (mm)	Discharge (m^3/s)	Screen Pos.	Debris Length (mm)	Ratio of debris length to bar spacing	Passed Through	Blocked
T3S1P4A60B100QHD050	60	100	0.035	4	50	0.50	97	3
T3S1P4A60B100QHD075	60	100	0.035	4	75	0.75	98	2
T3S1P4A60B100QHD100	60	100	0.035	4	100	1.00	97	3
T3S1P4A60B100QHD150	60	100	0.035	4	150	1.50	83	17
T3S1P4A60B100QHD200	60	100	0.035	4	200	2.00	71	29
T3S1P4A60B100QHD275	60	100	0.035	4	275	2.75	61	39
T3S1P4A60B100QHD300	60	100	0.035	4	300	3.00	60	40
T3S1P4A60B100QHD325	60	100	0.035	4	325	3.25	50	50
T3S1P4A60B100QHD350	60	100	0.035	4	350	3.50	64	36
T3S1P4A60B150QHD025	60	150	0.035	4	25	0.17	100	0
T3S1P4A60B150QHD050	60	150	0.035	4	50	0.33	98	2
T3S1P4A60B150QHD075	60	150	0.035	4	75	0.50	100	0
T3S1P4A60B150QHD100	60	150	0.035	4	100	0.67	100	0
T3S1P4A60B150QHD150	60	150	0.035	4	150	1.00	96	4
T3S1P4A60B150QHD200	60	150	0.035	4	200	1.33	89	11
T3S1P4A60B150QHD275	60	150	0.035	4	275	1.83	71	29
T3S1P4A60B150QHD300	60	150	0.035	4	300	2.00	64	36
T3S1P4A60B150QHD325	60	150	0.035	4	325	2.17	61	39
T3S1P4A60B150QHD350	60	150	0.035	4	350	2.33	76	24

Table D.2 Results from screen position testing part 2

Run ID	Rack Angle (Degrees)	Bar Spacing (mm)	Discharge (m^3/s)	Debris Length (mm)	Ratio of debris length to bar spacing	Passed Through	Blocked
T4S1P1A30B30QHD025	30	30	0.035	25	0.83	92	8
T4S1P1A30B30QHD050	30	30	0.035	50	1.67	37	63
T4S1P1A30B30QHD075	30	30	0.035	75	2.50	28	72
T4S1P1A30B30QHD100	30	30	0.035	100	3.33	28	72
T4S1P1A30B30QHD150	30	30	0.035	150	5.00	21	79
T4S1P1A30B30QHD200	30	30	0.035	200	6.67	22	78
T4S1P1A30B30QHD275	30	30	0.035	275	9.17	20	80
T4S1P1A30B30QHD300	30	30	0.035	300	10.00	22	78
T4S1P1A30B30QHD325	30	30	0.035	325	10.83	20	80
T4S1P1A30B30QHD350	30	30	0.035	350	11.67	25	75
T4S1P1A30B40QHD025	30	40	0.035	25	0.63	94	6
T4S1P1A30B40QHD050	30	40	0.035	50	1.25	70	30
T4S1P1A30B40QHD075	30	40	0.035	75	1.88	37	63
T4S1P1A30B40QHD100	30	40	0.035	100	2.50	33	67
T4S1P1A30B40QHD150	30	40	0.035	150	3.75	27	73
T4S1P1A30B40QHD200	30	40	0.035	200	5.00	25	75
T4S1P1A30B40QHD275	30	40	0.035	275	6.88	23	77
T4S1P1A30B40QHD300	30	40	0.035	300	7.50	21	79
T4S1P1A30B40QHD325	30	40	0.035	325	8.13	21	79
T4S1P1A30B40QHD350	30	40	0.035	350	8.75	22	78
T4S1P1A30B50QHD025	30	50	0.035	25	0.50	97	3
T4S1P1A30B50QHD050	30	50	0.035	50	1.00	88	12
T4S1P1A30B50QHD075	30	50	0.035	75	1.50	55	45
T4S1P1A30B50QHD100	30	50	0.035	100	2.00	44	56
T4S1P1A30B50QHD150	30	50	0.035	150	3.00	36	64
T4S1P1A30B50QHD200	30	50	0.035	200	4.00	39	61
T4S1P1A30B50QHD275	30	50	0.035	275	5.50	28	72
T4S1P1A30B50QHD300	30	50	0.035	300	6.00	30	70
T4S1P1A30B50QHD325	30	50	0.035	325	6.50	28	72
T4S1P1A30B50QHD350	30	50	0.035	350	7.00	28	72
T4S1P1A30B60QHD025	30	60	0.035	25	0.42	95	5

Run ID	Rack Angle (Degrees)	Bar Spacing (mm)	Discharge (m^3/s)	Debris Length (mm)	Ratio of debris length to bar spacing	Passed Through	Blocked
T4S1P1A30B60QHD050	30	60	0.035	50	0.83	92	8
T4S1P1A30B60QHD075	30	60	0.035	75	1.25	74	26
T4S1P1A30B60QHD100	30	60	0.035	100	1.67	45	55
T4S1P1A30B60QHD150	30	60	0.035	150	2.50	33	67
T4S1P1A30B60QHD200	30	60	0.035	200	3.33	31	69
T4S1P1A30B60QHD275	30	60	0.035	275	4.58	28	72
T4S1P1A30B60QHD300	30	60	0.035	300	5.00	27	73
T4S1P1A30B60QHD325	30	60	0.035	325	5.42	28	72
T4S1P1A30B60QHD350	30	60	0.035	350	5.83	33	67
T4S1P1A30B80QHD025	30	80	0.035	25	0.31	99	1
T4S1P1A30B80QHD050	30	80	0.035	50	0.63	96	4
T4S1P1A30B80QHD075	30	80	0.035	75	0.94	98	2
T4S1P1A30B80QHD100	30	80	0.035	100	1.25	70	30
T4S1P1A30B80QHD150	30	80	0.035	150	1.88	43	57
T4S1P1A30B80QHD200	30	80	0.035	200	2.50	46	54
T4S1P1A30B80QHD275	30	80	0.035	275	3.44	42	58
T4S1P1A30B80QHD300	30	80	0.035	300	3.75	41	59
T4S1P1A30B80QHD325	30	80	0.035	325	4.06	36	64
T4S1P1A30B80QHD350	30	80	0.035	350	4.38	37	63
T4S1P1A30B100QHD025	30	100	0.035	25	0.25	100	0
T4S1P1A30B100QHD050	30	100	0.035	50	0.50	97	3
T4S1P1A30B100QHD075	30	100	0.035	75	0.75	96	4
T4S1P1A30B100QHD100	30	100	0.035	100	1.00	95	5
T4S1P1A30B100QHD150	30	100	0.035	150	1.50	67	33
T4S1P1A30B100QHD200	30	100	0.035	200	2.00	48	52
T4S1P1A30B100QHD275	30	100	0.035	275	2.75	41	59
T4S1P1A30B100QHD300	30	100	0.035	300	3.00	46	54
T4S1P1A30B100QHD325	30	100	0.035	325	3.25	45	55
T4S1P1A30B100QHD350	30	100	0.035	350	3.50	43	57
T4S1P1A30B150QHD025	30	150	0.035	25	0.17	100	0
T4S1P1A30B150QHD050	30	150	0.035	50	0.33	99	1
T4S1P1A30B150QHD075	30	150	0.035	75	0.50	96	4
T4S1P1A30B150QHD100	30	150	0.035	100	0.67	95	5

Run ID	Rack Angle (Degrees)	Bar Spacing (mm)	Discharge (m^3/s)	Debris Length (mm)	Ratio of debris length to bar spacing	Passed Through	Blocked
T4S1P1A30B150QHD150	30	150	0.035	150	1.00	95	5
T4S1P1A30B150QHD200	30	150	0.035	200	1.33	80	20
T4S1P1A30B150QHD275	30	150	0.035	275	1.83	73	27
T4S1P1A30B150QHD300	30	150	0.035	300	2.00	68	32
T4S1P1A30B150QHD325	30	150	0.035	325	2.17	62	38
T4S1P1A30B150QHD350	30	150	0.035	350	2.33	63	37
T4S1P1A45B30QHD025	45	30	0.035	25	0.83	96	4
T4S1P1A45B30QHD050	45	30	0.035	50	1.67	43	57
T4S1P1A45B30QHD075	45	30	0.035	75	2.50	32	68
T4S1P1A45B30QHD100	45	30	0.035	100	3.33	30	70
T4S1P1A45B30QHD150	45	30	0.035	150	5.00	20	80
T4S1P1A45B30QHD200	45	30	0.035	200	6.67	19	81
T4S1P1A45B30QHD275	45	30	0.035	275	9.17	24	76
T4S1P1A45B30QHD300	45	30	0.035	300	10.00	28	72
T4S1P1A45B30QHD325	45	30	0.035	325	10.83	26	74
T4S1P1A45B30QHD350	45	30	0.035	350	11.67	25	75
T4S1P1A45B40QHD025	45	40	0.035	25	0.63	96	4
T4S1P1A45B40QHD050	45	40	0.035	50	1.25	73	27
T4S1P1A45B40QHD075	45	40	0.035	75	1.88	38	62
T4S1P1A45B40QHD100	45	40	0.035	100	2.50	30	70
T4S1P1A45B40QHD150	45	40	0.035	150	3.75	28	72
T4S1P1A45B40QHD200	45	40	0.035	200	5.00	28	72
T4S1P1A45B40QHD275	45	40	0.035	275	6.88	25	75
T4S1P1A45B40QHD300	45	40	0.035	300	7.50	27	73
T4S1P1A45B40QHD325	45	40	0.035	325	8.13	30	70
T4S1P1A45B40QHD350	45	40	0.035	350	8.75	21	79
T4S1P1A45B50QHD025	45	50	0.035	25	0.50	97	3
T4S1P1A45B50QHD050	45	50	0.035	50	1.00	87	13
T4S1P1A45B50QHD075	45	50	0.035	75	1.50	50	50
T4S1P1A45B50QHD100	45	50	0.035	100	2.00	40	60
T4S1P1A45B50QHD150	45	50	0.035	150	3.00	37	63
T4S1P1A45B50QHD200	45	50	0.035	200	4.00	35	65
T4S1P1A45B50QHD275	45	50	0.035	275	5.50	32	68

Run ID	Rack Angle (Degrees)	Bar Spacing (mm)	Discharge (m^3/s)	Debris Length (mm)	Ratio of debris length to bar spacing	Passed Through	Blocked
T4S1P1A45B50QHD300	45	50	0.035	300	6.00	35	65
T4S1P1A45B50QHD325	45	50	0.035	325	6.50	29	71
T4S1P1A45B50QHD350	45	50	0.035	350	7.00	33	67
T4S1P1A45B60QHD025	45	60	0.035	25	0.42	96	4
T4S1P1A45B60QHD050	45	60	0.035	50	0.83	93	7
T4S1P1A45B60QHD075	45	60	0.035	75	1.25	72	28
T4S1P1A45B60QHD100	45	60	0.035	100	1.67	45	55
T4S1P1A45B60QHD150	45	60	0.035	150	2.50	38	62
T4S1P1A45B60QHD200	45	60	0.035	200	3.33	49	51
T4S1P1A45B60QHD275	45	60	0.035	275	4.58	33	67
T4S1P1A45B60QHD300	45	60	0.035	300	5.00	33	67
T4S1P1A45B60QHD325	45	60	0.035	325	5.42	31	69
T4S1P1A45B60QHD350	45	60	0.035	350	5.83	30	70
T4S1P1A45B80QHD025	45	80	0.035	25	0.31	100	0
T4S1P1A45B80QHD050	45	80	0.035	50	0.63	95	5
T4S1P1A45B80QHD075	45	80	0.035	75	0.94	95	5
T4S1P1A45B80QHD100	45	80	0.035	100	1.25	66	34
T4S1P1A45B80QHD150	45	80	0.035	150	1.88	51	49
T4S1P1A45B80QHD200	45	80	0.035	200	2.50	47	53
T4S1P1A45B80QHD275	45	80	0.035	275	3.44	48	52
T4S1P1A45B80QHD300	45	80	0.035	300	3.75	50	50
T4S1P1A45B80QHD325	45	80	0.035	325	4.06	38	62
T4S1P1A45B80QHD350	45	80	0.035	350	4.38	35	65
T4S1P1A45B100QHD025	45	100	0.035	25	0.25	100	0
T4S1P1A45B100QHD050	45	100	0.035	50	0.50	99	1
T4S1P1A45B100QHD075	45	100	0.035	75	0.75	95	5
T4S1P1A45B100QHD100	45	100	0.035	100	1.00	93	7
T4S1P1A45B100QHD150	45	100	0.035	150	1.50	69	31
T4S1P1A45B100QHD200	45	100	0.035	200	2.00	49	51
T4S1P1A45B100QHD275	45	100	0.035	275	2.75	48	52
T4S1P1A45B100QHD300	45	100	0.035	300	3.00	41	59
T4S1P1A45B100QHD325	45	100	0.035	325	3.25	39	61
T4S1P1A45B100QHD350	45	100	0.035	350	3.50	33	67

Run ID	Rack Angle (Degrees)	Bar Spacing (mm)	Discharge (m^3/s)	Debris Length (mm)	Ratio of debris length to bar spacing	Passed Through	Blocked
T4S1P1A45B150QHD025	45	150	0.035	25	0.17	100	0
T4S1P1A45B150QHD050	45	150	0.035	50	0.33	100	0
T4S1P1A45B150QHD075	45	150	0.035	75	0.50	96	4
T4S1P1A45B150QHD100	45	150	0.035	100	0.67	94	6
T4S1P1A45B150QHD150	45	150	0.035	150	1.00	98	2
T4S1P1A45B150QHD200	45	150	0.035	200	1.33	80	20
T4S1P1A45B150QHD275	45	150	0.035	275	1.83	77	23
T4S1P1A45B150QHD300	45	150	0.035	300	2.00	73	27
T4S1P1A45B150QHD325	45	150	0.035	325	2.17	62	38
T4S1P1A45B150QHD350	45	150	0.035	350	2.33	68	32
T4S1P1A60B30QHD025	60	30	0.035	25	0.83	98	2
T4S1P1A60B30QHD050	60	30	0.035	50	1.67	36	64
T4S1P1A60B30QHD075	60	30	0.035	75	2.50	26	74
T4S1P1A60B30QHD100	60	30	0.035	100	3.33	24	76
T4S1P1A60B30QHD150	60	30	0.035	150	5.00	27	73
T4S1P1A60B30QHD200	60	30	0.035	200	6.67	23	77
T4S1P1A60B30QHD275	60	30	0.035	275	9.17	25	75
T4S1P1A60B30QHD300	60	30	0.035	300	10.00	20	80
T4S1P1A60B30QHD325	60	30	0.035	325	10.83	19	81
T4S1P1A60B30QHD350	60	30	0.035	350	11.67	21	79
T4S1P1A60B40QHD025	60	40	0.035	25	0.63	96	4
T4S1P1A60B40QHD050	60	40	0.035	50	1.25	70	30
T4S1P1A60B40QHD075	60	40	0.035	75	1.88	38	62
T4S1P1A60B40QHD100	60	40	0.035	100	2.50	29	71
T4S1P1A60B40QHD150	60	40	0.035	150	3.75	30	70
T4S1P1A60B40QHD200	60	40	0.035	200	5.00	26	74
T4S1P1A60B40QHD275	60	40	0.035	275	6.88	24	76
T4S1P1A60B40QHD300	60	40	0.035	300	7.50	25	75
T4S1P1A60B40QHD325	60	40	0.035	325	8.13	22	78
T4S1P1A60B40QHD350	60	40	0.035	350	8.75	20	80
T4S1P1A60B50QHD025	60	50	0.035	25	0.50	98	2
T4S1P1A60B50QHD050	60	50	0.035	50	1.00	88	12
T4S1P1A60B50QHD075	60	50	0.035	75	1.50	52	48

Run ID	Rack Angle (Degrees)	Bar Spacing (mm)	Discharge (m^3/s)	Debris Length (mm)	Ratio of debris length to bar spacing	Passed Through	Blocked
T4S1P1A60B50QHD100	60	50	0.035	100	2.00	45	55
T4S1P1A60B50QHD150	60	50	0.035	150	3.00	36	64
T4S1P1A60B50QHD200	60	50	0.035	200	4.00	32	68
T4S1P1A60B50QHD275	60	50	0.035	275	5.50	30	70
T4S1P1A60B50QHD300	60	50	0.035	300	6.00	34	66
T4S1P1A60B50QHD325	60	50	0.035	325	6.50	24	76
T4S1P1A60B50QHD350	60	50	0.035	350	7.00	32	68
T4S1P1A60B60QHD025	60	60	0.035	25	0.42	93	7
T4S1P1A60B60QHD050	60	60	0.035	50	0.83	86	14
T4S1P1A60B60QHD075	60	60	0.035	75	1.25	74	26
T4S1P1A60B60QHD100	60	60	0.035	100	1.67	48	52
T4S1P1A60B60QHD150	60	60	0.035	150	2.50	36	64
T4S1P1A60B60QHD200	60	60	0.035	200	3.33	28	72
T4S1P1A60B60QHD275	60	60	0.035	275	4.58	35	65
T4S1P1A60B60QHD300	60	60	0.035	300	5.00	30	70
T4S1P1A60B60QHD325	60	60	0.035	325	5.42	31	69
T4S1P1A60B60QHD350	60	60	0.035	350	5.83	32	68
T4S1P1A60B80QHD025	60	80	0.035	25	0.31	99	1
T4S1P1A60B80QHD050	60	80	0.035	50	0.63	96	4
T4S1P1A60B80QHD075	60	80	0.035	75	0.94	91	9
T4S1P1A60B80QHD100	60	80	0.035	100	1.25	70	30
T4S1P1A60B80QHD150	60	80	0.035	150	1.88	50	50
T4S1P1A60B80QHD200	60	80	0.035	200	2.50	45	55
T4S1P1A60B80QHD275	60	80	0.035	275	3.44	41	59
T4S1P1A60B80QHD300	60	80	0.035	300	3.75	35	65
T4S1P1A60B80QHD325	60	80	0.035	325	4.06	38	62
T4S1P1A60B80QHD350	60	80	0.035	350	4.38	32	68
T4S1P1A60B100QHD025	60	100	0.035	25	0.25	99	1
T4S1P1A60B100QHD050	60	100	0.035	50	0.50	92	8
T4S1P1A60B100QHD075	60	100	0.035	75	0.75	94	6
T4S1P1A60B100QHD100	60	100	0.035	100	1.00	94	6
T4S1P1A60B100QHD150	60	100	0.035	150	1.50	68	32
T4S1P1A60B100QHD200	60	100	0.035	200	2.00	52	48

Run ID	Rack Angle (Degrees)	Bar Spacing (mm)	Discharge (m^3/s)	Debris Length (mm)	Ratio of debris length to bar spacing	Passed Through	Blocked
T4S1P1A60B100QHD275	60	100	0.035	275	2.75	52	48
T4S1P1A60B100QHD300	60	100	0.035	300	3.00	50	50
T4S1P1A60B100QHD325	60	100	0.035	325	3.25	48	52
T4S1P1A60B100QHD350	60	100	0.035	350	3.50	42	58
T4S1P1A60B150QHD025	60	150	0.035	25	0.17	98	2
T4S1P1A60B150QHD050	60	150	0.035	50	0.33	96	4
T4S1P1A60B150QHD075	60	150	0.035	75	0.50	95	5
T4S1P1A60B150QHD100	60	150	0.035	100	0.67	92	8
T4S1P1A60B150QHD150	60	150	0.035	150	1.00	93	7
T4S1P1A60B150QHD200	60	150	0.035	200	1.33	74	26
T4S1P1A60B150QHD275	60	150	0.035	275	1.83	63	37
T4S1P1A60B150QHD300	60	150	0.035	300	2.00	64	36
T4S1P1A60B150QHD325	60	150	0.035	325	2.17	58	42
T4S1P1A60B150QHD350	60	150	0.035	350	2.33	58	42

Appendix E – Regression Analysis from Testing Phase 1

Response 1 Blockage
Transform: Logit Lower bound: 0 Upper bound: 100
Stepwise Regression with Alpha to Enter = 0.100, Alpha to Exit = 0.100
Forced Terms Intercept

Added	**Coefficient Estimate**	**t for H_0 Coeff=0**	**Prob > |t|**	**R-Squared**	**MSE**
D-Debris Length	1.59	-23.13	<0.0001	0.4688	1.41
B-Bar Spacing	-1.26	22.04	<0.0001	0.7054	0.78
D^2	-1.64	19.29	<0.0001	0.8177	0.48
BD	0.55	-8.94	<0.0001	0.8391	0.43
A-Screen Angle	-0.25	8.10	<0.0001	0.8549	0.39
B^2	0.42	-6.52	<0.0001	0.8645	0.36
C-Discharge	-0.13	4.51	<0.0001	0.8689	0.35

ANOVA for Response Surface Reduced Quadratic Model
Analysis of variance table [Partial sum of squares - Type III]

	Sum of Squares	df	Mean Square	F Value	p-value Prob > F	
Model	1393.74	7	199.11	568.17	< 0.0001	significant
A-Screen Angle	24.89	1	24.89	71.02	< 0.0001	
B-Bar Spacing	412.75	1	412.75	1177.81	< 0.0001	
C-Discharge	7.12	1	7.12	20.32	< 0.0001	
D-Debris Length	826.79	1	826.79	2359.34	< 0.0001	
BD	34.10	1	34.10	97.32	< 0.0001	
B^2	15.37	1	15.37	43.87	< 0.0001	
D^2	192.04	1	192.04	547.99	< 0.0001	
Residual	210.26	600	0.35			
Cor Total	1604.00	607				

The Model F-value of 568.17 implies the model is significant. There is only a 0.01% chance that a "Model F-Value" this large could occur due to noise.
Values of "Prob > F" less than 0.0500 indicate model terms are significant.
In this case A, B, C, D, BD, B^2, D^2 are significant model terms.
Values greater than 0.1000 indicate the model terms are not significant.
In this case A, B, C, D, AC, AD, BD, A^2, B^2, C^2, D^2 are significant model terms.

Std. Dev.	0.59	R-Squared	0.8689
Mean	-0.47	Adj R-Squared	0.8674
C.V. %	125.87	Pred R-Squared	0.8650
PRESS	216.58	Adeq Precision	107.286

The "Pred R-Squared" of 0.8650 is in reasonable agreement with the "Adj R-Squared" of 0.8674."Adeq Precision" measures the signal to noise ratio. A ratio greater than 4 is desirable. Your ratio of 107.286 indicates an adequate signal. This model can be used to navigate the design space.

Factor	**Coefficient Estimate**	**df**	**Standard Error**	**95% CI Low**	**95% CI High**	**VIF**
Intercept	-0.30	1	0.053	-0.40	-0.19	
A-Screen Angle	-0.25	1	0.030	-0.31	-0.19	1.00
B-Bar Spacing	-1.33	1	0.039	-1.40	-1.25	1.02
C-Discharge	-0.13	1	0.029	-0.19	-0.075	1.00
D-Debris Length	1.90	1	0.039	1.82	1.98	1.31
BD	0.55	1	0.056	0.44	0.66	1.30
B^2	0.41	1	0.063	0.29	0.54	1.01
D^2	-1.70	1	0.073	-1.84	-1.56	1.01

Final Equation in Terms of Coded Factors:

Logit(Blockage) = Ln[(Blockage + 0.00)/(100.00 - Blockage)] =

$$
\begin{aligned}
&-0.30 \\
&-0.25 \quad * A \\
&-1.33 \quad * B \\
&-0.13 \quad * C \\
&+1.90 \quad * D \\
&+0.55 \quad * B * D \\
&+0.41 \quad * B^2 \\
&-1.70 \quad * D^2
\end{aligned}
$$

Final Equation in Terms of Actual Factors:

Logit(Blockage) = Ln[(Blockage + 0.00)/(100.00 - Blockage)] =

$$
\begin{aligned}
&+0.051284 \\
&-0.016648 \quad * \text{Screen Angle} \\
&-53.42828 \quad * \text{Bar Spacing} \\
&-8.82257 \quad * \text{Discharge} \\
&+30.72767 \quad * \text{Debris Length} \\
&+56.44123 \quad * \text{Bar Spacing} * \text{Debris Length} \\
&+115.23579 \quad * \text{Bar Spacing}^2 \\
&-64.30326 \quad * \text{Debris Length}^2
\end{aligned}
$$

Appendix F – Regression Analysis from Testing Phase 2

Response **1** **Blocked**
Transform: **Logit** **Lower bound: 0** **Upper bound: 100**
Stepwise Regression with Alpha to Enter = 0.100, Alpha to Exit = 0.100

Forced Terms Intercept

Added	Coefficient Estimate	t for H_0Coeff=0	Prob > |t|	R-Squared	MSE
D-Debris Size	1.55	-20.63	<0.0001	0.4300	1.47
B-Bar Spacing	-1.28	20.32	<0.0001	0.6711	0.85
D^2	-1.73	17.57	<0.0001	0.7877	0.55
BD	0.69	-9.63	<0.0001	0.8179	0.47
A-Screen Angle	-0.27	7.87	<0.0001	0.8360	0.43
B^2	0.45	-6.46	<0.0001	0.8474	0.40

ANOVA for Response Surface Reduced Quadratic Model
Analysis of variance table [Partial sum of squares - Type III]

Source	Sum of Squares	df	Mean Square	F Value	p-value Prob > F	
Model	1235.50	6	205.92	517.21	< 0.0001	significant
A-Screen Angle	25.31	1	25.31	63.58	< 0.0001	
B-Bar Spacing	412.06	1	412.06	1034.97	< 0.0001	
D-Debris Size	795.95	1	795.95	1999.22	< 0.0001	
BD	41.69	1	41.69	104.72	< 0.0001	
B^2	16.60	1	16.60	41.68	< 0.0001	
D^2	198.33	1	198.33	498.15	< 0.0001	
Residual	222.56	559	0.40			
Cor Total	1458.06	565				

The Model F-value of 517.21 implies the model is significant. There is only a 0.01% chance that a "Model F-Value" this large could occur due to noise.

Values of "Prob > F" less than 0.0500 indicate model terms are significant.
In this case A, B, D, BD, B^2, D^2 are significant model terms.
Values greater than 0.1000 indicate the model terms are not significant.

Std. Dev.	0.63	R-Squared	0.8474
Mean	-0.30	Adj R-Squared	0.8457
C.V. %	212.60	Pred R-Squared	0.8429
PRESS	229.07	Adeq Precision	105.029

The "Pred R-Squared" of 0.8429 is in reasonable agreement with the "Adj R-Squared" of 0.8457.
"Adeq Precision" measures the signal to noise ratio. A ratio greater than 4 is desirable. Your ratio of 105.029 indicates an adequate signal. This model can be used to navigate the design space.

Factor	**Coefficient Estimate**	**df**	**Standard Error**	**95% CI Low**	**95% CI High**	**VIF**
Intercept	-0.32	1	0.058	-0.43	-0.20	
A-Screen Angle	-0.26	1	0.033	-0.33	-0.20	1.01
B-Bar Spacing	-1.43	1	0.045	-1.52	-1.35	1.08
D-Debris Size	2.14	1	0.048	2.05	2.23	1.50
BD	0.67	1	0.066	0.54	0.80	1.45
B^2	0.45	1	0.070	0.31	0.59	1.02
D^2	-1.89	1	0.084	-2.05	-1.72	1.07

Final Equation in Terms of Coded Factors:

Logit(Blocked) = Ln[(Blocked + 0.00)/(100.00 - Blocked)] =
-0.32
-0.26 * A
-1.43 * B
+2.14 * D
+0.67 * B * D
+0.45 * B^2
-1.89 * D^2

Final Equation in Terms of Actual Factors:

Logit(Blocked) = Ln[(Blocked + 0.00)/(100.00 - Blocked)] =
-0.17582
-0.017546 * Screen Angle
-59.44834 * Bar Spacing
+33.74227 * Debris Size
+68.93594 * Bar Spacing * Debris Size
+125.61712 * Bar Spacing^2
-71.39369 * Debris Size^2

Appendix G – Regression Analysis from Testing Phase 3

Response **1** **Blocked**
Transform: **Logit** **Lower bound: 0** **Upper bound: 100**
Stepwise Regression with Alpha to Enter = 0.100, Alpha to Exit = 0.100

Forced Terms Intercept

Added	**Coefficient Estimate**	**t for H0 Coeff=0**	**Prob > |t|**	**R- Squared**	**MSE**
B-Debris Length	1.85	-15.61	<0.0001	0.4838	1.75
A-Bar Spacing	-1.31	12.42	<0.0001	0.6766	1.10
B^2	-1.97	12.46	<0.0001	0.7981	0.69
C-Relative Velocity	-0.51	8.90	<0.0001	0.8457	0.53
AB	0.75	-7.51	<0.0001	0.8736	0.43
B^3	1.28	-6.00	<0.0001	0.8892	0.38
AB^2	0.70	-3.49	0.0006	0.8943	0.37
A^2	0.32	-3.27	0.0012	0.8986	0.35

ANOVA for Response Surface Reduced Cubic Model
Analysis of variance table [Partial sum of squares - Type III]

Source	**Sum of Squares**	**df**	**Mean Sqaure**	**F Value**	**p-value Prob > F**	
Model	790.21	8	98.78	280.23	< 0.0001	significant
A-Bar Spacing	104.63	1	104.63	296.85	< 0.0001	
B-Debris Length	31.89	1	31.89	90.47	< 0.0001	
C-Relative Velocity	43.04	1	43.04	122.09	< 0.0001	
AB	15.90	1	15.90	45.12	< 0.0001	
A^2	3.78	1	3.78	10.73	0.0012	
B^2	64.64	1	64.63	183.37	< 0.0001	
AB^2	5.24	1	5.24	14.86	0.0001	
B^3	11.50	1	11.50	32.62	< 0.0001	
Residual	89.18	253	0.35			
Cor Total	879.41	261				

The Model F-value of 280.23 implies the model is significant. There is only a 0.01% chance that a "Model F-Value" this large could occur due to noise.

Values of "Prob > F" less than 0.0500 indicate model terms are significant.
In this case A, B, C, AB, A^2, B^2, AB^2, B^3 are significant model terms.

Std. Dev.	0.59	R-Squared	0.8986
Mean	-0.30	Adj R-Squared	0.8954
C.V. %	197.74	Pred R-Squared	0.8885
PRESS	98.07	Adeq Precision	72.120

The "Pred R-Squared" of 0.8885 is in reasonable agreement with the "Adj R-Squared" of 0.8954. "Adeq Precision" measures the signal to noise ratio. A ratio greater than 4 is desirable. Your ratio of 72.120 indicates an adequate signal. This model can be used to navigate the design space.

Factor	**Coefficient Estimate**	**df**	**Standard Error**	**95% CI Low**	**95% CI High**	**VIF**
Intercept	-0.26	1	0.088	-0.44	-0.089	
A-Bar Spacing	-1.80	1	0.10	-2.00	-1.59	3.07
B-Debris Length	1.47	1	0.15	1.16	1.77	8.39
C-Relative Velocity	-0.52	1	0.047	-0.61	-0.42	1.00
AB	0.65	1	0.096	0.46	0.83	1.56
A^2	0.32	1	0.098	0.13	0.51	1.03
B^2	-1.82	1	0.13	-2.08	-1.55	1.44
AB^2	0.76	1	0.20	0.37	1.14	3.80
B^3	1.17	1	0.21	0.77	1.58	8.36

Final Equation in Terms of Coded Factors:

Logit(Blocked) = Ln[(Blocked + 0.00)/(100.00 - Blocked)] =

-0.26	
-1.80	* A
+1.47	* B
-0.52	* C
+0.65	* A * B
+0.32	* A^2
-1.82	* B^2
+0.76	* A * B^2
+1.17	* B^3

Final Equation in Terms of Actual Factors:

Logit(Blocked) = Ln[(Blocked + 0.00)/(100.00 - Blocked)] =

-1.01356	
-41.53535	* Bar Spacing
+73.90181	* Debris Length
-1.51795	* Relative Velocity
-113.14369	* Bar Spacing * Debris Length
+88.71015	* Bar Spacing^2
-265.90675	* Debris Length^2
+478.18207	* Bar Spacing * Debris Length^2
+273.78569	* Debris Length^3

Appendix H – Regression Analysis from Full Data Set

Response **1** **Blocked**
Transform: **Logit** **Lower bound: 0** **Upper bound: 100**
Stepwise Regression with Alpha to Enter = 0.100, Alpha to Exit = 0.100

Forced Terms Intercept

Added	**Coefficient Estimate**	**t for H_0 Coeff=0**	**Prob > |t|**	**R-Squared**	**MSE**
C-Debris Length	1.67	-26.98	<0.0001	0.4752	1.51
B-Bar Spacing	-1.28	24.20	<0.0001	0.6966	0.88
C^2	-1.74	21.99	<0.0001	0.8107	0.55
BC	0.61	-10.54	<0.0001	0.8337	0.48
E-Relative Velocity	-0.72	10.69	<0.0001	0.8545	0.42
B^2	0.39	-6.62	<0.0001	0.8621	0.40
A-Screen Angle	0.19	-5.16	<0.0001	0.8665	0.39

ANOVA for Response Surface Reduced Quadratic Model
Analysis of variance table [Partial sum of squares - Type III]

Source	**Sum of Squares**	**df**	**Mean Square**	**F Value**	**p-value Prob > F**	
Model	2009.40	7	287.06	740.15	< 0.0001	significant
A-Screen Angle	10.33	1	10.33	26.63	< 0.0001	
B-Bar Spacing	570.91	1	570.91	1472.04	< 0.0001	
C-Debris Length	1217.92	1	1217.92	3140.28	< 0.0001	
E-Relative Velocity	51.15	1	51.15	131.88	< 0.0001	
BC	52.99	1	52.99	136.62	< 0.0001	
B^2	18.03	1	18.03	46.49	< 0.0001	
C^2	280.06	1	280.06	722.11	< 0.0001	
Residual	309.49	798	0.39			
Cor Total	2318.9	805				

The Model F-value of 740.15 implies the model is significant. There is only a 0.01% chance that a "Model F-Value" this large could occur due to noise.

Values of "Prob > F" less than 0.0500 indicate model terms are significant.
In this case A, B, C, E, BC, B^2, C^2 are significant model terms.

Std. Dev.	0.62	R-Squared	0.8665
Mean	-0.392	Adj R-Squared	0.8654
C.V. %	159.98	Pred R-Squared	0.8634
PRESS	316.76	Adeq Precision	124.128

The "Pred R-Squared" of 0.8654 is in reasonable agreement with the "Adj R-Squared" of 0.8645. "Adeq Precision" measures the signal to noise ratio. A ratio greater than 4 is desirable. Your ratio of 124.128 indicates an adequate signal. This model can be used to navigate the design space.

Factor	**Coefficient Estimate**	**df**	**Standard Error**	**95% CI Low**	**95% CI High**	**VIF**
Intercept	0.20	1	0.058	0.086	0.32	
A-Screen Angle	0.19	1	0.038	0.12	0.27	2.04
B-Bar Spacing	-1.36	1	0.035	-1.43	-1.29	1.02
C-Debris Length	2.03	1	0.036	1.95	2.10	1.32
E-Relative Velocity	-1.05	1	0.092	-1.23	-0.87	2.04
BC	0.60	1	0.052	0.50	0.71	1.31
B^2	0.39	1	0.057	0.28	0.50	1.01
C^2	-1.79	1	0.067	-1.92	-1.66	1.02

Final Equation in Terms of Coded Factors:

Logit(Blocked) = Ln[(Blocked + 0.00)/(100.00 - Blocked)] =

+0.20	
+0.19	* A
-1.36	* B
+2.032	* C
-1.05	* E
+0.60	* B * C
+0.39	* B^2
-1.79	* C^2

Final Equation in Terms of Actual Factors:

Logit(Blocked)	= Ln[(Blocked + 0.00)/(100.00 - Blocked)] =
+0.033990	
+0.012962	* Screen Angle
-53.87339	* Bar Spacing
+32.34954	* Debris Length
-1.24938	* Relative Velocity
+61.95619	* Bar Spacing * Debris Length
+108.67909	* Bar Spacing^2
-67.89552	* Debris Length^2

Appendix I – Regression Analysis from Summary Data Set

Response 1 Blocked
Transform: Logit Lower bound: 0 Upper bound: 100
Stepwise Regression with Alpha to Enter = 0.100, Alpha to Exit = 0.100

Forced Terms Intercept

Added	**Coefficient Estimate**	**t for H0 Coeff=0**	**Prob > |t|**	**R-Squared**	**MSE**
B-Bar Spacing	-0.97	20.44	<0.0001	0.8359	0.077
D-Relative Velocity	-0.52	7.64	<0.0001	0.9046	0.046
B^2	0.31	-6.15	<0.0001	0.9353	0.031
A-Screen Angle	0.18	-6.72	<0.0001	0.9588	0.020

ANOVA for Response Surface Reduced Quadratic Model
Analysis of variance table [Partial sum of squares - Type III]

Source	**Sum of Squares**	**df**	**Mean Square**	**F Value**	**p-value Prob > F**	
Model	37.07	4	9.27	459.81	< 0.0001	significant
A-Screen Angle	0.91	1	0.91	45.17	< 0.0001	
B-Bar Spacing	32.20	1	32.20	1597.80	< 0.0001	
D-Relative Velocity	3.33	1	3.33	165.16	< 0.0001	
B^2	1.18	1	1.18	58.75	< 0.0001	
Residual	1.59	79	0.020			
Cor Total	38.66	83				

The Model F-value of 459.81 implies the model is significant. There is only a 0.01% chance that a "Model F-Value" this large could occur due to noise.

Values of "Prob > F" less than 0.0500 indicate model terms are significant.
In this case A, B, D, B^2 are significant model terms.

Std. Dev.	0.14	R-Squared	0.9588
Mean	-0.22	Adj R-Squared	0.9567
C.V. %	64.72	Pred R-Squared	0.9529
PRESS	1.82	Adeq Precision	75.727

The "Pred R-Squared" of 0.9529 is in reasonable agreement with the "Adj R-Squared" of 0.9567.

"Adeq Precision" measures the signal to noise ratio. A ratio greater than 4 is desirable. Your ratio of 75.727 indicates an adequate signal. This model can be used to navigate the design space.

Factor	**Coefficient Estimate**	**df**	**Standard Error**	**95% CI Low**	**95% CI High**	**VIF**
Intercept	-0.35	1	0.034	-0.42	-0.28	
A-Screen Angle	0.18	1	0.027	0.13	0.23	2.02
B-Bar Spacing	-0.97	1	0.024	-1.01	-0.92	1.00
D-Relative Velocity	-0.82	1	0.064	-0.95	-0.69	2.02
B^2	0.31	1	0.040	0.23	0.39	1.00

Final Equation in Terms of Coded Factors:

Logit(Blocked) = Ln[(Blocked + 0.00)/(100.00 - Blocked)] =

-0.35	
+0.18	* A
-0.97	* B
-0.82	* D
+0.31	* B^2

Final Equation in Terms of Actual Factors:

Logit(Blocked) = Ln[(Blocked + 0.00)/(100.00 - Blocked)] =

+2.17217	
+0.011900	* Screen Angle
-31.44277	* Bar Spacing
-0.97528	* Relative Velocity
+85.19416	* Bar Spacing^2

Appendix J – Regression Analysis from simplified linear models

Full Data Set

Response 1 Blocked
Transform: Logit Lower bound: 0 Upper bound: 100
Stepwise Regression with Alpha to Enter = 0.100, Alpha to Exit = 0.100

Forced Terms Intercept

Added	**Coefficient Estimate**	**t for H0 Coeff=0**	**Prob > |t|**	**R-Squared**	**MSE**
C-Debris Length	1.67	-26.98	<0.0001	0.4752	1.51
B-Bar Spacing	-1.28	24.20	<0.0001	0.6966	0.88
E-Relative Velocity	-0.65	6.98	<0.0001	0.7139	0.83
A-Screen Angle	0.21	-3.86	0.0001	0.7191	0.81

ANOVA for Response Surface Reduced Linear Model

Analysis of variance table [Partial sum of squares - Type III]

Source	**Sum of Squares**	**df**	**Mean Square**	**F Value**	**p-value Prob > F**	
Model	1667.60	4	416.90	512.73	< 0.0001	significant
A-Screen Angle	12.12	1	12.12	14.90	0.0001	
B-Bar Spacing	520.97	1	520.97	640.72	< 0.0001	
C-Debris Length	1190.80	1	1190.80	1464.52	< 0.0001	
E-Relative Velocity	48.04	1	48.04	59.08	< 0.0001	
Residual	651.29	801	0.81			
Cor Total	2318.90	805				

The Model F-value of 512.73 implies the model is significant. There is only a 0.01% chance that a "Model F-Value" this large could occur due to noise.

Values of "Prob > F" less than 0.0500 indicate model terms are significant.
In this case A, B, C, E are significant model terms.
Values greater than 0.1000 indicate the model terms are not significant.

Std. Dev.	0.90	R-Squared	0.7191
Mean	-0.39	Adj R-Squared	0.7177
C.V. %	231.64	Pred R-Squared	0.7155
PRESS	659.66	Adeq Precision	93.715

The "Pred R-Squared" of 0.7155 is in reasonable agreement with the "Adj R-Squared" of 0.7177."Adeq Precision" measures the signal to noise ratio. A ratio greater than 4 is desirable. Your ratio of 93.715 indicates an adequate signal. This model can be used to navigate the design space.

Factor	**Coefficient Estimate**	**df**	**Standard Error**	**95% CI Low**	**95% CI High**	**VIF**
Intercept	-0.46	1	0.058	-0.58	-0.35	
A-Screen Angle	0.21	1	0.055	0.10	0.32	2.04
B-Bar Spacing	-1.29	1	0.051	-1.39	-1.19	1.00
C-Debris Length	1.74	1	0.046	1.65	1.83	1.00
E-Relative Velocity	-1.02	1	0.13	-1.28	-0.76	2.04

Final Equation in Terms of Coded Factors:

Logit(Blocked) = Ln[(Blocked + 0.00)/(100.00 - Blocked)] =
-0.46
+0.21 * A
-1.29 * B
+1.74 * C
-1.02 * E

Final Equation in Terms of Actual Factors:

Logit(Blocked) = Ln[(Blocked + 0.00)/(100.00 - Blocked)] =
-0.035617
+0.014036 * Screen Angle
-21.49494 * Bar Spacing
+10.73375 * Debris Length
-1.21050 * Relative Velocity

Aggregated Data Set

Response 1 Blocked
Transform: Logit Lower bound: 0 Upper bound: 100
Stepwise Regression with Alpha to Enter = 0.100, Alpha to Exit = 0.100

Forced Terms Intercept

Added	**Coefficient Estimate**	**t for H0 Coeff=0**	**Prob > |t|**	**R-Squared**	**MSE**
B-Bar Spacing	-0.97	20.44	<0.0001	0.8359	0.077
E-Relative Velocity	-0.52	7.64	<0.0001	0.9046	0.046
A-Screen Angle	0.18	-5.12	<0.0001	0.9282	0.035

ANOVA for Response Surface Reduced Linear Model

Analysis of variance table [Partial sum of squares - Type III]

Source	**Sum of Squares**	**df**	**Mean Square**	**F Value**	**p-value Prob > F**	
Model	35.88	3	11.96	344.69	< 0.0001	significant
A-Screen Angle	0.91	1	0.91	26.24	< 0.0001	
B-Bar Spacing	32.32	1	32.32	931.30	< 0.0001	
D-Relative Velocity	3.33	1	3.33	95.92	< 0.0001	
Residual	2.78	80	0.035			
Cor Total	38.66	83				

The Model F-value of 344.69 implies the model is significant. There is only a 0.01% chance that a "Model F-Value" this large could occur due to noise.

Values of "Prob > F" less than 0.0500 indicate model terms are significant.
In this case A, B, D are significant model terms.
Values greater than 0.1000 indicate the model terms are not significant.

Std. Dev.	0.10	R-Squared	0.9282
Mean	-0.22	Adj R-Squared	0.9255
C.V. %	84.92	Pred R-Squared	0.9200
PRESS	3.09	Adeq Precision	64.606

The "Pred R-Squared" of 0.9200 is in reasonable agreement with the "Adj R-Squared" of 0.9255.

"Adeq Precision" measures the signal to noise ratio. A ratio greater than 4 is desirable. Your ratio of 64.606 indicates an adequate signal. This model can be used to navigate the design space.

Factor	Coefficient Estimate	df	Standard Error	95% CI Low	95% CI High	VIF
Intercept	-0.20	1	0.037	-0.27	-0.12	
A-Screen Angle	0.18	1	0.035	0.11	0.25	2.02
B-Bar Spacing	-0.97	1	0.032	-1.03	-0.91	1.00
D-Relative Velocity	-0.82	1	0.084	-0.99	-0.65	2.02

Final Equation in Terms of Coded Factors:

Logit(Blocked) = Ln[(Blocked + 0.00)/(100.00 - Blocked)] =
-0.20
+0.18 * A
-0.97 * B
-0.82 * D

Final Equation in Terms of Actual Factors:

Logit(Blocked) = Ln[(Blocked + 0.00)/(100.00 - Blocked)] =
+1.63507
+0.011900 * Screen Angle
-16.13607 * Bar Spacing
-0.97528 * Relative Velocity

Appendix K – Macros for Blockage Estimation Tool

```
'/^^^^^^^^^^^^^^^^^^^^^^^^^^^^^^^^^^^^^^^^^^^^^^^^^^^^^^^^^^^^^^^^^^^^^^^^^^^^^^^^^^^^^^^^^/
'/* WELCOME TO THE CODE FOR THE CULVERT BLOCKAGE ESTIMATOR */
'/^^^^^^^^^^^^^^^^^^^^^^^^^^^^^^^^^^^^^^^^^^^^^^^^^^^^^^^^^^^^^^^^^^^^^^^^^^^^^^^^^^^^^^^^^/
'/####################################################/
'/# SET UP THE GLOBAL CONSTANTS AND VARIABLES #/
'/####################################################/
''/* ****************/
'/* Spreadsheet name */
'/* ****************/
Public Const Workbook As String = "Blockage_estimator.xlsm"
'
'/* **********************************/
'/* The position of the parameter  decription */
'/* **********************************/
Public Const R_angle_txt As String = "C8"              '/* Screen Angle */
Public Const R_bar_spacing_txt As String = "C10"       '/* Bar Spacing */
Public Const R_debris_length_txt As String = "C12"     '/* Debris Length */
Public Const R_position_txt As String = "C14"          '/* Relative Velocity */
'
'/* ******************************/
'/* The position of the Input parameters */
'/* ******************************/
Public Const R_angle As String = "E8"                  '/* Screen Angle */
Public Const R_bar_spacing As String = "E10"           '/* Bar Spacing */
Public Const R_debris_length As String = "E12"         '/* Debris Length */
Public Const R_position As String = "E14"              '/* Relative Velocity */
Public Const R_model_type As String = "B1"             '/* 1 - Empirical model */
'                                                      /* 2 – Linear  model */
'
'/* ******************************/
'/* The position of the output parameters */
'/* ******************************/
Public Const R_blockage As String = "N10"              '/* Blockage */
Public Const R_blockage_low As String = "O10"          '/* Worksheet Model */
Public Const R_blockage_high As String = "P10"         '/* Worksheet Model */
'
'/* ******************/
'/* Error check variables */
'/* ******************/
Public angle_error As Integer
Public bar_spacing_error As Integer
Public debris_length_error As Integer
Public position_error As Integer
Public calculation_error As Integer
Public Const R_error_message As String = "B16"

'/* ****************/
'/* The input constants */
'/* ****************/
Public extrapolation_flag As Integer
Public bar_spacing_min As Double
Public bar_spacing_max As Double
Public debris_length_min As Double
```

```
Public debris_length_max As Double
Public bar_spacing_min_str As String
Public bar_spacing_max_str As String
Public debris_length_min_str As String
Public debris_length_max_str As String
Public position_min As Double
Public position_max As Double
Public position_min_str As String
Public position_max_str As String
'
'/* ******************/
'/* The output variables */
'/* *****************/
Public Blockage As Double                    '/* Estimated % trapped by the trash screen */
Public error_message As String
'
Option Explicit                              'All the data are declared
'
'/################/
'/# NAVIGATION #/
'/################/
'
'/****************************************************** /
'/* THIS SUBROUTINE TAKES YOU TO THE HELP PAGE  */
'/*******************************************************/
Sub help()
Worksheets("Help").Activate
Range("A1").Select
End Sub
'
'/**********************************************************************/
'/* THIS SUBROUTINE TAKES YOU TO THE BLOCKAGE  MODEL PAGE */
'/**********************************************************************/
Sub show_model()
Worksheets("Model").Activate
Range("E10").Select
Call initialise_data
End Sub
'
'/###################/
'/# INITIALISATION #/
'/###################/
'/*******************************************/
'/* THIS SUBROUTINE SETS INITIAL DATA */
'/*******************************************/
Sub initialise_data()

ActiveSheet.Unprotect

Worksheets("Model").Range(R_angle) = 45
Worksheets("Model").Range(R_bar_spacing_txt) = "Bar Spacing (m)"
Worksheets("Model").Range(R_bar_spacing) = 0.15
Worksheets("Model").Range(R_debris_length_txt) = "Debris Length (m)"
Worksheets("Model").Range(R_debris_length) = 0
Worksheets("Model").Range(R_position_txt) = "Relative Velocity"
Worksheets("Model").Range(R_position) = 1.2
```

```
Worksheets("model").angle_spin.Visible = True
Worksheets("model").bar_spacing_spin.Visible = True
Worksheets("model").debris_length_spin.Visible = True
Worksheets("model").position_spin.Visible = True

angle_error = 0
bar_spacing_error = 0
debris_length_error = 0
position_error = 0
calculation_error = 0
extrapolation_flag = 0

Call run_model

End Sub

'/**********************************************/
'/* THIS SUBROUTINE SETS PARAMETER LIMITS */
'/**********************************************/
Sub set_param_limits()

bar_spacing_min = 0.01
bar_spacing_max = 2
bar_spacing_min_str = "0.01"
bar_spacing_max_str = "2"
debris_length_min = 0.025
debris_length_max = 5
debris_length_min_str = "0.025"
debris_length_max_str = "5"
position_min = 0.1
position_max = 10
position_min_str = "0.1"
position_max_str = "10"

End Sub

'/#########################/
'/# ALL THE VALIDATIONS #/
'/#########################/
'
'/*****************************************************/
'/* THIS SUBROUTINE VALIDATES THE ANGLE ENTERED   */
'/*****************************************************/
Sub validate_angle()

ActiveSheet.Unprotect  '/* not sure why need to do this but can't change the color if you don't */

If Worksheets("Model").Range(R_angle) > 90 Then
   Worksheets("Model").Range(R_angle).Select
      With Selection.Interior
            .ColorIndex = 3
      End With
   Worksheets("Model").Range(R_error_message) = "ERROR angle must be between 1 and 90 
degrees"
   angle_error = 1
```

```
ElseIf Worksheets("Model").Range(R_angle) < 1 Then
    Worksheets("Model").Range(R_angle).Select
        With Selection.Interior
                .ColorIndex = 3
        End With
    Worksheets("Model").Range(R_error_message) = "ERROR angle must be between 1 and 90
degrees"
    angle_error = 1

Else
    Worksheets("Model").Range(R_angle).Select
        With Selection.Interior
                .ColorIndex = 2
        End With
    Worksheets("Model").Range(R_error_message) = " "
    angle_error = 0
End If

'/* Check if within range modelled, if not dispay a warning */
If Worksheets("Model").Range(R_angle) < 30 Or Worksheets("Model").Range(R_angle) > 60
Then
    extrapolation_flag = 1
End If

ActiveSheet.Protect

End Sub


'/***********************************************************/
'/* THIS SUBROUTINE VALIDATES THE BAR SPACING ENTERED    */
'/***********************************************************/
Sub validate_bar_spacing()

ActiveSheet.Unprotect  '/* not sure why need to do this but can't change the color if you don't */

If Worksheets("Model").Range(R_bar_spacing) > bar_spacing_max Then
    Worksheets("Model").Range(R_bar_spacing).Select
        With Selection.Interior
              .ColorIndex = 3
         End With
     error_message = "ERROR bar spacing must be between " + bar_spacing_min_str + " and " _
                                             +  bar_spacing_max_str
     Worksheets("Model").Range(R_error_message) = error_message
     bar_spacing_error = 1

ElseIf Worksheets("Model").Range(R_bar_spacing) < bar_spacing_min Then
     Worksheets("Model").Range(R_bar_spacing).Select
         With Selection.Interior
                 .ColorIndex = 3
         End With
     error_message = "ERROR bar spacing must be between " + bar_spacing_min_str + " and "  _
                                            +  bar_spacing_max_str
     Worksheets("Model").Range(R_error_message) = error_message
     bar_spacing_error = 1
```

```
Else
     Worksheets("Model").Range(R_bar_spacing).Select
         With Selection.Interior
                 .ColorIndex = 2
      End With
     Worksheets("Model").Range(R_error_message) = " "
     bar_spacing_error = 0
End If

'/* Check if within range modelled, if not dispay a warning */
If Worksheets("Model").Range(R_bar_spacing) < 0.03 Or
Worksheets("Model").Range(R_bar_spacing) > 0.15 Then
        extrapolation_flag = 1
End If

ActiveSheet.Protect

End Sub


'/**************************************************************/
'/* THIS SUBROUTINE VALIDATES THE DEBRIS LENGTH ENTERED   */
'/**************************************************************/
Sub validate_debris_length()
ActiveSheet.Unprotect  '/* not sure why need to do this but can't change the color if you don't */

If Worksheets("Model").Range(R_debris_length) > debris_length_max Then
    Worksheets("Model").Range(R_debris_length).Select
        With Selection.Interior
                .ColorIndex = 3
        End With
    Worksheets("Model").Range(R_error_message) = "ERROR debris length must be between "
+ debris_length_min_str + _
                                        " and " + debris_length_max_str
    debris_length_error = 1

ElseIf Worksheets("Model").Range(R_debris_length) > 0 And
Worksheets("Model").Range(R_debris_length) < debris_length_min Then
    Worksheets("Model").Range(R_debris_length).Select
        With Selection.Interior
                .ColorIndex = 3
        End With
    Worksheets("Model").Range(R_error_message) = "ERROR If a debris length is entered it
must be between " + debris_length_min_str + _
                                        " and " + debris_length_max_str
   debris_length_error = 1

Else
    Worksheets("Model").Range(R_debris_length).Select
        With Selection.Interior
                .ColorIndex = 2
        End With
    Worksheets("Model").Range(R_error_message) = " "
    debris_length_error = 0
End If
```

```
'/* Check if within range modelled, if not dispay a warning */
If Worksheets("Model").Range(R_debris_length) < 0.025 Or
Worksheets("Model").Range(R_debris_length) > 0.35 Then
       extrapolation_flag = 1
End If

ActiveSheet.Protect

End Sub

'/*****************************************************************/
'/* THIS SUBROUTINE VALIDATES THE RELATIVE VELOCITY ENTERED  */
'/*****************************************************************/
Sub validate_position()

ActiveSheet.Unprotect  '/* not sure why need to do this but can't change the color if you don't */

If Worksheets("Model").Range(R_position) > position_max Then
    Worksheets("Model").Range(R_position).Select
       With Selection.Interior
            .ColorIndex = 3
        End With
     error_message = "ERROR relative velocity must be between " + position_min_str + " and " _
                                     + position_max_str
     Worksheets("Model").Range(R_error_message) = error_message
     position_error = 1

ElseIf Worksheets("Model").Range(R_position) < position_min Then
     Worksheets("Model").Range(R_position).Select
        With Selection.Interior
               .ColorIndex = 3
        End With
     error_message = "ERROR relative velocity must be between " + position_min_str + " and " _
                                  +  position_max_str
     Worksheets("Model").Range(R_error_message) = error_message
     position_error = 1

Else
     Worksheets("Model").Range(R_position).Select
        With Selection.Interior
               .ColorIndex = 2
      End With
     Worksheets("Model").Range(R_error_message) = " "
     position_error = 0
End If

'/* Check if within range modelled, if not dispay a warning */
If Worksheets("Model").Range(R_position) < 0.97 Or Worksheets("Model").Range(R_position)
> 1.8 Then
       extrapolation_flag = 1
End If

ActiveSheet.Protect

End Sub
```

```
'/##################/
'/# CALCULATIONS #/
'/##################/
'
'/****************************************************************/
'/* THIS SUBROUTINE RUNS THE CALCULATIONS FOR AN ESTIMATE */
'/* WHERE DEBRIS LENGTH HAS BEEN INCLUDED                 */
'/****************************************************************/
Sub logit_full_calculation_model()

If Worksheets("Sheet1").Range(R_model_type) = 1 Then           '/*Empirical model*/
    Worksheets("Model").Activate
    ActiveSheet.Unprotect
    Range("N10").Select
    Worksheets("Model").Range(R_blockage) = _
            0.03399 + _
            (0.012962 * (Worksheets("Model").Range(R_angle))) + _
            (-53.87339 * (Worksheets("Model").Range(R_bar_spacing))) + _
            (32.34954 * (Worksheets("Model").Range(R_debris_length))) + _
            (-1.24983 * (Worksheets("Model").Range(R_position))) + _
            (61.95619 * (Worksheets("Model").Range(R_bar_spacing)) *
(Worksheets("Model").Range(R_debris_length))) + _
            (108.67909 * (Worksheets("Model").Range(R_bar_spacing)) *
(Worksheets("Model").Range(R_bar_spacing))) + _
            (-67.89552 * (Worksheets("Model").Range(R_debris_length)) *
(Worksheets("Model").Range(R_debris_length)))

Else                                                             '/*Linear model*/
   Worksheets("Model").Activate
   ActiveSheet.Unprotect
   Range("N10").Select
   Worksheets("Model").Range(R_blockage) = _
            0.035617 + _
            (0.014036 * (Worksheets("Model").Range(R_angle))) + _
            (-21.49494 * (Worksheets("Model").Range(R_bar_spacing))) + _
            (10.73375 * (Worksheets("Model").Range(R_debris_length))) + _
            (-1.2105 * (Worksheets("Model").Range(R_position)))
End If

Worksheets("Model").Range(R_blockage) = _
             Exp(Worksheets("Model").Range(R_blockage))

Worksheets("Model").Range(R_blockage) = (100 *_
            Worksheets("Model").Range(R_blockage)) / (1 + _
            Worksheets("Model").Range(R_blockage))

If Worksheets("Model").Range(R_blockage) < 0 Then
    Worksheets("Model").Range(R_blockage) = 0
ElseIf Worksheets("Model").Range(R_blockage) > 100 Then
    Worksheets("Model").Range(R_blockage) = 100
End If
End Sub
'
```

```
'/*************************************************************/
'/* THIS SUBROUTINE RUNS THE CALCULATIONS FOR AN ESTIMATE */
'/* WHERE NO DEBRIS LENGTH IS BEEN INCLUDED                */
'/*************************************************************/
Sub logit_summary_calculation_model()

If Worksheets("Sheet1").Range(R_model_type) = 1 Then   '/*Empirical model*/
  Worksheets("Model").Activate
  ActiveSheet.Unprotect
  Range("N10").Select
  Worksheets("Model").Range(R_blockage) = _
        2.17217 + _
        (0.0119 * (Worksheets("Model").Range(R_angle))) + _
        (-31.44277 * (Worksheets("Model").Range(R_bar_spacing))) + _
        (-0.97528 * (Worksheets("Model").Range(R_position))) + _
        (85.19416 * (Worksheets("Model").Range(R_bar_spacing)) *
(Worksheets("Model").Range(R_bar_spacing)))

Else                                                   '/*Linear model*/
  Worksheets("Model").Activate
  ActiveSheet.Unprotect
  Range("N10").Select
  Worksheets("Model").Range(R_blockage) = _
        1.63507 + _
        (0.0119 * (Worksheets("Model").Range(R_angle))) + _
        (-16.13607 * (Worksheets("Model").Range(R_bar_spacing))) + _
        (-0.97528 * (Worksheets("Model").Range(R_position)))
End If

Worksheets("Model").Range(R_blockage) = Exp(Worksheets("Model").Range(R_blockage))

Worksheets("Model").Range(R_blockage) = (100 * Worksheets("Model").Range(R_blockage))
/ (1 + Worksheets("Model").Range(R_blockage))

If Worksheets("Model").Range(R_blockage) < 0 Then
   Worksheets("Model").Range(R_blockage) = 0
ElseIf Worksheets("Model").Range(R_blockage) > 100 Then
   Worksheets("Model").Range(R_blockage) = 100
End If

End Sub

'/#######################################/
'/# AT LAST THE ACTUAL MODEL ITSELF #/
'/#######################################/
'
'/**************************************/
'/* THIS SUBROUTINE RUNS THE MODEL   */
'/**************************************/
Sub run_model()
Worksheets("Model").Activate
ActiveSheet.Unprotect

'/* SET UP CONSTANTS AND VARIABLES */
Call set_param_limits
```

```
'/* CHECK THE VALIDATIONS */
extrapolation_flag = 0

'/* CHECK THE ANGLE */
angle_error = 0
Call validate_angle
If angle_error = 1 Then
Worksheets("Model").Activate
   ActiveSheet.Unprotect
   Range("N10").Select
      Worksheets("Model").Range(R_blockage) = ""
   Exit Sub
End If

'/* CHECK THE BAR SPACING */
bar_spacing_error = 0
Call validate_bar_spacing
If bar_spacing_error = 1 Then
Worksheets("Model").Activate
   ActiveSheet.Unprotect
   Range("N10").Select
      Worksheets("Model").Range(R_blockage) = ""
   Exit Sub
End If

'/* CHECK THE DEBRIS_LENGTH */
debris_length_error = 0
Call validate_debris_length
If debris_length_error = 1 Then
Worksheets("Model").Activate
   ActiveSheet.Unprotect
   Range("N10").Select
      Worksheets("Model").Range(R_blockage) = ""
   Exit Sub
End If

'/* CHECK THE RELATIVE VELOCITY */
position_error = 0
Call validate_position
If position_error = 1 Then
Worksheets("Model").Activate
   ActiveSheet.Unprotect
   Range("N10").Select
      Worksheets("Model").Range(R_blockage) = ""
   Exit Sub
End If


'/* CHECK IF EXTRAPOLATIONS HAVE BEEN USED */
If extrapolation_flag = 1 Then
   Worksheets("model").warning_msg.Visible = True
Else
   Worksheets("model").warning_msg.Visible = False
End If
```

```
'/* DO THE CALCULATIONS   */
calculation_error = 0

If Worksheets("Model").Range(R_debris_length) = 0 Or
Worksheets("Model").Range(R_debris_length) = "" Then
   Call logit_summary_calculation_model
Else
   Call logit_full_calculation_model
End If

If calculation_error = 1 Then
   Exit Sub
End If
End

End Sub

'/^^^^^^^^^^^^^^^^^^^^^^^^^^^^^^^^^^^^^^^^^/
'/* SUPPLEMENTARY FUNCTIONALITY    */
'/^^^^^^^^^^^^^^^^^^^^^^^^^^^^^^^^^^^^^^^^/
'/********************/
'/* FORM CONTROL    */
'/********************/
Private Sub angle_spin_SpinDown()
   Call run_model
End Sub

Private Sub angle_spin_SpinUp()
   Call run_model
End Sub

Private Sub bar_spacing_spin_SpinUp()
   ActiveSheet.Unprotect
   Worksheets("Model").Range(R_bar_spacing) = Worksheets("Model").Range(R_bar_spacing)
+ 0.01
   Call run_model
   ActiveSheet.Protect
End Sub

Private Sub bar_spacing_spin_SpinDown()
   ActiveSheet.Unprotect
   Worksheets("Model").Range(R_bar_spacing) = Worksheets("Model").Range(R_bar_spacing)
- 0.01
   Call run_model
   ActiveSheet.Protect
End Sub

Private Sub debris_length_spin_SpinUp()
   ActiveSheet.Unprotect
   Worksheets("Model").Range(R_debris_length) =
Worksheets("Model").Range(R_debris_length) + 0.1
   Call run_model
   ActiveSheet.Protect
End Sub

Private Sub debris_length_spin_SpinDown()
```

```
   ActiveSheet.Unprotect
   If Worksheets("Model").Range(R_debris_length) < 0.11 Then
     Worksheets("Model").Range(R_debris_length) = 0
   Else
      Worksheets("Model").Range(R_debris_length) =
Worksheets("Model").Range(R_debris_length) - 0.1
   End If
   Call run_model
   ActiveSheet.Protect
End Sub

Private Sub discharge_spin_SpinUp()
   ActiveSheet.Unprotect
   Worksheets("Model").Range(R_discharge) = Worksheets("Model").Range(R_discharge) +
0.01
   Call run_model
   ActiveSheet.Protect
End Sub

Private Sub discharge_spin_SpinDown()
   ActiveSheet.Unprotect
   Worksheets("Model").Range(R_discharge) = Worksheets("Model").Range(R_discharge) -
0.01
   Call run_model
   ActiveSheet.Protect
End Sub

Private Sub position_spin_SpinUp()
   ActiveSheet.Unprotect
   Worksheets("Model").Range(R_position) = Worksheets("Model").Range(R_position) + 0.1
   Call run_model
   ActiveSheet.Protect
End Sub

Private Sub position_spin_SpinDown()
   ActiveSheet.Unprotect
   If Worksheets("Model").Range(R_position) < 0.11 Then
     Worksheets("Model").Range(R_position) = 0
   Else
     Worksheets("Model").Range(R_position) = Worksheets("Model").Range(R_position) - 0.1
   End If
      Call run_model
   ActiveSheet.Protect
End Sub
```